BINARY VAPOR-LIQUID PHASE EQUILIBRIUM FOR CARBON DIOXIDE + HEAVY NORMAL PARAFFINS

By

KHALED A. MASSOUD-GASEM

Bachelor of Science in Chemical Engineering
The University of California, Berkeley
Berkeley, California
1976

Master of Science in Chemical Engineering
and Petroleum Refining
Colorado School of Mines
Golden, Colorado
1979

Submitted to the Faculty of the Graduate College
of the Oklahoma State University
in partial fulfillment of the requirements
for the degree of
DOCTOR OF PHILOSOPHY
May, 1986

BINARY VAPOR-LIQUID PHASE EQUILIBRIUM

FOR CARBON DIOXIDE + HEAVY

NORMAL PARAFFINS

Thesis approved:

Robert S. Robinson Jr.
Thesis Adviser

Billy L Cryna

Jan Chapman

J P Chandler

Norman N Durham
Dean of the Graduate College

PREFACE

An experimental apparatus was constructed for the determination of bubble point pressures for binary mixtures of CO_2 + heavy normal paraffins (HNP) at temperatures from 323 K to 423 K and pressures to 96 bar. Precise bubble point data were obtained for CO_2 binaries involving n-eicosane, n-octacosane, n-hexatriacontane and n-tetratetracontane, all of which are solids at room temperature. Correlative efforts for CO_2 + n-paraffins (n-C_4 and above) included the following items: (1) Interaction parameters were determined for the Soave-Redlich-Kwong (SRK) and Peng-Robinson (PR) equations of state using least square regressions. (2) In order to provide the HNP pure-component properties required for the equations of state, new correlations based on existing experimental data have been developed for the critical temperature, critical pressure and the acentric factor of the HNP's in terms of the paraffin carbon number. (3) Sensitivity analyses were performed to assess the effects of errors in the estimated hydrocarbon critical properties on the values of the regressed interaction parameters and predicted phase properties. (4) Several parameter generalization schemes for interaction parameters for the SRK and PR equations in terms of pure hydrocarbon properties have been developed to extend their predictive capabilities to CO_2 + HNP systems for which no experimental data are available. (5) The data were analyzed using the Krichevsky-Kasarnovsky model. This provided

estimates of Henry's constants and CO_2 partial molar volumes and demonstrated the internal consistency of the acquired data.

God I thank for the opportunities of time, place and the encounters with so many wonderful and enlighted people, some directly and many through their writings. Needless to say, this study was influenced by numerous contributions of so many, to those, to my teachers through the years, to my colleagues and to my friends goes my deepest sense of appreciation and indebtedness.

Ebb and flow is the trait of all research endeavors. Undertaking my Ph.D. work under the advisement of Professor R. L. Robinson, Jr. has, I believe, lessened the severity and the frustration of the ebb cycles of this work. I extend my sincere thanks and expressions of gratitude to Professor Robinson. His intelligent guidance, authoritative knowledge of thermodynamics and depth of experience have significantly contributed to the completion of this study.

I would also like to express my thanks to my advisory committee members: Professor B. L. Crynes, Professor Jan Wagner, Professor J. Chandler and the late Professor J. H. Erbar for their valuable suggestions and fruitful discussions. My special thanks go to my dear friend Carlos Ruiz for his valuable assistance and to Mrs. Kenda Morris for her help and patience in typing this manuscript.

I am eternally in debt to the peoples of Libya for their continued financial and moral support throughout the years.

Most of all, to all members of my family, especially my parents and my wife, I dedicate this humble work in recognition of their sacrifices and ever present love.

TABLE OF CONTENTS

Chapter Page

LIST OF TABLES

LIST OF FIGURES

Figure Page

NOMENCLATURE

A	- aP^2/R^2T^2
A_i	- correlation constant
AAD	- absolute average deviation
a	- equation of state cohesive energy constant
B	- bP/RT
b	- equation of state covolume
CN	- paraffin carbon number
C_{ij}	- equation of state first interaction parameter
D	- saturated liquid density
Dev	- deviation, $Y_{calc}-Y_{exptl}$
D_{ij}	- equation of state second interaction parameter
E	- expected value
e	- random experimental error
F	- constraint function
f	- fugacity
g	- joint probability
$H_{2,1}$	- Henry's constant of solute (2) in solvent (1)
I	- number of solute injections
K	- Boltzman's constant
L	- likelihood function
ℓ	- number of parameters in a model
M	- number of phases present
Max	- maximum

Min - minimum

MW - molecular weight

m - measured variable

N - number of components in a system

NPT - number of data points

n - number of data points or number of experiments

P - system pressure

R - universal gas constant

S - objective function

SG - specific gravity

T - system temperature

V - molar volume

$\overline{V}$ - partial molar volume

VP - vapor pressure

u - number of independent variables

X - property value

x - liquid mole fraction

y - vapor mole fraction

z - compressibility factor

ZRA - Rackett compressibility factor

Greek Symbols

α - temperature functionality for the a parameter

β - temperature functionality for the b parameter

γ - activity coefficient

Δ - change in property

ε - residual vector

θ - parameter vector

λ - correlation parameter

μ - chemical potential

ν - number of degrees of freedom

ρ - density

σ - standard error

ϕ - fugacity coefficient

Ω_a, Ω_b - equation of state pure component parameters

ω - acentric factor

Subscripts

BPP - bubble point

b - boiling point point

c - critical state

calc - calculated value

exptl - experimental value

HC - hydrocarbon

i - component or data point index

j - component or data point index

k - component or data point index

ij - interaction parameter index

r - reduced property

Superscripts

J,K	- indices
ℓ or L	- liquid phase
m	- measured value
t	- matrix transpose
v	- vapor phase
$^\circ$	- standard state
',",	- phase index
∞	- infinite value or infinite dilution

CHAPTER I

INTRODUCTION

Phase equilibria thermodynamics is an essential element in the rational design and development of a multitude of industrial processes as well as in the enhancement of our understanding of fluid-phase behavior involving pure fluids and mixtures. The phase behavior of carbon dioxide, CO_2, mixtures is receiving particular attention in recent years. This attention has been motivated, in part, by interest in CO_2 as a miscible displacement fluid for recovery of petroleum from reservoirs and as a supercritical solvent in diverse industrial applications.

Several studies (1-5) have been devoted to assessments of the abilities of various cubic equations of state (EOS) to describe the phase behavior of CO_2-containing mixtures. However, limited experimental data involving CO_2 and heavy hydrocarbons has resulted in inadequate characterization for such mixtures.

The purpose of this study was to obtain solubility data for CO_2 in the following members of the normal paraffin homologous series: n-eicosane (n-C_{20}), n-octacosane (n-C_{28}), n-hexatriacontane (n-C_{36}), n-tetratetracontane (n-C_{44}). These studies were designed to provide the needed information for the further development of generalized predictive methods, including those utilizing van der Waals type cubic EOS, an additional topic of study in this investigation.

This study proceeded in three distinct phases dealing with experimental data acquisition, reduction and correlation. Chapter II contains a concise outline of the correlating framework for the representation of the experimental data using classical phase equilibria thermodynamics based on the works of Willard Gibbs(6).

A discussion of the experimental apparatus design and experimental procedure is presented in Chapters II-V. Presentation of experimental data along with the relevant error analysis and consistency tests are given in Chapter VI.

Chapter VII outlines the data reduction procedure employed. A description is given for the optimality criterion used along with details of its implementation for the phase equilibrium problem at hand.

Most, if not all, viable models for mixture representation involve pure component properties, and such data for heavy n-paraffins (the domain of this study) are scarce. Thus, Chapter VII is devoted to the development of a new correlating framework for pure fluid properties which provides better capability for extrapolating to high carbon numbers.

In Chapter IX, the Soave-Redlich-Kwong (7) and Peng-Robinson (8) EOS were studied for the representation of the acquired experimental data. This included EOS parameter selection for the purposes of data reduction, assessment of molar volume predictions, and sensitivity analyses of the effects of input data errors on the quality of the predictions. Finally, generalized correlations were developed for SRK and PR parameters involving a variety of schemes with different degrees of complexity.

Put concisely, this investigation contains the three ingredients of applied engineering research: (1) logical use of the framework of thermodynamics, (2) experimentation, and (3) inference using the tools of statistics and numerical analysis. Although no effort was made to include details of proofs or derivations for some of the principal relations or postulates used, appropriate references are given for such details.

CHAPTER II

THERMODYNAMIC FRAMEWORK

Within the framework of classical thermodynamics, the general criterion for equilibrium between a fixed number, M, of stable heterogeneous phases in a non-reactive system containing N components can be expressed in terms of temperature T, pressure P and chemical potential μ with the following equations (9):

$$T' = T'' \ldots = T^M \tag{2.1}$$

$$P' = P'' \ldots = P^M \tag{2.2}$$

$$\mu_i' = \mu_i'' \ldots = \mu_i^M \qquad (i = 1, N) \tag{2.3}$$

These conditions for equilibria, as advanced by Gibbs (6), signify uniformity of temperature, pressure, and lack of irreversible constituent mass transfer between the phases throughout the system.

In preference to quantifying the condition of equal chemical potential in terms of the measurable properties of T, P, and phase compositions x_i, use of an auxiliary function named fugacity, f_i, has been well established as a procedure which gives better behaved functionality at the limiting conditions of ideal fluid behavior (9). Thus, an equivalent condition to Equation (2.3) can be stated as:

$$f_i' = f_i'' \ldots = f_i^M \qquad (i = 1, N) \tag{2.4}$$

where $f_i = f_i(T, P, x_i)$. Material balance constraints require that:

$$\sum_{i=1}^{N} x_i' = \sum_{i=1}^{N} x_i'' = \ldots = \sum_{i=1}^{N} x_i^M = 1.0 \tag{2.5}$$

The (M-1)N equations expressed by equations (2.4) and the 2 + M(N-1) variables may be used with the phase rule (9) to determine the number of independent variables, ν, that must be specified for complete description of system in equlibrium as:

$$\nu = N - M + 2 \tag{2.6}$$

Classical thermodynamics provides us with two procedures for calculating the fugacity in terms of T, P and x_i, both based on property deviation concepts. The first procedure uses the fugacity coefficient, $\hat{\phi}_i$, as the deviation function or:

$$f_i' = \hat{\phi}_i' \, P x_i' \tag{2.7}$$

where the deviation function, $\hat{\phi}_i$, is in reference to an ideal gas mixture. Thus, by definition:

$$\hat{\phi}_i' = 1$$

$$\lim P \text{ --->} 0$$

This choice of reference has been found to be suitable in most cases for vapors and dense fluids. The second procedure using the ideal solution as the reference state is based on the activity coefficient deviation function, γ_i, or:

$$f_i = \gamma_i \, f_i^o \, x_i \tag{2.8}$$

This alternate approach, however, is normally used only for dense fluid phases, and special care is required in specifying the standard state fugacity, f_i^o, where $\gamma_i = 1$ (9).

The fugacity coefficient, $\hat{\phi}_i$, and the activity coefficient, γ_i, are related to volumetric properties of the mixture by the following exact relations (9):

$$\ln \hat{\phi}_i = \frac{1}{RT} \int_o^P \left(\overline{V}_i - \frac{RT}{P}\right) dP \tag{2.9}$$

and

$$\ln \gamma_i = \frac{1}{RT} \int_o^P \left(\overline{V}_i - V_i\right) dP \tag{2.10}$$

where $\overline{V}_i$ and V_i represent the partial molar volume and the molar volume of the component, respectively.

Although classical thermodynamics offers an efficient organizational tool for equilibria calculations, it does not provide an explicit expression for the interrelation among the observables, e.g., $V_i = f(T, P, x_i)$. This fact transforms the conceptual difficulties in phase equilibria thermodynamics to proper selection or development of models which would express such a relation concisely and accurately.

Since no theoretical models exist which describe the relationship among the observables with the desired accuracy (except for highly idealized conditions), over the years semi-empirical models have been developed. These are in most cases specialized models, thus achieving a reasonable degree of success for the specific purposes intended. This empiricism in the model formulation requires experimentation to provide the needed data for model selection and development, which in turn translates to two specific requirements:

(1) phase equilibrium data for the mixtures of interest;

(2) the proper mathematical and statistical tools to incorporate the experimental results into the selected models (through some model parameters).

Parallel to the two approaches for calculating fugacity, two methods have evolved in VLE calculation, and while the first employs an EOS for both the liquid and the vapor phase fugacity calculations, the second method uses the EOS for the vapor phase and a liquid solution model for the liquid phase. A representation of experimental data for CO_2 + n-paraffins will be given in this study utilizing both methods.

Emphasis, however, will be placed on the EOS approach, due to its simple extensions to multi-component systems as well as offering a continuity in the critical region, which the two-model approach is incapable of producing.

Regardless of the models selected for correlating the experimental data, ideally such models should give a concise statement of the gained knowledge of phase behavior for the systems considered. To this end, efforts are extended to employ models which have some theoretical basis, allowing a set of model parameters to describe experimental data without significant loss of accuracy. Also, a preference is given to models which have predictive capabilities for mixture equilibrium properties that can be employed using pure substance data input.

CHAPTER III

PREVIOUS EXPERIMENTAL WORK

This chapter describes the previous experimental work pertinent to the present study. Two distinct areas of interest are reviewed briefly: (1) experimental apparatus which have been used in VLE experiments, and (2) experimental VLE data involving carbon dioxide and heavy normal paraffins which are solid at room temperature.

Experimental Apparatus

Experimental techniques for VLE data acquisition enjoy considerable attention due to the constant industrial demand for such data. Experimental schemes for equipment design and selection of the attributes of the measured properties, (as being constant or variable during the experiment) are guided by the Gibbs phase rule. For a binary VLE system, the rule, as expressed by Equation (2.6), specifies two degrees of freedom among four variables: temperature, pressure, and liquid and vapor compositions.

Three general methods exist for equilibria determinations. The compositions of the coexisting phases may be measured as a function of pressure at a constant temperature (isothermal), the phase compositions may be measured as a function of temperature at constant pressure (isobaric), or the pressures and temperatures at which condensation or boiling occur at constant composition may be determined.

Experimental implementation of the above mentioned methods which are in current use (10-13) may be classified as:

(1) static or fluid recirculation methods (when considering phase-contacting cell design);

(2) synthetic or analytic in dealing with phase composition determination;

(3) visual or graphical regarding the bubble point determination.

Attention in this study is directed to the bubble point approach, primarily because the vapor phase composition is considered a redundant measurement of importance only in consistency tests based on the Gibbs-Duhem equation (14). Furthermore, the added difficulties in operating analytical instruments, such as a chromatograph, make a synthetic approach (where known amounts of system components are equilibriated) more attractive when dealing with high melting point solvents such as those considered here. This is even more true in the present situation since the vapor phase for systems involving CO_2 + heavy paraffins is practically pure CO_2.

Although the bubble point approach and its numerous modifications have been used since 1877 (11), the method employed in this study is more in the context of the works of Sage, et al. (13), with the added design details for handling solvents which are solid at room temperature. The method consists of the introduction of known amounts of well-degassed pure components into a variable-volume thermostated equilibrium cell. The bubble point is established by identifying the break point in a pressure-volume curve.

Variations in the design of bubble point apparatus revolve mainly on the experimental schemes used to:

(1) affect volume changes of the equilibrum mixture;

(2) ensure proper contacting of the fluid 'phases' present;

(3) identify the bubble point.

Reported methods for varying the volume in the equilibrium cell include the use of a piston-cylinder assembly (15) and the use of mercury as an incompressible involatile fluid piston (10,13). The latter, used in the present work, has the added advantage that the mercury can act as an excellent mixing agent during agitation. (To ensure the attainment of equilibrium in a reasonable time, the cell contents are mechanically agitated.) Several methods have been employed to accomplish this: rocking the equilibrium cell, magnetic stirring (89), or a more involved method of rocking the entire constant temperature bath housing the equilibrium cell (16).

Regarding bubble point determinations, although visual observations may prove very useful in many instances, especially when encountering liquid phase splitting or solid formation, bubble point determination by phase boundary discontinuities is very reliable. This method, however, is recommended only at conditions well below the critical point where a clear distinction exists between the liquid and the vapor compressibilities.

Experimental Data

CO_2 + hydrocarbon vapor-liquid equilibria data are of interest in a number of industrial processes, including processing of petroleum products, production of coal liquids, and enhanced oil recovery. Accordingly, several investigators (1-5) have compiled references for CO_2-hydrocarbon binary mixtures. These compilations include data for

aromatics, naphthenes and normal paraffins which are liquids at room temperature. Limited data, however, are available on systems involving CO_2 and heavy normal paraffin solvents which are solids at room temperature. At the inception of this work, only two studies were found in the literature dealing with such systems. Data on CO2 + n-eicosane has been reported by Huie, et al. (17), and CO_2 with traces of n-octacosane presented by McHugh, et al. (18). More recently, however, Fall and Luks (19), reported VLE data binaries involving the heavy normal paraffins for n-C_{22} and n-C_{32}.

The literature search included the chemical abstracts for the period from 1907 to 1983, major data compilations such as that by Wichterle, et al. (20), and the specialized journals. Only VLE experiments pertaining to normal paraffins which are used in this study appear in Table I. Data employed were selected so as to place special emphasis on heavy n-paraffins. Accordingly, only representative data were included for n-paraffins lighter than n-C_{10}. CO_2 supercritical temperature range considered extends from 310-510 K.

TABLE I

EXPERIMENTAL DATA FOR CO_2 + n-PARAFFINS
USED IN THIS STUDY

Paraffin Carbon Number, CN	Temperature Range, K	Pressure Range, Bar	CO_2 Liquid Mole Fraction Range, X_{CO_2}	Ref.
4	310.9 - 410.9	5.5 - 75.4	0.00 - 0.91	21
6	313.2 - 393.2	8.6 - 116.0	0.03 - 0.92	15
7	310.7 - 477.2	1.8 - 133.1	0.02 - 0.95	22
10	277.6 - 510.9	3.5 - 172.4	0.05 - 0.91	13
20	323.2 - 373.2	6.2 - 67.6	0.07 - 0.50	This Work
22	323.2 - 373.2	9.6 - 71.8	0.12 - 0.59	19
28	323.2 - 423.2	8.1 - 96.0	0.07 - 0.62	This Work
32	348.2 - 398.2	9.5 - 72.3	0.10 - 0.56	19
36	373.2 - 423.2	5.2 - 86.5	0.06 - 0.50	This Work
44	373.2 - 423.2	5.8 - 70.8	0.08 - 0.50	This work

CHAPTER IV

EXPERIMENTAL APPARATUS AND MATERIALS

The general arrangement of the equipment used in this study is illustrated in Figure 1. The apparatus employs a static type equilibrium cell which may be used in bubble point determinations over wide ranges of temperature, pressure and liquid composition. The central part of the apparatus is a high-pressure, variable volume rocking cell housed in a constant temperature bath.

A distinct feature of the apparatus is its capability for handling solvents which are solids at room temperature. Solvent solidification presents significant problems in conventional equilibrium apparatus; this may explain in part the lack of data for such systems. This chapter provides a general description of the apparatus. For additional details refer to Appendix A.

The Equilibrium Cell

The equilibrium cell is a 90 cc high-pressure stainless steel cylinder. The cell is mounted in an aluminum metal block attached to a motor-driven rocking assembly with a 1/50 horsepower variable speed motor, Bodine Electric Company, model series 200, type NSH-12. The effective volume of the cell (EC) can be varied by the introduction or withdrawal of mercury at the bottom of the cell. Solvent and solute injections, on the other hand, are made at the top of the cell through a

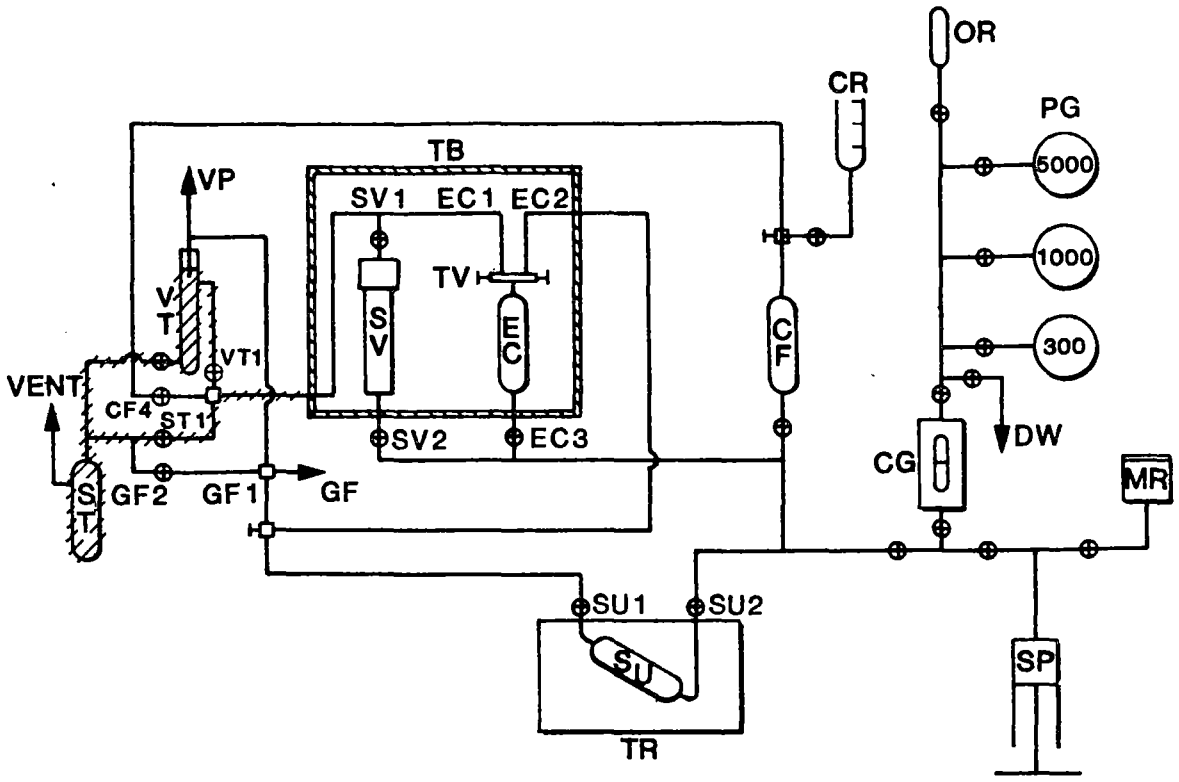

CF - CLEANING FLUID CYLINDER
CG - MERCURY-OIL CONTACT GAUGE
CR - CLEANING FLUID RESERVOIR
DW- TO DEAD-WT. GAUGE
EC - EQUILIBRIUM CELL
GF - TO GAS-FEED CYLINDERS
VT - VACUUM TRAP
MR - MECURY RESERVOIR
OR - OIL RESERVOIR
PG - PRESSURE GAUGES
SP - SCREW PUMP
ST - SOLVENT TRAP
SU - SOLUTE STORAGE CYLINDER
SV - SOLVENT STORAGE CYLINDER
TB - CONSTANT TEMPERATURE BATH
TR - REFRIGERATED TEMPERATURE BATH
TV - THREE-WAY VALVE
VP - TO VACUUM SYSTEM
HEATING TAPE

Figure 1. Schematic Representation of Experimental Apparatus

1/16 inch stainless steel three-way valve (TV) (HIP Inc., catalog number 65-15AF1). To minimize possible dead volume within the cell, a short segment of 1/16 inch tubing is employed to connect the cell to the three-way valve.

While the equilibrium cell is rocking, it is brought from a vertical to a horizontal position at a controlled speed of up to 100 cycles/min, using a motor speed controller (Bodine Electric Company, model 901, type BSH-200). Thus the mercury not only provides an excellent fluid piston for volume control, but also acts as an excellent mixing agent. This is achieved by the constant mercury "sloshing" during the rocking motion.

In the early apparatus construction trials, a Jerguson sight gauge was used as the equilibrium cell. This was used to permit visual observations of the equilibrating mixture. However, frequent leaks (which were attributed to the gasketing system used) led to the use of the present "blind" cell.

Storage and Injecting Assembly

As indicated in Figure 1, several storage cylinders were employed in this experiment. While some reservoirs such as (SV) and (SU) are intended for injection purposes, others such as (CF) and (MR) are merely for clean-up procedures and material storage. The solvent reservoir (SV), a 125 cc high-pressure reactor bomb with screw-top closure (HIP, Inc., catalog number OC-3), is placed inside the high-temperature bath (TB) in order to accommodate heavy solvents (solids at room temperature). The reservoir may be filled with the solid solvent by removing the top of the bomb. The solute is stored in a high-pressure

(5000 psi rating) stainless steel cylinder (SU). The cylinder in turn is housed in an external constant temperature refrigerated bath (TR), so that the solute may be injected as a gas or liquid as desired.

Injections of solvent or solute into the equilibrium cell are done volumetrically by injecting mercury at the bottom of either the solvent or the solute cylinders, thus displacing an equal quantity of fluid into the rocking cell. The injected volumes are metered from a precision screw pump (SP) with a storage capacity of 500 cc maintained at room temperature. Mercury needed to replace that lost during the cleaning procedure is placed in a 250 cc aluminum reservoir (MR) with a tight removable lid. The mercury reservoir is connected to the screw pump, thus mercury replacement is easily accomplished.

Cleaning fluid may be delivered to the equilibrium cell (or the other fluid reservoirs) in the same fashion as described for solvent injections from storage in a 250 cc high pressure stainless steel cylinder. Additional fluid is obtained from a 150 cc glass burette (CR). Similarly, reserve oil for the pressure gauges is stored in an open top 75 cc stainless steel cylinder.

Pressure Generation and Measurement

Pressures are measured on three precision bourdon-tube gauges (PG) which are calibrated periodically against a dead-weight tester (not shown). The three gauges have full scale readings of 300, 1000 and 5000 psi (Dresser Industries models AE05132, AD15868 and CMM5000). While the imprecision of the 300 and 1000 gauges is estimated to be 0.07% of the full scale, the imprecision of the 5000 gauge is estimated at $\pm$ 1.6 psia. Pressures are transmitted directly from the equilibrium cell to

the gauges through the mercury-filled lines. The pressure gauges are oil-filled and are connected to the mercury system through mercury-oil contact in a Jerguson sight gauge (CG); suitable head corrections are applied for the mercury.

Pressure generation is achieved by reduction of the effective volume of the equilibrium cell or storage reservoir. This in turn is accomplished by the introduction (or withdrawal for pressure reduction purposes) of mercury into the cell. A calibrated Ruska hand pump, model 2411, is used to house and to transmit the mercury into the different storage cylinders.

Constant Temperature Baths

Two commercial constant temperature baths were used in this experiment. The first, (TB) is a high-temperature Hotpack air oven, model 200001, used to house the equilibrium cell and the solvent cylinder. Temperature control of the oven is maintained within 0.1 K by a Hallikainen proportional-integral controller, model 1053A. Temperature measurements within 0.1 K were made using a calibrated platinum resistance thermometer connected to a Fluke digital readout, model 2180A. Repeated ice melting point checks confirm the reported imprecision of 0.1 K or less. The second bath (TR), which contains the solute cylinder, is a constant temperature refrigerated bath, Neslab model RTE-4. The unit, which is designed to operate between -30°C and +100°C, is equipped with a circulating pump, proportional temperature controller (0.01°C stability), and stainless steel refrigerator coils. Water is used as a heating (or cooling) medium. Temperature of the water bath is measured by a mercury-in-glass thermometer with divisions

of 0.1°C. The thermometer was calibrated at 50°C with the platinum resistance thermometer which indicated an uncertainty of 0.1°C in the temperature measurement.

Degassing Assembly

The degassing assembly consists of the solvent storage cylinder (SV) and the vacuum trap (VT), which is a 100 cc, 1-inch diameter glass tube with a top rubber stopper. While the former houses the solvent in the solid or liquid phase, the latter prevents the vaporized solvent from reaching the line leading to the vacuum system. In addition, the vacuum trap is used to collect mercury accompanying the discarded hydrocarbon mixture during the cleaning procedure. Excess hydrocarbon and mercury collected in the trap are transferred to a solvent trap (ST), a 250 cc stainless steel cylinder.

To prevent solvent solidification in the vacuum trap or the connecting lines, a heating tape (signified by +++ in Figure 1) is used. Heat input is controlled by a variable power source (a variac).

The Vacuum System

The main components of the vacuum system are shown in Figure 2. Vacuum is achieved by a 100 l/m free air displacement Sargent-Welch mechanical pump (A), model 8811. A glass cold trap (E) immersed in liquid nitrogen is used to trap condensable materials so that they do not reach the vacuum pump. Elimination of condensables reduces the chance for corrosion and damage to the vacuum pump and promotes efficient vacuuming. While all the vacuum lines are 1/2-inch-OD copper tubing, glass-to-metal connections are made of vacuum rubber tubing

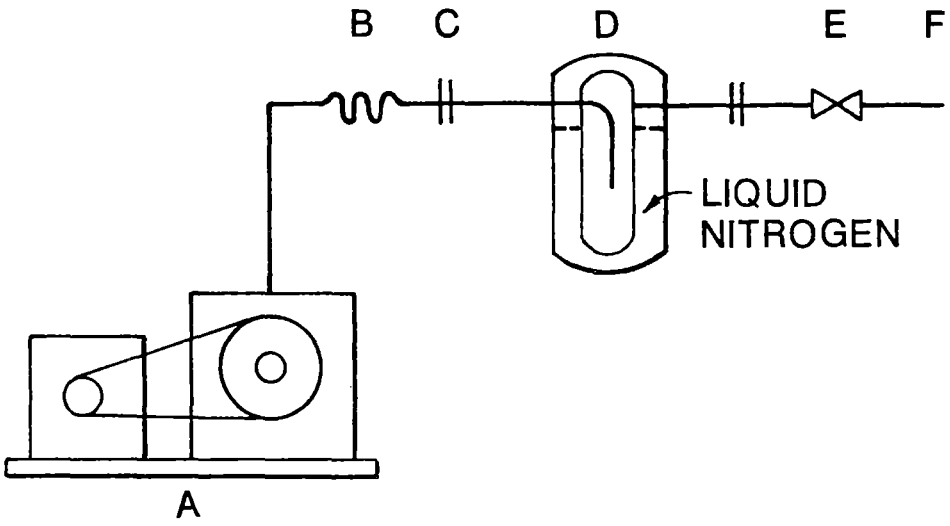

A. MECHANICAL VACUUM PUMP
B. CAJON FLEXIBLE BELLOWS TUBING
C. ULTRA-TORR UNIONS
D. GLASS COLD TRAP
E. SHUTOFF VALVE
F. CONNECTION TO DEGASSING ASSEMBLY

Figure 2. Details of Vacuum System

(B). Tubing clamps are applied to such connections to prevent leaks. The cold trap is connected to the vacuum pump lines by Cajon Ultra-Torr unions (C). The pressure in the vacuum system is measured with a thermocouple vacuum gauge, Sargent-Welch model 1515.

Auxiliary Equipment

High Pressure Valves and Tubing

A leak-tight system is an absolute requisite for a bubble point determination procedure. Accordingly, careful selection of fittings and tubing is essential. In this experiment, 1/8 inch stainless steel tubing and valves were used in the majority of the apparatus. Exceptions included the 1/16 inch tubing used in the coils (three feet long and six inches in diameter) leading to the 1/16 inch three-way valve (TV). Also, 1/4 inch tubing was used in portions of the lines leading to the vacuum system and the dead-weight tester. Taper seal valves fitted with teflon packing (HIP Inc.) and rated at 15,000 psi were used almost exclusively.

Although most fittings and valves performed satisfactorily with rare occurrence of leaks, the three-way valve (TV) and the 1/16 inch coils connecting it to the fluid reservoirs required frequent service. This included coil replacement to avoid line rupture which is induced by the constant rubbing of the coils during rocking of the equilibrium cell (EC), frequent replacement of the three-way valve teflon packing to prevent leaks and, when this was not successful, replacement of the valve itself.

Barometer

The barometric pressure determination required to convert from gauge pressure measurements to absolute pressure were normally made using a quartz Bourdon tube gauge, Texas Instruments (TI) Inc., Model 141. The gauge as calibrated by the manufacturer, had a reported accuracy of 0.015% of full scale. When the TI gauge was not available, an inverted-tube mercury barometer was used, which reasonably agreed with the TI gauge measurements.

Materials

The carbon dioxide used in this study had a stated purity of 99.99 mol% and was supplied by Linde Specialty Gases. The normal paraffins were of a reported purity of 99 mol% as supplied by Alfa Products. No further purification of the chemicals was attempted.

CHAPTER V

EXPERIMENTAL PROCEDURE

This chapter contains descriptions of the experimental procedure for the bubble point data obtained. Procedural steps included apparatus clean-up, pressure testing, solvent degassing, solvent and solute injection and bubble point determination. In addition, frequent calibration checks were performed on the pressure gauges and the thermometers prior to injection, and vapor pressure measurements for propane and ammonia were made to ensure that the system as a whole was functioning properly. Although details and the motivation behind each step are discussed in the following sections, as an over-view, the success of such an experiment is highly dependent on a leak-tight system, impurities-free mixtures (especially from incondensibles such as air), proper accounting for the amount of material injected, and reliable temperature and pressure measurement and control.

Two alternative approaches are possible for data acquisition. The first is to maintain a constant temperature while several consecutive injections are made to vary the composition. The second approach is to hold the mixture composition constant and vary the temperature. While the latter offers the advantage of having fewer clean-ups for the equilibrium cell, the former reduces both the possibilities for leaks due to thermal stress and the difficulties associated with establishing

temperature control. Accordingly, the isothermal approach was used in this work.

In implementing the procedure outlined, two assumptions were made: that the mercury vapor pressure is negligible (<0.02 psi at the maximum temperature of 423 K), and that the hydrocarbon solvent is incompressible at the injection conditions; thus, variations of density with pressure can be safely ignored and solvent injections may be done at elevated pressures of about 200 psia.

Apparatus Clean-up

The purpose of this step is to clean the equilibrium cell, the solvent storage cylinder, and the connecting lines of any hydrocarbon that may be present. The procedure used is as follows:

(1) The line connecting the solvent cylinder and the vacuum trap (VT) are heated using the tape heater.

(2) While the valves VT2, CF4, GF2, and EO2 are closed, valve ST1 is opened to allow for the displacement of heated hydrocarbon solvent into the solvent trap (ST). The displacement is done by injecting mercury from the screw pump (SP).

(3) CO_2 gas at 500 psi is vented through the solvent cylinder to help remove the hydrocarbon material.

(4) While the valves SV2 and EC3 are closed, the cleaning fluid cylinder (CF) is charged with pentane, and a pressure of 500 psi is generated.

(5) A 15 cc volume is created in the solvent cylinder by withdrawing mercury (into the screw pump). During withdrawal

of mercury, a pressure head is maintained by pentane through the line connected to the (CF4) valve.

(6) Pentane is injected into the solvent cylinder to fill the volume created in the previous step. Pressure in the cylinder is increased to 700 psi, and pentane is allowed to dissolve the remaining hydrocarbon for about 20 minutes. During this step valve (CF4) is kept closed, while valve SV2 is opened.

(7) The pentane/hydrocarbon solution is displaced into the solvent trap (ST) in the manner followed in step 2. A pressure of 700 psi is maintained in the solvent cylinder to keep pentane in the liquid phase, however.

(8) Steps 3 through 8 are repeated at least four times increasing the amount of pentane used by 5 cc. each time.

For the clean-up of the equilibrium cell, the above procedure is used with one exception: the pentane/hydrocarbon mixture in step 6 is allowed to rock for 15 minutes after each injection.

Pressure Testing

The method used for the determination of the bubble point pressure, namely locating the break-point in the pressure-volume curve, makes leaks in the pressure system detrimental. Thus pressure testing the system, to test for leaks, is an essential element of the overall effort. To accomplish this, first the equilibrium cell is pressurized with helium gas and a leak test is performed at room temperature using a highly sensitive helium leak detector. Secondly, the cell is pressurized with helium gas at the temperature of the experiment and a pressure test is carried out at a pressure level higher than those which

would be encountered during the experimental run. All elements of the pressure system are included in the test (e.g., the screw pump and the appropriate pressure gauges). The duration of the test may extend from 12 hours in routine checks to over 24 hours after major maintenance service.

Similar steps are taken when pressure testing the solvent or the solute storage cylinder. In such cases, however, a tolerance is exhibited for one or two psi of overnight pressure loss when using helium, since both cylinders are not part of the equilibrium system.

Degassing Procedure

Since the determination of the bubble point pressure involves identification of the pressure at which complete condensation of the vapor phase mixture occurs, the mixture must be free of any noncondensibles such as air. The degassing procedure followed in this study is described below.

(1) Approximately 40 gm of hydrocarbon solvent are placed in the solvent cylinder (SV) as solid flakes or powder. About 20 cc of clearance above the solvent level are provided for vacuuming. The air filling this clearance is removed by purging the cylinder with CO_2 gas at 30 psi through the CO_2 feed line (GF).

(2) While valves EC1 and SU1 are closed, vacuum is established on the solvent through the heated vacuum trap (VT) for at least one hour.

(3) The oven is then heated to the desired system temperature, and vacuum is maintained on the now-melted solvent.

(4) While vacuuming, gradual mercury injections of about 5 cc every half hour are made into the bottom of the solvent cylinder, thus reducing the clearance above the hydrocarbon solvent.

(5) After a minimum of three hours of vacuuming and mercury injections, a continuous flow of the hydrocarbon solvent (3 to 5 cc) is seen dripping in the vacuum trap. At this point the SV1 valve is closed and the pressure in the solvent cylinder is raised to 200 psi.

Injection Procedure

Establishing the binary mixture composition for which the bubble point is to be determined is achieved by injecting known amounts of solvent and solute into the equilibrium cell. The details for solvent and solute injections are given in this section.

Solvent Injection

(1) Having maintained the constant temperature air bath at the desired temperature for at least six hours, a provision is made for 20 cc of free volume in the equilibrium cell (by withdrawing mercury from the bottom of the cell).

(2) After purging the equilibrium cell with high pressure CO_2 several times along with short periods of vacuuming, vacuum is maintained for at least an hour as the last step in preparing the equilibrium cell for injection. The pressure lines connecting the screw pump to the equilibrium cell are also evacuated, thus removing air or any other volatile contaminants.

(3) The pressure lines are pressurized to about 200 psi using the mercury pump after isolating the equilibrium cell by closing valve EC3. Next, valve VS2 is opened, thus connecting the pressure system to the solvent storage cylinder.

(4) Pressure is stabilized in the solvent cylinder at the desired injection pressure (usually around 200 psi). At this point, the solvent reservoir pressure, the pump reading, the oven temperature, and the room temperature are recorded. A sample record is given in Appendix A.

(5) A predetermined amount of hydrocarbon solvent is injected into the equilibrium cell. This is accomplished by injecting an equivalent amount of mercury into the solvent reservoir.

(6) While valve EC1 is closed, the solvent cylinder pressure is reestablished and the final pump reading and room temperature are recorded.

(7) As a last step, the solvent cylinder is isolated by closing valve SV2.

Solute Injection

(1) For a given solvent injection, the amount of solute needed to obtain the desired liquid mole fraction is determined.

(2) The solute storage cylinder pressure is stabilized at the desired level, while only valves GF1, SU4 and SU2 are open to the pressure system.

(3) A record is made of the solute cylinder pressure, the initial pump reading, and temperature along with room temperature and the barometric pressure.

(4) The amount of solute (CO_2), as determined in step 1, is injected into the equilibrium cell. Pressure is reestablished in the solute cylinder, and a record is made of the final pump reading and the final room temperature.

After applying proper thermal expansion corrections (details given in Appendix A) to the solvent and solute volumes injected, the mixture liquid mole fraction is calculated. The corrections applied are due to temperature differences between the screw pump mercury and the solvent and the solute cylinders. The densities of the solvent liquids were obtained from the literature (63), as were the CO_2 densities (24).

Solute Preparation

To prepare the solute (CO_2) for injection at the desired temperature the following steps are taken:

(1) Having set the refrigerator bath at the desired temperature, and while the value SU2 is closed, the solute cylinder (SU) is evacuated through the vacuum trap.

(2) Mercury is injected into the solute cylinder, through valve SU2 while SU1 is closed, until pressure starts to build up, indicative of a completely mercury-filled cylinder.

(3) Mercury is then withdrawn from the bottom of the solute cylinder while 50 cc of high pressure CO_2 is admitted into the cylinder. This and the previous step establish a proper head correction datum point for the solute cylinder.

(4) Filling and purging of CO_2 from the solute cylinder is continued for at least five times to help remove any traces of the cleaning fluid or air.

(5) Vacuum is applied to the purged solute cylinder for at least one-half hour.

(6) The purging and filling sequence is repeated, and finally the solute cylinder is filled with CO_2 at roughly the desired injection pressure.

Bubble Point Determination

After each injection of solute into the solvent in the rocking cell, the bubble point pressure of the mixture is determined. This is done by injecting known amounts of mercury into the cell to alter the system volume. After each mercury injection, the cell is rocked for at least 15 minutes to bring the system to equilibrium and then the pressure is recorded. This process is repeated to obtain pressure readings in both the single-phase liquid and the vapor-liquid two-phase regions. The bubble point pressure is located by observing the break point in a pressure-volume curve as the system passes from a two-phase to an all-liquid condition. Example plots are shown in Figure 3.

Attainment of equilibrium is determined by the constancy of pressure for a minimum of 15 minutes. This translates to a time requirement of about 45 minutes when dealing with the two phase and double that in the single phase region. Room temperature variations have a significant effect on this process due to expansion and contraction of the exposed mercury in the pressure lines and the screw pump. Thus efforts were made to maintain the room temperature constant within 0.5 K, especially when gathering data in the single phase region.

The compositions of the bubble point liquids are determined from the precisely known volumes of pure solvent and solute injected into the

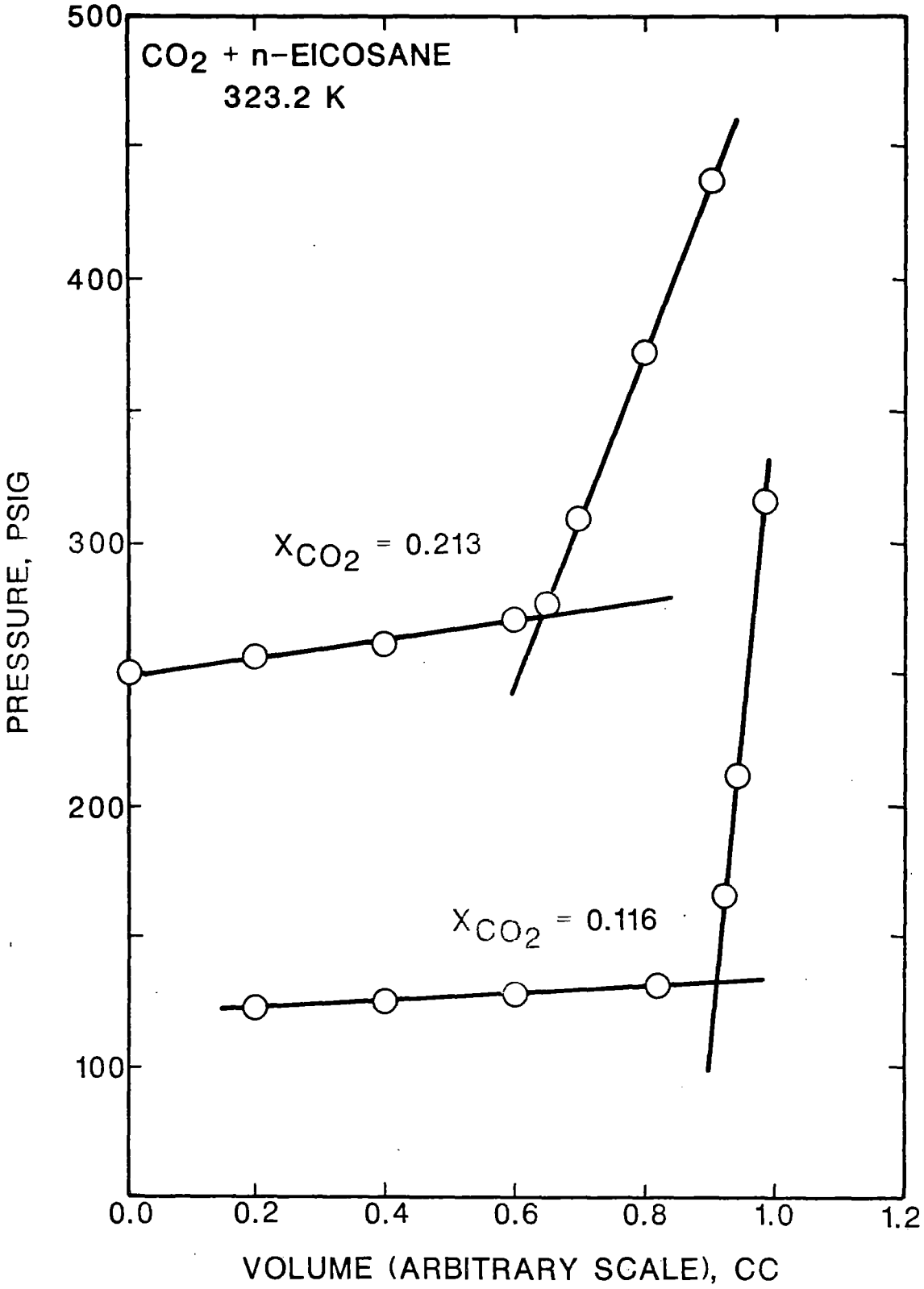

Figure 3. Graphical Bubble Point Determination

cell; thus, no compositional analyses are required. Calculation procedure for the liquid mole fraction is given in Appendix A.

CHAPTER VI

PRESENTATION AND ANALYSIS OF EXPERIMENTAL DATA

Proper evaluation of the acquired data is an essential element in the overall experimental effort. While error analysis provides estimates for the experimental uncertainties due to random disturbances, experimental consistency tests are the primary guard against systematic errors. Accordingly, this chapter contains a presentation for the experimental data obtained along with error analysis and an assessment for the consistency of the reported values.

Presentation of Experimental Data

Isothermal bubble point pressure data for CO_2 binaries involving the normal paraffins n-eicosane (n-C_{20}), n-octacosane (n-C_{28}), n-hexatriacontane (n-C_{36}), and n-tetratetracontane (n-C_{44}) were obtained in this study. The raw experimental data are presented in Tables II through V. The measurements cover a temperature range of 323 to 423 K (122 to 302°F) and pressures to approximately 96 bar (1400 psia), which translates to CO_2 mole fractions of up to 0.54. A typical graphical representation of the experimental data is given in Figure 4 for the CO_2 + n-octacosane system.

Tables VI and VII contain the raw experimental data for the CO_2 + benzene and ethane + n-dodecane (n-C_{12}) binaries. These data were

TABLE II

BUBBLE POINT PRESSURE DATA FOR
CO_2 + n-EICOSANE

Mole fraction CO_2	Bubble Point Pressure bar	(psia)
----------323.2 K (122°F)----------		
0.073	6.2	(90.0)
0.098	8.55	(124.5)
0.116	10.10	(146.5)
0.180	16.24	(235.5)
0.212	19.72	(286.0)
0.235	21.99	(319.0)
0.242	22.72	(329.5)
0.251	23.82	(345.5)
0.300	29.47	(427.5)
0.322	31.82	(461.5)
0.335	33.37	(484.0)
0.399	41.88	(607.0)
0.425	46.06	(668.0)
0.501	57.67	(836.5)
----------373.2 K (212°F)----------		
0.090	10.69	(155.0)
0.153	19.06	(276.5)
0.214	27.65	(401.0)
0.249	33.16	(481.0)
0.314	44.02	(638.5)
0.332	47.30	(686.0)
0.371	54.81	(795.0)
0.416	64.29	(932.5)
0.430	67.57	(980.0)

TABLE III

BUBBLE POINT PRESSURE DATA FOR
CO_2 + n-OCTACOSANE

Mole fraction CO_2	Bubble Point Pressure bar	(psia)
----------348.2 K (167°F)----------		
0.099	8.45	(122.5)
0.160	14.48	(210.0)
0.231	22.41	(325.0)
0.301	31.23	(453.0)
0.399	46.23	(670.5)
0.470	59.33	(860.5)
0.551	77.22	(1120.0)
0.617	96.04	(1393.0)
----------373.2 K (212°F)----------		
0.082	8.07	(117.0)
0.098	9.72	(141.0)
0.149	15.65	(227.0)
0.215	23.75	(344.5)
0.289	34.75	(504.0)
0.339	42.88	(622.0)
0.391	52.36	(759.5)
0.465	68.12	(988.0)
0.558	93.46	(1355.5)
----------423.2 K (302°F)----------		
0.070	8.41	(122.5)
0.107	13.38	(194.0)
0.155	20.24	(293.5)
0.226	29.34	(425.5)
0.301	45.37	(658.0)
0.397	66.81	(969.0)
0.490	92.53	(1342.0)

TABLE IV

BUBBLE POINT PRESSURE DATA FOR
CO_2 + n-HEXATRIACONTANE

Mole fraction CO_2	Bubble Point Pressure bar	(psia)
----------373.2 K (212°F)----------		
0.062	5.24	(76.0)
0.101	8.72	(126.5)
0.172	15.79	(229.0)
0.178	16.62	(241.0)
0.206	19.48	(282.5)
0.280	28.68	(416.0)
0.335	36.44	(528.5)
0.375	42.82	(621.0)
0.390	45.05	(653.5)
0.459	58.78	(856.0)
----------423.2 K (302°F)----------		
0.097	10.17	(147.5)
0.147	16.10	(233.5)
0.191	21.96	(318.5)
0.280	35.27	(511.5)
0.302	39.23	(569.0)
0.393	56.74	(823.0)
0.405	60.09	(871.5)
0.502	86.53	(1255.0)

TABLE V

BUBBLE POINT PRESSURE DATA FOR
CO_2 + n-TETRATETRACONTANE

Mole fraction CO_2	Bubble Point Pressure bar	(psia)
----------373.2 K (212°F)----------		
0.080	5.79	(84.0)
0.122	9.38	(136.0)
0.188	15.37	(223.0)
0.233	19.99	(290.0)
0.343	33.57	(486.0)
0.401	41.85	(607.0)
0.502	61.12	(886.5)
----------423.2 K (302°F)----------		
0.091	8.14	(118.0)
0.152	14.41	(209.0)
0.193	19.24	(279.0)
0.270	29.30	(425.0)
0.319	36.54	(530.0)
0.398	50.92	(738.5)
0.485	70.81	(1027.0)

TABLE VI

BUBBLE POINT PRESSURE DATA FOR
ETHANE + n-DODECANE at 373.2 K (212°F)

Mole fraction Ethane	Bubble Point Pressure bar	(psia)
0.111	7.76	(112.5)
0.179	13.48	(195.5)
0.204	15.58	(226.0)
0.244	19.27	(279.5)
0.279	24.37	(353.5)
0.300	24.89	(361.0)
0.399	35.51	(515.0)
0.403	35.71	(518.0)
0.487	46.26	(671.0)
0.534	52.33	(759.0)

TABLE VII

BUBBLE POINT PRESSURE DATA FOR
CO_2 + BENZENE at 313.2 K (40°F)

Mole fraction CO_2	Bubble Point Pressure bar	(psia)
0.056	7.58	(110.0)
0.101	12.62	(183.0)
0.191	21.93	(318.0)
0.260	29.54	(428.5)
0.405	42.57	(617.5)
0.531	51.71	(750.0)

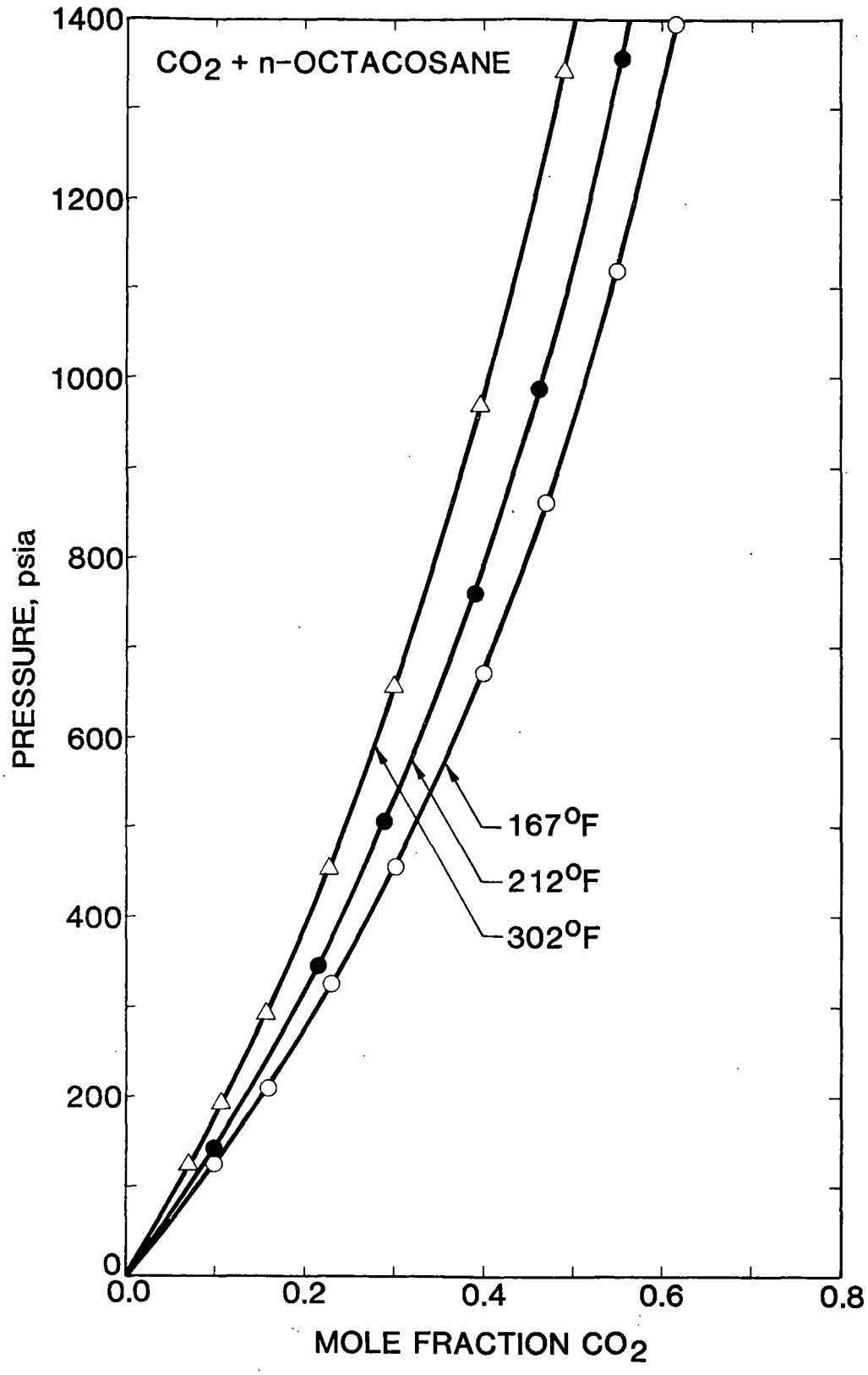

Figure 4. Bubble Point Pressure Data for CO_2 + n-Octacosane System

obtained in the early stages of the study as part of the efforts to verify the integrity of the experimental apparatus and procedures.

Consistency of Experimental Data

One of the major problems encountered in phase equilibrium studies has been the verification of the thermodynamic consistency of the data obtained. Although many techniques have been developed over the years, some more complicated than others, a number of the simpler methods still give reliable conclusions about the consistency of the data obtained experimentally. Some of those simpler tests are used here. Three types of consistency tests are performed before the experimental data are accepted as being consistent. These are instrumental, external, and internal consistency tests.

Instrumental Consistency

Instrumental consistency for the temperature, pressure, and volume measuring devices is established by frequent calibrations, as will be discussed in the following sections. In addition, vapor pressures of pure propane and ammonia were determined at several temperatures to ensure proper combined temperature and pressure measurement. Representative vapor pressure values obtained are given in Table VIII along with the reported literature values. Comparison of the data sets indicates good agreement. The slight differences exhibited may be attributed to differences in the purity of the materials used in the different investigations. Selection of propane and ammonia for these measurements was based on the convenient range of their vapor pressures.

TABLE VIII

VAPOR PRESSURE MEASUREMENTS

Temperature (°F)	Vapor pressure, psia				Ref No.
	Experimental		Literature		
	Propane	Ammonia	Propane	Ammonia	
80.0		149.6		153.0	23
86.3	157.8		158.1		23
120.0		286.4		286.4	23
150.0		429.4		432.2	23
180.3		618.0		619.0	23

External Consistency

External consistency tests are used to verify the accuracy of the apparatus and the procedures employed, by comparison of results obtained using the present apparatus to those of other investigators at the same (or similar) experimental conditions. For such a purpose, bubble point pressure data were measured on three systems for which literature data exist: ethane + n-dodecane, CO_2 + benzene, and CO_2 + n-eicosane. Data comparisons appear in Figures 5 and 6, where the data from the various sources are shown in terms of their deviations from simple polynomial functions fit to the present data given in Tables VI and VII.

Among the various data for ethane + n-dodecane (25-27), the present work results are in best agreement with those of Legret, et al. (25); the results shown in Figure 5 indicate differences in bubble point

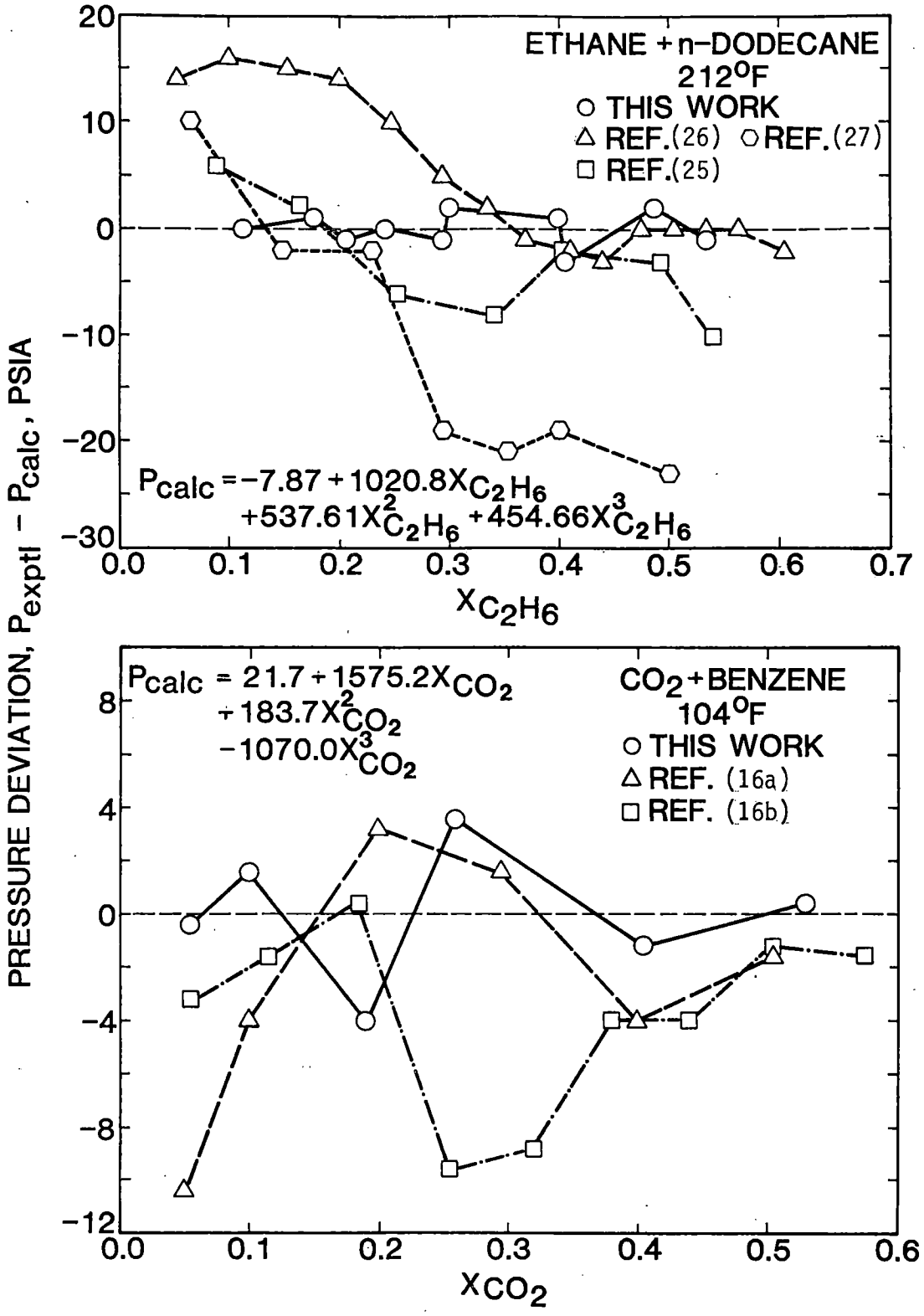

Figure 5. Comparison of Bubble Point Pressure Data for Ethane + n-Dodecane and CO_2 Benzene Systems

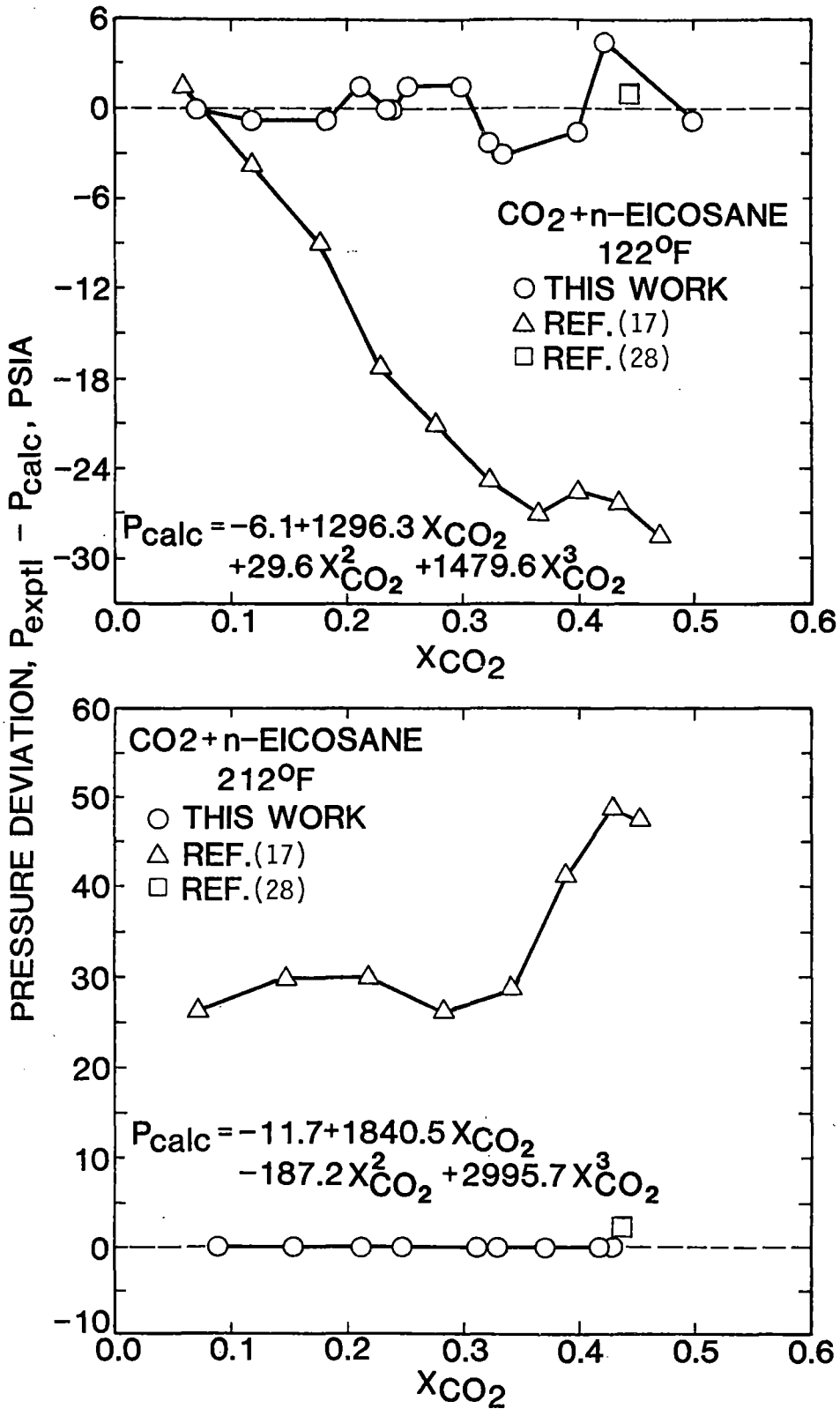

Figure 6. Comparison of Bubble Point Pressure Data for n-Eicosane System

pressures of about 4 psia. While deviations of up 20 psi are observed among the different studies, no general agreement is evident for the direction or magnitude of such deviations from the present data.

Comparison of CO_2 + benzene data obtained in this study at 104°F with those acquired by Gupta, et al. (16) indicates good agreement, among all the data reported. Agreement is excellent, in particular, with the bubble point measurements (16a). And although variations exist at CO_2 mole fraction below 0.35, the deviations observed are on the average within the combined uncertainties in the reported data.

The present data for CO_2 + n-eicosane are in substantial disagreement with those of Huie, et al. (17). Deviations shown in Figure 6 are as large as 28 psi for the 122°F isotherm. Similarly, deviations of up to 49 psi were obtained for the 212°F isotherm. Also shown in Figures 6-8 are two bubble point pressure measurements made at Amoco Production Company (28) in an effort to resolve the observed discrepancies in the n-eicosane data for which no other experimental data existed. Amoco's data for the two isotherms, along with recently acquired data by Fall and Luks (90) at 122°F, confirm the validity of the present measurements for n-eicosane system.

The combined comparisons described above were taken as confirmation of the proper operation of the present apparatus and procedures. Measurements were then performed on the heavier paraffin solvents.

Internal Consistency

Internal consistency tests are used to check the consistency of the data collected on the same apparatus at different experimental conditions. In such tests, the pressure-to-mole fraction ratio (P/x_{CO_2})

is plotted against the CO_2 mole fraction. The amount of scatter in such a plot is indicative of the precision of data analyzed, and the quality of variations of (P/x_{CO_2}) with x_{CO_2} among the different isotherms is a reflection on the accuracy of the data obtained. Figures 7 through 13 present such plots for the binary systems considered. Smoothness of the curves obtained, along with minimum scatter observed, are ample evidence of the high precision of the data obtained.

Examination of (P/x_{CO_2}) plots for the test systems discussed above included in Figures 7, 8, 12, and 13 confirm the conclusions reached earlier. As shown in Figures 7 and 8 for the n-eicosane system, equally excellent agreement exists between Amoco's data and the present work data at 122 and 212°F. In contrast, Huie's data exhibit marked deviations from the present work on both isotherms. While Huie's data indicate lower BPP's for 122°F isotherm, higher BPP's are indicated for the 212°F isotherm.

The (P/x_{CO_2}) plot for CO_2 + benzene (Figure 12) system shows general agreement among the various investigators with slight variations at CO_2 mole fractions below 0.1. Finally, the results of $(P/x_{C_2H_6})$ for ethane further demonstrate that excellent agreement exist between the present work and Lagert's over the whole composition range reported. Agreement with Lee (26) and Meskel-Lesavre (27), however, is limited to high and low mole fractions, respectively.

Krichevsky-Kasarnovsky Analysis

To this point, no particular solution model has been employed for the analysis of the data used; hence, no hidden model bias affected the

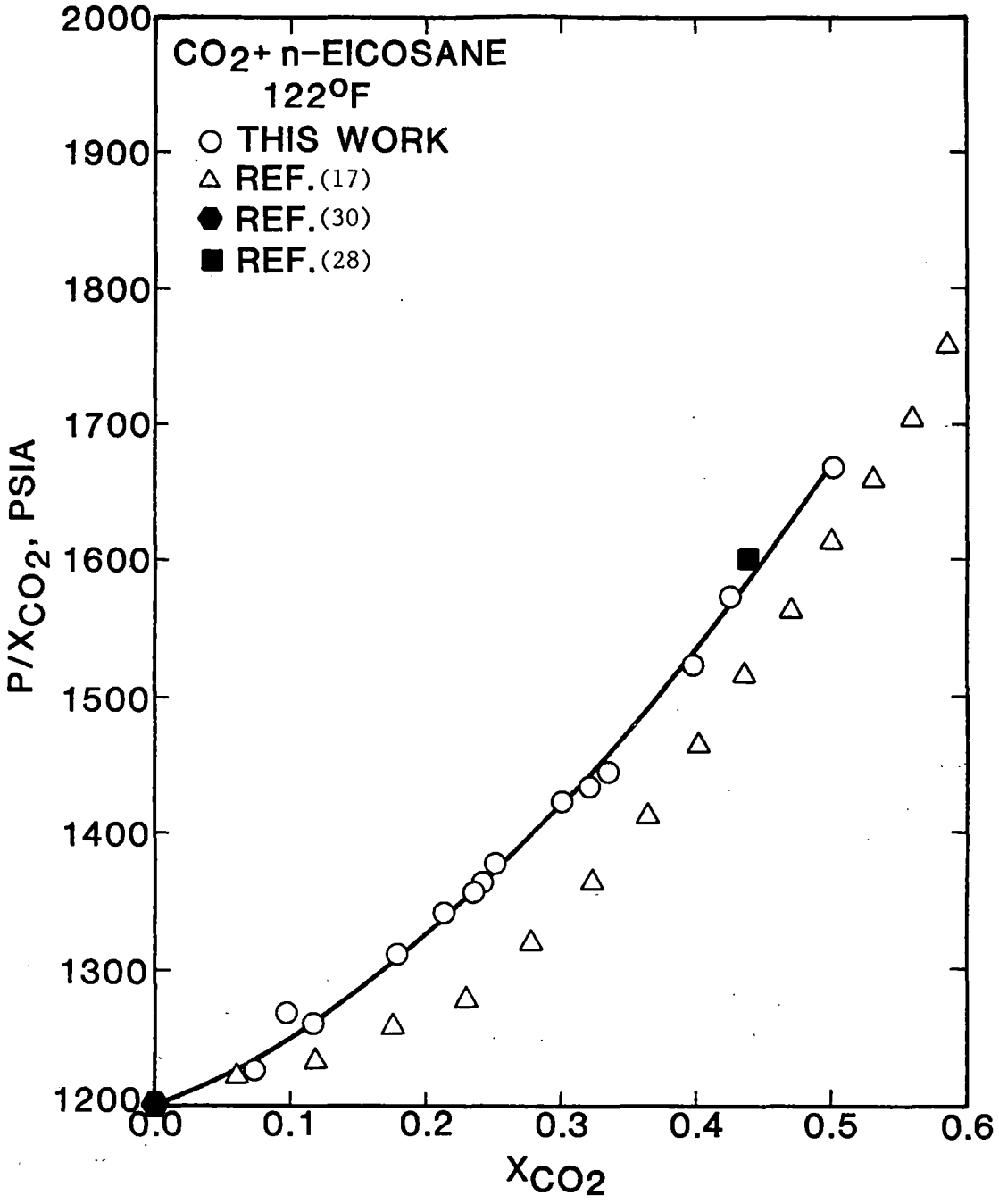

Figure 7. Comparison of Bubble Point Data for CO_2 + n-Eicosane at 122°F

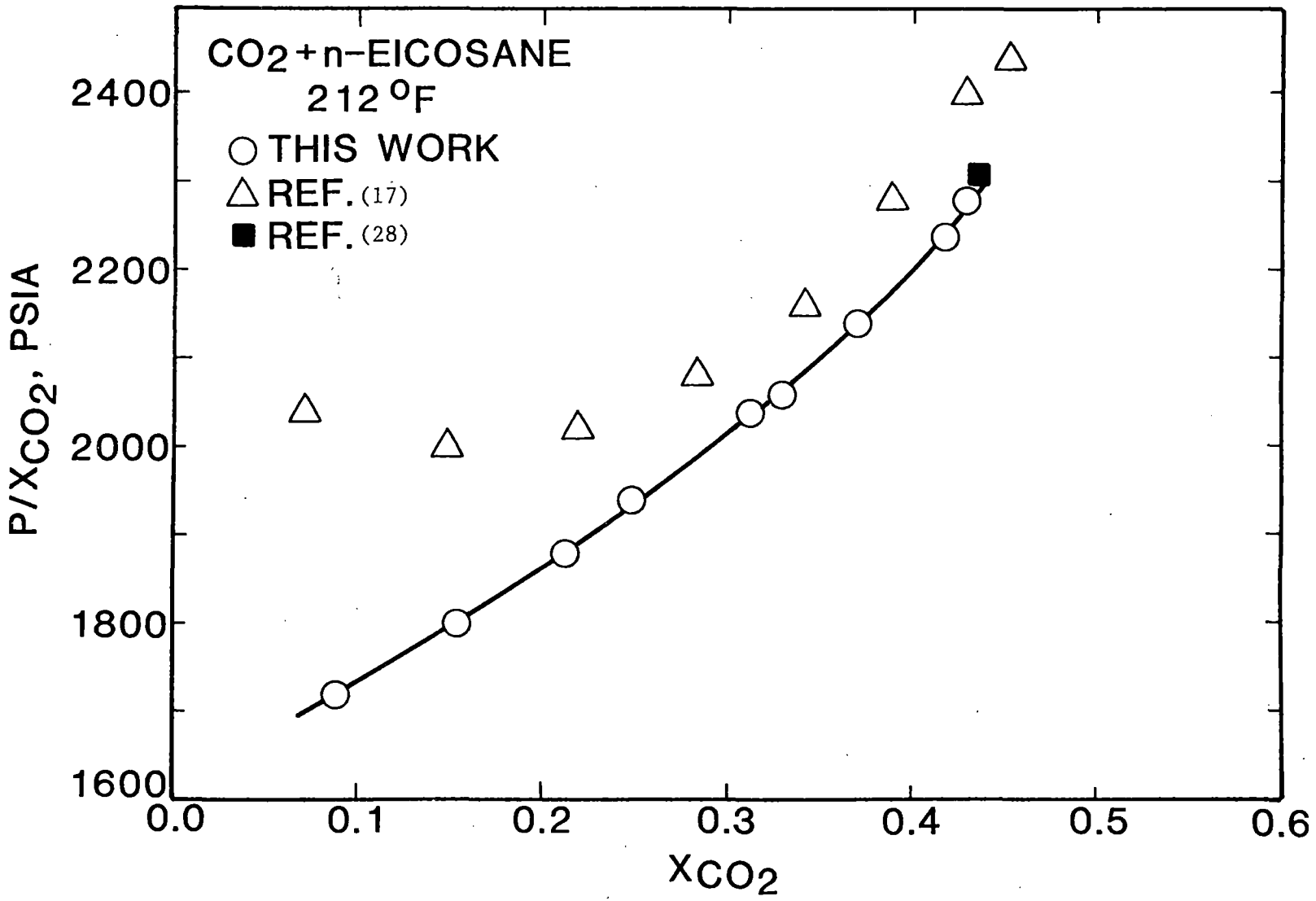

Figure 8. Comparison of Bubble Point Data for CO_2 + n-Eicosane at 212°F

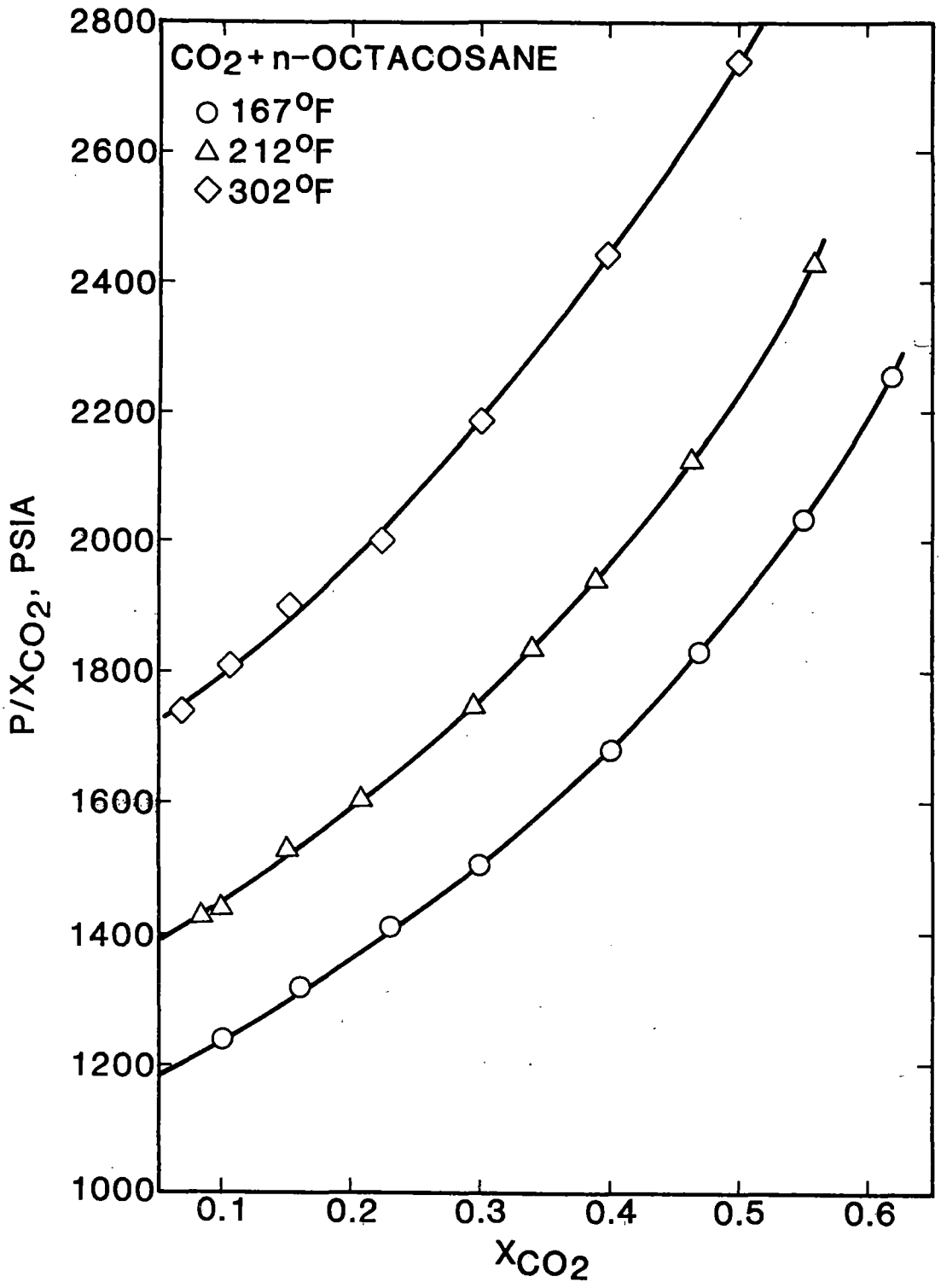

Figure 9. Bubble Point Data for CO_2 + n-Octacosane at 167°F, 212°F and 302°F

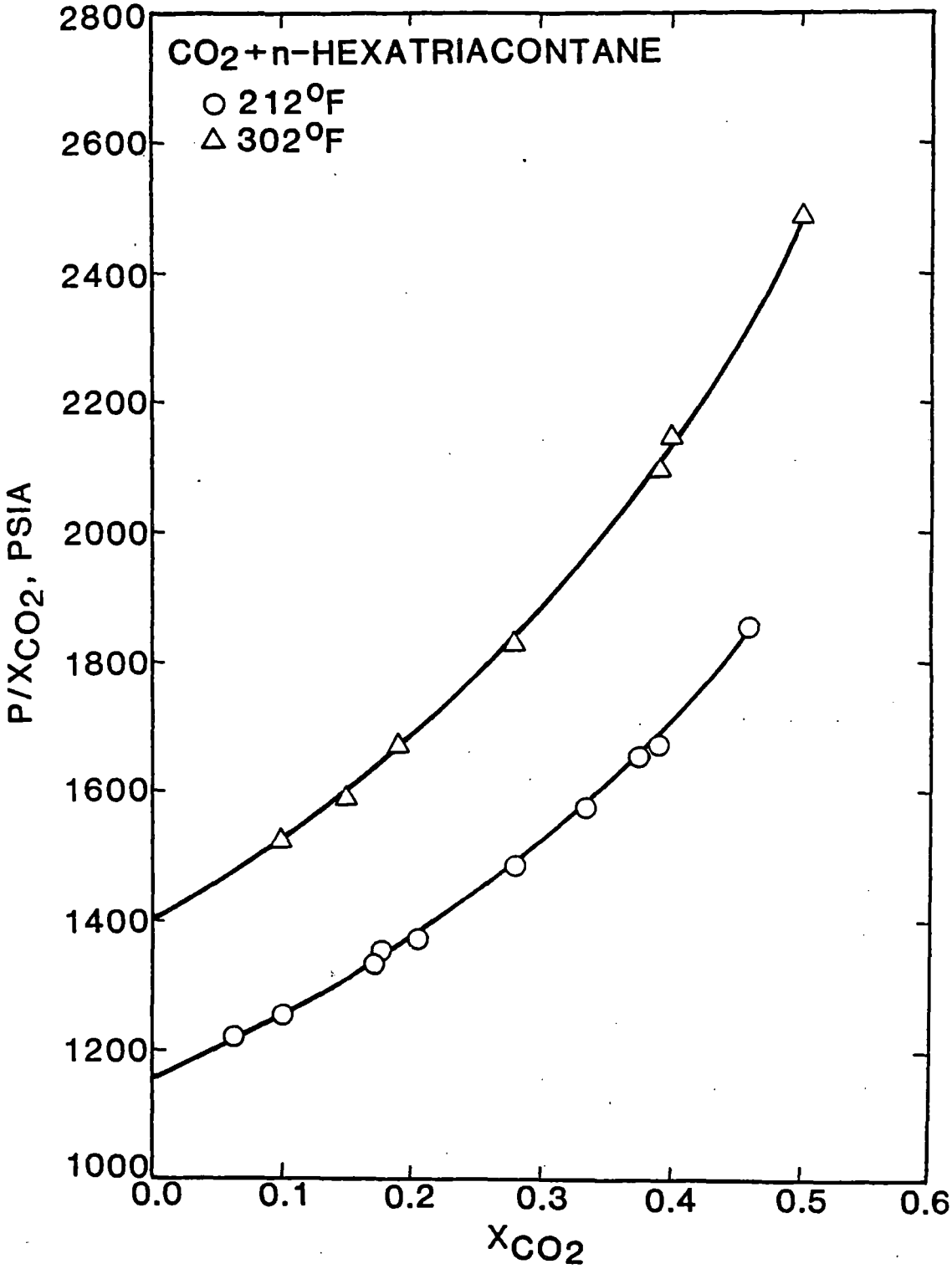

Figure 10. Bubble Point Data for CO_2 + n-Hexatriacontane at 212°F and 302°F

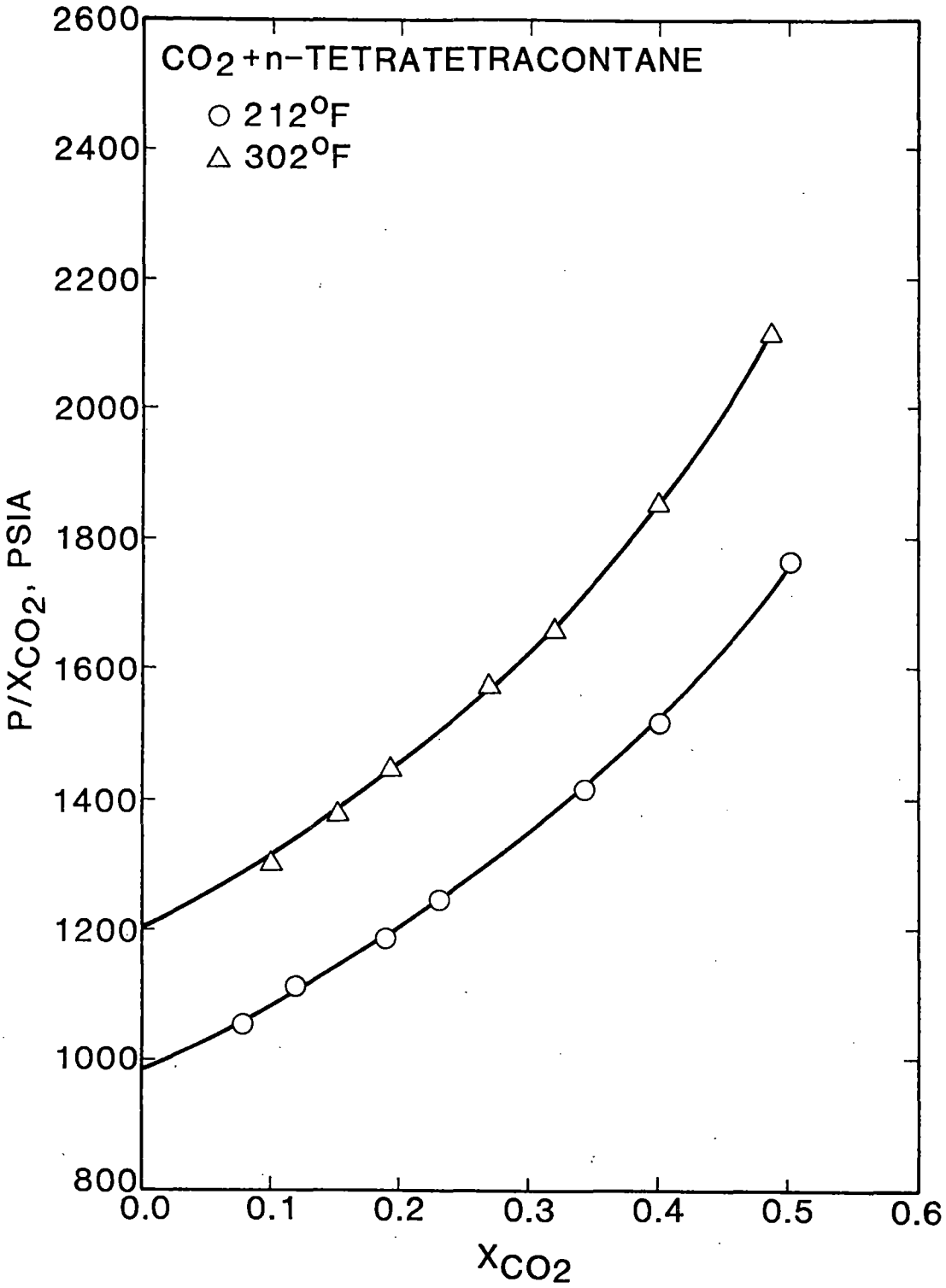

Figure 11. Bubble Point Data for CO_2 + n-Tetratetracontane at 212°F and 302°F

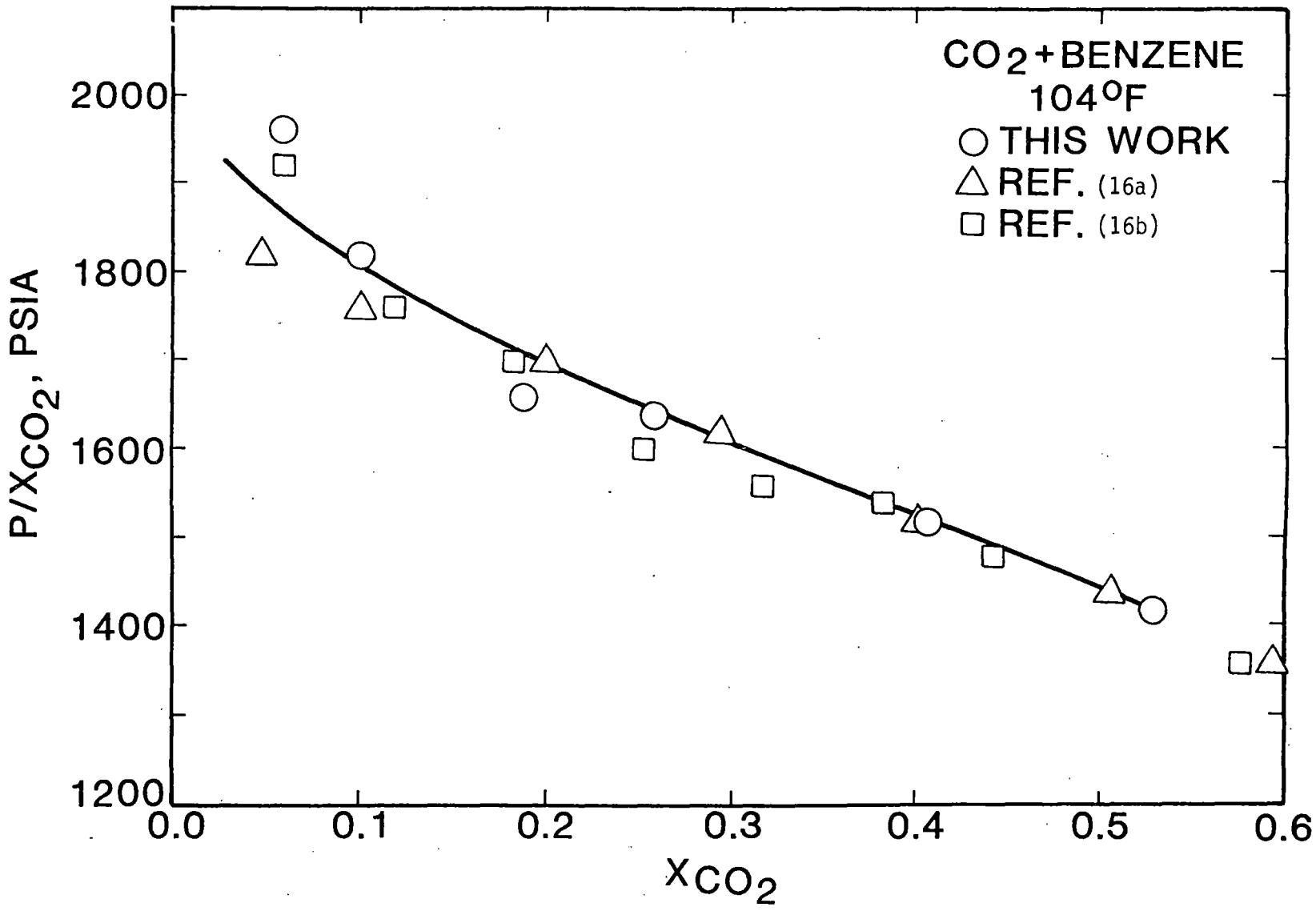

Figure 12. Comparison of Bubble Point Data for CO_2 + Benzene at 104°F

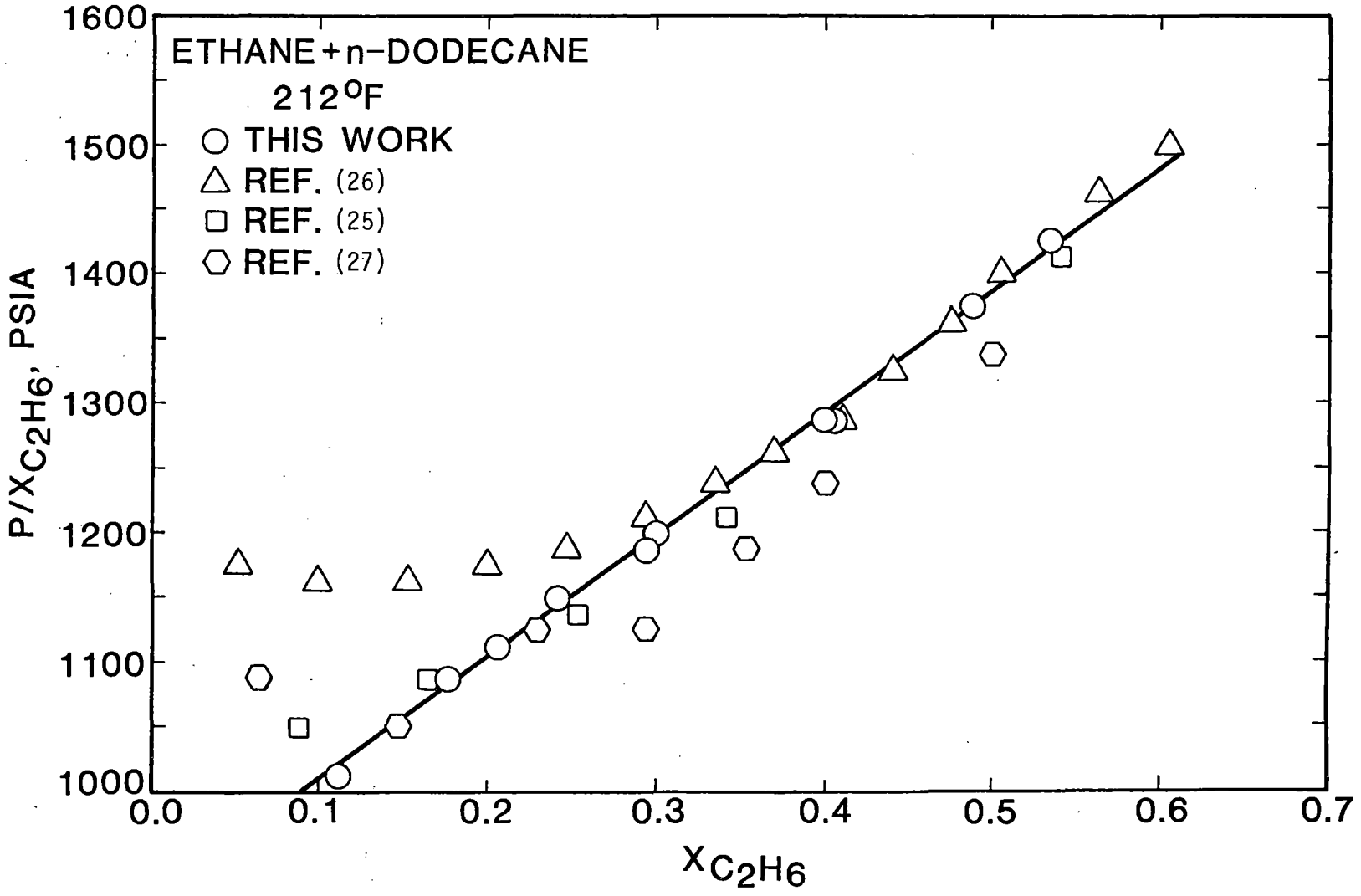

Figure 13. Comparison of Bubble Point data of Ethane + n-Dodecane at 212°F

conclusions reached. To further explore the consistency of the data, the Krichevsky-Kasarnovsky solution model analysis was applied to the data.

At mole fractions below 0.45, CO_2 solubility in normal paraffins can be represented excellently by Krichevsky-Kasarnovsky (KK) equation (29):

$$\ln (f_{CO_2}/x_{CO_2}) = \ln (H_{CO_2,HC}) + (\bar{V}^{\infty}_{CO_2}/RT)(P - P_{HC}) \qquad (6.1)$$

In Equation (6.1), the fugacity of pure CO_2 was substituted for the fugacity of CO_2 in the vapor-phase mixture since the vapor phase is essentially pure CO_2. The pure CO_2 data were taken from the literature (24). The model fits the solubility data with average deviations of less than 0.002 in CO_2 mole fraction; these deviations are less than 0.5% of the measured values of the solubility.

The experimental data were regressed according to Equation (6.1) to obtain values for Henry's constant and the infinite-dilution partial molar volume of CO_2. The resulting parameters are given in Table IX and Figures 14 and 15. The Henry's constant of 1200 psia at 323.2 K obtained for n-eicosane is in excellent agreement with the value of 1203 psia interpolated from the data of Chai, et al. (30). However, care must be exercised in attributing physical significance to the values in Table IX. Investigations using more complex models indicate that the Henry's constants in Table IX should be no more than a few percent from the true values. The reported partial volumes of CO_2, however, may be considerably less accurate.

TABLE IX

HENRY'S CONSTANT AND INFINITE-DILUTION PARTIAL MOLAR VOLUME FOR CARBON DIOXIDE IN HEAVY NORMAL PARAFFINS

Hydrocarbon Solvent	Temperature K	(°F)	Henry's Constant bar	(psia)	Partial Molar Volume cm3/g-mol	(ft3/lb-mol)
$n\text{-}C_{20}$	313.2	(122)	82.39	(1195)	47.6	(0.762)
	373.2	(212)	112.94	(1638)	79.0	(1.265)
$n\text{-}C_{28}$	348.2	(167)	81.15	(1177)	130.8	(2.096)
	373.2	(212)	93.77	(1360)	138.5	(2.219)
	423.2	(302)	115.56	(1676)	150.6	(2.412)
$n\text{-}C_{36}$	373.2	(212)	81.22	(1178)	170.2	(2.726)
	423.2	(302)	98.53	(1429)	188.7	(3.022)
$n\text{-}C_{44}$	373.2	(212)	70.60	(1024)	211.3	(3.385)
	423.2	(302)	85.22	(1236)	225.5	(3.612)

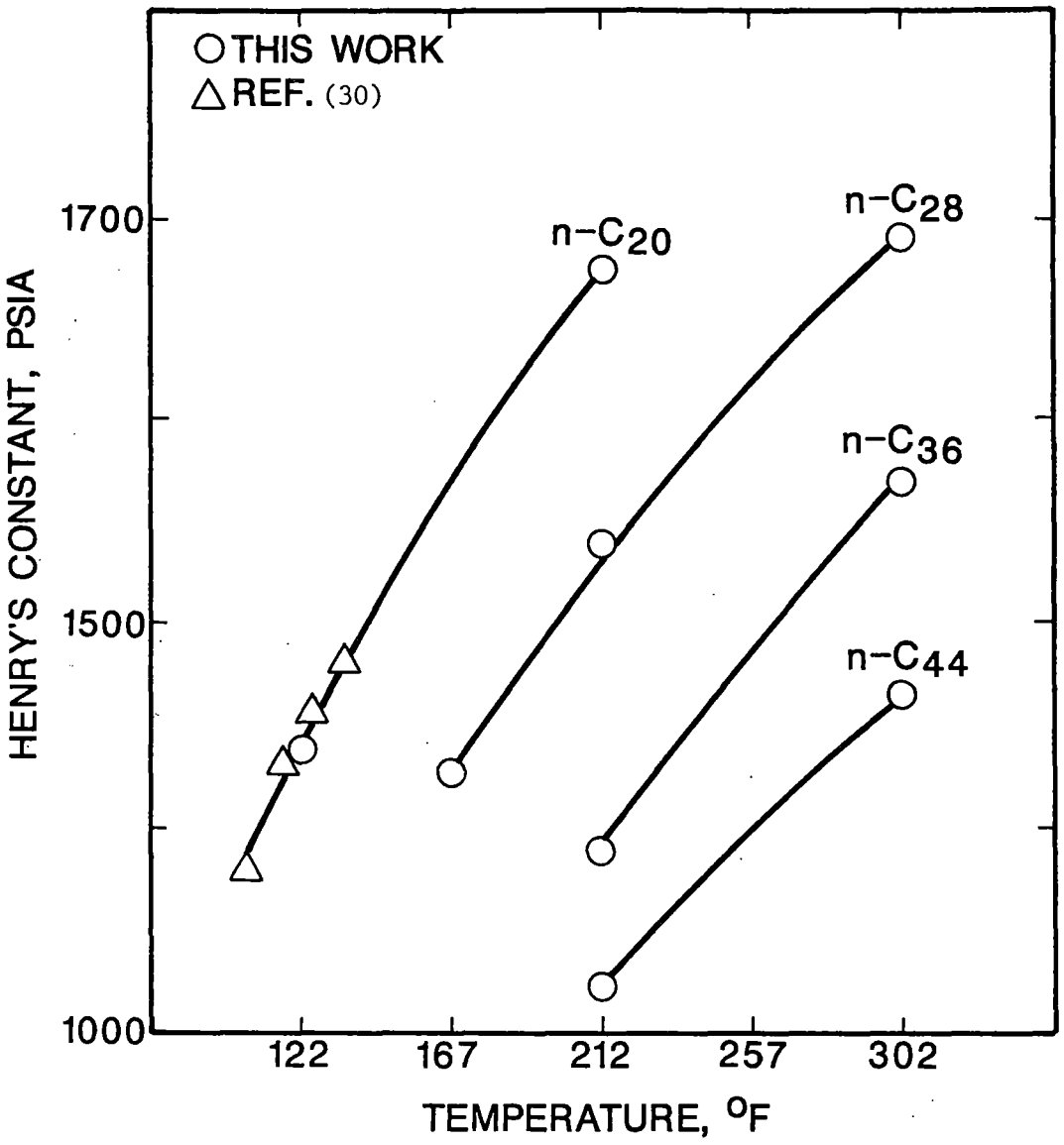

Figure 14. Henry's Constants for CO_2 + n-Paraffin Binaries

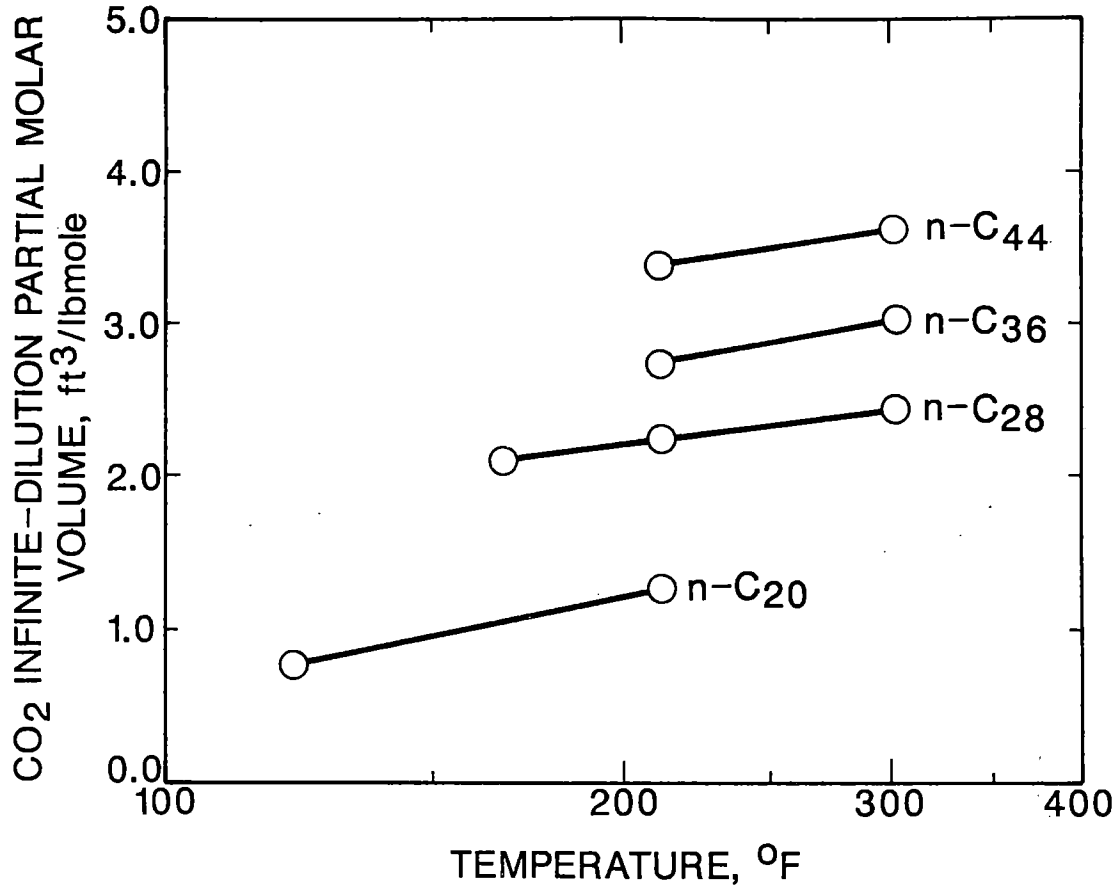

Figure 15. CO_2 Partial Molar Volumes for CO_2 + n-Parrafin Binaries

The totality of the instrumental, external and internal consistency analysis performed lead to the conclusion that the data are consistent for the systems under investigation.

Analysis of Errors in Experimental Data

In reporting experimental data, an estimate is required for the possible uncertainty in the reported experimental values. Two types of errors are normally encountered: systematic and random errors. The former are attributed to an inherent bias in the procedure used which results in a consistent deviation of the observable from its "true value". Random errors, on the other hand, are assumed to result from a large number of small disturbances about the "true value".

Random errors reflect the imprecision of the data obtained, and their random nature makes them amenable to the tools of statistical analysis. Systematic errors, however, indicate inaccuracy in the procedures used. Detection and elimination of such errors is the only measure available in this case.

Prior to discussing the uncertainty in the reported bubble point measurements, definitions are given for precision and accuracy. Precision is considered here to be the measure of reproducibility of a given observation when replicate runs are made under the same prevailing conditions for both instruments and environment. Accuracy refers to the success of obtaining the true value of a quantity. Instrument accuracy is established by comparisons with reliable and accepted standards. As shown in Appendix B, pressure gauge calibrations were made against a dead weight gauge with a certification traceable to the National

Bureau of Standards. The platinum resistance thermometer and the displacement pump calibrations were performed according to established procedures as given in Appendix B.

Three sources of variability which contribute to the uncertainty in reported bubble point pressures were accounted for in an experiment.

(1) Variability due to imprecisions in temperature, volume, and pressure measurements, which are generally called instrumental or prime errors. Repeated measurements and periodic calibrations established the magnitudes of such errors. These were found to be as follows (reported in terms of standard deviations as detailed in Appendix B):

$$\sigma_T = 0.1 \text{ K}$$

$$\sigma_V = 0.006 \text{ V}$$

$$\varepsilon_p = \begin{array}{l} 0.2 \text{ psia (300 psi gauge)} \\ 0.7 \text{ psia (1000 psi gauge)} \\ 1.6 \text{ psia (5000 psi gauge)} \end{array}$$

(2) Uncertainty in calculated variables such as the liquid mole fraction, or dependent ones such as the bubble point pressure, which are determined by error propagation. For a typical run of three CO_2 injections of 5 cc each, one hydrocarbon injection of 10 cc, and estimating the uncertainties in the densities as:

$$\sigma\rho_{CO_2} = 0.001 \, \rho_{CO_2}$$

$$\sigma\rho_{HC} = 0.003\ \rho_{HC}$$

an estimate of the uncertainty in the liquid mole fraction can be obtained as follows, based on a derivation given in Appendix B:

$$\sigma_{x_1} = \sigma_{x_2} = 0.009\ x_1 x_2 \tag{6.2}$$

The above equation leads to a maximum estimate error in the liquid mole fraction of:

$$\sigma_{x_1} = \sigma_{x_2} = 0.002$$

The uncertainty due to prime and propagated errors in the pressure measurements are given by

$$\sigma_p^2 = \varepsilon_p^2 + (\partial P/\partial x_1)_T^2\ \sigma_{x_1}^{\ 2} + (\partial P/\partial T)^2\ \sigma_T^2 \tag{6.3}$$

Assuming that the temperature contribution term is negligible and substituting for σ_x^2, the following relation is obtained:

$$\sigma_p^2 = \varepsilon_p^{\ 2} + (\partial P/\partial x_1)_T^2\ (0.009\ x_1 x_2)^2 \tag{6.4}$$

where the rate of pressure change with respect to the mole fraction $(\partial P/\partial x_1)$, is determined numerically using experimental P and x_1 values.

(3) To quantify the uncertainty attributed to the procedure used in determining the bubble point pressure, which is not measured directly, two steps were taken. First, during the course of the experiments, repeated bubble point pressure determinations were made on each of several fluid mixtures at fixed temperature and composition. This was done by repeating the pressure-volume transverse (such as those shown in Figure 3) several times for a specific mixture and comparing the pressures at which the "breaks" occurred in the plots. Variations observed in excess of those attributed to the prime errors discussed above are regarded as errors associated with the traversing/plotting procedure used.

Secondly, at different levels of temperature and pressure the test described above was repeated to reveal any correlations between these two factors and the procedural errors. The results obtained indicate such a correlation exists between the pressure level and the observed imprecision of the measured bubble point pressure. This correlation can be expressed as follows based on reproducibility data given in Table B.7:

$$\sigma_p = 0.0024\ P\ (\text{psia}) \qquad (6.5)$$

Equation (6.4) includes both the prime and the procedural error but not the propagated error due to uncertainty in the mole fraction. To account for such a contribution Equations (6.4) and (6.5) are combined

to give the expected error in the bubble point pressure as expressed by the following equation:

$$\sigma_{BPP} = [(0.0024\ P)^2 + (\partial P/\partial X_1)^2\ (0.009\ X_1 X_2)^2]^{1/2} \qquad (6.6)$$

Additional details are given in Appendix B.

CHAPTER VII

DATA REDUCTION

This chapter addresses the problem of estimating the ℓ parameters of a nonlinear model from n experiments were n exceeds ℓ. For each experiment, there are r measured (or functions of measured) variables, Z_i^m . These are assumed to contain random experimental errors or:

$$Z_i^m = Z_i + e_i \tag{7.1}$$

where Z_i signifies the variable "true value".

A relation (more normally called a constraint) presumably exists which express the functionality among the "true values" of the variables of interest such that:

$$F(Z_i, \Theta) = 0 \tag{7.2}$$

where Θ is a vector of ℓ unknown parameters (31). Then upon substitution of the experimentally observed values Z_i into Equation (7.2), the residual, due to the disagreement between experimental and values, can be defined as:

$$\varepsilon_i = F(Z_i^m, \Theta) \tag{7.3}$$

Having such a disagreement, along with the fact that the number of constraint equations n exceeds the number of parameters ℓ, an exact solution for Equation (7.2) is not possible in terms of Z_i. Consequently, an optimality criterion is needed to establish estimates for both the parameters and the measured variables, and to quantify a measure of confidence in the estimates obtained.

Assuming that the errors involved are random in nature and small in magnitude, the principle of maximum likelihood, MLH, as advanced by Fisher (32), provides a powerful probablistic basis for the deriviation of an optimality criterion. In essence, the principle defines the optimum parameters as those for which the likelihood of obtaining the observed set of experimental data as a whole is maximum.

Undertaking a framework as such is done in pursuit of attaining the statistically "best" estimates for the model parameters. This is in contrast to curve fitting the data which leads in most cases to suboptimization, a situation in which the parameter estimates obtained fail to reasonably predict variables other than those fitted (32,33).

No attempt is made here to review the details of the MLH approach to data reduction; the reader is referred to numerous publications on the subject (35-37). However, most of the commonly used optimality criteria (objective functions) in data reduction stem from this approach. This includes variations of unweighed and weighed least squares regressions.

Under the assumptions that the variables of interest, dependent and independent, are subject to small random errors and that the experimental measurements of such variables are independent, then the likelihood for obtaining a given measurement is proportional to the

probability of its occurrence (38,39). Furthermore, the likelihood for r measurements (response factors) in a given experiment is the joint probability of their occurrence as a set or:

$$L(Z_i^m, Z_i, \theta) = g(Z_i^m, Z_i) \tag{7.4}$$

where $g(Z_i^m, Z_i)$ represents the joint probability density for all measured variables. Accordingly, the likelihood of all measurements taken as a whole is the product of the joint probability density functions of n experiments:

$$L(Z_i^m, Z_i, \theta) = \prod_1^n g(Z_i^m, Z_i) \tag{7.5}$$

To obtain MLH estimates for Z_i and θ, the likelihood function, L, is maximized, or equivalently the logarithm of the reciprocal is minimized as follows (39):

$$\text{minimize } S = \sum_i^n \ln (1/g (Z_i^m, Z_i, \theta)) \tag{7.6}$$

thus, obtaining the general form for the MLH optimality criterion, where no distinction is made between dependent and independent variables and all are assumed to contain random errors.

As indicated by Equation (7.6) the application of the MLH method requires that a form be specified for the probability density function. If the errors ε_i are assumed to be normally distributed, then

the expected value for the error and the variance-covariance matrix are given by:

$$E(\varepsilon) = 0$$

$$E(\varepsilon\varepsilon^t) = \sigma$$

Then the joint probability function for the measurements vector Z is demonstrably as follows (31):

$$g(Z_i^m, Z_i) = \frac{1}{(2)^{(1/2r)} |\sigma_i|^{1/2}} \exp \{-1/2\ \varepsilon^t \sigma_i^{-1} \varepsilon\} \qquad (7.7)$$

Thus, by substituting the above definition into Equation (7.6) the optimality criterion becomes:

$$\text{minimize: } S = \sum_{i=1}^{n} 1/2\ (\varepsilon^t \sigma^{-1} \varepsilon + \ln |\sigma| + n/r \ln (2\pi)) \qquad (7.8)$$

subject to the constraints of Equation (7.2). Now, if the vector of r observations in the i^{th} experiment has the variance-covariance matrix σ_i then for a given experiment

$$\varepsilon_i^t \sigma_i^{-1} \varepsilon_i = \sum_{j=1}^{r} \sum_{k=1}^{r} \sigma^{jk} \varepsilon_j \varepsilon_k \qquad (7.9)$$

and the further assumation is made the term $\ln|\sigma|$ is constant (39), the general MLH criterion reduces to:

$$\text{minimize: } S = \sum_{i=1}^{n} \sum_{j=1}^{r} \sum_{k=1}^{r} \sigma_i^{jk} \varepsilon_{ij} \varepsilon_{ik} \tag{7.10}$$

subject to the constraints of Equation (7.2).

Using the above equation, a weighted least square regression (WLSR) criterion can be obtained by assuming negligible covariance ($\sigma^{jk} = 0$ if $j \neq k$) or:

$$\text{minimize } S = \sum_{i=1}^{n} \sum_{j=1}^{r} \sigma_i^{jj} \varepsilon_{ij}^2 \tag{7.11}$$

Furthermore, setting σ_i^{jj} to a value of 1.0, the least squares regression (LSR) criterion is obtained as:

$$\text{minimize } S = \sum_{i=1}^{n} \sum_{j=1}^{r} \varepsilon_{ij}^2 \tag{7.12}$$

Vapor-Liquid Equilibrium Data Reduction

Data reductions for binary VLE experimental data have generated considerable attention in recent years. This is especially so when dealing with proper selection or development of optimality criterion (13,31,36,37,55). A number of proposed methods have been suggested, depending on whether the study is dealing with a complete information

set where all measurable variables (T, P, x, y) are available, or dealing with subsets such as (T, P, x) or (T, P, y).

Inspection of such methods reveals a common trend of emphasis on proper assessment of weighing factors as required by Equation (7.10), or the elements of the variance-covariance matrix in a more general sense. Several studies have concluded that in most cases unweighed regression as signified by Equation (7.11), leads to different values for the estimated model parameters depending on the variable minimized in a given subset (34). In contrast, proper weighing produces the same parameter estimates using a given information subset regardless of which variable residuals are minimized.

The Optimality Criterion

For a binary vapor-liquid system at equilibrium, the measured properties (temperature T, pressure P, the liquid-phase mole fraction x, and the vapor-phase mole fraction y) represent the full set of information regarding the data reduction.

Applying Equation (7.10), where assumptions of negligible covariance between the different measured variable in a (T, P, x) information subset the following criterion is obtained:

$$\text{minimize: } S = \sum_{i=1}^{n} \left[\frac{(P_i - P_i^m)^2}{\sigma_{iP}^2} + \frac{(T_i - T_i^m)^2}{\sigma_{iT}^2} + \frac{(x_i - x_i^m)^2}{\sigma_{ix}^2} \right] \quad (7.13)$$

The decision to pursue an experimental design where the vapor-phase mole fraction measurements are not made is based on the fact that such measurements constitute only a redundancy (13), since a (T, P, x) data subset is sufficient to establish accurately the solution model parameters. Measurements of the vapor-phase composition, when allowed for, may be used for internal consistency calculations.

Returning to Equation (7.13), and assuming that the contributions for all terms, relative to that of the pressure residual, are small, along with the fact that lack-of-fit in the model exceeds (in some cases) the magnitude of the random experimental errors, the equation can be reduced to:

$$\text{minimize: } S = \sum_{i=1}^{n} \frac{(P_i^m - P_i)^2}{\sigma_{iP}^2} \tag{7.15}$$

where

$$\sigma_{iP}^2 = \varepsilon_{iP}^2 + (\partial P/\partial x)_i^2 \, \sigma_{x_i}^2 \tag{7.16}$$

The evaluation of σ_{iP}^2 above is in accordance with Equation (7.13) where an assumption of negligible covariance is used, along with discounting the effect temperature uncertainty on the pressure variance.

Reflecting on the steps taken to derive the optimality criterion as given by Equations (7.10) and (7.11), clearly, while the deriviation started with the most general formulation under the MLH framework where all variables are assumed subject to error, due to the assumptions made regarding data and model, the criterion obtained is that of effective variance-weighted least squares regression.

Constraint Equations

As mentioned earlier for a binary VLE system, the full information set is given by (T, P, x, y). However, according to the Gibbs phase rule, Equation (2.6), only two variables must be specified to completely describe the system. This leads to having two independent variables (e.g., T, x) and two dependent ones (e.g., P, y). The functional relationship between these variables as described by the thermodynamic framework, Equations (2.4) and (2.5), represents the constraint equations in the data reduction procedure. The terms dependent and independent are used here only in constraint formulation, rather than in optimality criterion derivation where all variables are assumed subject to error.

Specifically, selecting T and x_1 as the independent variables, the constraint equations can be written as:

$$\log (x_1K_1 + x_2K_2) = 0 \tag{7.17}$$

and

$$y_1 = K_1x_1/(K_1x_1 + K_2x_2) \tag{7.18}$$

where by definition:

$$K_i = \hat{\Phi}_i^L / \hat{\Phi}_i^V$$

and

$$\sum_{i=1}^{i=N} x_i = 1.0$$

These constraints are equivalent to equations suggested by Anderson (31) using a two model approach in which:

$$P = x_1 \gamma_i f_1^0 / \Phi_1^V + x_2 \gamma_2 f_2^0 / \Phi_2^V \tag{7.19}$$

and

$$y_1 = \frac{1}{1 + (x_2 \gamma_2 f_2^0 \Phi^V{}_1 / x_1 \gamma_1 f_1^0 \Phi_2^V} \tag{7.20}$$

Data reduction based on total pressure as expressed by Equation (7.19) is first attributed to Barker (41).

Implementation

The steps in numerical implementation of any data reduction algorithm, once a theoretical framework has been selected, are highly

dependent on the optimality criterion used. The degree of complexity of such a criterion is (as shown earlier) a product of the assumptions made and the extent of the simplifications undertaken (31,35,42,43).

Parallel to the development of the criteria represented by Equations (7.10), (7.11) and (7.12) for the MLH, WLSR, and LSR approaches, respectively, algorithms have been advanced, each taking advantage of the problem structure at hand. For the general case represented by Equation (7.10), most numerical implementations involve (1) linearization of the constraints, Equation (2.2), using Taylor series expansion; (2) adjoining the objective function, Equation (7.10), to the linearized constraints by introducing extraneous parameters such as Lagrange multipliers (31,43), thus transforming the problem into the domain of unconstrained optimization; (3) selection of a numerical routine to solve simultaneously for ℓ unknown parameters Θ and nm variable estimates Z. The storage requirements and the computational efficiency ascribed to these algorithms differ with the linearization and the transformation steps taken (35,43).

In application of the WLSR algorithms, in contrast, estimates for the parameters and the variables are obtained sequentially in two separate steps. First estimates are made for the unknown parameters, aiming to satisfy the criterion given by Equation (7.11). Then a separate convergence routine is used to satisfy the constraint equations in order to obtain estimates for the measured variables Z^m. The sequence is repeated until an overall convergence is achieved by satisfying both the optimality criterion and the constraints.

For the purposes of this study WLSR procedure along the lines described above is used for experimental data reduction as will be discussed in Chapter IX.

CHAPTER VIII

PROPERTY PREDICTIONS FOR PURE NORMAL PARAFFINS

Pure substance physical properties (such as the critical constants, acentric factor, vapor pressure and liquid density) constitute an essential element in most models for correlating phase behavior of pure fluids and mixtures alike. The literature contains ample experimental data for the critical constants of n-paraffins up to n-C_8, limited data for n-paraffins up to n-C_{17}, and practically no experimental measurements for n-C_{18} and heavier molecules (44,45). The experimental difficulties, coupled with inadequate theoretical models for the predictions of the needed properties, make empirical and semi-empirical correlations a necessity. Numerous correlations for the properties of interest have been advanced (44,46,47,48,49). However, representation of the properties at higher carbon numbers is often inadequate.

Properties investigated here include: the normal boiling point T_b, the critical temperature T_c, the critical pressure P_c, and the acentric factor ω. In addition, efforts in this study were extended to provide generalized correlations for structure dependent input data for selected saturated liquid density models. No attempt, however, was made to discuss the details of previous works cited or tested (such a discussion can be found elsewhere as given by appropriate references), rather comparisons are given for the results obtained from correlations which showed reasonable promise.

Proposed Correlation

The equation proposed here for correlating the structure dependent properties of pure n-paraffins is:

$$Y = \left[\frac{C_1}{C_4} - \left(\frac{C_1}{C_4} - C_3^{1-C_2}\right) \exp\left(- C_4 (CN - 1)(1-C_2)\right)\right]^{\frac{1}{1-C_2}} \qquad (8.1)$$

where

Y = Pure Physical Property

C_1 = Correlation Constant

C_2 = Scaling coefficient

C_3 = Property value at initial scaling variable (e.g., P_c for CN=1) where $Y_0 = C_3$

C_4 = Growth rate

Y^∞ = Property value at infinite scaling variable , where

$$Y^\infty = \left(\frac{C_1}{C_4}\right)^{\frac{1}{1-C_2}}$$

CN = Carbon number of n-paraffin

The above expressions are widely used in botany and animal science in growth studies (50-51). Application of such a correlation as expressed

by Equation (8.1) is intuitive, but is guided by the following observations:

(1) The rate of change in given property with respect to the correlation variable (e.g. the carbon number) is a function of the property value.

(2) There exists a limiting value for a given property, reached asymptotically as the correlating variable tends to infinity.

The correlation as expressed by Equation (8.1), which will be referred to as asymptotic behavior correlation (ABC), has considerable flexibility and is capable of reproducing a variety of curvatures, including exponential and sigmoid. This correlating procedure requires knowledge of initial property value ($Y=Y_0$) and infinite property value ($Y=Y_\infty$), to allow proper graduation or scaling between such values. Unfortunately, while the former is available by selecting the correlation coordinate as (Carbon Number-1), values for the latter are non-existent except for a semi-empirical estimate for T_b^∞ (52). Thus, the missing constants are treated as regressed parameters with the hope that lower carbon number data would project reasonable values for such parameters.

Careful testing of the fitting capabilities of ABC for several properties has revealed its high fidelity in representing the available experimental data. Acceptance of the estimates obtained for a given property are based on reasonable agreement with established relationships among a set of properties, when available, and/or the quality of predictions attained using an acceptable behavior model (such SRK EOS for vapor pressure predictions) employing such estimates.

Choice of the carbon number as the correlation coordinate for structure dependent property is natural when dealing with n-paraffin. Extension to other classes of compounds using this approach would, however, require a definition for the effective carbon number. Using the molecular weight, as suggested by some authors (53), produced comparable results for the properties tested since CN and the molecular weight are linearly related for n-paraffins.

Pure n-Paraffin Data Source

Basic data for n-paraffins up to n-C_{17} including T_b, T_c, P_c, V_c and ω used for correlating purposes were taken from the TRAPP Data Library of the National Bureau of Standards (54). For saturated liquid density data Table XVII contains the list of references for the experimental data used.

Results

Table X presents the summary of the results obtained for the different properties using the ABC correlation. Absolute average percent deviations (%AAD) of 0.04, 0.08, 0.38, 0.59, and 0.68 were obtained for T_b, T_c, P_c, V_c and ω respectively. This represents a significant improvement over several popular correlations, such as those advanced by Lydersen (49), Kesler and coworkers (46), or the more recent one proposed by Chao (53). Following is an account of the results obtained for each property considered.

TABLE X

SUMMARY OF RESULTS FOR PURE n-PARAFFINS PROPERTY PREDICTIONS

	Physical Property										
	T_b, K			T_c, K				P_c, bar			
	ABC	ZOW	CHA	ABC*	LYD	L-K	CHA	ABC	LYD	L-K	CHA
Ref No		52	53		49	46	53		49	46	53
No Pt	17	17	17	16	17	14	17	16	16	14	16
Excld**	--	--	--	C_2	--	C_1-C_3	--	C_1	C_1	C_1-C_3	C_1
RMSE	0.21	1.89	0.72	0.52	4.57	3.52	1.16	0.13	0.49	0.86	0.41
BIAS	0.16	0.19	-0.33	0.43	-3.07	-2.49	-0.14	-.003	-0.11	-0.79	0.19
AAD	0.16	0.71	0.54	0.43	3.52	2.72	1.00	0.10	0.41	0.78	0.31
%AAD	0.04	0.50	0.15	0.08	0.62	0.42	0.19	0.38	1.85	3.70	1.30
ABC constants:											
C_1	0.31391E04			0.36173E-1				0.91316E01			
C_2	-0.76229E00			0.47775E00				0.99371E00			
C_3	0.11163E03			0.58524E00				0.55280E02			
C_4	0.16693E-1			0.43358E-1				0.90409E01			

*Correlated as T_b/T_c.
**Not included in regression or statistics.

TABLE X (continued)

	Physical Property								
	V_c, cc/gmol				ω				SG
	ABC	LYD	RED	CHA	ABC	PIT	L-K	CHA	ABC
Ref No		49	47	53		47	46	53	
No Pt	16	17	17	16	15	15	17	16	17
Excld*	C_1	--	--	C_2	C_1-C_2	C_1-C_3	C_1	C_1	--
RMSE	5.15	12.2	39.9	12.3	0.0040	0.0065	0.0017	0.0096	0.0041
BIAS	0.39	-8.71	19.5	3.01	0.0005	0.0006	0.0007	0.0036	-0.0015
AAD	3.61	10.01	23.2	7.43	0.0003	0.0053	0.0014	0.0079	0.0033
%AAD	0.59	1.87	3.06	1.08	0.68	1.79	0.39	1.67	0.45
ABC constants:									
C_1	0.36056E02				0.36056E02				0.83629E-1
C_2	0.93988E-1				0.99371E00				-0.82383E00
C_3	0.91516E02				0.91516E02				0.24681E00
C_4	0.14756E-1				0.14756E-1				0.13088E00

*Not included in regression or statistics.

Normal Boiling Point Predictions

The importance of the normal boiling point, T_b, lies in its utility as a correlating parameter for other essential fluid properties. Efforts to correlate T_b, however, are not as extensive as those for the critical properties since by definition T_b can be calculated using a reliable vapor pressure equation. Lack of experimental vapor pressure data for paraffins beyond n-C_{28} created a need for a viable correlating procedure.

Comparison of the T_b predictions obtained using the ABC correlation to experimental measurements as given in Table XI and to those determined by methods considered in Table X indicate the superiority of the ABC procedure for lower CN. More significantly in dealing with heavy paraffins is the extrapolation quality of the tested correlation. Figure 16 contains predictions for n-paraffins up to n-C_{100}; reasonable agreement between the ABC predictions and those of the Zwolinski method is evident. Poor T_b predictions obtained using Chao's correlation at high CN is not surprising, since this method is recommended for CN below n-C_{30}.

Applying the the ABC correlation a value of 990 K was obtained for as an estimate for the limiting value of T_b, T_b^{∞}. This is in reasonable agreement with Zwolinski's (52) estimate of 1078 K. Forcing a value of 1078 K for T_b^{∞} when using the ABC correlation resulted in worsened predictions for the lower carbon numbers.

Critical Temperature Predictions

A review of predictive methods for critical properties by Spencer and Daubert (49) concluded that the Lydersen group contribution and the

TABLE XI

NORMAL BOILING POINT PREDICTION
USING ASYMPTOTIC BEHAVIOR CORRELATION

DATA	CARBON NUMBER	TB(K) EXPTL	TB(K) CALC	DEV	%DEV
1	1	111.63	111.63	-0.00	-0.00
2	3*	231.05	230.47	-0.58	-0.25
3	4	272.65	272.69	0.04	0.01
4	5	309.21	309.37	0.16	0.05
5	6	341.88	342.05	0.18	0.05
6	7	371.58	371.66	0.08	0.02
7	8	398.82	398.78	-0.04	-0.01
8	9	423.97	423.83	-0.14	-0.03
9	10	447.30	447.11	-0.19	-0.04
10	11	469.08	468.87	-0.21	-0.04
11	12	489.47	489.29	-0.18	-0.04
12	13	508.62	508.51	-0.12	-0.02
13	14	526.73	526.65	-0.08	-0.01
14	15	543.87	543.83	-0.04	-0.01
15	16	560.01	560.12	0.11	0.02
16	17	575.20	575.60	0.40	0.07

MODEL OVERALL STATISTICS

PAR(1).. PAR(N)= 0.313914D 04 -0.762291D 00 0.111630D 03
0.166931D-01

RMSE = 0.2133 K		NO PT =	16
AAD = 0.1590 K		%AAD =	0.043
MIN DEV= -0.5793 K		MIN %DEV =	-0.251
MAX DEV= 0.3995 K		MAX %DEV =	0.069
BIAS = -0.0392 K		C-VAR =	0.001
RESTRICTIONS :	NONE	R-SQR	=0.999309
AUX. MODELS :	0000000000 / 0000000000	EXP REF =	

*n-C_2 is not included in parameter regression

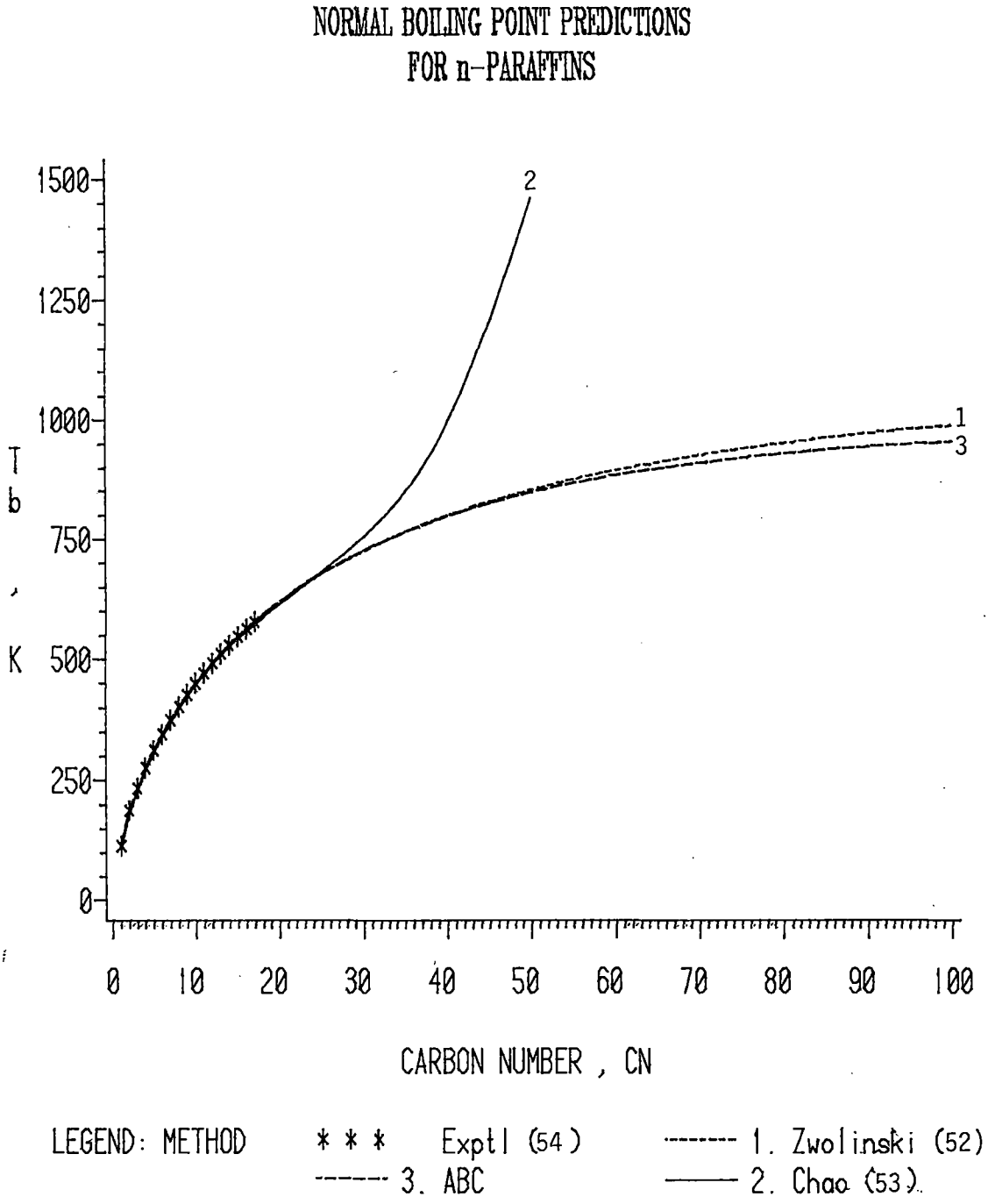

Figure 16. Normal Boiling Point Predictions for n-Paraffins

Nokay correlation with revised constants gave best results for n-paraffins. Comparison of the ABC predictions to those of the Lydersen method indicates a considerable improvement using the ABC correlation as signified by an AAD of 0.08% compared to 0.62% for Lydersen's method. Application of the Lee-Kesler correlation (46) results in similar precision to that obtained by Lydersen's method, thus leading to inferior predictions to those obtained by the present method as indicated by the results of Table X.

While correlating T_c in terms of the carbon number gave excellent results for the fitted data, extrapolated T_c values obtained at higher carbon numbers were rather low in comparison to T_b. To obviate this problem (T_b/T_c) ratio was correlated in preference to T_c leading to improved extrapolations and simultaneously retaining good quality predictions for lower CN, as shown in Table XII. A need for such a recourse is dictated by the lack of information in the T_c data used to produce proper projections at higher CN. Comparison of T_c estimates at higher CN using the different methods indicate that values obtained from the ABC correlation fall intermediate to those obtained from the other methods, as shown by Figure 17.

The Lee-Kesler correlation requires specific gravity at 60°F (SG) as a correlating variable. To extend the use of this correlation to heavy n-paraffins (which are solid at 60°F) estimates for SG were obtained using the ABC correlation employing the lower CN data. Obviously, the application of SG for solids is not within the nature of SG definition. However, viewing SG as merely a correlating variable allowed for estimates to be made as given in Table XIII.

TABLE XII

CRITICAL TEMPERATURE PREDICTION
USING ASYMPTOTIC BEHAVIOR CORRELATION

DATA	CARBON NUMBER	TC(K) EXPTL	TC(K) CALC	DEV	%DEV
1	1	190.55	190.74	0.19	0.10
2	2	305.33	304.66	-0.67	-0.22
3	3	369.82	369.86	0.04	0.01
4	4	425.16	424.55	-0.61	-0.14
5	5	469.75	469.61	-0.14	-0.03
6	6	507.89	507.63	-0.26	-0.05
7	7	540.14	540.51	0.37	0.07
8	8	568.82	569.39	0.57	0.10
9	9	594.56	595.04	0.48	0.08
10	10	617.55	618.04	0.49	0.08
11	11	638.74	638.89	0.16	0.02
12	12	658.25	657.93	-0.32	-0.05
13	13	676.15	675.42	-0.73	-0.11
14	14	692.95	691.68	-1.27	-0.18
15	15	706.75	706.85	0.10	0.01
16	16	720.55	720.91	0.36	0.05
17	17	733.35	733.95	0.60	0.08

MODEL OVERALL STATISTICS

PAR(1).. PAR(N)= 0.361753D-01 -0.477753D 00 0.585240D 00
0.433584D-01*

RMSE = 0.5216 K		NO PT =	17
AAD = 0.4319 K		%AAD =	0.082
MIN DEV= -1.2652 K		MIN %DEV =	-0.219
MAX DEV= 0.5991 K		MAX %DEV =	0.100
BIAS = -0.0382 K		C-VAR =	0.001

RESTRICTIONS : NONE R-SQR =0.999258
AUX. MODELS : 0000000000 / 0000000000 EXP REF =

*Correlation Constants reported here are for T_b/T_c ratio

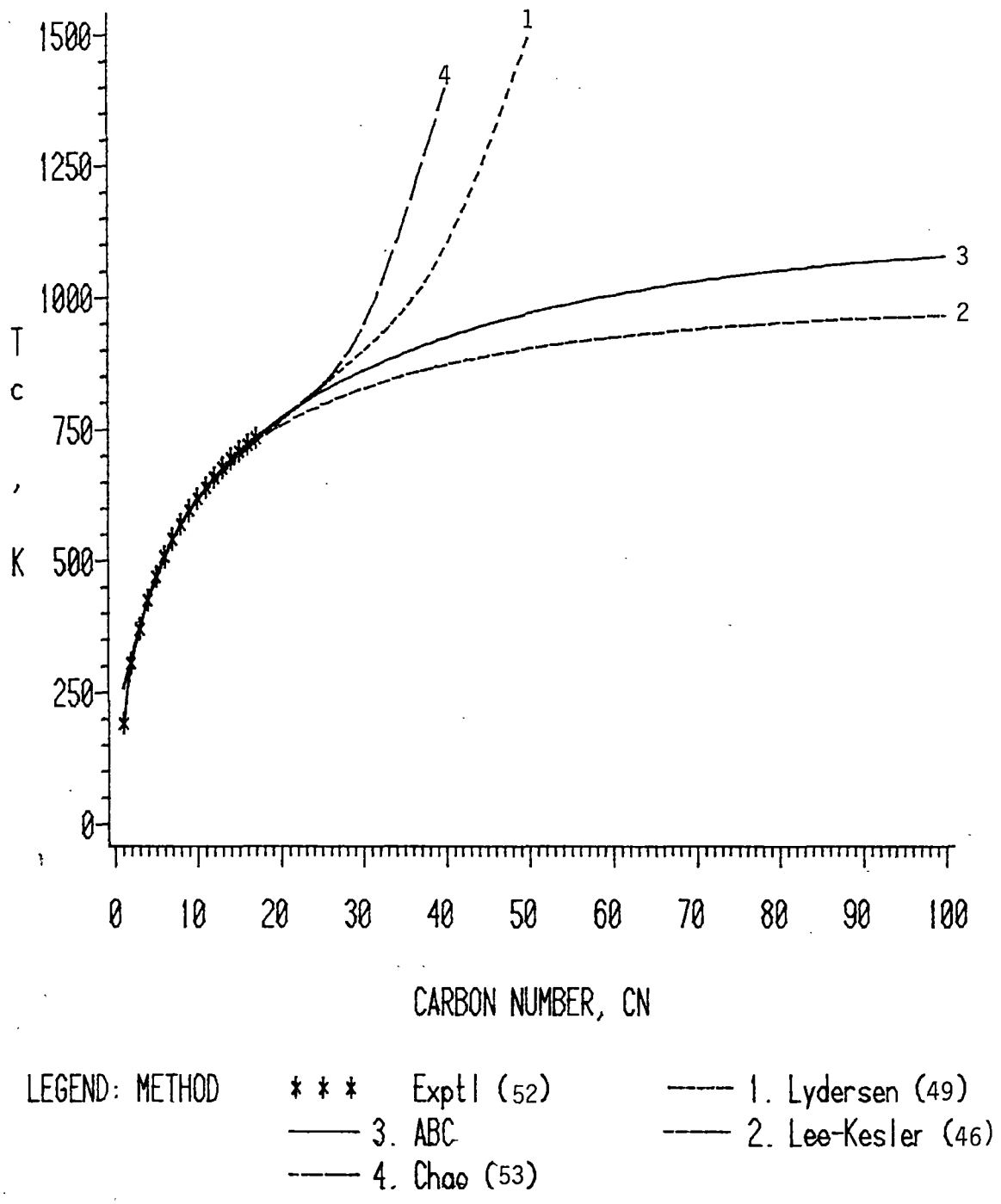

Figure 17. Critical Temperatures Predictions for n-Paraffins

TABLE XIII

SPECIFIC GRAVITY (60/60) PREDICTION
USING ASYMPTOTIC BEHAVIOR CORRELATION

CARBON NUMBER		SG(60/60) EXPTL	SG(60/60) CALC	DEV.	%DEV
1	1	0.2470	0.2468	-0.0002	-0.08
2	2	0.4100	0.4104	0.0004	0.11
3	3	0.5077	0.5081	0.0004	0.09
4	4	0.5844	0.5753	-0.0091	-1.56
5	5	0.6310	0.6239	-0.0071	-1.12
6	6	0.6640	0.6602	-0.0038	-0.58
7	7	0.6882	0.6876	-0.0006	-0.09
8	8	0.7068	0.7085	0.0017	0.25
9	9	0.7217	0.7247	0.0030	0.42
10	10	0.7342	0.7372	0.0030	0.41
11	11	0.7443	0.7470	0.0027	0.36
12	12	0.7526	0.7546	0.0020	0.26
13	13	0.7601	0.7605	0.0004	0.06
14	14	0.7667	0.7652	-0.0015	-0.20
15	15	0.7721	0.7688	-0.0033	-0.42
16	16	0.7773	0.7717	-0.0056	-0.72
17	17	0.7817	0.7739	-0.0078	-0.99

MODEL OVERALL STATISTICS

PAR(1).. PAR(N)= 0.836289D-01 -0.823825D 00 0.246807D 00
0.130883D 00

RMSE	= 0.0041	NO PT	= 17
AAD	= 0.0031	%AAD	= 0.454
MIN DEV=	-0.0091	MIN %DEV	= -1.558
MAX DEV=	0.0030	MAX %DEV	= 0.417
BIAS	= -0.0015	C-VAR	= 0.006

RESTRICTIONS : NONE R-SQR =0.998665
AUX. MODELS : 0000000000 / 0000000000 EXP REF =

Critical Pressure Predictions

Measured values of the critical pressures, P_c, are generally accepted as having lower accuracy than measured values of T_c (51). Hence several investigators (55) treat P_c as an adjustable parameter in vapor pressure equations. ABC predictions for P_c, given in Table XIV, reflect this tendency as indicated by an AAD of 0.38% in comparison to 0.08 % for T_c. This degree of precision, however, is excellent when compared to that obtained with the recommended approach of Lydersen, or similarly the Lee-Kesler method shown in Table X.

Efforts to obtain reasonable extrapolation for P_c at higher CN were guided by values of P_c estimated using the Antoine vapor pressure equation at the critical temperature. Justification in employing this procedure is based on the observation that the Antoine equation fitted using data below T_c always underpredicts the true critical by about 7%.

Inspection of Figure 18 indicates that P_c values obtained at high CN using the ABC correlation tend to be higher than those predicted by the Lee-Kesler method.

Critical Volume Predictions

Previous assessments of critical volume estimations (49) have deemed the Lydersen method most reliable when T_c and P_c are not available. By comparison, the Reidel equation was found to be more accurate when such properties are known for the compounds of interest. Evaluation of the ABC predictions along with those of the above mentioned methods reveals that a better representation of the available experimental data was obtained by the former, as indicated by Tables XV and X. Figure 19 depicts the variation in the value of V_c estimates as

TABLE XIV

CRITICAL PRESSURE PREDICTION
USING ASYMPTOTIC BEHAVIOR CORRELATION

DATA	CARBON NUMBER	PC(BAR) EXPTL	PC(BAR) CALC	DEV	%DEV
1	2	48.71	48.38	-0.33	-0.68
2	3	42.47	42.66	0.19	0.44
3	4	37.96	37.87	-0.10	-0.25
4	5	33.76	33.83	0.07	0.21
5	6	30.28	30.42	0.14	0.45
6	7	27.35	27.50	0.15	0.55
7	8	24.98	25.01	0.03	0.13
8	9	22.88	22.86	-0.02	-0.07
9	10	20.97	21.00	0.03	0.14
10	11	19.38	19.38	-0.01	-0.04
11	12	18.06	17.96	-0.11	-0.59
12	13	16.83	16.72	-0.12	-0.68
13	14	15.73	15.62	-0.11	-0.71
14	15	14.65	14.65	-0.00	-0.01
15	16	13.76	13.79	0.03	0.24
16	17	12.92	13.02	0.10	0.81

MODEL OVERALL STATISTICS

PAR(1).. PAR(N)= 0.913158D 01 0.993706D 00 0.552796D 02
0.904089D 01

RMSE = 0.1252 BAR NO PT = 16
AAD = 0.0955 BAR %AAD = 0.375
MIN DEV= -0.3314 BAR MIN %DEV = -0.709
MAX DEV= 0.1858 BAR MAX %DEV = 0.809
BIAS = -0.0029 BAR C-VAR = 0.005

RESTRICTIONS : NONE R-SQR =0.996658
AUX. MODELS : 0000000000 / 0000000000 EXP REF =

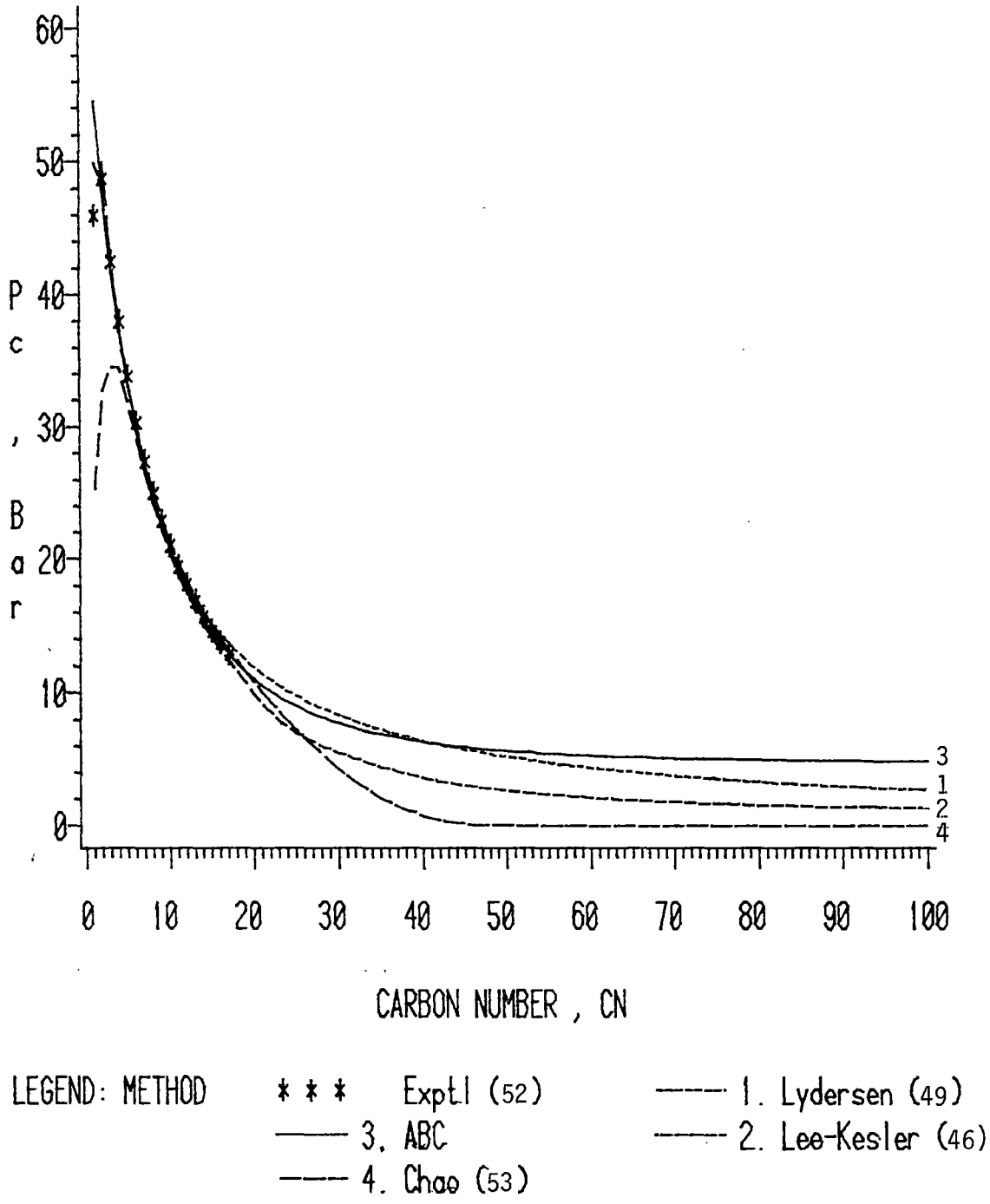

Figure 18. Critical Pressure Predictions for n-Paraffins

TABLE XV

CRITICAL VOLUME PREDICTION
USING ASYMPTOTIC BEHAVIOR CORRELATION

DATA	CARBON NUMBER	VC(CC/MOL) EXPTL	VC(CC/MOL) CALC	DEV	%DEV
1	2	147.06	146.21	-0.85	-0.58
2	3	201.61	202.18	0.57	0.28
3	4	256.41	258.89	2.48	0.97
4	5	313.60	316.02	2.42	0.77
5	6	373.22	373.37	0.15	0.04
6	7	431.97	430.78	-1.19	-0.28
7	8	490.00	488.15	-1.85	-0.38
8	9	548.90	545.38	-3.52	-0.64
9	10	607.53	602.42	-5.11	-0.84
10	11	665.00	659.19	-5.81	-0.87
11	12	719.70	715.68	-4.02	-0.56
12	13	775.20	771.82	-3.38	-0.44
13	14	827.13	827.60	0.47	0.06
14	15	880.28	882.98	2.70	0.31
15	16	930.23	937.96	7.73	0.83
16	17	977.00	992.50	15.50	1.59

MODEL OVERALL STATISTICS

PAR(1).. PAR(N)= 0.360560D 02 0.939880D-01 0.915160D 02
0.147560D-01

RMSE = 5.1551 CC/MOL		NO PT =	16
AAD = 3.6090 CC/MOL		%AAD =	0.589
MIN DEV= -5.8054 CC/MOL		MIN %DEV =	-0.873
MAX DEV= 15.4984 CC/MOL		MAX %DEV =	1.586
BIAS = 0.3916 CC/MOL		C-VAR =	0.009
RESTRICTIONS :	NONE	R-SQR	=0.986566
AUX. MODELS :	0000000000 / 0000000000	EXP REF =	

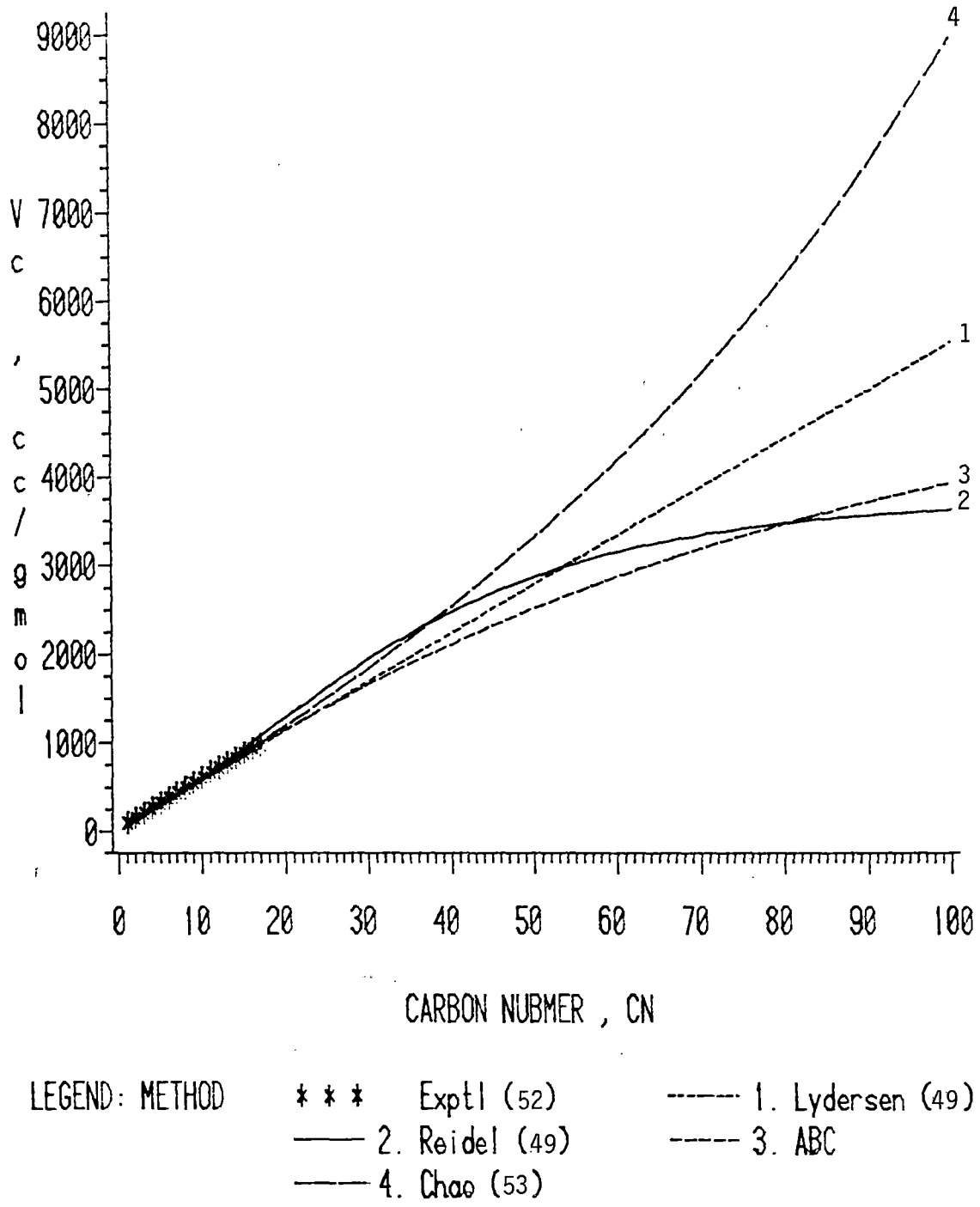

Figure 19. Critical Volume Predictions for n-Paraffins

given by the different methods, where difference in estimates of up to 100% are observed.

Acentric Factor Predictions

The acentric factor, ω, defined by Pitzer (48) as:

$$\omega = -\log P_r \text{ (at } T_r = 0.7) - 1.0 \qquad (8.2)$$

is one of the more increasingly used pure fluid constants. Introduced as a measure of acentricity (nonsphericity) of molecules, it is commonly used to account for deviation of the intermolecular potential of a given fluid from that of simple fluid, or the interaction between the various parts of a complex molecule.

As indicated by Equation (8.2), calculation of values for ω require vapor pressure measurements at $T_r = 0.7$ as well as T_c and P_c. Similarly, correlations proposed by Lee-Kesler and Edmister (49) require T_b, T_c, and P_c. Results of application of the ABC procedure using only the CN as correlating variable are given in Table XVI along with a summary of statistics for the other methods considered. As indicated by the above mentioned results, the Lee-Kesler correlation gives slightly better predictions, if not comparable ones, for the lower CN. However, for higher carbon numbers the superiority of the ABC Correlation predictions is rather obvious considering both the Lee-Kesler and Chao equations.

Evaluation of the higher CN estimates of ω using the ABC procedure to those obtained using the Pitzer definition, as shown in Figure 20 employing values for T_c and P_c determined by the ABC correlation signify

TABLE XVI

ACENTRIC FACTOR PREDICTION
USING ASYMPTOTIC BEHAVIOR CORRELATION

DATA	CARBON NUMBER	W EXPTL	W CALC	DEV	%DEV
1	3	0.1542	0.1526	-0.0016	-1.05
2	4	0.2004	0.2016	0.0012	0.61
3	5	0.2511	0.2506	-0.0005	-0.21
4	6	0.2978	0.2991	0.0013	0.45
5	7	0.3499	0.3470	-0.0029	-0.84
6	8	0.3995	0.3940	-0.0055	-1.38
7	9	0.4451	0.4401	-0.0049	-1.11
8	10	0.4885	0.4852	-0.0033	-0.68
9	11	0.5301	0.5291	-0.0010	-0.19
10	12	0.5708	0.5720	0.0012	0.21
11	13	0.6096	0.6137	0.0041	0.68
12	14	0.6442	0.6543	0.0101	1.57
13	15	0.6918	0.6937	0.0019	0.28
14	16	0.7311	0.7320	0.0009	0.13
15	17	0.7623	0.7691	0.0068	0.89

MODEL OVERALL STATISTICS

PAR(1).. PAR(N)= 0.736969D-01 0.148801D 00 0.570769D-01
0.446205D-01

RMSE =	0.0041	NO PT =	15
AAD =	0.0032	%AAD =	0.684
MIN DEV=	-0.0055	MIN %DEV =	-1.381
MAX DEV=	0.0101	MAX %DEV =	1.574
BIAS =	0.0005	C-VAR =	0.009

RESTRICTIONS : NONE R-SQR =0.978100
AUX. MODELS : 0000000000 / 0000000000 EXP REF =

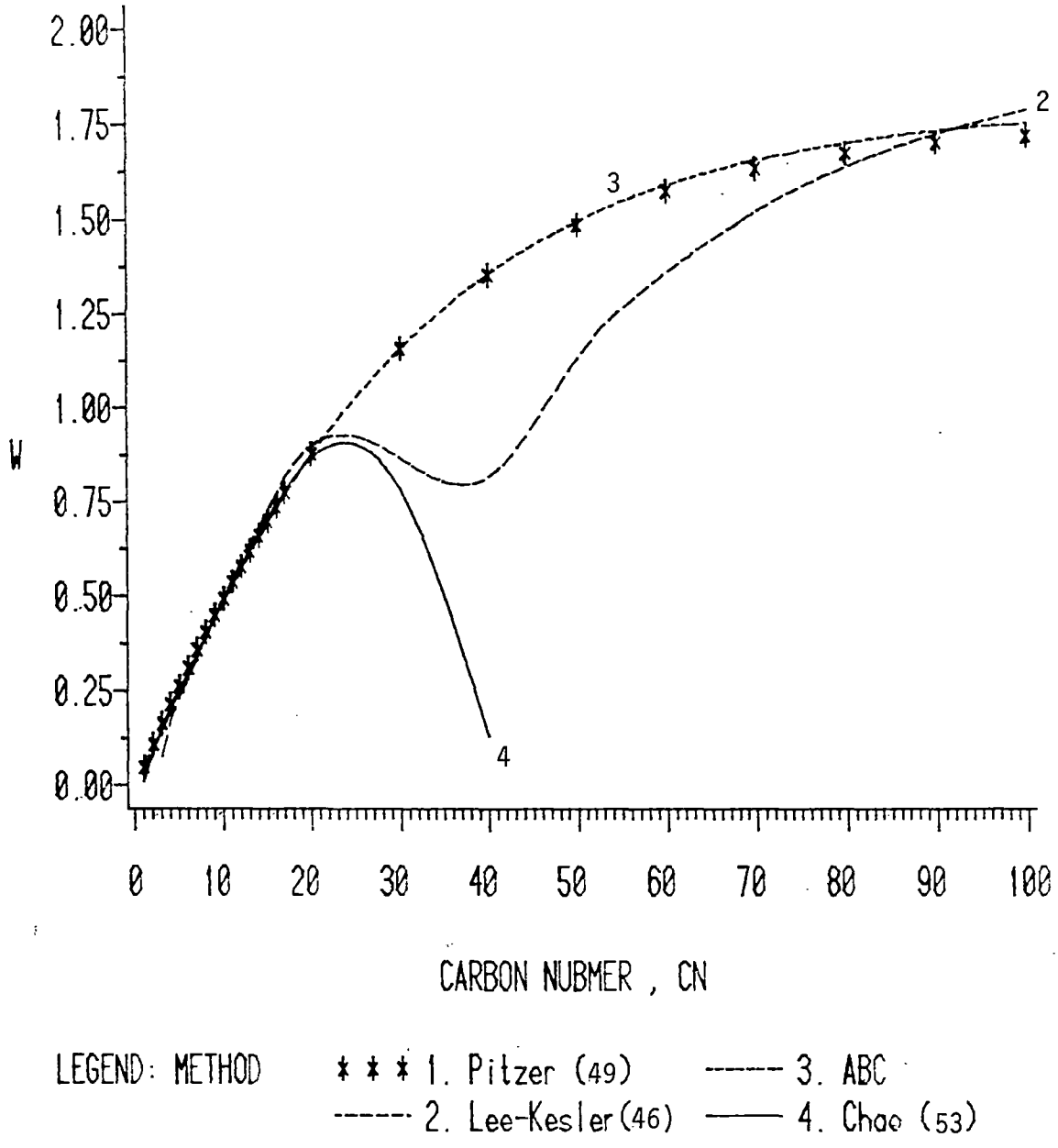

Figure 20. Acentric Factor Predictions for n-Paraffins

an excellent degree of internal consistency among T_c, P_c and the vapor pressure equation used.

Saturated Liquid Density Predictions

As was mentioned earlier efforts here are directed toward the development of generalized correlations for structure dependent input data for selected predictive models. Table XVII presents the summary of results of using the modified Rackett equation (56) for the prediction of pure n-paraffin liquid density. Input values for the correlation variable needed for this equation, ZRA, were generalized using the ABC correlation as given in Table XVIII. Similarly, a generalized correlation is provided for the prediction of the characteristic volume employed by the Hankinson-Thomson equation (57). The constants given in Table XVIII for the characteristic volume were determined using the actual acentric factor rather than the SRK EOS acentric factor proposed by the original authors.

As indicated by the results of Tables XVII and XVIII, better density predictions are obtained for n-paraffins using the modified Rackett equation, especially for the lower carbon numbers. Ignoring results obtained for n-C_{44} and n-C_{64} an overall %AAD of 0.27 and 0.51 was obtained form the two equations respectively. Such results reflect a comparable precision to that of observed by individual parameter regressions for each substance. However, for the purposes of parameter regressions, the results of which are given in Tables XVII-XVIII, density data for n-C_{44} and n-C_{64} were not included so as to avoid worsened overall predictions.

TABLE XVII

SATURATED LIQUID DENSITY PREDICTION
USING RACKETT EQUATION

I	CN	REF	TRMIN	TRMAX	RMSE	BIAS	AAD	%AAD	NO PT
1	3	92	0.626	0.975	0.91	0.17	0.67	0.13	4
2	4	92	0.643	0.831	4.39	-3.90	3.90	0.71	3
3	5	92	0.658	0.936	1.23	-0.06	1.03	0.19	4
4	6	92	0.673	0.935	1.56	0.25	1.34	0.25	4
5	7	92	0.685	0.962	2.28	1.51	1.51	0.28	4
6	8	92	0.700	0.975	2.06	0.77	1.72	0.38	4
7	9	63	0.493	0.711	2.00	1.80	1.80	0.26	4
8	10	63	0.523	0.685	1.17	0.83	1.01	0.15	3
9	11	63	0.506	0.663	0.65	0.29	0.63	0.09	3
10	12	63	0.491	0.643	0.45	-0.29	0.29	0.04	3
11	13	63	0.479	0.627	0.79	-0.77	0.77	0.11	3
12	14	63	0.467	0.612	1.14	-1.10	1.10	0.15	3
13	15	63	0.457	0.599	1.30	-1.20	1.20	0.17	3
14	16	63	0.448	0.587	1.26	-1.09	1.09	0.15	3
15	17	63	0.440	0.576	1.07	-0.66	0.82	0.11	3
16	20	63	0.419	0.549	2.57	2.31	2.31	0.32	3
17	22	63	0.408	0.471	5.32	4.97	4.97	0.66	2
18	28	63	0.382	0.501	5.08	-4.44	4.44	0.58	3
19	30	63	0.434	0.492	6.61	-6.40	6.40	0.86	2
20	32	63	0.398	0.426	11.95	-11.89	11.89	1.54	2
21	36	63	0.470	0.525	1.62	-0.84	1.38	0.19	2
22	40	63	0.458	0.458	7.71	7.71	7.71	1.04	1
23	44	63	0.395	0.448	20.53	20.40	20.40	2.69	2*
24	64	63	0.367	0.465	157.43	157.43	157.43	20.79	3*

MODEL OVERALL STATISTICS

PAR(1).. PAR(N)= 0.506728D-04 -0.285000D 01 0.285932D 00
0.227043D-01

RMSE	= 32.7053 KG/M3	NO PT	= 71
AAD	= 9.2258 KG/M3	%AAD	= 1.254
MIN DEV	=-13.0074 KG/M3	MIN %DEV	= -1.670
MAX DEV	=158.4926 KG/M3	MAX %DEV	= 21.762
BIAS	= 6.7626 KG/M3	C-VAR	= 0.050

RESTRICTIONS : NONE R-SQR =0.827862
AUX. MODELS : 3333300000 / 1111100000 EXP REF =

*Not included in regression

TABLE XVIII

SATURATED LIQUID DENSITY PREDICTION
USING HANKINSON AND THOMSON MODEL

I	CN	REF	TRMIN	TRMAX	RMSE	BIAS	AAD	%AAD	NO PT
1	3	92	0.626	0.975	5.04	-5.01	5.01	1.09	4
2	4	92	0.643	0.831	2.80	-2.03	2.35	0.43	3
3	5	92	0.658	0.936	3.85	3.72	3.72	0.70	4
4	6	92	0.673	0.935	4.17	4.03	4.03	0.75	4
5	7	92	0.685	0.962	5.04	4.82	4.82	0.96	4
6	8	92	0.700	0.975	4.56	3.65	3.65	0.83	4
7	9	63	0.493	0.711	2.71	2.49	2.49	0.36	4
8	10	63	0.523	0.685	1.24	0.77	1.05	0.15	3
9	11	63	0.506	0.663	0.91	-0.19	0.78	0.12	3
10	12	63	0.491	0.643	1.31	-1.05	1.05	0.16	3
11	13	63	0.479	0.627	1.86	-1.73	1.73	0.25	3
12	14	63	0.467	0.612	2.33	-2.27	2.27	0.33	3
13	15	63	0.457	0.599	2.67	-2.62	2.62	0.37	3
14	16	63	0.448	0.587	2.90	-2.86	2.86	0.40	3
15	17	63	0.440	0.576	2.95	-2.92	2.92	0.41	3
16	20	63	0.419	0.549	2.55	-2.48	2.48	0.34	3
17	22	63	0.408	0.471	1.54	-1.43	1.43	0.19	2
18	28	63	0.382	0.501	2.67	2.34	2.34	0.30	3
19	30	63	0.434	0.492	3.21	3.09	3.09	0.41	2
20	32	63	0.398	0.426	4.65	4.63	4.63	0.60	2
21	36	63	0.470	0.525	4.62	4.37	4.37	0.60	2
22	40	63	0.458	0.458	7.19	7.19	7.19	0.97	1
23	44	63	0.395	0.448	8.63	8.54	8.54	1.12	2
24	64	63	0.367	0.465	3.15	-1.68	2.71	0.36	3

MODEL OVERALL STATISTICS

PAR(1).. PAR(N)= 0.751894D-01 0.247215D 00 0.106977D 00
0.100000D-09

RMSE =	3.6817 KG/M3	NO PT =	71
AAD =	3.1216 KG/M3	%AAD =	0.514
MIN DEV=	-6.0132 KG/M3	MIN %DEV =	-1.334
MAX DEV=	9.7869 KG/M3	MAX %DEV =	2.215
BIAS =	0.7077 KG/M3	C-VAR =	0.006

RESTRICTIONS : NONE R-SQR =0.997204
AUX. MODELS : 3333300000 / 1111100000 EXP REF =

A less popular equation for liquid density prediction is that of Meisner (58). In contrast to the Rackett correlation (56) this equation gives excellent predictions for the higher CN paraffins and poor predictions for octane and lighter paraffins. Table XIX contains a summary of results for this method where %AAD within 0.15 are observed CN > 8.

Discussion

As indicated by the above mentioned results, a significant improvement is realized in the quality of the pure property predictions using the ABC correlation. Omission of some light members of the homologous series (methane or ethane) to improve the quality of fit should not be viewed as detrimental in assessing the potential of the ABC procedure. Trials to account for CH_2 and CH_3 group contributions eliminated this shortcoming. Simplicity in using CN as a correlating variable however was favored.

Elimination of multiple input data, which are required by most of the existing predictive methods, is an added advantage of this proposed unified correlating framework. Also, lack of multiple data input is a significant factor when the effects of input data error propagation on the prediction quality are considered.

To further test the soundness of property estimates obtained at higher carbon numbers, vapor pressure predictions were made employing SRK EOS along with the ABC pure paraffin property estimates. Table XXIV contains the SRK vapor pressure predictions at $T = T_b$ and $T = 0.7\ T_r$. %AAD of 1% and a maximum deviation of 2% for n-C_{44} is indictive of the viability of the T_b, T_c, P_c and ω values used. Contrasting the quality

TABLE XIX

SATURATED LIQUID DENSITY PREDICTION
USING MEISNER CORRELATION

I	CN	REF	TRMIN	TRMAX	RMSE	BIAS	AAD	%AAD	NO PT
1	3	92	0.626	0.975	37.14	22.90	23.44	6.41	4
2	4	92	0.643	0.831	5.02	-2.04	4.70	0.84	3
3	5	92	0.658	0.936	22.76	13.11	13.73	3.13	4
4	6	92	0.673	0.935	23.10	14.23	14.51	3.23	4
5	7	92	0.685	0.962	36.15	22.35	22.35	5.34	4
6	8	92	0.700	0.975	46.33	27.65	27.81	7.09	4
7	9	63	0.493	0.711	0.81	0.03	0.72	0.11	4
8	10	63	0.523	0.685	0.91	-0.40	0.87	0.13	3
9	11	63	0.506	0.663	0.87	-0.16	0.78	0.12	3
10	12	63	0.491	0.643	0.80	0.05	0.69	0.10	3
11	13	63	0.479	0.627	0.73	0.26	0.69	0.10	3
12	14	63	0.467	0.612	0.66	0.43	0.61	0.08	3
13	15	63	0.457	0.599	0.70	0.57	0.57	0.08	3
14	16	63	0.448	0.587	0.73	0.65	0.65	0.09	3
15	17	63	0.440	0.576	0.78	0.73	0.73	0.10	3
16	20	63	0.419	0.549	0.77	0.67	0.67	0.09	3
17	22	63	0.408	0.471	1.66	0.26	1.64	0.22	2
18	28	63	0.382	0.501	0.99	0.43	0.97	0.13	3
19	30	63	0.434	0.492	1.15	1.15	1.15	0.15	2
20	32	63	0.398	0.426	0.76	-0.60	0.60	0.08	2
21	36	63	0.470	0.525	1.04	0.47	0.92	0.13	2
22	40	63	0.458	0.458	1.06	1.06	1.06	0.14	1
23	44	63	0.395	0.448	0.55	-0.27	0.48	0.06	2
24	64	63	0.367	0.465	2.00	-1.93	1.93	0.25	3

MODEL OVERALL STATISTICS

PAR(1).. PAR(N)= 0.119600D 03 0.128160D 00 0.802600D 00
0.557000D-05

RMSE	= 18.2542 KG/M3	NO PT	= 71
AAD	= 6.5147 KG/M3	%AAD	= 1.536
MIN DEV	= -7.1145 KG/M3	MIN %DEV	= -1.246
MAX DEV	= 90.8335 KG/M3	MAX %DEV	= 24.352
BIAS	= 5.6609 KG/M3	C-VAR	= 0.028

RESTRICTIONS : NONE R-SQR =0.797746
AUX. MODELS : 3333300000 / 1111100000 EXP REF =

of vapor pressure predictions at lower and higher CN indicates little loss of accuracy beyond n-C_{17}, past which only ABC pure properties estimates were used. Based on all the above arguments regarding simplicity, internal consistency and accuracy in comparison with available experimental data, one may safely assume the viability of the ABC pure n-paraffin predictions. Accordingly, Table XX contains pure fluid properties used for EOS representation of experimental data, the subject of the next chapter. Notice that experimental data (54) were used where available. Above n-C_{17}, however, needed properties were estimated using the ABC correlation.

TABLE XX

PURE FLUID PROPERTIES USED IN EOS PREDICTIONS

COMPONENT	T_b, K	T_c, K	P_c, bar	ω
CO_2		304.21	73.83	0.2250
n-C_4	272.65	425.16	37.96	0.2004
n-C_6	341.88	507.89	30.28	0.2978
n-C_7	371.58	540.14	27.36	0.3499
n-C_{10}	447.30	617.50	20.97	0.4885
n-C_{20}	617.78	770.50	11.17	0.8738
n-C_{22}	642.83	791.70	10.22	0.9381
n-C_{28}	706.35	845.43	8.26	1.1073
n-C_{32}	740.97	875.10	7.42	1.2022
n-C_{36}	770.74	901.07	6.82	1.2847
n-C_{44}	818.87	944.29	6.04	1.4179

CHAPTER IX

EQUATION OF STATE REPRESENTATION OF EXPERIMENTAL DATA

As was discussed in Chapter II, classical thermodynamics does not provide explicit expressions for interrelationships among observables: temperature T, pressure P, volume V and composition x. Such expressions, which are the basis for the predictive capabilities in practical applications, may be represented by an equation of state, EOS. By definition, an equation of state is a mathematical relation among the above-mentioned variables which can be expressed as $f(T, P, V, x) = 0$, or as $P = f(T, V, x)$ in a pressure explicit form.

Cubic Equations of State

Theoretical developments of EOS based on the kinetic theory or statistical mechanics involving intermolecular forces suffer from severe limitations (60,59). Consequently simplified molecular models have been used where simple structures are envisioned for the fluids and averaging is employed for the molecular interactions. From such developments evolved the works of van der Waals (VDW) in 1873 (61).

According to VDW molecular model, the system pressure may be viewed as a result of two contributions: one due to molecular attraction effects and the other due to repulsion effects, or:

$$P = P_r + P_a \tag{9.1}$$

For P_r and P_a van der Waals used the following simple relations:

$$P = \frac{RT}{V-b} - \frac{a}{V^2}$$

The qualitative success of van der Waals equation of state in representing fluid phase behavior, coupled with its inherent simplicity (a two-constant, closed form equation amenable to analytic solution) has lead to numerous modifications in an effort to bring about quantitative agreement with experimental data. A "generalized" VDW EOS may be written which includes scores of such proposed modifications (62):

$$P = \frac{RT}{V-b} - \frac{\theta(V-\eta)}{(V-b)(V^2+\sigma V+\varepsilon)} \tag{9.2}$$

Table XXI illustrates how three currently popular equations, namely the Redlich-Kwong (RK), the Soave-Redlich-Kwong (SRK) and the Peng-Robinson (PR) EOS, may be obtained by proper specification of the parameters in Equation (9.2).

TABLE XXI

CUBIC EOS PARAMETER SPECIALIZATIONS

Equation	Parameter Specialization θ	η	σ	ε	Ref.
VDW	a	b	0	0	61
RK	a	b	b	0	67
SRK	a	b	b	0	7
PR	a	b	2b	$-b^2$	8

Characterization of the cubic EOS constants a and b, termed the attraction law constant and the covolume respectively, represents another avenue of improving the performance of such equations. Table XXII presents parameter characterizations for the cubic EOS considered, where a general definition for the constants a and b may be given as:

$$a = a_c \alpha = \Omega_a \, (R^2 T_c^2 / P_c) \alpha \tag{9.3}$$

$$b = b_c \beta = \Omega_b \, (R T_c / P_c) \beta \tag{9.4}$$

As indicated by the equations above, while a_c and b_c are determined at the critical state, α and β are introduced to permit variation with temperature of parameters a and b. For the SRK and PR equations, for example,

$$\alpha = [1 + m(1-Tr^{1/2})]^2, \qquad \beta = 1 \tag{9.5}$$

$$m = m_0 + m_1\omega + m_2\omega^2 \tag{9.6}$$

TABLE XXII

CUBIC EOS PARAMETER CHARACTERIZATION

EOS	Ω_a	Ω_b	β	m_0	m_1	m_2
VDW	27/64	1/3	1	0	0	0
RK	0.42747	0.08664	1	0	0	0
SRK	0.42747	0.08664	1	0.480	1.574	-1.76
PR	0.45724	0.0778	1	0.37464	1.54226	0.26992

As indicated by the above equations, while a_c and b_c are determined at the critical state, α is introduced to account for parameter a variation with temperature. Historically, Wilson (64) was first to propose modification of the temperature dependence of "a" for the RK a's temperature dependence; however, significant improvements in the quality of the predictions by the equation were not realized until Soave (7) proposed the simple correlation given by Equation (9.3). Zudkevitch and Joffe (65) and Chang and Lu (66) proposed to make both a and b temperature dependent.

Extension to Mixtures

The most general forms of the mixing rules most accepted to extend VDW cubic EOS to calculation of mixture properties are the following:

$$a = \sum_{i}^{n} \sum_{j}^{n} x_i x_j \, a_{ij} \tag{9.7}$$

$$b = \sum_{i}^{n} \sum_{j}^{n} x_i x_j \, b_{ij} \tag{9.8}$$

where

$$a_{ij} = (1-C_{ij}) \, (a_i a_j)^{1/2} \tag{9.9}$$

$$b_{ij} = (1+D_{ij}) \, (b_i+b_j)/2 \tag{9.10}$$

The C_{ij} and D_{ij} values in Equations (9.7) and (9.8) are empirical factors which must, at present, be determined from experimental data on the i-j binary mixture. The C_{ij} and D_{ij} account for deviations from the simple "mixing rules":

$$a_{ij} = (a_i a_j)^{1/2} \tag{9.11}$$

$$b_{ij} = (b_i+b_j)/2 \tag{9.12}$$

If Equations (9.11) and (9.12) are substituted into Equations (9.7) and (9.8), the results are:

$$a^{1/2} = \sum_{i}^{n} x_i a_i^{1/2} \tag{9.13}$$

$$b = \sum_{i}^{n} x_i b_i \qquad (9.14)$$

which are the original rules of Redlich and Kwong (67) and permit mixture properties to be calculated from a knowledge of pure component properties only.

While simple mixing rules, as given above, or use of a single interaction parameter (one C_{ij} per binary pair) are sufficient for some mixtures, others (especially those exhibiting some polarity or a dissimilarity in size among species) require further attention (68,69). Chao and coworkers (70), dealing with CO_2 + heavy hydrocarbon systems, for example, suggested using modified mixing rules based on conformal solutions to account for dissimilarity in size. Turek, et al. (3) on the other hand, dealing with similar systems of CO_2 binaries, proposed the introduction of an additional interaction parameter, D_{ij}, in the covolume to account for dissimilarities in molecular sizes.

Recently, more theoretically based mixing rules have been suggested employing the local composition concept (71); however, the simplicity of the classical mixing rules (with one or two interaction parameters) continues to make them attractive, particularly so when the availability of such parameters in the literature is considered.

Although EOS such as the SRK and the PR EOS have enjoyed considerable success in many applications, recognized deficiencies still exist (72,73). Some of these are inherent in the cubic nature of the equation, while others are attributable to the characterization of the EOS constants a and b. Poor description for the a and b at supercritical temperatures (72), unsatisfactory liquid density

predictions (73), and inadequate mixing rules when dealing with dissimilar molecules (68) are recognized shortcomings falling in the second category.

Efforts in this chapter are directed at EOS representation of the experimental VLE data for CO_2 + n-paraffins extending from n-C_4 to n-C_{44}. Only two variations of van der Waals cubic EOS are considered here, specifically the Soave-Redlich-Kwong and Peng-Robinson EOS.

The specific objectives are:

1. To modify the EOS constants to provide the best fit for the system under study, while maintaining the simplicity and the generality of the original equations.
2. To improve the liquid density predictions for the two equations.
3. To provide generalized binary interaction parameters for the CO_2 + n-paraffins in terms of pure hydrocarbon properties.

To achieve these objectives, methods used or generalizations proposed are guided by the following considerations:

1. The proper prediction of the pure component equilibrium properties is a necessary, but not a sufficient, condition for obtaining the proper mixture characterization.
2. Using a cubic EOS, only a compromise fit can be achieved in describing experimental reality.
3. Classical mixing rules may serve the purpose for similar size molecules; however, for asymmetric systems the need exists for better rules.
4. Although the EOS weaknesses are recognized, a systematic attack on the problem is yet to be seen. No claim is made for such a

study here, but rather attempts are made to explore a few promising areas.

Representation of CO_2 + n-Paraffin Systems

Cubic EOS representation for CO_2 + hydrocarbon binaries through regressed interaction parameters, as provided for by Equations (9.7) and (9.8) have been discussed by several investigators (1-5). While some have considered modified mixing rules, most works were in the context of a single parameter C_{ij}. The assumption that C_{ij} is independent of temperature, pressure, and composition for normal fluids is used in most cases.

In reviewing previous works it becomes evident that the scarcity of experimental data beyond n-decane and the lack of such data beyond n-C_{20} have made most conclusions regarding EOS predictive abilities for heavy hydrocarbons speculative.

Data Reduction and Evaluation

As mentioned earlier, new data have become available for CO_2 in binary mixtures with n-C_{22} and n-C_{32} from the work of Fall and Luks (19) and for n-C_{20}, n-C_{28}, n-C_{36} and n-C_{44} from the present work. Both these sets are isothermal P-x_{CO_2} measurements, i.e., the bubble point pressure is presented as a function of liquid mole fraction CO_2 or, alternatively, the solubility of CO_2 (mole fraction) as a function of pressure. In the EOS evaluations of the present work, these data were combined for analysis with selected data at lower carbon numbers,(n-C_4, n-C_6, n-C_7 and n-C_{10}) taken from the literature, as given in Table I.

For the purposes of this study, the WLSR reduction procedure is used employing Equation (7.15) as the optimality criterion and Equation (7.17) and (7.18) as constraint equations. Definitions for the component fugacity coefficient, $\hat{\phi}_i$, required by the above equations for the SRK and PR EOS are given in Appendix C. Marquardt's (74) least squares procedure is used to obtained optimum parameter estimates.

In specifying Equation (7.15) as our objective function, a weighting factor, σ_i, is required for each data point. Weighting factors for the data acquired in this study are based on Equation (7.5) with values of (dP/dx) obtained by numerical differentiation of experimental (P-x) data. However, in most cases insufficient information is given regarding estimates for the expected errors in reported experimental data. This led to the assignment of equal weights to all data point used, thus reverting to LSR objective function, or

$$S = \sum_{i=1}^{n} (P_{calc} - P_{exptl})_i^2 \qquad (9.15)$$

Nontheless, a separate table for optimum parameter estimates using weighted least square regression for the present data is given in Appendix C.

Results in this study are evaluated using the following statistics: bubble point pressure root-mean-square error (RMSE), bias, absolute average deviation (AAD), and percent absolute average deviation (% AAD). Definitions and formulae for all statistics are given in Table XXIII. Although employment of all the above statistics may seem excessive, each was found to serve a definite purpose. For example, while RMSE gives an indication of the overall performance of the model

TABLE XXIII

STATISTICS USED IN THIS STUDY

Statistic	Definition*	Description
$\overline{X}$ or mean	$\frac{\sum_{i}^{n} X_i}{n}$	The arithmetic average of n observations.
DEV	$(X_{cal}-X_{exp})$	Deviation of a calculated value for a variable from the experimentally observed one.
AAD	$\frac{\sum^{n} \lvert DEV \rvert}{n}$	The arithmetic average of the absolute values of the deviations of n observations about the mean.
BIAS	$\frac{\sum^{n} DEV}{n}$	The arithmetic average of the deviations of n observations.
RMSE	$\left(\frac{\sum^{n} DEV^2}{n}\right)^{1/2}$	The standard deviation of n observations. It is the root of the mean of the squared deviations.

*for more details see Ref. 81.

for a given data set, comparisons of RMSE to AAD provides needed information on the distribution of the deviations.

Along with numerical statistics, residual plots were used extensively to evaluate the quality of fit for the data at hand. These include deviation and percent deviation residual plots. Appendix C contains a sample for the evaluation procedures used in this study.

Several separate cases were studied to test the abilities of the EOS. The various cases included those employed by various investigators and cover a range from very simple to more complex models for data representation. Specific cases include the following:

Case	Description
1. $C_{ij} = 0$	The simplest case, equivalent to Equations (9.13) and (9.14) (the basic RK rules) and permits predictions from pure component data only. $D_{ij} = 0$.
2. C_{ij}	A separate value of C_{ij} is determined for each binary pair, independent of temperature. $D_{ij} = 0$. Corresponds to Equations (9.7) (9.9) and (9.14). This is in the most commonly employed EOS representation in the literature.
3. $C_{ij}(T)$	A separate value of C_{ij} is determined for each system at each temperature. $D_{ij} = 0$. This case permits the interaction parameter C_{ij} to be temperature dependent.
4. C_{ij}, D_{ij}	A separate pair of interaction parameters are determined for each binary pair, independent of temperature. This case assesses the benefits of including a second interaction parameter in EOS.

5. $C_{ij}(T)$, $D_{ij}(T)$ A separate pair of interaction parameters is determined for each binary at each temperature. This case evaluates the need for temperature dependencies of both C_{ij} and D_{ij}.

In the cases described above, no generalization of parameters, in terms of carbon number or temperature, was employed. Specific parameter values were evaluated, as required by the model. (Generalizations are described in a later section.)

Pure Component SRK EOS Prediction

While good pure component property prediction, vapor pressure in particular, is not a sufficient condition for obtaining reasonable EOS representation for binary mixtures, it is a necessary one. Accordingly, vapor pressure predictions were performed on pure n-paraffin solvents at the normal boiling point temperature, T_b, and at $T=0.7\ T_c$. Selection of these temperatures is dictated by the very low vapor pressure observed for the n-paraffins considered at the experimental temperatures considered, and also to duplicate Soave's (7) choice of temperatures in matching vapor pressure data for the compounds he considered.

Table XXIV presents the results of SRK EOS vapor pressure predictions for n-paraffins with carbon numbers extending from 4 to 44. The quality of the predictions obtained for the heavy paraffins (%DEV $\leq$ 2) is slightly worse than that obtained for lighter paraffins (%DEV $\leq$ 1); however, the deviations observed are well within the expected error for SRK vapor pressure predictions. Similarly, good predictions (%AAD = 1) are obtained for CO_2 vapor molar volumes at temperatures encountered for the binary systems (Table XXV).

TABLE XXIV

PURE n-PARAFFINS VAPOR PRESSURE PREDICTIONS
USING SRK EOS

DATA	CN	T(K) EXPTL*	X(CO2) EXPTL	P(BAR) EXPTL	P(BAR) CALC	DEV	%DEV
1	4	272.65	0.0000	1.014	1.003	-0.010	-1.03
2	7	371.58	0.0000	1.014	1.011	-0.003	-0.29
3	7	378.10	0.0000	1.222	1.221	-0.001	-0.08
4	10	447.30	0.0000	1.014	1.019	0.005	0.50
5	10	432.25	0.0000	0.680	0.681	0.001	0.14
6	16	560.12	0.0000	1.014	1.023	0.009	0.93
7	16	504.74	0.0000	0.258	0.257	-0.001	-0.44
8	20	617.78	0.0000	1.014	1.028	0.015	1.45
9	20	539.35	0.0000	0.149	0.151	0.002	1.38
10	22	642.83	0.0000	1.014	1.030	0.017	1.64
11	22	554.19	0.0000	0.121	0.120	-0.001	-0.84
12	28	706.35	0.0000	1.014	1.032	0.018	1.82
13	28	591.91	0.0000	0.068	0.067	-0.001	-1.25
14	32	740.97	0.0000	1.014	1.030	0.016	1.58
15	32	612.57	0.0000	0.050	0.049	-0.001	-2.03
16	36	770.74	0.0000	1.014	1.025	0.011	1.10
17	36	630.75	0.0000	0.038	0.037	-0.000	-1.28
18	44	818.87	0.0000	1.014	1.011	-0.003	-0.30
19	44	661.00	0.0000	0.026	0.025	-0.000	-1.91

MODEL OVERALL STATISTICS

RMSE = 0.0088 BAR		NO PT =	19
AAD = 0.0061 BAR		%AAD =	1.053
MIN DEV= -0.0105 BAR		MIN %DEV =	-2.028
MAX DEV= 0.0184 BAR		MAX %DEV =	1.817
BIAS = 0.0038 BAR		C-VAR =	0.018
RESTRICTIONS : NONE		R-SQR =	0.981970
AUX. MODELS : 000 000 000			

*T_b values used are obtained as described in Chapter VIII

TABLE XXV

CO_2 VAPOR MOLAR VOLUME PREDICTIONS
USING SRK EOS

Data	T,K	P,bar	Vapor Molar Volume, lit/gmol		
			Exptl (24)	Calc	%Dev
1	273.15	34.818	0.4526	0.4613	1.93
2	323.15	35.000	0.6558	0.6576	0.28
3	373.15	35.000	0.8123	0.8159	0.44
4	423.15	35.000	0.9543	0.9596	0.56
5	473.15	35.000	1.1089	1.1096	0.66
6	532.15	35.000	1.1219	1.1227	0.64
7	323.15	59.998	0.3258	0.3285	0.83
8	373.15	59.998	0.4415	0.4462	1.05
9	432.15	59.998	0.5356	0.5420	1.19
10	473.15	59.998	0.6212	0.6287	1.21
11	523.15	59.998	0.7020	0.6287	1.20
				%AAD =	0.91

This coupled with the results of similar testing on the viability of SRK EOS performed by Chao and coworkers (70) on other heavy hydrocarbons lead us to believe the adequacy of the SRK and PR EOS in representing the systems considered in the present work.

Single Parameter, C_{ij}, Predictions

Prior to discussing the results obtained using optimum C_{ij}, efforts were directed to assessment of the prediction abilities of cubic EOS in the absence of interaction parameters, $C_{ij} = D_{ij} = 0$ (Case 1). Table XXVI presents the results obtained for the CO_2 binaries considered. Very large deviations are observed for the predicted bubble point pressures in comparison to the experimental values (RMSE = 13 bar and %AAD = 22).

Although the need for an interaction parameter is dictated by the dissimilarity in molecular species involved and molecular size considerations, one may be interested to note that the greatest deviations occur for the intermediate size carbon numbers (n-C_{10} to n-C_{28}). The molecular size aside, having CO_2 as a constituent imposes an added element of complexity in behavior, due to its quadrapole effect, which translates to poorer results than would be expected for a similar size non-polar substance.

In comparison, Table XXVII presents the results obtained using an optimum "lumped C_{ij}" approach, where C_{ij}, specific to each binary system, is assumed independent of temperature, pressure, and composition (Case 2). While an adequate representation is obtained for systems involving paraffins lighter than n-decane, large deviations are observed for n-decane and heavier paraffins. Deviations within 3% AAD (RMSE

TABLE XXVI

C_{ij} = 0 BPP

CALCULATIONS USING SRK EOS

ISO	CN	T(K)	C(I,J)	D(I,J)	RMSE BAR	BIAS BAR	AAD BAR	%AAD	NO PT
1	4	310.9	0.0000	0.0000	6.89	-6.15	6.15	24.4	18
2	4	344.3	0.0000	0.0000	7.83	-6.70	6.70	17.8	17
3	4	377.6	0.0000	0.0000	5.14	-4.51	4.52	10.6	12
4	4	410.9	0.0000	0.0000	1.45	-1.28	1.28	3.1	7
5	6	313.1	0.0000	0.0000	10.55	-9.79	9.79	23.0	8
6	6	353.1	0.0000	0.0000	13.51	-12.52	12.52	28.1	15
7	6	393.1	0.0000	0.0000	15.69	-14.94	14.94	22.5	14
8	7	310.6	0.0000	0.0000	8.13	-6.73	6.73	22.6	23
9	7	352.6	0.0000	0.0000	13.99	-12.99	12.99	23.9	17
10	7	394.3	0.0000	0.0000	13.50	-12.61	12.61	17.6	16
11	7	477.2	0.0000	0.0000	7.04	-6.31	6.31	9.6	7
12	10	277.6	0.0000	0.0000	8.85	-8.07	8.07	45.0	11
13	10	310.9	0.0000	0.0000	15.23	-14.16	14.16	38.6	11
14	10	344.3	0.0000	0.0000	20.16	-18.63	18.63	32.4	8
15	10	377.6	0.0000	0.0000	23.78	-21.62	21.62	28.6	10
16	10	410.9	0.0000	0.0000	24.29	-21.75	21.75	25.2	11
17	10	444.3	0.0000	0.0000	21.91	-19.49	19.49	22.3	11
18	10	477.6	0.0000	0.0000	19.67	-17.55	17.55	20.2	11
19	10	510.9	0.0000	0.0000	16.66	-14.67	14.67	20.0	9
20	16	463.0	0.0000	0.0000	5.72	-5.44	5.44	15.3	4
21	20	323.1	0.0000	0.0000	11.92	-10.41	10.41	36.4	13
22	20	373.1	0.0000	0.0000	12.17	-10.75	10.75	25.1	9
23	22	323.1	0.0000	0.0000	18.76	-16.72	16.72	36.8	14
24	22	348.1	0.0000	0.0000	13.47	-11.61	11.61	27.3	19
25	22	373.1	0.0000	0.0000	9.53	-7.97	7.97	21.3	11
26	28	348.1	0.0000	0.0000	17.73	-13.40	13.40	25.1	8
27	28	373.1	0.0000	0.0000	11.75	-8.29	8.29	16.7	9
28	28	423.1	0.0000	0.0000	6.80	-3.90	4.12	6.3	7
29	32	348.1	0.0000	0.0000	11.53	-9.43	9.43	19.9	11
30	32	373.1	0.0000	0.0000	8.79	-7.65	7.65	14.0	11
31	32	398.1	0.0000	0.0000	3.70	-2.14	2.67	5.8	15
32	36	373.1	0.0000	0.0000	3.49	-2.03	2.19	5.6	10
33	36	423.1	0.0000	0.0000	3.29	0.25	2.47	8.0	8
34	44	373.1	0.0000	0.0000	2.43	0.45	1.93	10.8	7
35	44	423.1	0.0000	0.0000	5.52	5.31	5.31	22.1	7

MODEL OVERALL STATISTICS

RMSE	= 13.0551 BAR	NO PT	= 399
AAD	= 10.2760 BAR	%AAD	= 21.830
MIN DEV	=-35.8824 BAR	MIN %DEV	= -58.332
MAX DEV	= 7.2835 BAR	MAX %DEV	= 34.725
BIAS	= -9.9658 BAR	C-VAR	= 26.110
RESTRICTIONS	: NONE	R-SQR	=0.652412
AUX. MODELS	: 000 000 000		

TABLE XXVII

C_{ij} BPP
CALCULATIONS USING SRK EOS

ISO	CN	T(K)	C(I,J)	D(I,J)	RMSE BAR	BIAS BAR	AAD BAR	%AAD	NO PT
1	4	310.9	0.1472	0.0000	0.85	0.45	0.61	1.7	18
2	4	344.3	0.1472	0.0000	0.20	-0.03	0.13	0.4	17
3	4	377.6	0.1472	0.0000	1.10	-0.85	0.89	1.8	12
4	4	410.9	0.1472	0.0000	1.34	-1.17	1.20	2.8	7
5	6	313.1	0.1355	0.0000	1.33	0.61	1.13	2.2	8
6	6	353.1	0.1355	0.0000	1.23	0.22	1.04	2.5	14
7	6	393.1	0.1355	0.0000	1.26	-1.04	1.09	2.5	15
8	7	310.6	0.1096	0.0000	0.94	-0.36	0.79	2.3	23
9	7	352.6	0.1096	0.0000	0.84	-0.48	0.59	1.1	17
10	7	394.3	0.1096	0.0000	0.90	0.71	0.79	2.2	16
11	7	477.2	0.1096	0.0000	1.01	-0.29	0.83	1.4	7
12	10	277.6	0.1215	0.0000	1.39	-0.82	1.22	8.5	11
13	10	310.9	0.1215	0.0000	1.64	-0.42	1.49	5.1	11
14	10	344.3	0.1215	0.0000	3.79	1.00	2.74	4.0	8
15	10	377.6	0.1215	0.0000	2.67	0.49	1.92	2.1	10
16	10	410.9	0.1215	0.0000	2.16	-0.37	1.71	1.8	11
17	10	444.3	0.1215	0.0000	2.33	-1.55	1.99	2.4	11
18	10	477.6	0.1215	0.0000	3.75	-2.95	3.35	4.3	11
19	10	510.9	0.1215	0.0000	6.04	-5.40	5.40	7.8	9
20	16	463.0	0.0877	0.0000	0.20	-0.02	0.18	0.6	4
21	20	323.1	0.1080	0.0000	1.26	-0.84	0.85	2.3	13
22	20	373.1	0.1080	0.0000	1.60	1.55	1.55	4.7	9
23	22	323.1	0.1033	0.0000	2.45	-1.78	1.87	3.5	14
24	22	348.1	0.1033	0.0000	1.54	1.38	1.43	5.2	19
25	22	373.1	0.1033	0.0000	2.48	2.32	2.32	7.8	11
26	28	348.1	0.0878	0.0000	3.78	-1.13	2.70	7.1	8
27	28	373.1	0.0878	0.0000	2.39	1.69	2.29	9.6	9
28	28	423.1	0.0878	0.0000	5.02	4.68	4.68	16.4	7
29	32	348.1	0.0534	0.0000	4.04	-2.56	2.90	5.5	11
30	32	373.1	0.0534	0.0000	1.62	-0.05	1.38	3.7	11
31	32	398.1	0.0534	0.0000	4.17	3.96	3.96	12.4	15
32	36	373.1	0.0205	0.0000	2.01	-0.40	1.42	5.9	10
33	36	423.1	0.0205	0.0000	3.30	2.33	3.22	11.5	8
34	44	373.1	-0.0215	0.0000	3.62	-1.26	2.34	8.7	7
35	44	423.1	-0.0215	0.0000	3.79	3.40	3.43	16.3	7

MODEL OVERALL STATISTICS

RMSE	= 2.4291 BAR	NO PT	= 399
AAD	= 1.7105 BAR	%AAD	= 4.582
MIN DEV=	-9.4233 BAR	MIN %DEV	= -14.782
MAX DEV=	8.7905 BAR	MAX %DEV	= 28.746
BIAS	= 0.0021 BAR	C-VAR	= 4.858
RESTRICTIONS	: NONE	R-SQR	=0.993712
AUX. MODELS	: 000 000 000		

within 1 bar) are obtained for the light paraffin binaries, which is typical of cubic EOS predictions (1,70). For heavier paraffins (C_{10} - C_{44}), however, deviations of up to 16% (RMSE = 5 bar) are observed.

As indicated in Table XXVII, the predictions show a marked improvement over Case 1 ($C_{ij} = D_j = 0$) with a reduction in the overall %AAD from 22 to 4.6% (RMSE from 13 to 2.4 bar). However, this improvement is only limited for the heavy paraffins in which the size effects are dominant.

Turning the attention to the magnitude of the C_{ij} parameters obtained, Figure 21 presents C_{ij} (▲) as a function of the carbon number, CN. The results obtained indicate a disagreement with the suggestion Robinson (76) that a constant value of C_{ij} of about 0.13 for may be adequate for the heavier paraffins. While this may hold reasonably well for paraffins up to n-C_{20} (the data based used to draw such conclusions), the newly acquired data indicate pronounced variations in the C_{ij} value at higher CN. In addition, the rate of decrease in C_{ij} value beyond n-C_{20} is significant, resulting in a negative C_{ij} for n-C_{44}.

Interaction Parameter Temperature Dependence

Considering the temperature dependence of C_{ij} has been recognized as an important factor in improving the cubic EOS predictions (4,69). While this is not a favorable undertaking, due to the added complexity of having to deal with several parameters for a given binary, the results given in Table XXVIII nevertheless indicate the existence of a significant temperature dependence of C_{ij} for the systems studied. Comparison of results given in Table XXVIII for $C_{ij}(T)$ (Case 3) to those

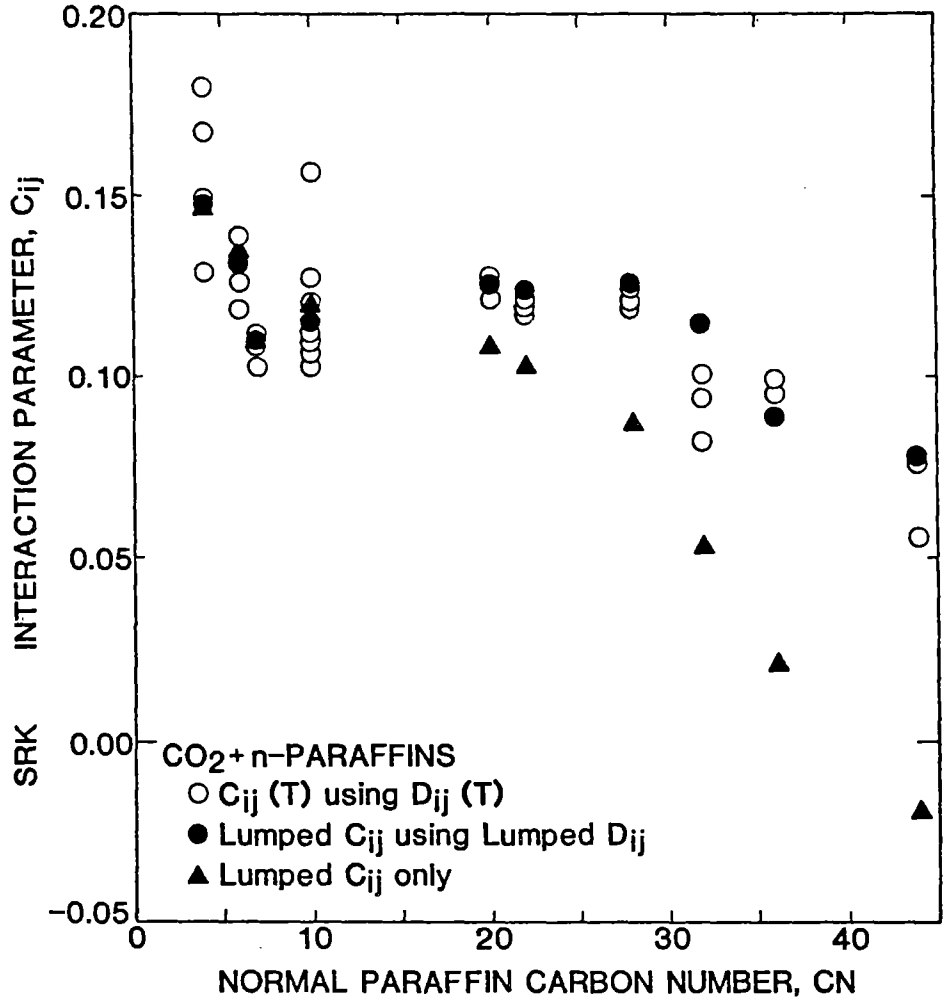

Figure 21. CO_2 + n-Paraffins First Interaction Parameter, C_{ij}

TABLE XXVIII

$C_{ij}(T)$ BPP

CALCULATIONS USING SRK EOS

ISO	CN	T(K)	C(I,J)	D(I,J)	RMSE BAR	BIAS BAR	AAD BAR	%AAD	NO PT
1	4	310.9	0.1359	0.0000	0.47	-0.16	0.39	1.6	18
2	4	344.3	0.1473	0.0000	0.20	-0.02	0.13	0.4	17
3	4	377.6	0.1679	0.0000	0.24	0.08	0.21	0.6	12
4	4	410.9	0.2254	0.0000	0.35	-0.06	0.30	0.7	7
5	6	313.1	0.1263	0.0000	0.93	-0.29	0.87	2.0	8
6	6	353.1	0.1308	0.0000	1.12	-0.37	0.90	2.8	14
7	6	393.1	0.1410	0.0000	0.98	-0.47	0.80	1.8	15
8	7	310.6	0.1106	0.0000	0.93	-0.29	0.78	2.3	23
9	7	352.6	0.1113	0.0000	0.76	-0.24	0.49	0.8	17
10	7	394.3	0.1048	0.0000	0.74	0.01	0.61	1.6	16
11	7	477.2	0.1076	0.0000	1.17	-0.32	0.96	1.5	7
12	10	277.6	0.1275	0.0000	1.27	-0.32	1.04	6.8	11
13	10	310.9	0.1210	0.0000	1.63	-0.51	1.48	5.2	11
14	10	344.3	0.1137	0.0000	2.69	-1.09	2.48	4.8	8
15	10	377.6	0.1169	0.0000	2.23	-0.73	1.91	2.6	10
16	10	410.9	0.1207	0.0000	2.14	-0.56	1.71	1.8	11
17	10	444.3	0.1269	0.0000	1.99	-0.56	1.59	1.7	11
18	10	477.6	0.1356	0.0000	2.75	-0.85	2.15	2.6	11
19	10	510.9	0.1737	0.0000	1.83	-0.52	1.48	2.3	9
20	16	463.0	0.0877	0.0000	0.20	-0.03	0.18	0.6	4
21	20	323.1	0.1166	0.0000	0.46	0.19	0.42	1.9	13
22	20	373.1	0.0988	0.0000	0.73	0.27	0.67	2.3	9
23	22	323.1	0.1132	0.0000	0.73	0.30	0.61	2.1	14
24	22	348.1	0.0974	0.0000	1.11	0.44	0.99	3.6	19
25	22	373.1	0.0862	0.0000	0.84	0.31	0.67	2.8	11
26	28	348.1	0.1005	0.0000	2.33	1.29	2.15	8.6	8
27	28	373.1	0.0840	0.0000	2.31	1.17	2.07	8.6	9
28	28	423.1	0.0554	0.0000	2.57	1.22	2.19	8.8	7
29	32	348.1	0.0741	0.0000	1.67	0.68	1.50	5.5	11
30	32	373.1	0.0567	0.0000	1.52	0.48	1.35	3.9	11
31	32	398.1	0.0259	0.0000	1.95	0.67	1.69	5.8	15
32	36	373.1	0.0328	0.0000	1.59	0.66	1.32	7.3	10
33	36	423.1	0.0103	0.0000	3.07	1.28	2.72	9.5	8
34	44	373.1	0.0074	0.0000	2.32	1.07	2.16	12.5	7
35	44	423.1	-0.0481	0.0000	2.82	1.22	2.55	11.4	7

MODEL OVERALL STATISTICS

RMSE	= 1.5401 BAR	NO PT	= 399
AAD	= 1.1290 BAR	%AAD	= 3.523
MIN DEV	= -5.7531 BAR	MIN %DEV	= -12.023
MAX DEV	= 6.6148 BAR	MAX %DEV	= 24.378
BIAS	= 0.0609 BAR	C-VAR	= 3.080
RESTRICTIONS	: NONE	R-SQR	=0.998119
AUX. MODELS	: 000 000 000		

of lumped C_{ij} of Case 2 indicates a reduction in RMSE from 2.5 to 1.5 bar translating to reduction in %AAD from 4.5 to 3.5%.

As shown in Figure 22,in most cases the lumped C_{ij} parameter is an intermediate value to those obtained for the different isotherms. Further, Figure 22 shows that only n-heptane data shows no obvious dependence of C_{ij} on temperature, while for lighter paraffins (n-C_4 and n-C_6) C_{ij} is increasing with temperature, for heavier paraffins (n-C_{20} and above) a definite decrease of C_{ij} with temperature is evident. Data for n-C_{10} system, on the other hand, produces a parabolic behavior, as was noted by Kato (4).

Viewed in totality, the optimum C_{ij}-temperature curves, as shown in Figure 22, produce a spray-type behavior with a pinch point around 260 K. This is in contrast to conclusions reached by Lin (5), in which no C_{ij} temperature dependence was deemed necessary for K-value predictions. The differences in the effect of temperature on the quality of the EOS predictions may be explained by the fact that K-value predictions are significantly less sensitive to C_{ij} than are bubble point pressure calculations for the CO_2 systems, as was discussed by Graboski (2).

Modified SRK Predictions

In addition to the use of interaction parameters, two other routes exist for possible improvements in the predictive ability of a cubic EOS. These are modified characterization of the EOS constant a and b of Equation (9.2) and modified mixing rules. In dealing with CO_2 + hydrocarbon systems, Graboski (2) considered paraffins up to n-decane and suggested a modification for the supercritical temperature

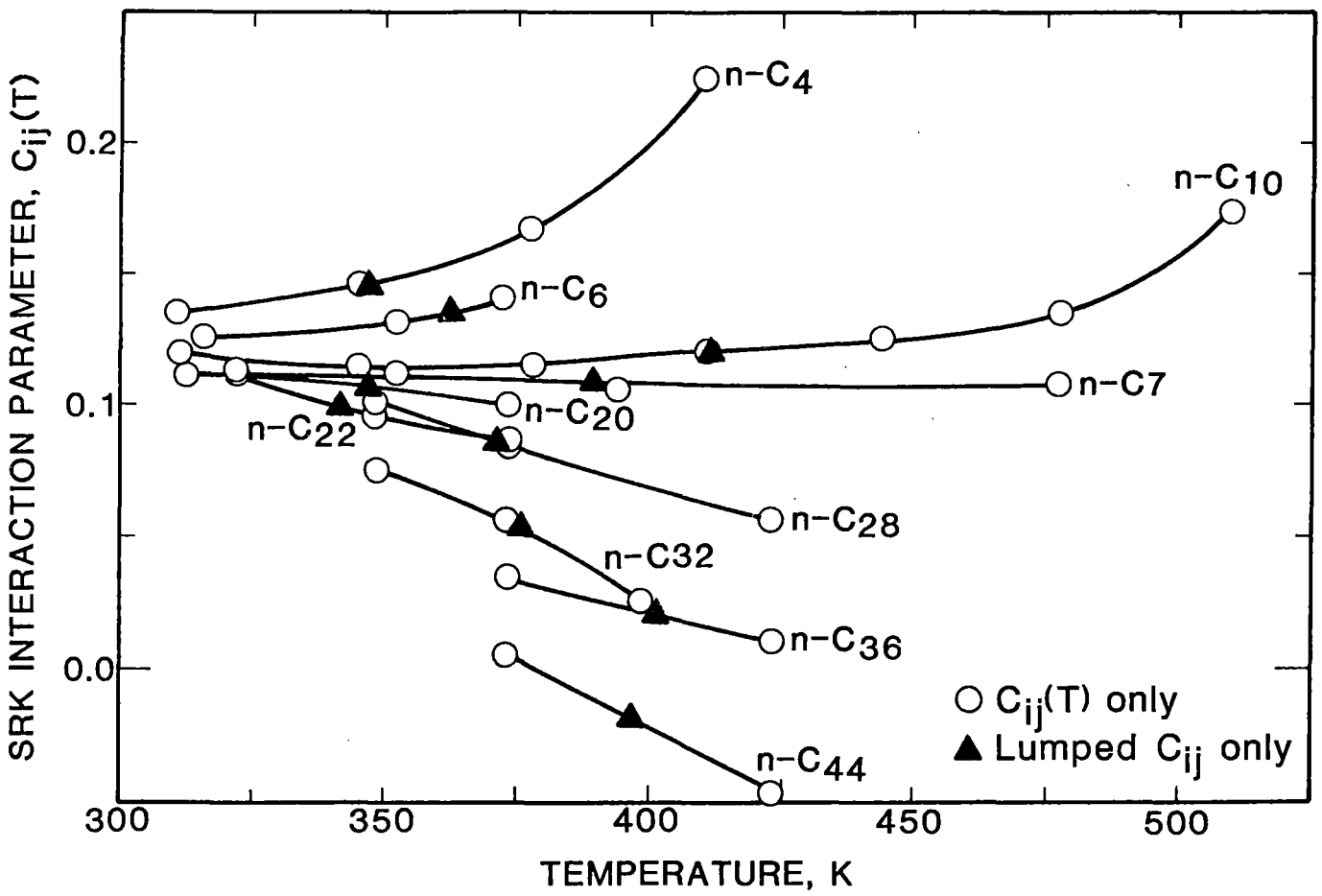

Figure 22. Effects of Temperatures and n-Paraffin Carbon Number on SRK Interaction Parameter C_{ij}

dependence of the constant "a" through the term m of Equation (9.6) to secure better predictions for "heavier hydrocarbons". By comparison to predictions made based on the original SRK definition of the term m, predictions using Graboski's modification offer no improvement for the systems considered, as shown in Table XXIX. Also given in the same table are the results of Simonet's (77) recommendations for the characterization of the EOS constants a and b, where Ω_a and Ω_b were correlated as a function of reduced temperature. Again, no improvement is observed in the quality of the predictions. Thus, the original SRK formulation was retained and improved property predictions were sought through modified mixing rules or an increased number of regressed model parameters.

Selection of Regressed Parameters

To improve predictions by increasing the number of the regressed parameters (in mixing rules, the critical properties, or the acentric factor), some desirable characteristics should be sought in selecting such parameters (78). First, the number of regressed parameters should be kept at minimum for a given binary to facilitate extensions to multicomponent systems. Second, parameters selected should have the least amount of correlation among them (so as not to be highly demanding regarding the quality of the experimental data required). Finally, such parameters should be amenable to generalization based on pure fluid properties.

In dealing with CO_2 + heavy n-paraffins, a disparity in molecular size is rather obvious. This effect is well reflected by the inadequacy of single interaction parameter predictions (Table XXVII) for n-C_{10} and

heavier molecules and suggests modification of the mixing rules for the covolume b. Following the recommendation of Turek, et al. (3) as expressed by Equation (9.10) for the covolume b, an additional interaction parameter, D_{ij}, was used to account for molecular size variations.

TABLE XXIX

COMPARISON OF RESULTS FOR SRK CONSTANTS CHARACTERIZATION FOR SYSTEMS CONSIDERED

	Parameter Used	Bubble Point Pressure, Bar				
		RMSE	BIAS	AAD	%AAD	NRMSE
Original SRK (7)	None	13.06	-9.97	10.78	2.83	8.98
Original SRK (7)	C_{ij}	2.43	0.003	1.71	4.58	1.00
Graboski (2) modified m of Equation (9.5)	C_{ij}	2.43	-.008	1.71	4.59	1.00
Simonet (77) modified Ω_a and Ω_b	C_{ij}	3.41	-.164	2.50	6.78	1.40

Selection of D_{ij} as an additional model parameter is well supported by results in Table XXX for CO_2 + n-decane at 344.3K. This table also shows the effect of varying pure decane properties such as the acentric factor ω and the critical properties T_c and P_c. Comparison of the deviations resulting from a given parameter or combination of parameters

TABLE XXX

CUBIC EOS PARAMETER SELECTION (CO_2 + n-DECANE at 344.2 K, SRK)

Case	Parameter Used	Parameter Values	Bubble Point Pressure, Bar					Molar Volume %AAD	
			RMSE*	BIAS	AAD	%AAD	NRMSE*	Liquid	Vapor
2	none	-------	20.16	-18.64	18.64	32.4	32.52	18.8	83.8
2	C_{ij}	0.1137	2.69	-1.10	2.48	4.86	4.34	19.1	7.4
3	D_{ij}	0.1160	11.75	9.59	-4.54	19.7	18.95	25.2	24.2
4	ω	0.4708	2.02	-18.35	18.35	32.3	32.30	19.0	67.0
5	C_{ij}, ω	0.2034, 0.0183	0.87	-0.33	0.74	1.3	1.40	30.7	3.2
6	C_{ij}, P_c	0.0773, 27.64	2.12	-0.57	1.90	3.45	3.56	7.6	5.9
7	C_{ij}, T_c	0.1584, 553.1	0.75	-0.16	0.66	1.09	1.21	17.5	2.4
8	C_{ij}, D_{ij}	0.1069, 0.0202	0.62	0.13	0.56	1.72	1.00	20.2	3.9

*NRMSE = RMSE/(RMSE of Case 8)

indicates lower deviations are obtained using C_{ij} and D_{ij} simultaneously. A bubble point pressure RMSE of 0.62 bar is obtained as compared to 2.69 bar using C_{ij} only or even the worse predictions using D_{ij} only (RMSE = 11.8 bar). Inspection of the other parameter selections used reveals that only the choice of C_{ij} and T_c gives comparable results (RMSE = 0.75 bar) to those obtained using C_{ij} and D_{ij}.

Treatment of the critical properties and the acentric factor as additional regressed model parameters is an often-used empirical procedure (91) to attain better cubic EOS representation of experimental data. While some improvement may be obtained in the prediction of properties included in the reduction procedure, due to the added model flexibility, overall results usually suffer from obvious suboptimization. As an example of such tendencies, the selection of the acentric factor as an additional model parameter for the system under study may be cited. Such a selection leads to worsened molar volume predictions as shown in Table XXX. Furthermore, three-dimensional plots (Figures 23 and 24) exploring the sensitivity of the predictions obtained to variations in the regressed parameters indicate a limited flexibility exists employing the acentric factor or the critical properties. This fact is well illustrated by Figure 24 where very poor predictions for the BPP pressure are observed when using poor property estimates, particularly so when using poor critical temperature estimates.

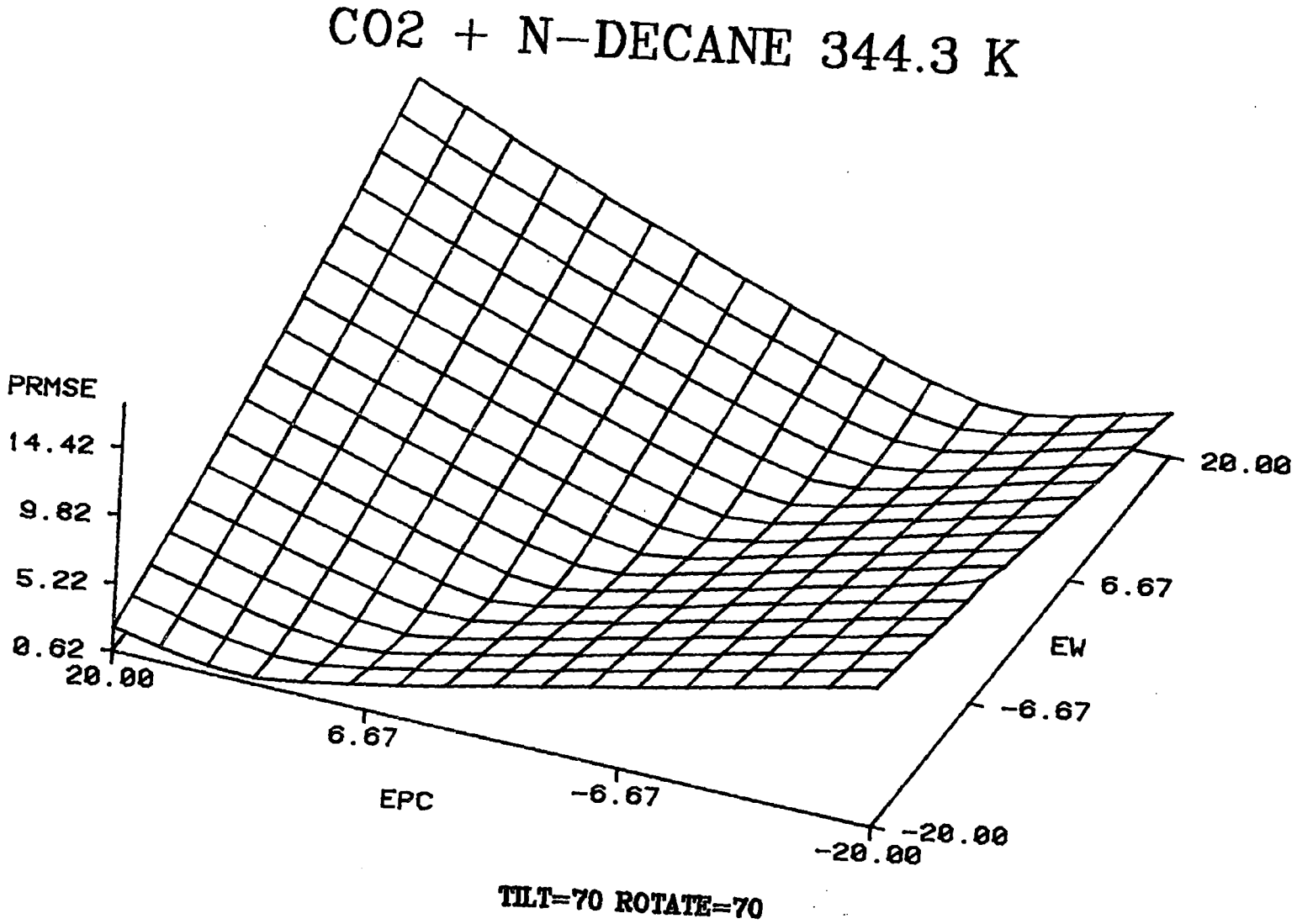

Figure 23. Sensitivity of SRK BPP Predictions to P_c and ω

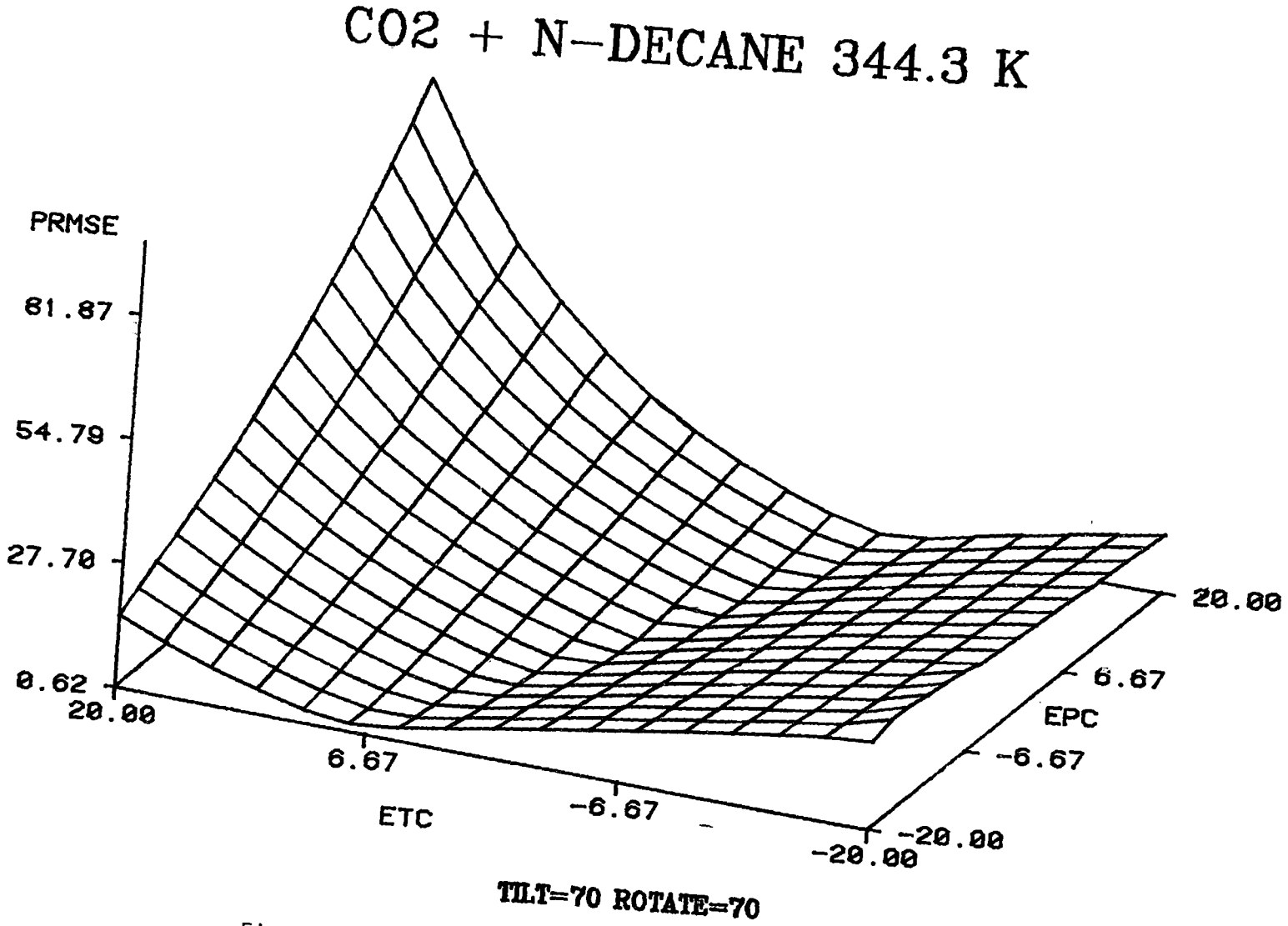

Figure 24. Sensitivity of SRK BPP Predictions to T_c and P_c

Effects of C_{ij} and D_{ij} on Predicted Properties

The influence of C_{ij} and D_{ij} on the quality of SRK EOS predictions can be shown as three-dimensional plots for different CO_2 + n-paraffin binaries. These figures depict the bubble point pressure deviations (as expressed by PRMSE in bars) resulting from variations in C_{ij} and D_{ij}. Variations in the interaction parameters for a given system are expressed as percentage changes from the optimum values (denoted as EC_{ij} and ED_{ij}) for C_{ij} and D_{ij}, respectively.

As shown in Figures 25 through 28, three-dimensional plots for CO_2 binaries involving n-C_4, n-C_{10}, n-C_{20} and n-C_{36} indicate that, while changes in C_{ij} have a definite effect on PRMSE for all size molecules considered, the role of D_{ij} varies depending on molecular size. For lower carbon number n-paraffins (n-C_4), variations in D_{ij} have little or no effect on the PRMSE obtained; however, a clear dependence of the resulting PRMSE on D_{ij} value is observed at high carbon numbers Furthermore, inspection of the plots reveals a gradual change in the relation between the two regressed parameters from being slightly correlated at lower carbon numbers to exhibiting strong correlation at higher carbon numbers. This tendency is supported by the observed gradual rotation of the minimum-PRMSE axis from being parallel to the EC_{ij} and ED_{ij} plane falling perpendicular on the EC_{ij} coordinate for n-C_4 to having a tilted diagonal projection on the EC_{ij} - ED_{ij} plane for n-C_{36}.

To examine the effect of C_{ij} and D_{ij} on mole fraction residuals as a function of pressure for both liquid and vapor phase predictions CO_2 + n-C_{10} at 344.3 K binary (12) was selected. Figure 29 reveals that the introduction of C_{ij} adjusts the liquid mole fraction residuals from a

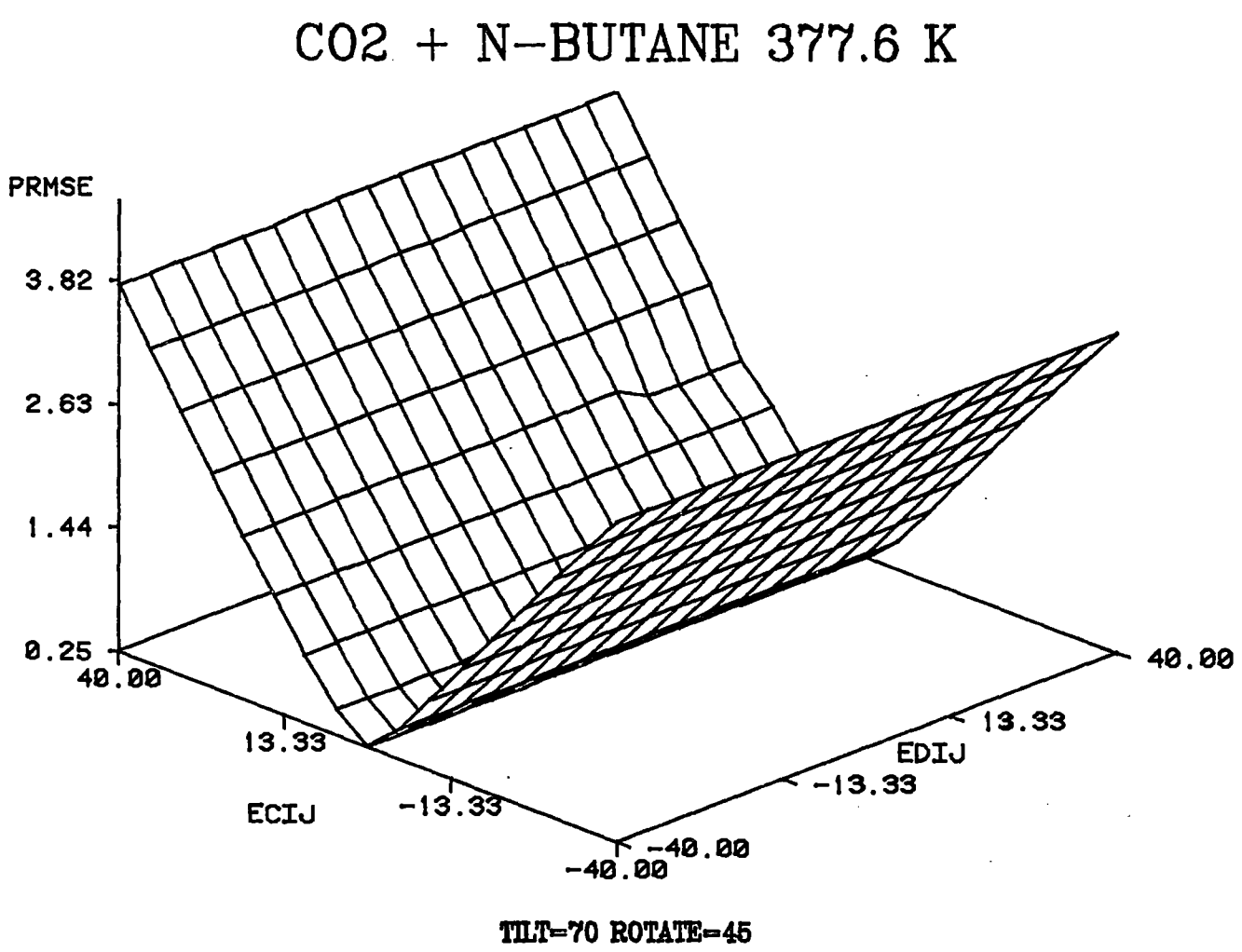

Figure 25. Sensitivity of SRK and BPP Predictions to C_{ij} and D_{ij} at Different CN

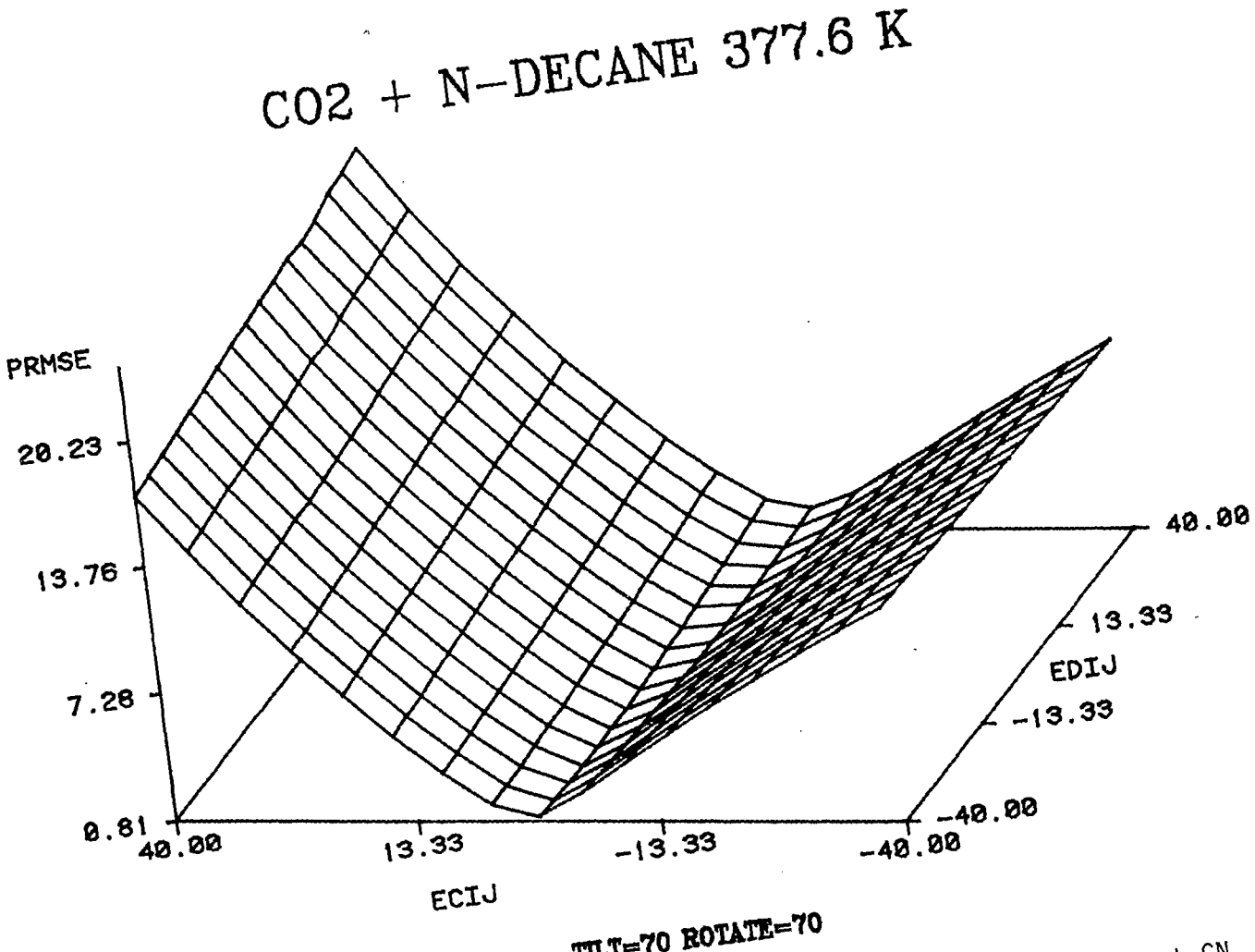

Figure 26. Sensitivity of SRK BPP Predictions to C_{ij} and D_{ij} at Different CN

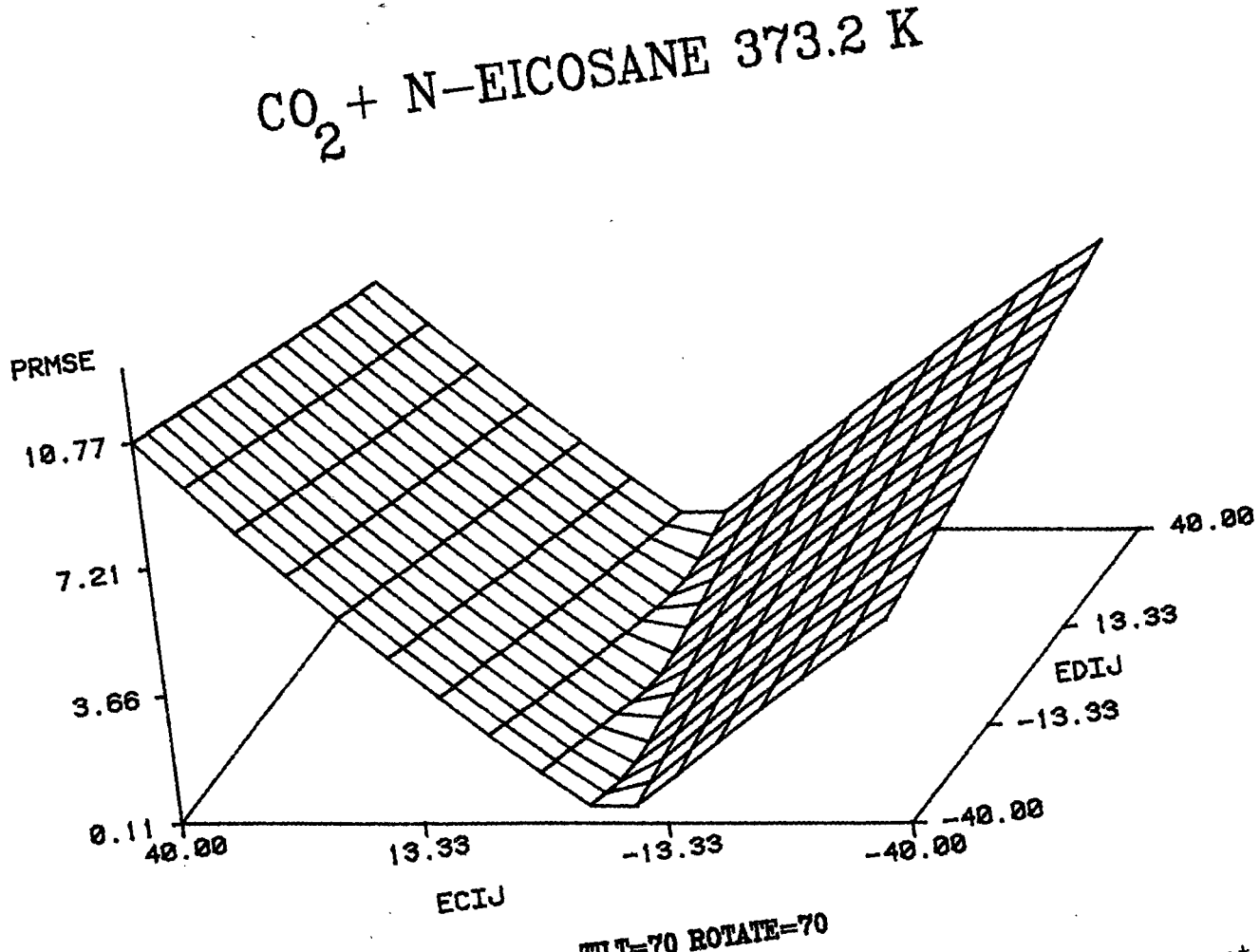

Figure 27. Sensitivity of SRK BPP Predictions to C_{ij} and D_{ij} at Different CN

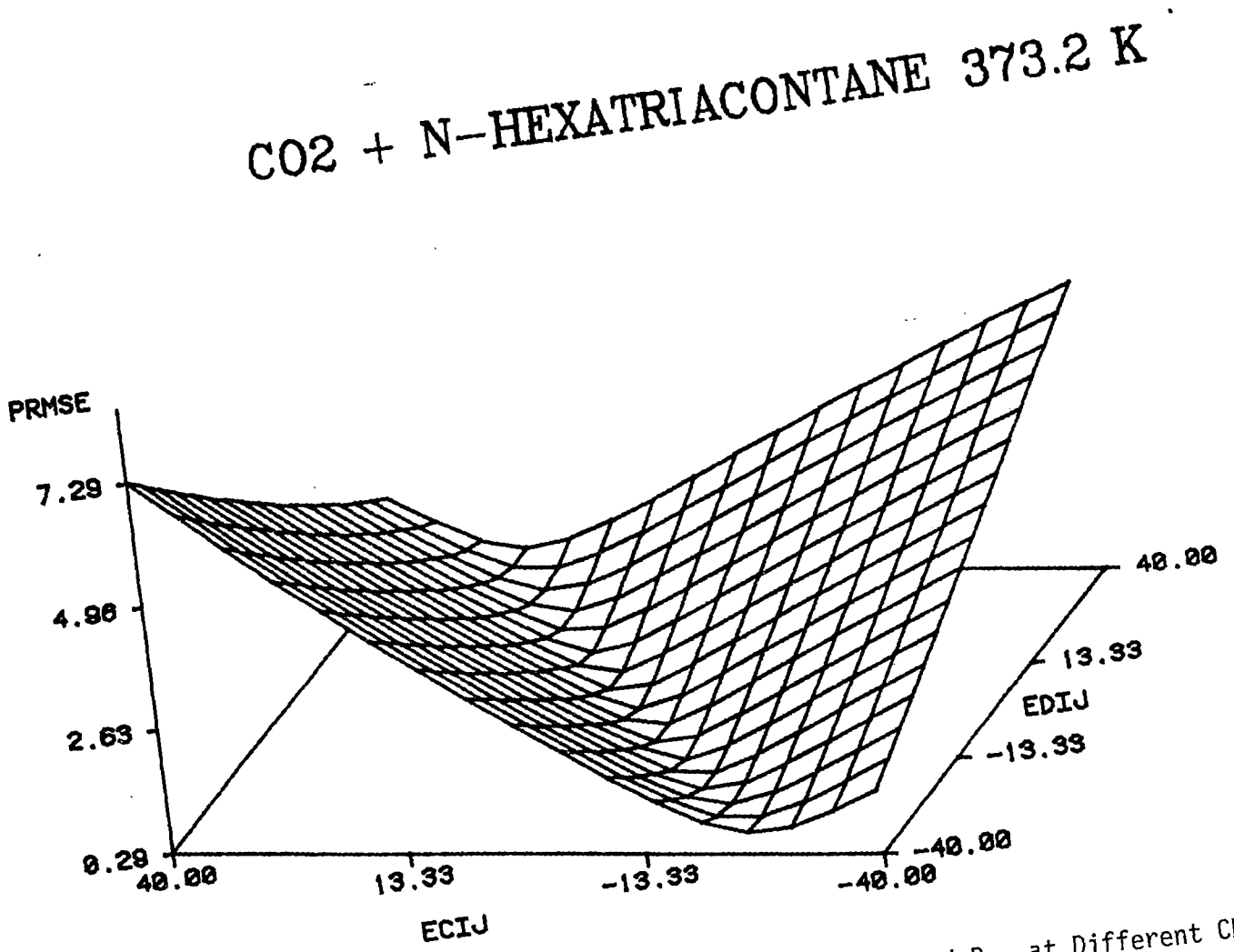

Figure 28. Sensitivity of SRK BPP Predictions to C_{ij} and D_{ij} at Different CN

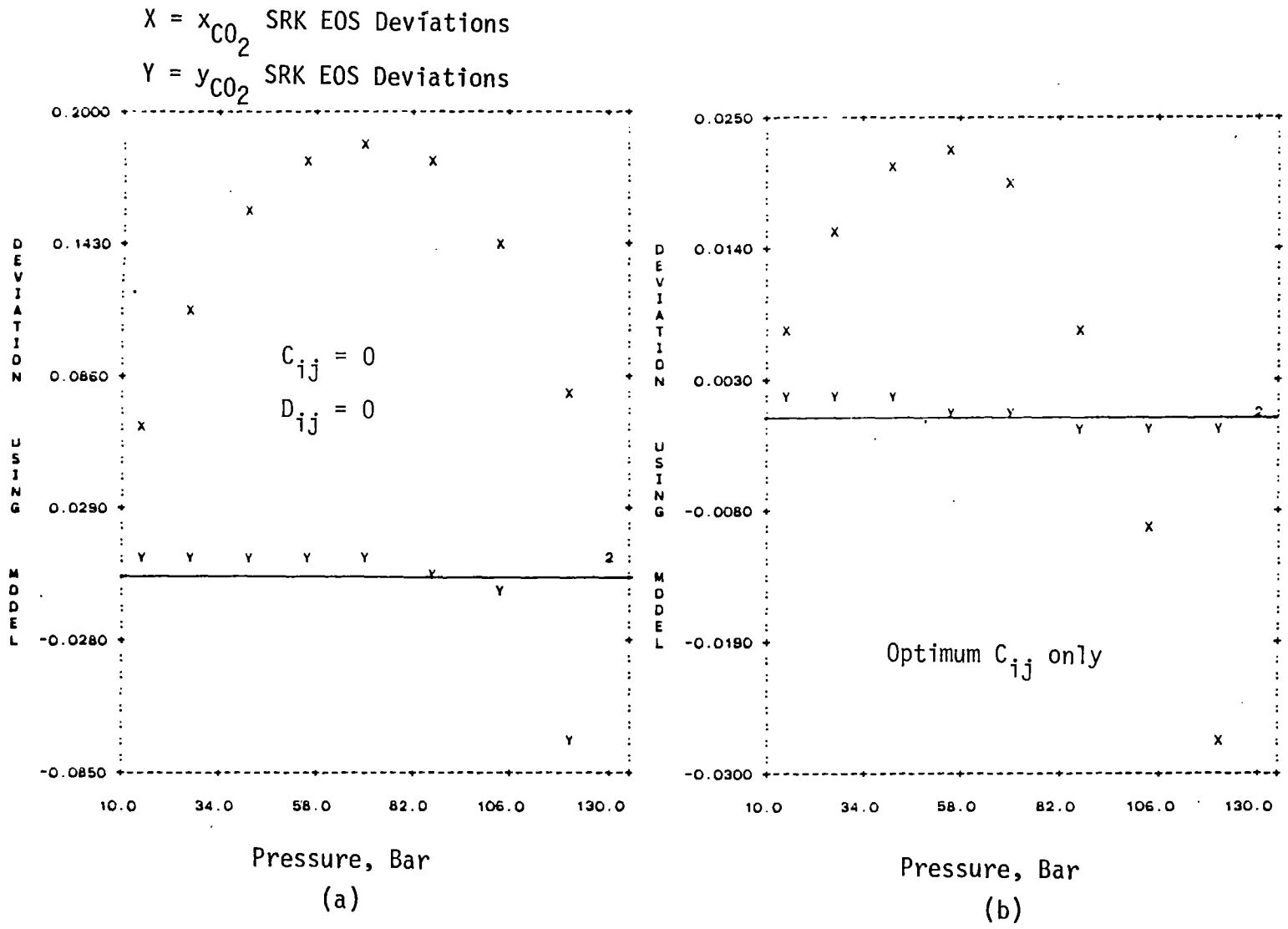

Figure 29. Effects of C_{ij} and D_{ij} on Phase Composition Predictions

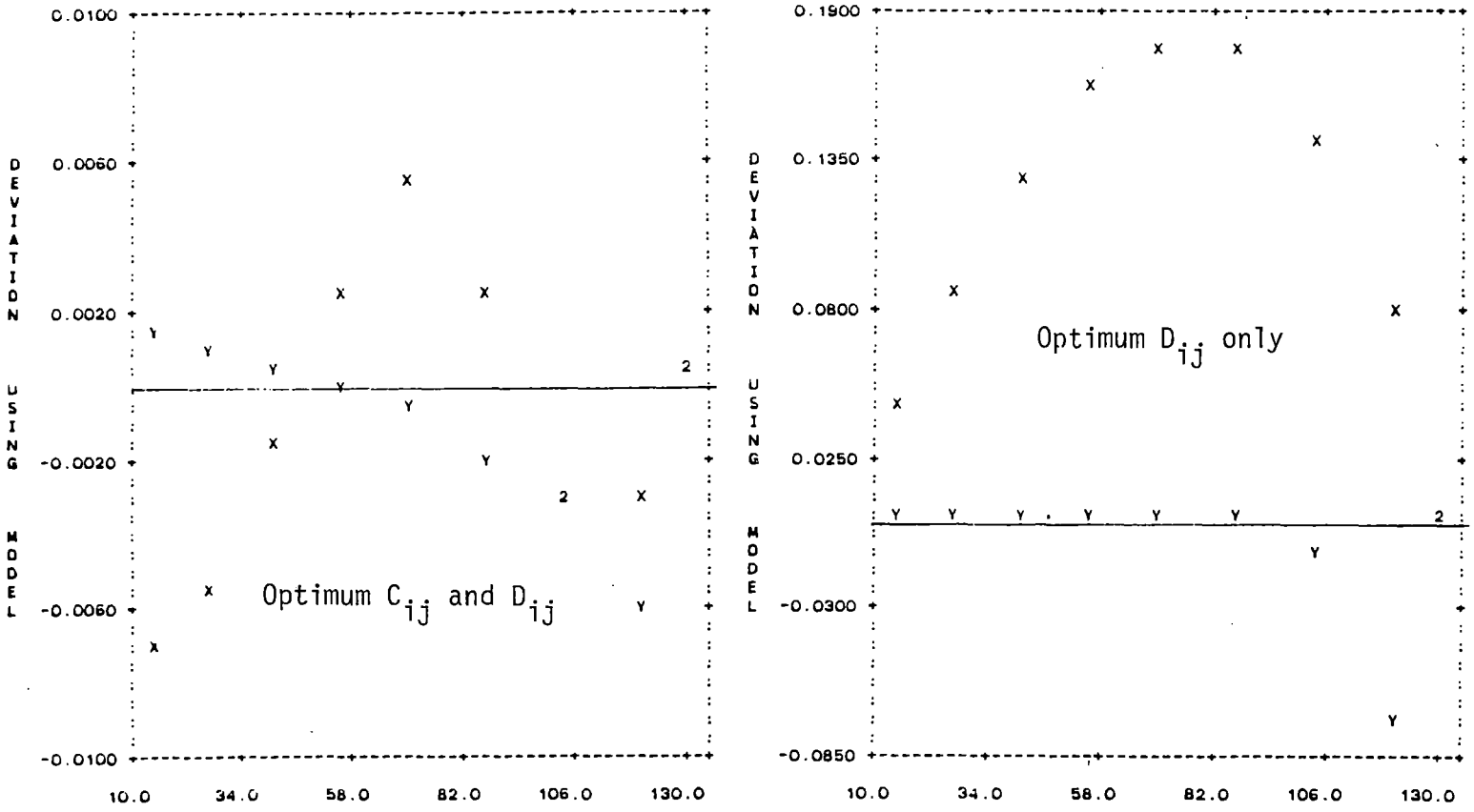

Figure 29. (Continued)

dome-like shape completely positive with deviations up to 0.19 for C_{ij} = 0 to a similar but shifted curve resulting in negative deviations at higher pressure. In contrast, the introduction of D_{ij} results in limited reduction in the observed deviations, but significantly adjusts the residual distribution forcing negative deviations at lower pressures when used along with C_{ij} (Figure 29,c).

The effects of C_{ij} and D_{ij} on vapor phase composition predictions are not as significant as those observed for the liquid phase. As indicated in Figure 29, the magnitude of observed deviations are much lower and better distributed about the zero-line. Interestingly, the introduction of D_{ij} causes a slight worsening of the overall RMSE of in the vapor phases residuals as compared to using C_{ij} only. Nevertheless, the magnitude of the deviations are comparable if not better than those obtained for the liquid composition. The fact that vapor composition predictions fair well (though not included in the data reduction procedure) supports the argument that experimental measurements for such a property are not essential except for consistency tests purposes (14) or studies concerned with variations in vapor composition on a trace scale.

Finally, the translational and rotational effects of C_{ij} and D_{ij} on the predicted phase compositions may be illustrated also in terms of K-value plots. Figures 30 and 31 present plots K-values of CO_2 as a function of pressure at different levels of C_{ij} and D_{ij} for CO_2 + n-butane at 377 K (21). The plot contains evidence that variations of C_{ij} primarily force a translation in the K-value curve; in contrast, varying values of D_{ij} at a fixed level of C_{ij} cause more of a rotation to the curve.

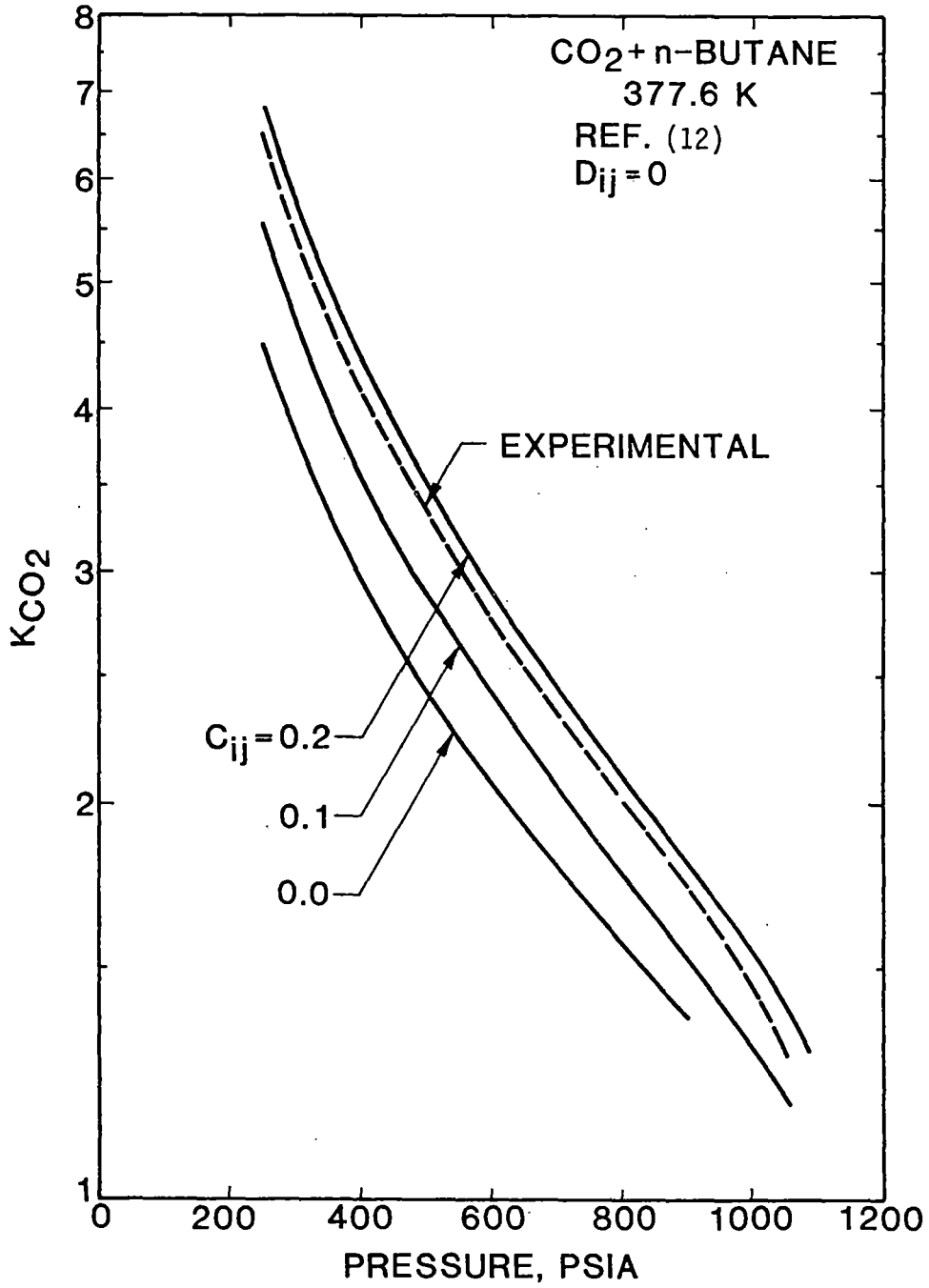

Figure 30. Effects of C_{ij} on K-Value Predictions

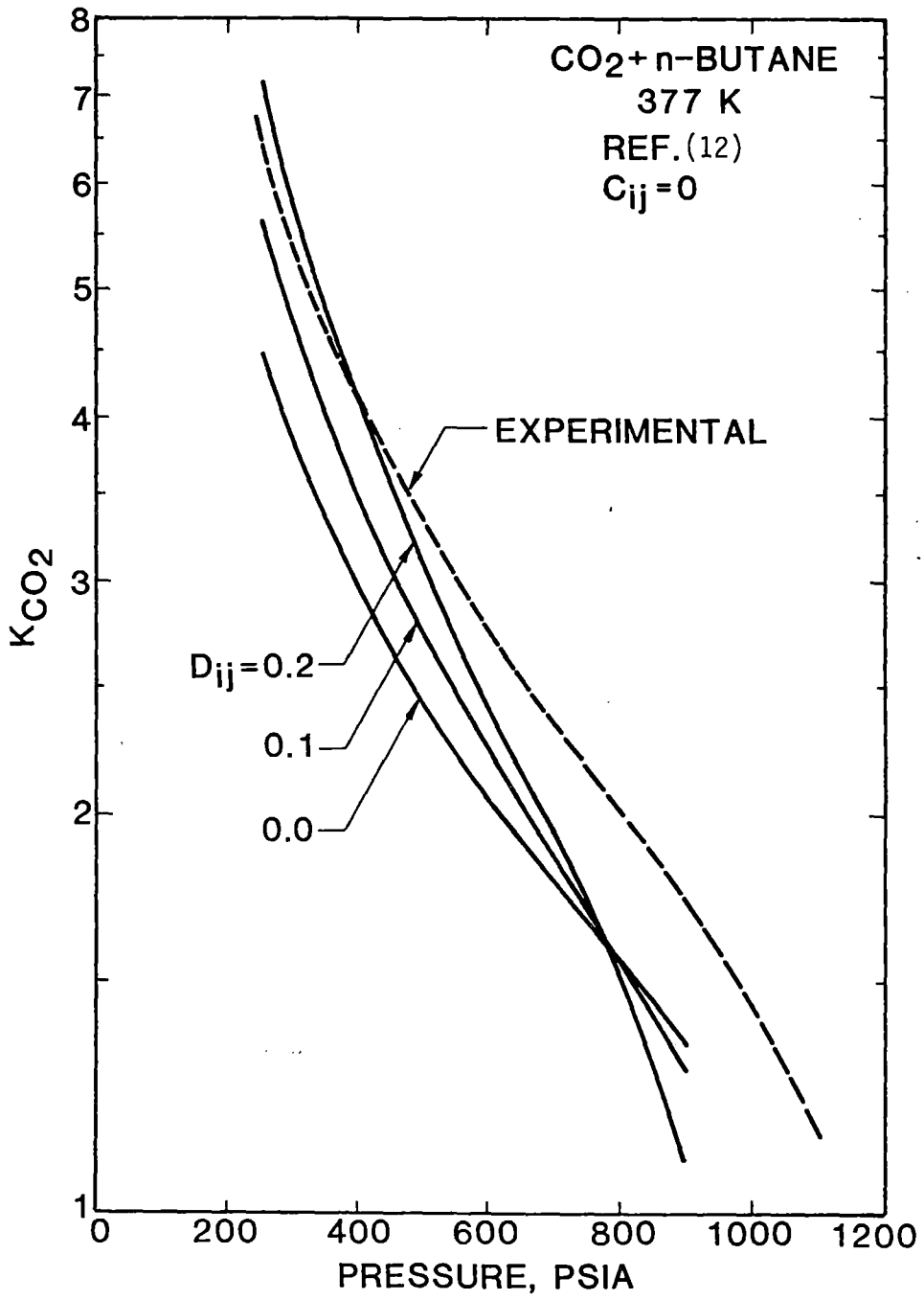

Figure 31. Effects of D_{ij} on K-Value Predictions

Two Parameter (C_{ij} and D_{ij}) Representation

Having accepted the need for a second interaction parameter, D_{ij}, to modify the covolume mixing rules, efforts were extended to implement this modification with minimal added complexity. This was done by first assessing the EOS predictions using temperature-independent parameters, (lumped C_{ij} and D_{ij}, Case 4), then proceeding to temperature-dependent parameters, $C_{ij}(T)$ and $D_{ij}(T)$ (Case 5), if necessary.

Table XXXI presents the results obtained for SRK EOS using lumped C_{ij} and D_{ij} parameters, (Case 4). While a significant improvement is evident in the EOS predictions in comparison with the base case when C_{ij} and D_{ij} are set at zero, the results indicate only a moderate improvement over lumped C_{ij} predictions. The deviations observed, however, overall RMSE of 1.7 bar and 2.8 %AAD, are comparable to those obtained using temperature-dependent C_{ij} as shown in Table XXVIII. Of significance is the observation that the predictive abilities for the EOS in both cases ($C_{ij}(T)$ or lumped C_{ij} and D_{ij}) deteriorate for heavy paraffins, including n-C_{10}.

While the introduction of D_{ij} is significant in improving the quality of the predictions, the temperature dependence for the two parameters is still important for the heavy paraffins. This temperature effect for the interaction parameters C_{ij} and D_{ij}, as shown in Table XXXII, is quite evident for n-C_{10} and heavier paraffins. Considerable improvement in the quality of the predictions results when both C_{ij} and D_{ij} are made functions of temperature, as seen from the overall RMSE of 0.6 bar and 1.2 %AAD. Values for the optimum C_{ij} and D_{ij} parameters are presented in Figures 21 and 32. In contrast to single parameter

TABLE XXXI

LUMPED C_{ij} AND D_{ij} BPP
CALCULATIONS USING SRK EOS

ISO	CN	T(K)	C(I,J)	D(I,J)	RMSE BAR	BIAS BAR	AAD BAR	%AAD	NO PT
1	4	310.9	0.1487	-0.0042	0.81	0.39	0.56	1.5	18
2	4	344.3	0.1487	-0.0042	0.18	-0.07	0.14	0.5	17
3	4	377.6	0.1487	-0.0042	1.13	-0.88	0.92	1.9	12
4	4	410.9	0.1487	-0.0042	1.36	-1.19	1.22	2.8	7
5	6	313.1	0.1313	0.0120	1.42	0.77	1.28	2.6	8
6	6	353.1	0.1313	0.0120	0.84	0.28	0.66	1.4	14
7	6	393.1	0.1313	0.0120	1.13	-0.99	0.99	1.8	15
8	7	310.6	0.1096	0.0004	0.93	-0.34	0.78	2.3	23
9	7	352.6	0.1096	0.0004	0.84	-0.46	0.57	1.0	17
10	7	394.3	0.1096	0.0004	0.93	0.74	0.83	2.3	16
11	7	477.2	0.1096	0.0004	1.00	-0.28	0.81	1.3	7
12	10	277.6	0.1149	0.0187	0.76	0.42	0.49	2.4	11
13	10	310.9	0.1149	0.0187	1.14	0.92	0.96	2.8	11
14	10	344.3	0.1149	0.0187	2.36	2.00	2.00	3.7	8
15	10	377.6	0.1149	0.0187	1.60	1.49	1.49	3.2	10
16	10	410.9	0.1149	0.0187	1.19	0.57	1.03	2.6	11
17	10	444.3	0.1149	0.0187	1.56	-0.66	1.31	2.0	11
18	10	477.6	0.1149	0.0187	3.12	-2.40	2.40	2.2	11
19	10	510.9	0.1149	0.0187	5.51	-4.71	4.71	6.2	9
20	16	463.0	0.0836	0.0015	0.20	-0.02	0.19	0.6	4
21	20	323.1	0.1265	-0.0079	1.14	-1.08	1.08	4.3	13
22	20	373.1	0.1265	-0.0079	1.38	1.26	1.26	3.1	9
23	22	323.1	0.1294	-0.0133	1.62	-1.53	1.53	4.9	14
24	22	348.1	0.1294	-0.0133	0.83	0.39	0.66	1.7	19
25	22	373.1	0.1294	-0.0133	1.30	0.76	0.94	2.5	11
26	28	348.1	0.1306	-0.0193	1.79	-1.70	1.70	6.0	8
27	28	373.1	0.1306	-0.0193	0.70	-0.44	0.64	3.1	9
28	28	423.1	0.1306	-0.0193	2.60	2.00	2.00	4.6	7
29	32	348.1	0.1149	-0.0211	2.50	-2.44	2.44	8.8	11
30	32	373.1	0.1149	-0.0211	1.18	-0.89	1.06	3.2	11
31	32	398.1	0.1149	-0.0211	2.63	1.89	2.16	4.9	15
32	36	373.1	0.0883	-0.0176	1.62	-1.48	1.48	6.4	10
33	36	423.1	0.0883	-0.0176	1.81	1.61	1.61	4.5	8
34	44	373.1	0.0762	-0.0226	2.47	-2.29	2.29	10.9	7
35	44	423.1	0.0762	-0.0226	2.28	1.82	1.82	4.7	7

MODEL OVERALL STATISTICS

RMSE	= 1.6992 BAR	NO PT	= 399
AAD	= 1.2162 BAR	%AAD	= 3.124
MIN DEV	= -9.2287 BAR	MIN %DEV	= -22.350
MAX DEV	= 5.4384 BAR	MAX %DEV	= 15.458
BIAS	= -0.1837 BAR	C-VAR	= 3.398
RESTRICTIONS	: NONE	R-SQR	=0.992684
AUX. MODELS	: 000 000 000		

TABLE XXXII

$C_{ij}(T)$ AND $D_{ij}(T)$ BPP
CALCULATIONS USING SRK EOS

ISO	CN	T(K)	C(I,J)	D(I,J)	RMSE BAR	BIAS BAR	AAD BAR	%AAD	NO PT
1	4	310.9	0.1280	0.0131	0.43	-0.14	0.29	0.9	18
2	4	344.3	0.1494	-0.0045	0.17	-0.04	0.14	0.5	17
3	4	377.6	0.1672	0.0008	0.24	0.06	0.22	0.6	12
4	4	410.9	0.1802	0.0807	0.13	0.05	0.10	0.3	7
5	6	313.1	0.1190	0.0150	0.79	-0.30	0.58	1.1	8
6	6	353.1	0.1268	0.0151	0.67	-0.15	0.53	1.2	14
7	6	393.1	0.1390	0.0131	0.45	-0.01	0.37	0.8	15
8	7	310.6	0.1026	0.0158	0.74	-0.26	0.51	1.9	23
9	7	352.6	0.1121	-0.0004	0.73	-0.13	0.49	0.8	17
10	7	394.3	0.1085	-0.0075	0.45	0.09	0.30	1.1	16
11	7	477.2	0.1124	0.0191	0.55	0.17	0.47	1.1	7
12	10	277.6	0.1020	0.0260	0.39	0.01	0.32	2.4	11
13	10	310.9	0.1090	0.0188	0.43	-0.03	0.33	1.0	11
14	10	344.3	0.1069	0.0202	0.62	0.13	0.56	1.7	8
15	10	377.6	0.1115	0.0202	1.08	0.80	0.85	2.6	10
16	10	410.9	0.1153	0.0161	1.11	0.32	1.00	2.2	11
17	10	444.3	0.1206	0.0168	1.09	0.22	0.98	1.8	11
18	10	477.6	0.1279	0.0269	1.29	0.27	1.17	2.0	11
19	10	510.9	0.1565	0.0301	1.00	0.12	0.83	1.2	9
20	16	463.0	0.0836	-0.0015	0.62	-0.58	0.58	1.8	4
21	20	323.1	0.1271	-0.0046	0.14	-0.00	0.10	0.3	13
22	20	373.1	0.1219	-0.0097	0.10	-0.01	0.09	0.3	9
23	22	323.1	0.1211	-0.0050	0.28	-0.00	0.23	0.7	14
24	22	348.1	0.1186	-0.0099	0.39	-0.01	0.33	1.1	19
25	22	373.1	0.1080	-0.0083	0.48	-0.01	0.39	1.4	11
26	28	348.1	0.1224	-0.0119	0.11	0.01	0.09	0.3	8
27	28	373.1	0.1200	-0.0147	0.14	-0.03	0.13	0.6	9
28	28	423.1	0.1180	-0.0215	0.73	-0.06	0.56	2.5	7
29	32	348.1	0.1005	-0.0107	0.41	-0.04	0.33	1.5	11
30	32	373.1	0.0939	-0.0127	0.41	-0.01	0.34	0.8	11
31	32	398.1	0.0822	-0.0168	0.77	-0.06	0.57	1.9	15
32	36	373.1	0.0948	-0.0152	0.29	-0.05	0.25	1.3	10
33	36	423.1	0.0992	-0.0242	0.47	-0.09	0.39	1.5	8
34	44	373.1	0.0776	-0.0170	0.29	-0.05	0.26	1.5	7
35	44	423.1	0.0546	-0.0230	0.30	-0.06	0.28	1.4	7

MODEL OVERALL STATISTICS

RMSE	= 0.6073 BAR	NO PT	= 399
AAD	= 0.4216 BAR	%AAD	= 1.228
MIN DEV	= -2.3034 BAR	MIN %DEV	= -11.697
MAX DEV	= 2.4339 BAR	MAX %DEV	= 11.984
BIAS	= -0.0009 BAR	C-VAR	= 1.215
RESTRICTIONS	: NONE	R-SQR	=0.999274
AUX. MODELS	: 000 000 000		

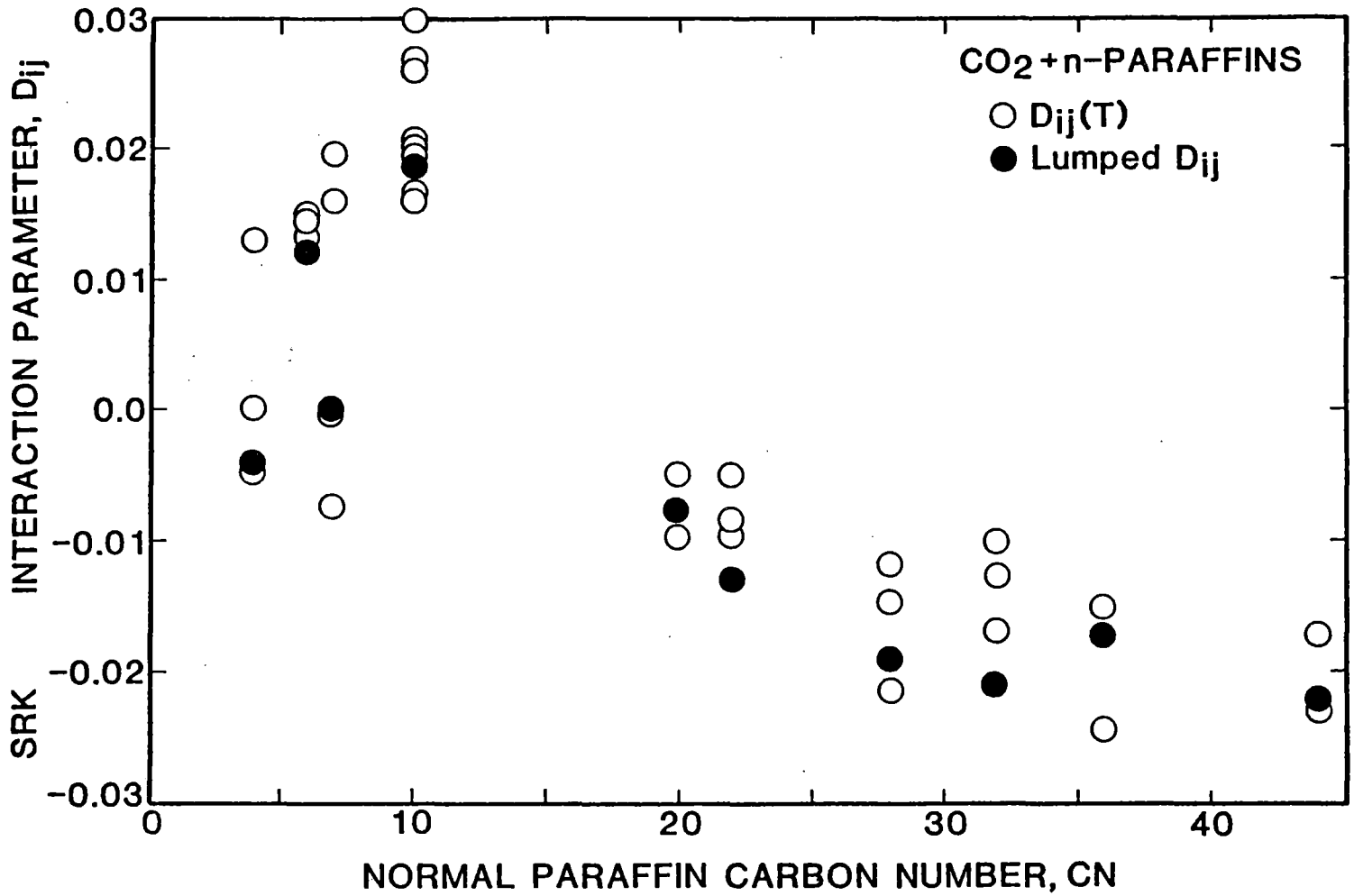

Figure 32. CO_2 + n-Paraffins Second Interaction Parameter, D_{ij}

regressions, C_{ij} values (when D_{ij} is introduced) remain positive for all paraffins considered. D_{ij} values, however, range from about 0.03 for n-C_{10} to -0.02 for n-C_{44}. In contrast, as shown in Figure 32, lighter paraffins D_{ij} shows random tendencies regarding both sign and magnitude.

Table XXXIII presents a summary of the results obtained using the different parameters in comparison to the base case where no interaction parameters are used, Case 1. As indicated in Table XXXIII and Figure 33, deviations from experimental values expressed in terms of bubble point pressure RMSE decrease progressively from 13.06 bar for Case 1 (C_{ij} and D_{ij} set to zero) to 0.62 bar for Case 5, in which C_{ij} and D_{ij} are temperature-dependent. The above results expressed as normalized RMSE indicate a 21-fold increase in RMSE going from the best of Case 5 to Case 1, where no interaction parameters are used. Also included in Table XXXIII are the summary of results for the PR EOS which are discussed in a separate section.

The results strongly suggest that two equally important factors effect the quality of the EOS predictions. First is the introduction of D_{ij} into the covolume mixing rules to account for molecular size effects. The second is accounting for the temperature-dependence of C_{ij} and D_{ij}. Table XXXIII and Figure 33 expressed the importance of the two factors.

Table XXXIV addresses the paraffin molecular size effects on the SRK EOS predictions applying the different parameters. Inspection of the results given for the different paraffins reveals that, although introduction of D_{ij} may be important for n-C_{10} and heavier paraffins, it is of no great value for the lighter paraffins. These conclusions are perhaps more obvious from Figure 33, in which the different lines

TABLE XXXIII

SUMMARY OF RESULTS FOR CUBIC EOS PRESENTATIONS FOR CO_2 + n-PARAFFINS
($n\text{-}C_4$ to $n\text{-}C_{44}$)

Case	Regressed Parameter	Bubble Point Pressure, Bar									
		RMSE*		BIAS		AAD		%AAD		NRMSE**	
		SRK	PR	SRK	PR	SRK	PR	SRK	PR	SRK	PR
1	none	13.06	12.23	-9.97	-9.06	10.78	9.58	21.83	20.51	21.41	21.09
2	C_{ij}	2.43	2.37	0.00	0.04	1.71	1.67	4.58	4.62	3.98	4.09
3	$C_{ij}(T)$	1.54	1.42	0.06	0.11	1.13	1.04	3.52	3.38	2.52	2.45
4	C_{ij}, D_{ij}	1.70	1.72	-0.18	-0.26	1.22	1.26	3.12	3.25	2.79	2.96
5	$C_{ij}(T)$, $D_{ij}(T)$	0.61	0.58	0.00	-0.05	0.42	0.40	1.23	1.15	1.00	1.00

*See Table XXIII for statistics definitions
**NRMSE = RMSE/(RMSE of Case 5)

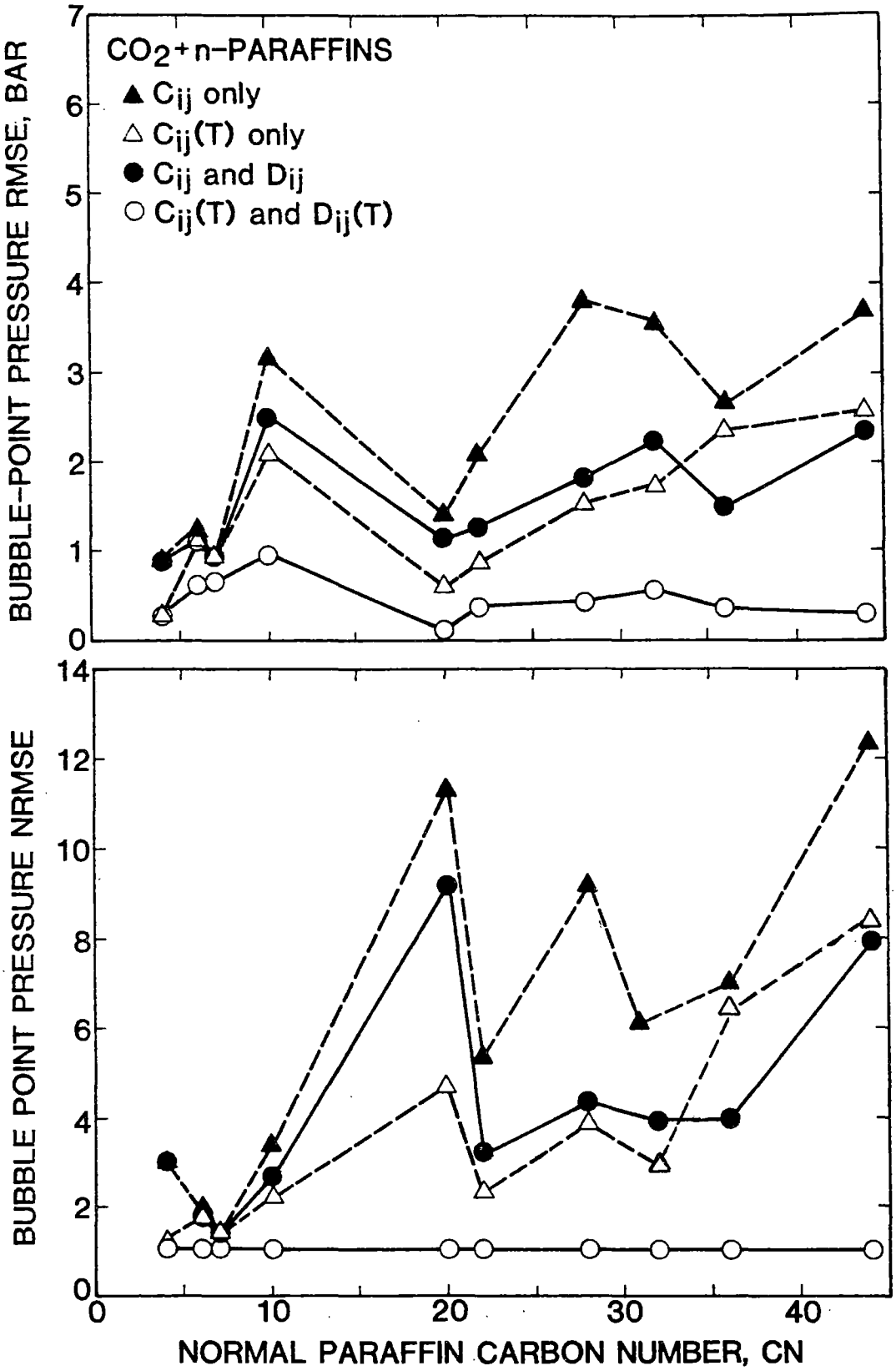

Figure 33. Temperature and Molecular Size Effects on SRK Predictions for CO_2 + n-Paraffins

TABLE XXXIV

EFFECTS OF PARAFFIN MOLECULAR SIZE ON SRK PREDICTIONS

CN	Temperature Range, K	No. PT.	Ref.	Bubble Point RMSE, Bar				
				None	C_{ij}	$C_{ij}(T)$	C_{ij}, D_{ij}	$C_{ij}(T)$, $D_{ij}(T)$
4	310.9 - 410.9	54	21	6.42	0.87	0.34	0.87	0.29
6	313.2 - 393.2	37	15	13.83	1.26	1.06	1.11	0.62
7	310.6 - 477.2	63	22	11.35	0.91	0.87	0.91	0.65
10	277.6 - 510.9	82	12	19.39	3.18	2.10	2.50	0.94
20	323.2 - 373.2	22	Present Work	12.02	1.41	0.59	1.15	0.13
22	323.2 - 373.2	44	19	14.59	2.11	0.91	1.25	0.39
28	348.2 - 423.2	24	Present Work	13.04	3.78	1.55	1.80	0.41
32	348.2 - 398.2	37	19	8.25	3.56	1.77	2.25	0.58
36	373.2 - 423.2	18	Present Work	3.41	2.66	2.37	1.30	0.38
44	373.2 - 423.2	14	Present Work	4.26	3.70	2.58	2.38	0.30

TABLE XXXIV (Continued)

CN	Temperature Range, K	No. PT.	Ref.	Bubble Point NRMSE, Bar				
				None	C_{ij}	$C_{ij}(T)$	C_{ij}, D_{ij}	$C_{ij}(T)$, $D_{ij}(T)$
4	310.9 - 410.9	54	21	22.14	3.00	1.17	3.00	1.00
6	313.2 - 393.2	37	15	22.31	2.03	1.71	1.79	1.00
7	310.6 - 477.2	63	22	17.46	1.40	1.34	1.40	1.00
10	277.6 - 510.9	82	12	20.63	3.38	2.23	2.66	1.00
20	323.2 - 373.2	22	Present Work	37.90	6.64	2.36	4.60	1.00
22	323.2 - 373.2	44	19	37.41	5.41	2.33	3.21	1.00
28	348.2 - 423.2	24	Present Work	31.80	9.22	3.78	4.39	1.00
32	348.2 - 398.2	37	19	14.22	6.14	3.05	3.88	1.00
36	373.2 - 423.2	18	Present Work	8.97	7.00	1.58	3.95	1.00
44	373.2 - 423.2	14	Present Work	14.2	12.33	8.60	7.93	1.00

reflect the parameter selections. Clearly indicated is the fact that, for paraffins below n-C_{10}, the differences in the magnitudes of the deviations observed from one case to the other are not as significant as those for the heavier paraffins.

Turning attention to the details of the temperature tendencies for C_{ij} and D_{ij}, the results obtained indicate a similar behavior for C_{ij} with temperature as was discussed for the single parameter case, $C_{ij}(T)$, and shown in Figure 22. For D_{ij} a definite decrease with temperature is observed as shown in Table XXXIV for n-C_{20} and heavier paraffins. For n-C_4 through n-C_{10} a random variation is observed for D_{ij} temperature-dependence. This is in agreement with the observation made previously of the high correlation between C_{ij} and D_{ij} at lower carbon numbers.

To further explore the nature of the interaction parameters temperature dependence, 3-dimensional plots were generated for the CO_2 + n-C_{10} system (12) at several temperatures showing PRMSE as a function of C_{ij} and D_{ij} (Figures 34 through 36). A gradual rotation in minimum-PRMSE axis is observed due the change in temperature similar to that observed due to molecular size variation (Figures 25 through 28) but opposite in direction. Also indicated by these plots is a reduced sensitivity to values of C_{ij} and D_{ij} at higher temperature, as indicated by lower over-all PRMSE. This observation tends to support the suggestion (4) to favor fitting lower temperature isotherms when lumped C_{ij} and D_{ij} are used.

Peng-Robinson EOS Representation

While most of the discussion has dealt with SRK EOS, conclusions drawn regarding equilibrium calculations apply equally well to the PR

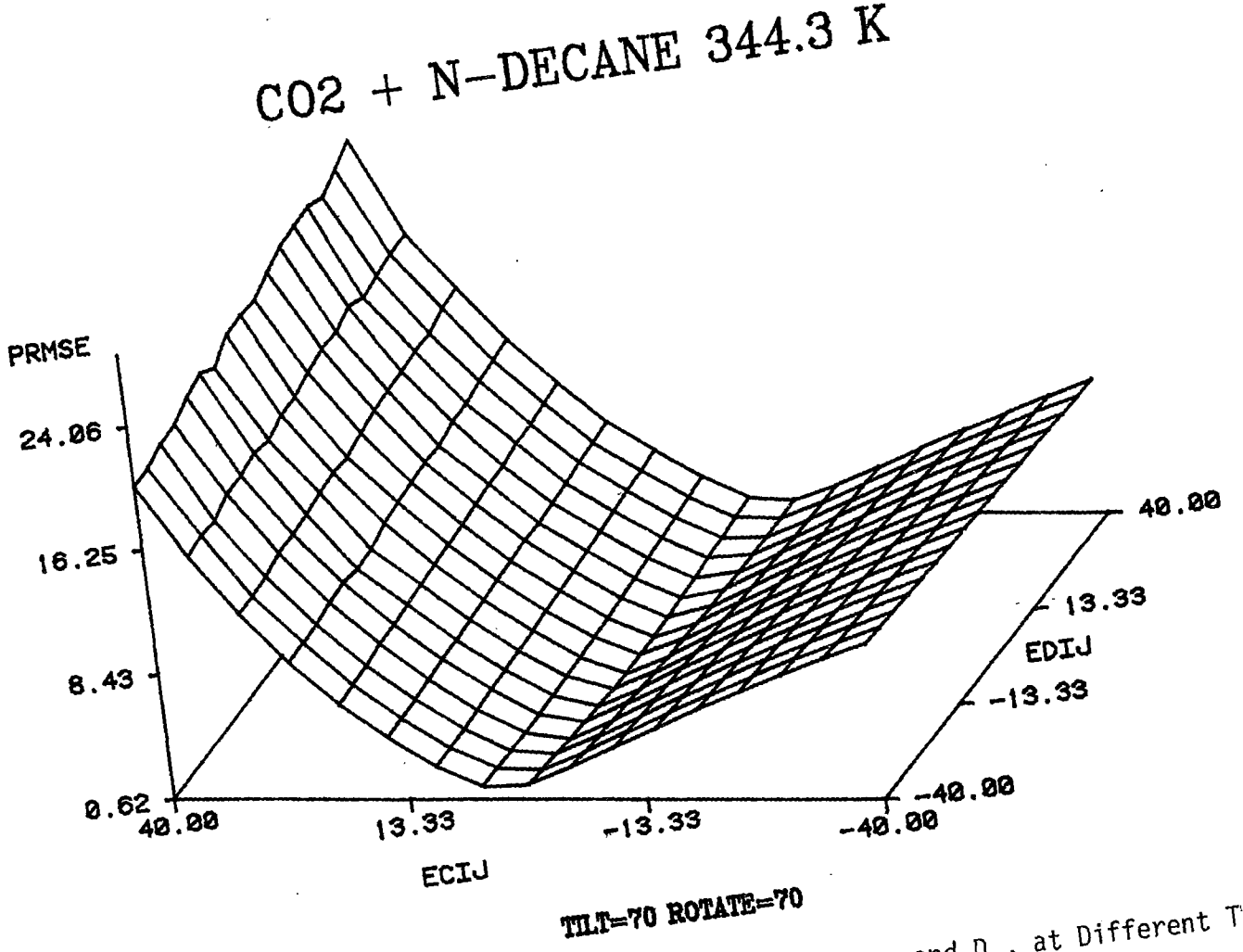

Figure 34. Sensitivity of SRK BPP Predictions to C_{ij} and D_{ij} at Different Temperature

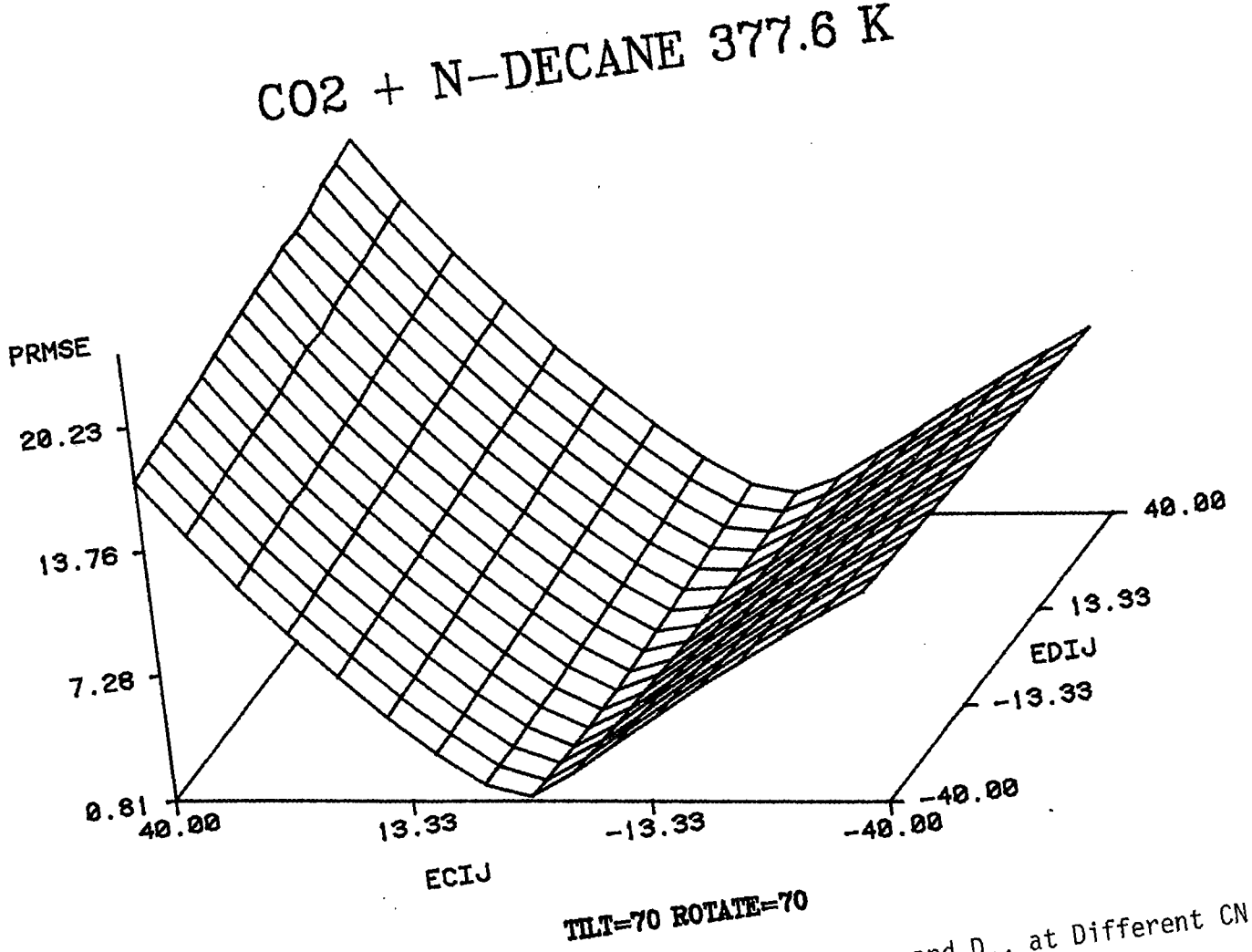

Figure 35. Sensitivity of SRK BPP Predictions to C_{ij} and D_{ij} at Different CN

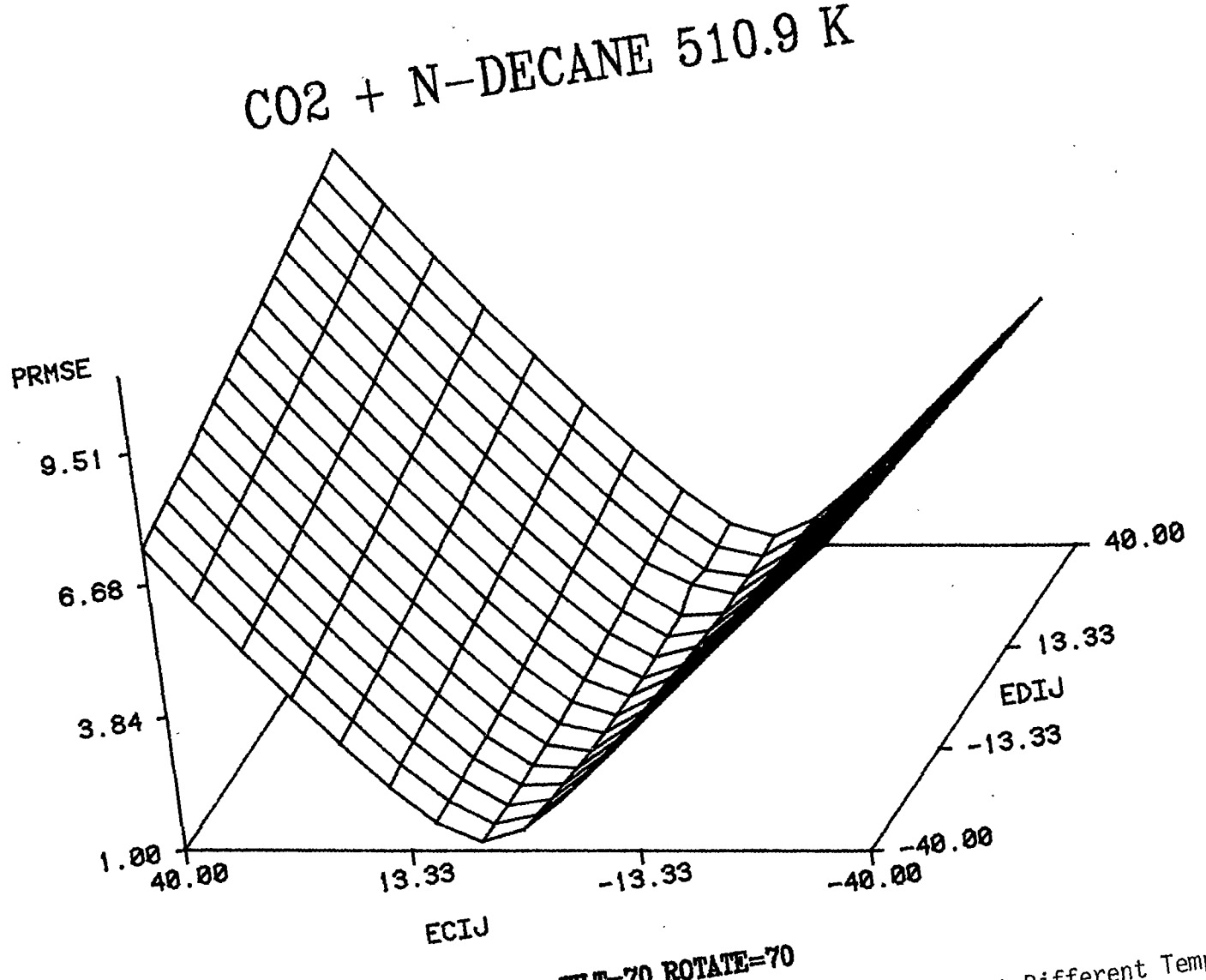

Figure 36. Sensitivity of SRK BPP Predictions to C_{ij} and D_{ij} at Different Temperature

EOS as indicated by Table XXXIII. Similarity in over-all statistics and the general tendencies for the optimun interaction parameters obtained is well established for the systems considered. However, comparison of interaction parameter values obtained from the two equations reveals that PR EOS employs slightly lower C_{ij} and D_{ij} values as indicated by the results given in Appendix C for this equation.

Comparisons of molar volume predictions appear in the next section.

Fluid Volume Predictions

Fluid volume predictions are a major weakness in the application of cubic EOS despite the improvement realized by PR EOS for many systems. To overcome this deficiency, some investigators (79,73) have introduced a third constant into the EOS. Perhaps the most attractive approach is that of volume translation, as was suggested by Martin (79), to improve pure fluid volume predictions. This stems from the fact that a separation between the equilibrium and volume calculations can be achieved as was further illustrated by Peneloux, et al. (80), for both pure fluids and mixtures.

Evidence has shown (80) that a translation along the volume axis of the form:

$$V = V - \sum_{i=1}^{N} A_i x_i \qquad (9.16)$$

leads to changes in the predicted volume without affecting the equilibrium property predictions (fugacity). Peneloux (80) related the volume correction constant, A_i, to the pure component Rackett compressibility factor, ZRA, by matching experimental saturated liquid

densities at Tr=0.7 for n-alkanes up to n-decane. Accordingly, the following correlation was advanced for the SRK EOS correction term:

$$A_i = a_1 \left(\frac{RT_c}{P_c}\right)(a_2 - ZRA_i)$$

Where values for a_1 and a_2 are given in Table XXXVI.

Table XXXV presents a summary of the results for molar volume predictions of some CO_2 + n-paraffin systems for which experimental data are available. Variations in the quality of the predictions due to volume translation or alteration of the values used for the interaction parameters (C_{ij} and D_{ij}) are also included in Table XXXV for the following specific case:

Case	Description
A	Using $C_{ij} = D_{ij} = 0$ and the original correlation parameters (Equation (9.16)) as given by Peneloux (80).
B	Using optimum $C_{ij}(T)$ and $D_{ij}(T)$ given in Table XXXII along with the original correlation parameters.
C	Using common C_{ij} and D_{ij}; constant values for C_{ij} and D_{ij} for all systems considered: SRK EOS $C_{ij} = 0.128$ $D_{ij} = -0.020$ PR EOS $C_{ij} = 0.085$ $D_{ij} = -0.024$
A*,B*	As in Cases A and B but using new correlation parameters obtained by fitting the data given in Tables XXXV and XXXVIII.

As indicated by the overall %AAD, substantial improvement in liquid molar volume predictions are realized by volume translation, practically

TABLE XXXV

MOLAR VOLUME PREDICTIONS FOR CO2 + n-PARAFFINS
USING SRK EOS

Case	CN	T(K)	ZRA	% AAD No Vol Tran V^{ℓ}	% AAD No Vol Tran V^{v}	% AAD Vol Tran V^{ℓ}	% AAD Vol Tran V^{v}	No. Pt.	Ref.
A	10	277.6	0.2510	21.1	99.1	1.4	98.7	11	12
B				23.0	2.7	3.4	2.4		
A*						1.4	98.6		
A	10	310.9	0.2510	22.9	106.2	5.7	104.9	12	12
B				24.2	20.6	7.0	19.2		
A*						5.2	104.7		
A	10	344.3	0.0251	16.8	58.7	5.6	58.3	9	12
B				18.9	5.7	6.7	3.9		
A*						5.0	58.3		
A	10	377.6	0.2510	19.2	45.2	3.5	44.7	11	12
B				20.7	3.6	4.2	1.9		
A*						2.5	44.6		
A	10	410.9	0.2510	20.2	40.3	4.8	38.1	12	12
B				20.1	4.8	4.6	3.0		
A*						3.5	37.9		
A	10	444.3	0.2510	20.7	34.5	5.8	32.3	12	12
B				21.1	5.8	5.2	4.0		
A*						4.3	32.0		
A	10	477.6	0.2510	21.1	30.8	7.1	28.0	12	12
B				20.4	8.2	6.5	5.6		
A*						5.7	27.7		
A	10	510.9	0.2510	22.6	30.3	9.0	27.3	10	12
B				21.3	8.2	7.9	5.9		
A*						7.6	27.1		
A	22	323.1	0.2241	47.7		4.9		14	19
B				47.2		4.4			
A*						1.3			
A	22	348.1	0.2241	47.1		4.2		19	19
B				46.4		3.5			
A*						1.2			
A	22	373.1	0.2241	45.3		2.8		11	19
B				44.8		2.4			
A*						1.7			
A	32	348.1	0.2213	54.7		6.5		11	19
B				53.9		5.7			

TABLE XXXV (Continued)

Case	CN	T(K)	ZRA	% AAD No Vol Tran V^{ℓ}	% AAD No Vol Tran V^{v}	% AAD Vol Tran V^{ℓ}	% AAD Vol Tran V^{v}	No. Pt.	Ref.
A*						1.7			
A	32	373.1	0.2213	52.9		5.7		11	19
B				52.0		4.8			
A*						1.1			
A	32	398.1	0.2213	51.8		4.9		15	19
B				51.0		4.1			
A*						1.2			

	Overall %AAD				Total No. Pt.
Case A	31.4	56.4	5.1	28.7	V^{ℓ}= 170
Case B	31.4	7.5	4.2	5.8	
Case A*			2.9	28.6	V^{v}= 65
Case B*			2.4	5.2	
Case C			2.3	11.7	

Only overall statistics are given for Cases B* and C.

independent of the values used for C_{ij} and D_{ij}. This is signified by a reduction in %AAD, from 31.4 for the original SRK predictions to 5.1 using corrected volumes. For vapor molar volume predictions, although acceptable deviations are obtained using optimum C_{ij} and D_{ij} values, still some improvement is attained when applying volume translation, as indicated by the reduction in %ADD from 7.5 to 5.8 (Case B).

In an attempt to further improve the molar volume predictions, the proposed correlation, as expressed by Equation (9.17), was refitted using experimental mixture molar volumes available for the CO_2 + n-paraffin systems reported. Table XXXV shows that favorable results are obtained as indicated by an overall %ADD of 2.4 and 5.2 for the liquid and the vapor respectively (Case B*). Original and refitted correlation parameters for Equation (9.17) are given in Table XXXVI for both the SRK and PR EOS.

Regarding the effect of binary interaction parameters on the corrected molar volume predictions, the results obtained indicate that, while liquid molar volumes are effected slightly by the values used for C_{ij} and D_{ij}, vapor molar volume predictions are quite sensitive to such values. Nevertheless, using common interaction parameters for all CO_2 + n-paraffin systems considered (Case C) produces comparable results for the liquid molar volumes (as shown in Table XXXV), and deviations for the vapor molar volumes double those obtained using optimum C_{ij} and D_{ij}.

Finally, comparison of PR and SRK EOS molar volume prediction, without volume translation, confirms the superiority of the former as

TABLE XXXVI

CORRELATION PARAMETERS FOR
VOLUME TRANSLATION

		Parameters for Equation (9.16)			
EOS	CASE	Original Ref. (80)		Refitted	
		a_1	a_2	a_1	a_2
SRK	A	.40768	.29441	.44943	.29441
	B	----	----	.44943	.29441
	C	----	----	.44943	.29441
PR	A	----	----	.30483	.29441
	B	----	----	.30483	.29383
	C	----	----	.30483	.37531

shown in Table XXXVII. However, applying volume translation to the volumes obtained from the two equations brings equality of predictive abilities as signified by an identical overall %ADD for both liquid and vapor volumes (2.4 and 5.2 respectively).

Sensitivity Analysis

The confidence placed in the estimates given, be it the EOS regressed parameters (C_{ij}, D_{ij}) or the predicted variables, is a direct reflection on the model and the experimental data used. Uncertainty in such estimates is attributable to three sources of variations, or errors. These are: (1) errors in the experimental data (x, P); (2) errors in the model input data, which are in this case the critical properties and the acentric factor (T_c,P_c and ω); and finally (3) errors due to lack of fit, or model deficiency, which according to the previous discussion can be assumed insignificant if $C_{ij}(T)$ and $D_{ij}(T)$ are used simultaneously. The assertion made about the last factor (regarding the absence of lack of fit) allows statistical treatment for the other two factors.

While variations due to experimental data (x, P) are accounted for by the standard errors for C_{ij} and D_{ij}, special efforts are needed to investigate the effects of errors in the EOS input variables (since the complexity of the model considered precludes the possibility of error propagation analysis).

Statistical treaties have established that the ability to draw certain inferences regarding the reliability of a given estimate obtained is affected by three different elements (81): the estimate mean value (μ), the estimate variance (σ) and the probability

TABLE XXXVII

MOLAR VOLUME PREDICTIONS FOR CO2 + n-PARAFFINS
USING PR EOS

				% AAD					
				No Vol Tran		Vol Tran			
Case	CN	T(K)	ZRA	V^{ℓ}	V^{v}	V^{ℓ}	V^{v}	No. Pt.	Ref.
A	10	277.6	0.2510	7.8	93.1	6.9	92.2	11	12
B				9.5	1.8	5.2	17.5		
A	10	310.9	0.2510	9.3	96.5	9.0	95.4	12	12
B				11.3	16.0	7.8	14.9		
A	10	344.3	0.0251	8.3	52.0	9.3	52.0	9	12
B				9.0	2.4	7.1	2.5		
A	10	377.6	0.2510	7.0	38.4	5.1	37.9	11	12
B				7.3	26.9	4.5	3.4		
A	10	410.9	0.2510	7.8	31.5	4.1	29.6	12	12
B				7.5	1.9	4.1	2.8		
A	10	444.3	0.2510	8.5	26.8	3.8	24.4	12	12
B				7.6	20.8	3.5	2.0		
A	10	477.6	0.2510	9.5	22.7	3.7	20.4	12	12
B				8.1	42.5	2.9	2.6		
A	10	510.9	0.2510	10.8	21.9	2.6	19.5	10	12
B				8.8	2.62	2.0	15.5		
A	22	323.1	0.2241	32.0		0.7		14	19
B				31.7		0.6			
A	22	348.1	0.2241	31.5		0.9		19	19
B				30.9		1.2			
A	22	373.1	0.2241	29.9		1.9		11	19
B				29.5		2.3			
A	32	348.1	0.2213	38.7		2.6		11	19
B				38.0		2.0			
A	32	373.1	0.2213	37.1		1.8		11	19
B				36.3		1.0			
A	32	398.1	0.2213	36.1		1.2		15	19
B				35.3		0.6			

	Overall %AAD				Total No. Pt.
Case A	20.7	48.5	3.5	24.8	V^{ℓ} = 170
Case B	20.4	15.4	2.4	5.2	V^{v} = 65
Case C			4.0	10.5	

Only overall statistics are given for Case C.

distribution for the errors in the estimate (F(x)).

The objective in this section is to briefly explore the influence of the variations in input variables on the predicted property, namely the BPP for the CO_2 + n-paraffin systems. To achieve such an objective a statistical procedure was implemented to provide answers to the following questions:

1) For a given level of error in input variables (T_c, P_c and ω) what is the range of error in the predicted variable as signified by BPP RMSE?
2) For a given level of confidence, e.g. 95%, what is the range of error in the predicted variable (BPP) RMSE at fixed level of error in the input variables (T_c, P_c, ω)?
3) For a given confidence level for BPP RMSE, what is the range for the C_{ij} and D_{ij} values?
4) Which input variable or input parameter most affects the value of the predicted variable?

The Statistical Procedure Used

The most widely used approach in conducting sensitivity or risk analysis is based on the method of statistical trials (83,84), or as more commonly called Monte Carlo simulations. Using this method involves the introduction of real random fluctuations in the input variables or model parameters under study. For such a purpose, a random number generator and an assumed error distribution are employed by knowing the amount of variation or the uncertainty in each input variable. The overall uncertainty in the predicted variable may be obtained by performing as many simulations as deemed necessary.

The main drawback in using this method is the computational cost involved, especially when dealing with an iterative procedure such as that used in EOS predictions. Accordingly, for the purposes of this study a limited number of simulations are performed using maximum expected errors in the the input variables as fluctuations to the nominal input values. And while this approach does not account for the stochasticity of the error variations, it does provide reasonable estimates for the desired statistics and illustrates the synergistic effects of different sources of errors.

To estimate the overall uncertainty, as well as the confidence interval for the BPP RMSE, C_{ij}, and D_{ij} the following statistical procedure was employed:

1. Using the nominal input variables (T_c, P_c and ω), regressed $C_{ij}(T)$ and $D_{ij}(T)$ were obtained along with estimates for their standard errors ($S_{C_{ij}}$, $S_{D_{ij}}$). Values obtained for C_{ij} and D_{ij} in this step were later used as nominal input parameters.
2. Variations in the input variables (T_c, P_c and ω) were introduced as fluctuations about the nominal values. These variations were given the values of 0.0, $3S_i$ and $-3S_i$, consecutively, expressed as percentages of the nominal values used. Estimates used for S_i were based on the results of Chapter VI dealing with pure fluid properties.
3. Variability due to experimental data (x, P) was simulated using standard errors in C_{ij} and D_{ij} obtained during data reduction as fluctuations to the parameter nominal values as was done in step (2).

4. Estimates for the mean, maximum and minimum BPP RMSE were then obtained along with the standard deviations for the input variables, C_{ij} and D_{ij}.
5. The standardized probability distribution for the BPP RMSE, C_{ij} and D_{ij} were then calculated according to the following definition (82) :

$$F(Z) = 1/\sqrt{2\pi}\ EXP\ (-\ Z^2/2) \tag{9.17}$$

where

$$Z = (X - \mu)/\sigma \tag{9.18}$$

The normal error distribution is assumed and a squared standard deviation was used to estimate the variance.

6. The confidence interval for the variable of interest, corresponding to any confidence level, is defined as (82):

$$\bar{X} - Z\ \sigma/\sqrt{n} \leq \mu \leq \bar{X} + Z\ \sigma/\sqrt{n} \tag{9.19}$$

where Z is the standard normal deviate which may be obtained from cumulative normal tables. Accordingly, the 95% confidence limits for estimating BPP RMSE may be calculated as:

$$\text{Mean BPP RMSE} - 1.96\ S_{\text{BPP RMSE}} / \sqrt{n} \leq \mu \leq \text{Mean BPP RMSE} + 1.96\ S_{\text{BPP RMSE}}/\sqrt{n} \tag{9.20}$$

where n is the number of simulations performed.

Assumption of normality for the probability distribution is quite reasonable according to the central limit theorm (82), since this analysis deals with sample means. Figure 37 presents a typical distribution curve obtained for the n-C_{36} system. Normality for the error distribution allows for simple mathematical manipulation to draw inferences regarding the estimates obtained.

Results and Discussion

The results of the sensitivity analysis performed on both pure n-paraffins and CO_2 + n-paraffins are discussed in this section. Sample simulations runs are included in Appendix D.

Table XXXVIII presents the results of sensitivity analysis for the pure n-paraffins normal boiling point pressure predictions for the systems considered. Average variations of 5% about the experimental values are observed for all paraffins (with slightly worse deviations for the heavy paraffins) when the expected random errors in T_c, P_c and ω are used. By comparison using an error level of about 10% for all input variables produces significantly higher deviations, up to 53% as seen for n-C_{36}. With regard to heavy paraffins, this inflated error level in the input variables is quite reasonable considering the fact that most estimates for such properties are obtained through extrapolation of lower paraffin experimental data. However, one may be reassured in this case by observing similar variations in the predicted BPP for both the heavy and light paraffins, as indicated by the sensitivity analyses for the the n-C_{10} and n-C_{36} system given in Tables XXXVIII. This is

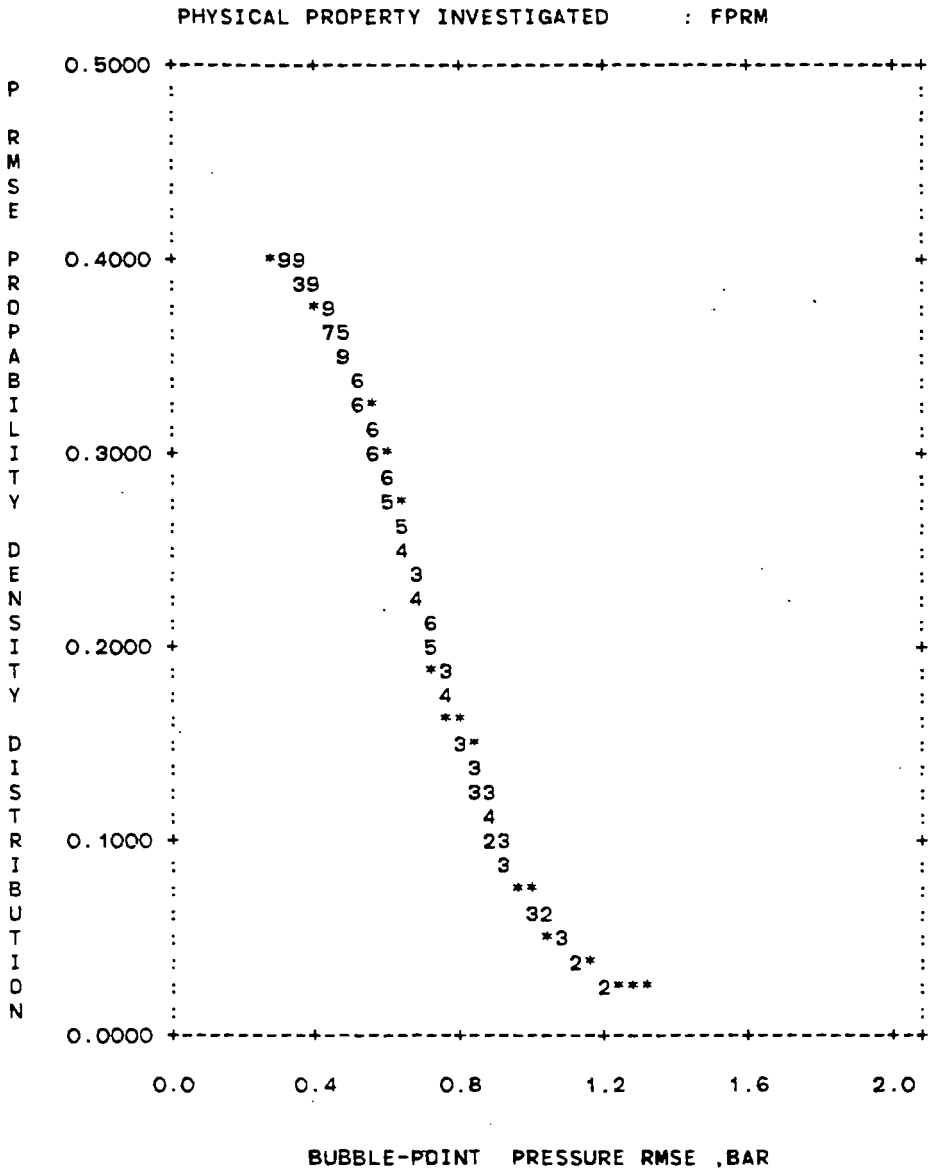

Figure 37. Normal Probability Distribution for BPP RMSE of n-C_{36} at the Normal Boiling Point

TABLE XXXVIII

EFFECT OF VARIATIONS IN THE INPUT VARIABLES ON THE SRK NORMAL BOILING POINT PREDICTIONS FOR n-PARFFINS

System	T_b, K	Error Level in T_c, P_c, ω (%)	BPP RMSE, bar		
			$\hat{\mu}$	$\hat{\sigma}$	%Error
$n\text{-}C_4$	272.65	0.5, 1., 2.	0.0396	0.0374	4.0
$n\text{-}C_{10}$	447.27	0.5, 1., 2.	0.0443	0.0476	4.4
		5., 10., 10.	0.4393	0.5333	43.9
$n\text{-}C_{20}$	617.78	0.5, 1., 2.	0.0499	0.0467	5.0
$n\text{-}C_{28}$	706.35	0.5, 1., 2.	0.0526	0.0472	5.3
$n\text{-}C_{36}$	770.74	0.5, 1., 2.	0.0523	0.0517	5.2
		5., 10., 10.	0.5297	0.6487	53.0
$n\text{-}C_{44}$	818.82	0.5, 1., 2.	0.0519	0.0578	5.2

indicative of consistent pure property prediction using the ABC correlation.

Regarding BPP predictions for CO_2 binaries, simulation runs were performed on n-C_{10} and n-C_{36} (at close temperatures) thus representing both light and heavy paraffins. The results of the simulation runs given in Table XXXIX indicate the following to be true for the two systems considered, and probably so for all CO_2 + n-paraffins in general:

1) Expected levels of variability in the input variables T_c, P_c and ω prior to interaction parameters regression has no effect on the resultant BPP RMSE, and only minor effects on the values obtained for C_{ij} and D_{ij} (Case 0). Such variations at fixed level of C_{ij} and D_{ij}, however, contribute an additional 33% to the nominal values for BPP RMSE and to the C_{ij} standard deviations (Case 2).
2) Using the interaction parameters standard error obtained during regression (due to variations in experimental (x, P) data, Case 3) simulate reasonably well (within 10%) the amount of variations in the actual (x, P) data as given by Case 1.
3) Excessive variability in input variables (T_c, P_c, ω at 5% error level) about triples the amount of observed RMSE for the two systems considered, as signified by Case 2*. Such variations, however, have more pronounced effects on the n-C_{10} system than those observed for n-C_{36}, a fact which may attributed to the near-critical points in the n-C_{10} data system.
4) Variation of 10% in the values of C_{ij} and D_{ij} used resulted in a two-fold increase in the observed BPP RMSE as indicated by

TABLE XXXIX

ESTIMATES SENSITIVITY ANALYSIS FOR CO_2 + n-PARAFFINS TEST SYSTEMS

Case	Variations Due to	BPP RMSE, BAR $\hat{\mu}$	BPP RMSE, BAR $\hat{\sigma}$	NRMSE	C_{ij} $\hat{\mu}$	C_{ij} $\hat{\sigma}$	D_{ij} $\hat{\mu}$	D_{ij} $\hat{\sigma}$	x_{CO_2} $\hat{\mu}$	x_{CO_2} $\hat{\sigma}$	NRMSE
					$n\text{-}C_{10}$ @ 344.3 K						
Input variables error levels: T_c = 0.5%, P_c = 1.0%, ω = 2.0%, C_{ij} = 0.6%, D_{ij} = 7.6%											
0	x, P	0.6215		1.00	.1069	.0006	.0202	.0015	.0044	.0002	1.00
1	x, P, T_c, P_c, ω	0.6215	0.0652		.1069	.0008	.0202	.0016			
2	T_c, P_c, ω	0.8546	0.3347	1.38	.1069		.0202		.0059	.0020	1.34
2*	T_c, P_c, ω(all 5%)	4.213	2.079	6.79	.1069		.0202				
3	C_{ij}, D_{ij}	0.6783	0.0642	1.09	.1069	.0005	.0202	.0013	.0049	.0125	1.11
3*	C_{ij}, D_{ij}(all 10%)	2.325	2.079	3.74	.1069		.0202		.0148	.0125	3.39
4	T_c,P_c,ω,C_{ij},D_{ij}	0.8888	0.3701	1.43	.1069	.0005	.0202	.0013			1.50

TABLE XXXIX (Continued)

Case	Variations Due to	BPP RMSE, BAR $\hat{\mu}$	BPP RMSE, BAR $\hat{\sigma}$	NRMSE	C_{ij} $\hat{\mu}$	C_{ij} $\hat{\sigma}$	D_{ij} $\hat{\mu}$	D_{ij} $\hat{\sigma}$	x_{CO_2} $\hat{\mu}$	x_{CO_2} $\hat{\sigma}$	NRMSE
					$n\text{-}C_{36}$ @ 373.2 K						
Input variables error levels: T_c = 0.5%, P_c = 1.0%, ω = 2.0%, C_{ij} = 4.5%, D_{ij} = 6.6											
0	x, P	0.2897		1.00	.0948	.0043	-.0152	.0010	.0021	.0000	1.00
1	x, P, T_c, P_c,ω	0.2897			.0948	.0052	-.0152	.0011	.0024	.0005	1.14
2	T_c, P_c, ω	0.3585	0.0934	1.24	.0948		-.0152				
2*	T_c, P_c, ω (all 5%)	0.8741	0.7335	3.02	.0948		-.0152				
3	C_{ij}, D_{ij}	0.5222	0.2936	1.84	.0948	.0035	-.0152	.0008	.0035	.0000	1.67
3*	C_{ij}, D_{ij} (all 10%)	0.8799	0.7425	3.04	.0948	.0077	-.0152	.0012	.0056	.0000	2.67
4	T_c, P_c, ω, C_{ij},D_{ij}	0.5626	0.3651	1.94	.0948	.0035	-.0152	.0008			2.00

NRMSE = (RMSE/RMSE of Case 0)

Case 3. Such sensitivity would preclude rough estimates of C_{ij} and D_{ij} from being useful in obtaining accurate EOS predictions.

5) Inclusion of expected variations for C_{ij} and D_{ij}, as represented by $S_{C_{ij}}$ and $S_{D_{ij}}$ in addition to variations in T_c, P_c and ω resulted in 67% increase in the RMSE as indicated by Case 4. The added deviations are indicative of the presence of synergistic effects even at moderate levels of error.

6) The value used for the critical temperature, T_c, has greater influence on the EOS predictions than observed for P_c or ω.

Figures 38 and 39 present the regressed parameters obtained for some of the systems considered in this study (T about 373 K) along with the estimated uncertainty accounting for all input variables. Inspection of the amount of variability suggests an average error of about 0.005 for C_{ij} and 0.001 for D_{ij} may be adequate for the systems considered.

Comparable sensitivity analysis for the effects of variations of input variables on the solubility predictions, also given in Table XXXIX, reveals similar overall tendencies to those observed for the BPP predictions. Accepting that for heavy n-paraffins the vapor phase tends to be almost pure CO_2, this would indicate the sensitivity of K-value predictions to the input variables including C_{ij} and D_{ij}; a contradiction to conclusions drawn by previous investigators (2,5) asserting the low sensitivity of K-value predictions to the interaction parameters used.

As indicated by Table XL, while K-value predictions for the light paraffins show some tolerance to variations in C_{ij} values used, as exemplified by an increase of 0.02 in the value C_{ij} for n-C_4 system,

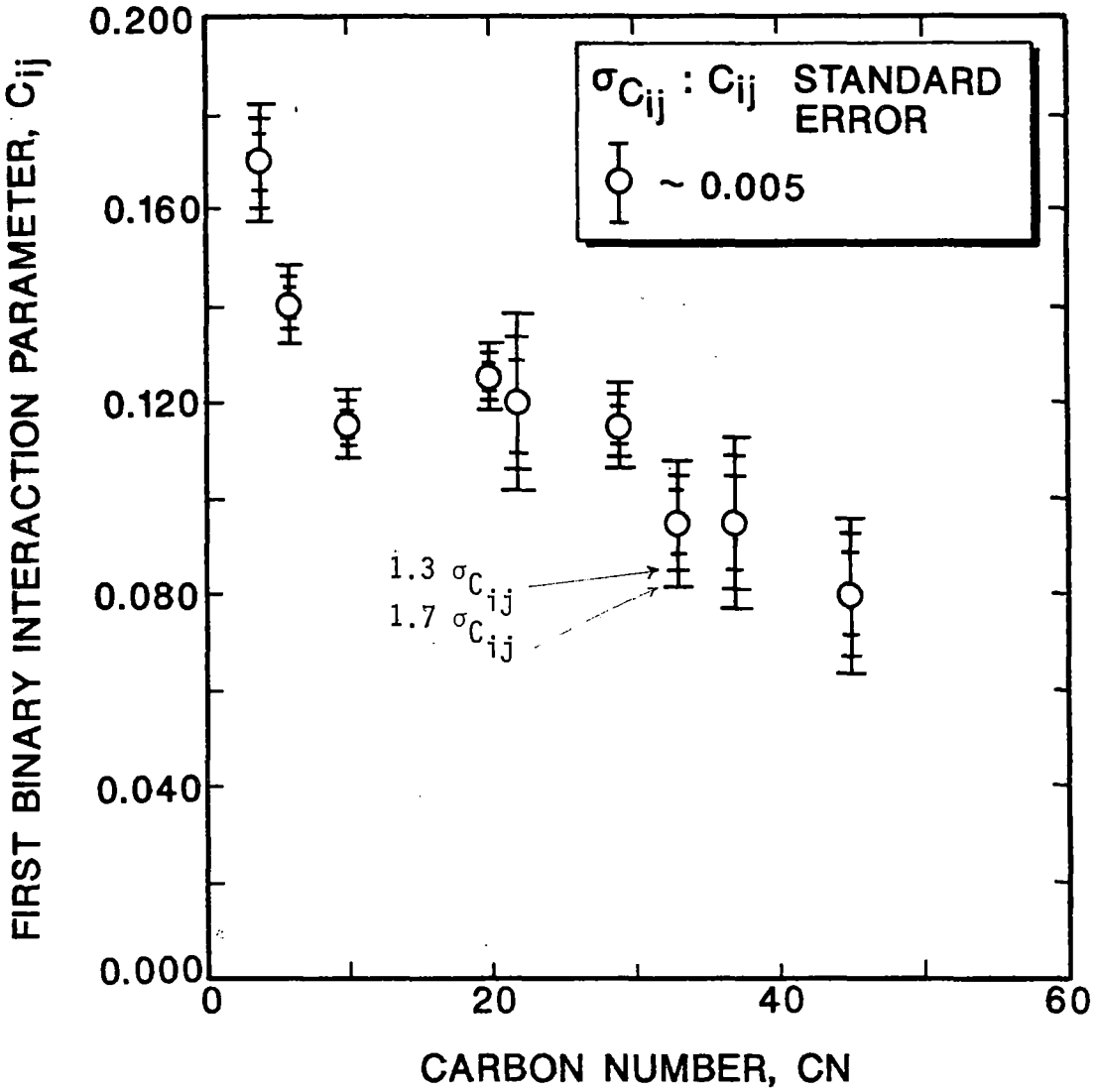

Figure 38. Effects of Input Data Variations on C_{ij} Values

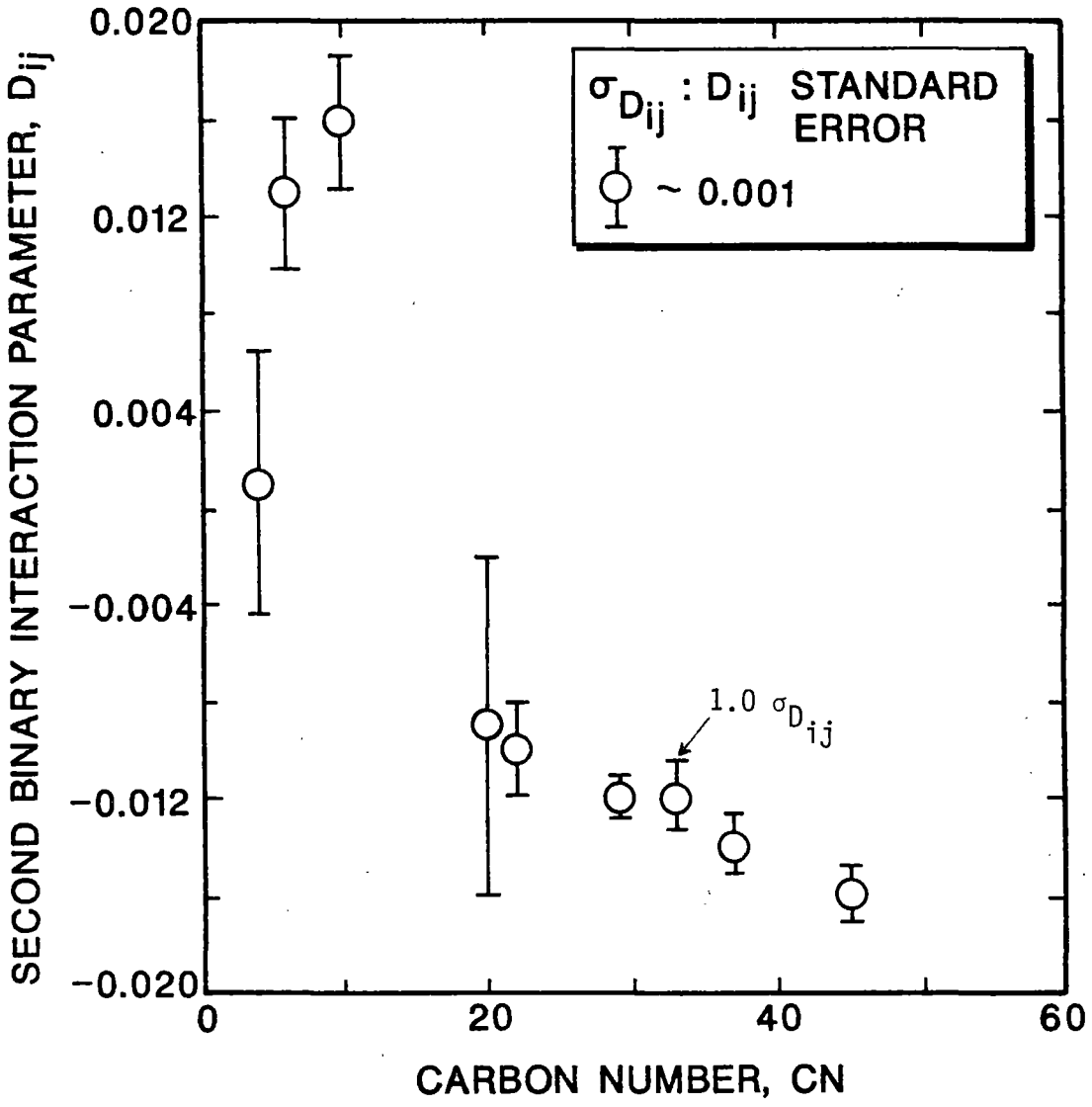

Figure 39. Effects of Input Data Variations on D_{ij} Values

such a level of error would certainly lead to unacceptable deviations for the heavier paraffins. Furthermore, for BPP predictions even for the lighter systems, 0.02 variation in C_{ij} would about double the BPP RMSE and %AAD.

TABLE XL

SENSITIVITY OF K-VALUE PREDICTIONS TO VARIATIONS IN THE C_{ij} VALUE (CO_2 + n-C_4, 311-411 K, REF. 12)

		BPP RMSE	%AAD		
CASE	PARAMETERS	BAR	BPP	K_{CO_2}	K_{n-C_4}
1	C_{ij} = .1472	0.86	1.4	6.2	3.9
2	C_{ij} = .1672	1.49	3.4	6.1	5.4
3	$C_{ij}(T)$, $D_{ij}(T)$	0.29	0.60	2.6	3.2

Parameter Generalization

The advantages offered by generalized EOS parameters in enhanced oil recovery simulations and many other calculations encountered in the petrochemical industry (such as when dealing with coal liquids) continue to generate ample interest in the development of generalized parameters correlations. This is particularly so when dealing with relatively simple equations of state such as the VDW type equations. Generalized parameters offer capabilities for interpolation and extrapolation to

conditions or systems for which no experimental data exist. Otherwise, this task is achieved by accessing numerous data tabulations leading in some cases to erroneous conclusions (3). This fact, along with the desired computational simplicity afford by such generalized correlations, makes them an attractive alternative.

Two distinct approaches have been followed in the literature. While the first approach considers soley the development of correlations for the optimum equation of state parameters (such as those presented in Table XXVII) in terms of some pure solvent properties (2,4,87). The second approach is more general and considers both the interaction parameters and the pure component parameters Ω_a and Ω_b of Equations (9.3, 9.4) (3,84,85). The additional effort is made to provide a better means for extrapolating the RK-type EOS constants a and b of Equations (9.3, 9.4) to temperatures above the light component critical temperature.

And while the motivations for parameter generalization are evident, the choice of correlating variables for such generalizations has been in most cases rather arbitrary. These include the critical properties, the acentric factor, the solubility parameter difference, the ionization potential or combinations these such as the cohesive energy parameter "a" of Equation (9.2), (2,86).

Addressing only CO_2 + hydrocarbon systems and considering first attempts made to correlate C_{ij}, Graboski (2) proposed the use of the solubility parameter difference as the correlating variable for the SRK interaction parameter. Thus, a temperature-independent correlation was given with a reported average BPP error of 14.6 psia for systems having carbon numbers up to n-decane. Concurrently, Huron, et al. (4)

concluded that a correlating scheme was not obvious for C_{ij} involving the binary systems they considered. Ezekwe (87) used a combination of the acentric factor and the solubility parameter difference to give a correlation for the SRK EOS interaction parameter C_{ij} for CO_2 binaries involving several hydrocarbons. Similar to Graboski's, the proposed correlation used a temperature-independent C_{ij}. In contrast to this, Kato, et al. (4) advanced a temperature-dependent correlation for the PR equation of state employing the acentric factor as the solvent characterization parameter. The C_{ij} values obtained from the correlation yielded a better fit to experimental data than that obtained using a temperature-independent values for C_{ij}. A drawback to this correlation, as was pointed out by Lin (5), is its failure to properly predict C_{ij} for CO_2 + non-paraffin systems. This is an expected state of affairs, since the correlation was based on normal paraffins extending to n-decane.

Lin (5), in a study devoted mainly to the PR equation of state interaction parameters, argued that there is no need to treat C_{ij} as temperature dependent in VLE calculation involving CO_2 + hydrocarbon mixtures. A proposed constant value for C_{ij} = 0.125 was suggested for such systems to preserve the inherent simplicity attributed to RK equations of state.

Using the second approach, where parameter generalization includes Ω_a and Ω_b of Equations (9.3, 9.4), Yarborough (88) applied the procedures proposed by Zudkevich and Joffe (65), and Chang and Lu (66) to advance correlations for Ω_a and Ω_b of the original RK equation in terms of reduced temperature and hydrocarbon acentric factor. The result was a correlation for Ω_a and Ω_b for hydrocarbons and other non-

polar components (CO_2, H_2S, N_2) for which critical properties are available or can be estimated. A limitation was placed on the applicability of such correlation to components not heavier than n-decane.

An extension to this work applied particularly to binaries involving CO_2 was given by Turek, et al. (3). This used modified mixing rules to include a second interaction parameter, D_{ij}. Also, a generalization was obtained for C_{ij} and D_{ij} simlutaneously with Ω_{a,CO_2} and Ω_{b,CO_2} for temperatures greater than the CO_2 critical temperature. While C_{ij} and D_{ij} were correlated in terms of the hydrocarbon acentric factor, Ω_{a,CO_2} and Ω_{b,CO_2} were made functions of CO_2 reduced temperature; this was observed to reduce the temperature dependence in the binary parameters C_{ij} and D_{ij} used to fit the binary VLE data.

Generalization Scheme

An inspection of Tables XXVIII and XXXII indicates that for most systems considered a temperature dependence for the interaction parameter(s) is definitely present. This is particularly true for the binaries involving larger molecules. And although a pressure dependence is not considered here, its influence on the interaction parameter values obtained can be detected by regressing data at different pressure levels. For example, Huron (6) observed a significant difference between C_{ij} values obtained from the critical loci and those obtained for VLE data.

Addressing only the temperature influence on the equation of state interaction parameters, the correlating variables are thus the temperature and the hydrocarbon solvent characterization parameter(s).

Two generalization schemes were pursued in the present work. First, the interaction parameter(s) C_{ij} or C_{ij} and D_{ij} were generalized as continuous functions of temperature and the solvent carbon number or other solvent properties. Secondly, the suggestions of Turek (3) were followed in surpressing the interaction parameter temperature-dependence by generalizing Ω_{a,CO_2} and Ω_{b,CO_2} as functions of the CO_2 reduced temperature. This allowed for the generalization of C_{ij} and D_{ij} only in terms of pure solvent properties.

1. Interaction Parameters Generalization

Although different correlating schemes were considered involving various combinations of hydrocarbon pure properties as correlating variables, only two correlations were judged worthy of pursuit and are thus presented in Table XLI. As indicated by Equations (9.21-9.24), the first correlation uses the solvent carbon number (a natural choice when dealing with n-paraffins) as a characterization parameter, while the second correlation employs the hydrocarbon reduced temperature and the acentric factor. To apply the first correlation to other hydrocarbons, such as aromatics, however, would require an effective carbon number characterization.

The interaction parameter temperature dependence in both correlations is expressed as a perturbation to temperature independent "lumped" interaction parameters, C_{ij} or D_{ij}. This approach allows for testing of a correlative scheme with a trend of increasing complexity. First, a test is made using common CO_2 + n-paraffin interaction parameters ($\overline{C}_{ij}$ or $\overline{C}_{ij}$ and $\overline{D}_{ij}$), then lumped parameters ($C_{ij}(\omega)$ or $C_{ij}(\omega)$ and $D_{ij}(\omega)$) and so on until finally temperature-dependent

TABLE XLI

CORRELATIONS FOR C_{ij} AND D_{ij} GENERALIZATION

No.	Correlation	
1	$C_{ij} = C_{ijo} (1 + A_4 (T - 212))$	(9.21)
	where $C_{ijo} = A_1 + A_2 CN + A_3 CN^2$	
	$D_{ij} = D_{ijo} (1 + A_7 (T - 212))$	(9.22)
	where $D_{ijo} = A_5 + A_6 \ln CN$	
	and T (=) °F	
2	$C_{ij} = C_{ijo} [1 + T_{r,HC} (A_4 + A_5 \omega_{HC})]$	(9.23)
	where $C_{ijo} = A_1 + A_2 \omega_{HC} + A_3 \omega^2_{HC}$	
	$Dij = D_{ijo} [1 + T_{r,HC} (A_9 + A_{10} \omega_{HC})]$	(9.24)
	where $D_{ijo} = A_6 + A_7 \omega_{HC} + A_8 \omega 2_{HC}$	(9.25)

parameters ($C_{ij}(\omega,T)$ and $D_{ij}(\omega,T)$) are considered. This kind of progression in the generalization scheme is useful in determining the minimum required level of complexity and providing correlations which, though less precise, may be quite adequate for certain intended purposes.

As shown by Equations (9.21-9.24), account for C_{ij} and D_{ij} temperature dependences in the first correlation is reflected by deviations from a base temperature of 212°F, while by comparison the second correlation employs the hydrocarbon reduced temperature scale.

2. Pure CO2 Parameter Generalization

In contrast to previous studies (3,84,85) where the original RK equation was considered for parameter generalization, the Soave and Peng-Robinson values for the pure component parameters Ω_a and Ω_b were retained for the hydrocarbon solvent and for CO_2 at temperatures up to its critical, T_{c,CO_2}. For temperatures greater than T_{c,CO_2} the correlations given in Table XLII were considered for the modification of the CO_2 supercritical behavior of Ω_a and Ω_b.

3. Parameter Generalization Regressions

The binary interaction parameters C_{ij} and D_{ij} and the supercritical pure parameters Ω_a and Ω_b were determined simultaneously by unweighted least squares regressions. Following this approach, rather than developing a general expression for individually regressed interaction parameters, is useful in reducing the undesirable effects of the correlation that exist between the different parameters. The objective function minimized and the numerical routine used are those previously

TABLE XLII

CORRELATIONS FOR CO_2 Ω_a AND Ω_b GENERALIZATIONS

No.	Correlations	
1	$\Omega_a = A_8 + A_9 T_{r,CO_2} + A_{10} T_r^2{}_{,CO_2}$, $T > T_{c,CO_2}$	(9.25)
	$\Omega_b = A_{11} + A_{12} T_{r,CO_2} + A_{13} T_r^2{}_{,CO_2}$, $T > T_{c,CO_2}$	(9.26)
2	$\Omega_a = \Omega_{ac} [1 + A_{11}(1 - T_{r,CO_2}) + A_{12}(1 - T_{r,CO_2})^2 + A_{13}(1 - T_{r,CO_2})^3]$	(9.27)
	where $\Omega_{ac} = 0.42747$ (SRK) or 0.45724 (PR)	
	$\Omega_b = \Omega_{bc} [1 + A_{14}(1 - T_{r,CO_2}) + A_{15}(1 - T_{r,CO_2})^2 + A_{16}(1 - T_{r,CO_2})^3]$	(9.28)
	where $\Omega_{bc} = 0.08664$ (SRK) or 0.0778 (PR)	

described in Chapter VII for attaining the non-generalized regressed interaction parameters in Tables XXVI through XXVIII. The data base (of Table I) was employed to regress parameters in the above mentioned correlations, with the exception that the n-C_7 system and the 277.6 K isotherm of n-C_{10} were deleted. Deviations obtained from the excluded isotherms were considerably larger, and constituted an obvious departure from the quality of fit obtained considering the rest of the data.

The specific functional relations used for the correlated parameters are summarized in their most general forms in Table XLI and XLII. The various correlating schemes tested here were obtained by selectively setting some of the coefficients A_1 through A_{10} in Table XLIII to zero. These functions, in reference to the second correlations, permit C_{ij} and D_{ij} to be represented as functions of ω_{HC} only, $T_{r,HC}$ only, or both variables simultaneously.

The specific cases investigated are described in Table XLIII. The cases studied include correlations similar to those used by previous investigators. For example, Case 6 employs a constant value for C_{ij} for all systems, as suggested by Robinson (76) and Lin (5). Case 11 is similar to the form used by Kato (4), Case 14 is of a form similar to that used bt Turek, et al. (3). Notice that Cases 1-5, not included in Table LXIII, were discussed earlier when dealing with individually regressed parameters.

Results and Discussion

Table XLIV presents a summary of results of the different generalization schemes involving both the interaction parameters (C_{ij}, D_{ij}) and the pure CO_2 parameters (Ω_{a,CO_2}, Ω_{b,CO_2}).

TABLE XLIII

SUMMARY OF GENERALIZATIONS STUDIED

Case	Correlation Framework No.	Parameters (A_i) Retained in Equations of Tables XLI and XLII
6. $\overline{C}_{ij}$		A_1
7. $\overline{C}_{ij}$, $\overline{D}_{ij}$		A_1, A_6
8. $C_{ij}(\omega)$	2	A_1-A_3
9. $\overline{C}_{ij}$, $D_{ij}(\omega)$	2	A_1, A_6-A_8
10. $C_{ij}(\omega)$, $D_{ij}(\omega)$	2	A_1-A_3, A_6-A_8
11. $C_{ij}(\omega, T)$	2	A_1-A_5
12. $\overline{C}_{ij}$, $D_{ij}(\omega, T)$	2	A_1, A_6-A_{10}
13. $C_{ij}(\omega, T)$, $D_{ij}(\omega)$	2	A_1-A_8
14a. $C_{ij}(CN, T)$, $D_{ij}(CN, T)$	1	A_1-A_7
14. $C_{ij}(\omega,T)$, $D_{ij}(\omega,T)$	2	A_1-A_7
15a. $C_{ij}(CN)$, $D_{ij}(CN)$ $\Omega_a(T)$, $\Omega_b(T)$	1	A_1-A_2, A_5-A_6, A_8,-A_{13}
15. $C_{ij}(\omega)$, $D_{ij}(\omega)$ $\Omega_a(T)$, $\Omega_b(T)$	2	A_1-A_3,A_6-A_8, A_{11}-A_{16}
16a. $C_{ij}(CN, T)$, $D_{ij}(CN, T)$ $\Omega_a(T)$, $\Omega_b(T)$	1	A_1-A_{13}
16. $C_{ij}(\omega, T)$ $D_{ij}(\omega, T)$ $\Omega_a(T)$, $\Omega_b(T)$	2	A_1-C_{16}
17. See Kato, et al. (4)		
18. See Lin (5), $\overline{C}_{ij}$		A_1 = 0.125 for PR EOS

TABLE XLIV

SUMMARY OF RESULTS FOR SRK PARAMETER GENERALIZATIONS

Case	BPP , Bar					X_{CO_2}				
	RMSE	BIAS	AAD	%AAD	NRMSE*	RMSE	BIAS	AAD	%AAD	NRMSE*
6	6.09	-.101	4.64	12.22	10.00	0.0334	-.0008	0.0270	10.39	6.07
7	3.68	-1.67	2.92	7.51	6.03	0.0217	0.0078	0.0180	7.42	3.95
8	3.06	-.280	2.23	5.87	5.01	0.0184	0.0012	0.0142	5.61	3.35
9	1.98	-.319	1.46	3.60	3.25	0.0111	0.0014	0.0086	3.29	2.02
10	1.94	-.291	1.43	3.74	3.18	0.0113	0.0013	0.0086	3.46	2.05
11	2.59	0.054	1.85	5.02	4.25	0.0154	-.0013	0.0116	4.46	2.80
12	1.76	-.286	1.28	3.18	2.99	0.0100	-.0001	0.0076	3.00	1.82
13	1.34	-.139	1.02	2.74	2.20	0.0082	-.0003	0.0063	2.71	1.49
14	1.20	-.092	0.90	2.38	1.97	0.0078	0.0001	0.0059	2.41	1.42
14a	1.50	-.293	1.10	2.77	2.46	0.0087	0.0008	0.0064	2.64	1.58
15	1.43	-.118	1.07	3.07	2.34	0.0099	0.0004	0.0073	3.22	1.80
15a	1.46	-.107	1.10	3.16	2.39	0.0108	0.0008	0.0076	3.11	1.96
16	0.87	-.034	0.67	1.84	1.43	0.0056	0.0000	0.0044	1.78	1.02
16a	1.07	-.071	0.80	2.19	1.75	0.0078	0.0002	0.0054	2.16	1.41
17	2.80	.273	1.83	5.07	4.59	0.0169	-.0024	0.0117	4.46	3.07

* RMSE / (RMSE of Case 5)

TABLE XLIV (Continued)

CASE GENERALIZED PARAMETER CONSTANTS (A_i) :

	1	2	3	4	5	6	7	8
	9	10	11	12	13	14	15	16
6	0.1000							
7	0.128					-.0200		
8	0.96387D-01	0.12741500	-.13466D00					
9	0.11825D000	0.00000d000	0.00000d000	0.00000d000	0.00000D000	0.42938D-01	-.56492D-01	0.27903D-02
10	0.13949D000	-.69723D-01	0.48124D-01	0.00000d000	0.00000D000	0.34864D-01	-.32706D-01	-.12628D-01
11	0.12517D00	-.22570D00	0.38685D00	-.21290D000	0.75220D000			
12	0.11862D000	0.00000D-00	0.00000D000	0.00000D000	0.00000D000	0.33402D-04	-.18647D-04	-.31344D-04
12	0.17550D004	-.29614D003						
13	0.61025D-01	-.53442D-01	0.17670D000	0.23016D001	-.30618D001	0.60409D-01	-.11649D000	0.43975D-01
14	0.66193D-01	-.75062D-01	0.17305D 00	0.25156D 01	-.31036D 01	-.50508D-05	0.78750D-04	-.93519D-04
14	0.32389D 04	-.19151D 04						
15	0.12865D000	-.35365D-01	0.28251D-01	0.00000D000	0.00000D000	0.35066D-01	-.36638D-01	-.90772D-02
15	0.00000D000	0.00000D000	0.40403D000	0.42271D000	-.30221D000	0.44397D000	-.74701D000	-.27151D001
16	0.67993D-01	0.16995D-01	0.13016D 00	0.11407D 01	-0.21357D 01	0.36395D-04	-0.21353D-04	-0.39392D-04
16	0.18954D 04	-.85526D 03	0.95589D 00	0.32887D 01	0.25592D 01	0.12677D 01	0.38509D 01	0.19917D 01

Parallel to the increased complexity of the generalization scheme used, in most cases increasing precision is achieved in the predictive ability of the EOS. The following is a discussion of the different generalization alternatives outlined in Table XLIV dealing specifically with the SRK EOS. Discussion pertaining to the PR EOS will be presented in a separate section.

Details regarding the extent and distribution of deviations from experimental data for the different paraffins considered, along with the details of correlation constants and detailed statistics for generalization schemes outlined in Table XLV are given in Appendix E. Discussion in the following sections will deal mainly with correlating schemes involving the second correlation for the interaction parameters and the CO_2 pure parameters, since similar but less precise results were generally observed using the first correlation.

The results given in Table XLIV indicate that some improvement is realized by employing common values for C_{ij} and D_{ij} (Case 7) over the suggested alternative (76, 5) of using only a common C_{ij} (Case 6). This is signified by a reduction in RMSE from 6.09 bar (0.0334 mole fraction) and %AAD of 12.2 for the single parameter approach to RMSE of 3.7 bar (0.0217 mole fraction) and %AAD of 7.5 using two parameters. In all cases, however, worsened representation is observed for the heavier molecules as shown in Cases 6 and 7 in Appendix E. This undesirable bias is not due to systematic errors in data used, but rather is expected based on the variation of C_{ij} with CN found previously (Figure 21). The previous recommendation by Robinson (76) for use of constant Cij, based on systems containing n-C_{10} and lighter paraffins, can be justified by results in Figure 21; variations in C_{ij} for CN < 10 are

rather random, with no clear temperature trend. However, the new data data at higher CN values shows that constant C_{ij} will not suffice at the higher carbon numbers. The value of C_{ij} = 0.100 (Case 6) is an obvious compromise and is incapable of accurate representation of data for the full range of CN.

Evaluations were next made for cases where interaction parameters were expressed as a function of the n-paraffin acentric factor. For C_{ij}-only (Case 8), the results are somewhat better than using constant values for C_{ij} and D_{ij}. Surprisingly, a constant value of C_{ij} used with an acentric factor dependent D_{ij} (Case 9) produces results comparable to to using both C_{ij} and D_{ij} as functions of ω_{HC} (Case 10). Both cases represent the data with RMSE values of about 2 bar and 0.01 mole fraction, with Case 9 requiring two fewer parameters than Case 10 (4 vs 6 parameters). The success of the C_{ij}, $D_{ij}(\omega)$ approach is consistent with the observation that inclusion of D_{ij} greatly reduces the variation of C_{ij} with CN. This result makes the C_{ij}, $D_{ij}(\omega)$ representation a reasonable, simple choice for general purpose applications. (One must recall, however, the introduction of the second parameter, D_{ij}, in either SRK or PR equation requires a rederivation of the fugacity coefficient expressions, as given in Appendix C.)

Cases 11 through 14 present results where C_{ij} and/or D_{ij} are permitted to vary both with temperature and ω_{HC}. Case 11 employs C_{ij} as a function of temperature and ω_{HC} in a manner similar to that suggested by Kato (4), but employs a simpler functional form. The results show no improvement over Case 8, where C_{ij} depends only on ω_{HC}. Results become progressively better for Cases 12-14 as the number of parameters in the models increase, with even the simplest case (Case 12) yielding RMSE of

less than 2 bar and 0.01 mole fraction. In fact Case 13, $C_{ij}(\omega,T)$, $D_{ij}(\omega)$ offers perhaps the best combination of accuracy and simplicity of all cases tested (RMSE of 1.3 bar and 0.008 mole fraction).

Using Ω_{a,CO_2} and Ω_{b,CO_2} values determined at the critical point along with the generalized temperature-dependent parameters, $C_{ij}(\omega,T)$ and $D_{ij}(\omega,T)$, results in about double the error margin given by regressed parameters. As shown in Table XLIV for Case 14, RMSE of 1.2 bar (0.0078 mole fraction) and %AAD of 2.4 are obtained using the second correlation. Details of the distribution of deviations for the different paraffins given in Table E.7 indicated worsened RMSE values using this correlation at very light and very heavy paraffins of the systems considered.

Surpressing the temperature dependence of the interaction parameters, by using lumped C_{ij} and D_{ij} with temperature dependent Ω_{a,CO_2} and Ω_{b,CO_2}, produces no significant improvement over previous cases, as indicated by the results given by Cases 15 and 15a. Furthermore, inspection of the results of Case 15, where the second correlation is used for Ω_{a,CO_2} and Ω_{b,CO_2} indicates better overall performance than that obtained using a correlating scheme for Ω_{a,CO_2} and Ω_{b,CO_2} similar to that proposed by Turek (3), as given by the first correlation, Equations (9.21, 9.22).

Finally, Cases 16 and 16a summarize the results of employing the complete temperature dependent generalization scheme involving $C_{ij}(\omega,T)$, $D_{ij}(\omega,T)$, and supercritical $\Omega_{a,CO_2}(T)$ and $\Omega_{b,CO_2}(T)$. The results for the test systems show the merits of the additional complexity of this approach. RMSE of 0.87 bar (0.0056 mole fraction) and %ADD of 1.84 as obtained for Case 16 reflect sufficient accuracy for most EOS predictive

purposes. As indicated by values of normalized RMSE, NRMSE, using regressed $C_{ij}(T)$ and $D_{ij}(T)$ as a reference best case (Case 1), the second correlation for all generalized parameters (Case 16) appears to be most successful in approximating the experimental precision of systems considered. This fact is supported by the least deviation, random bias with respect to molecular size expressed by the carbon number as shown in Table E.13.

Turning attention to the generalized parameter variations with solvent molecular size and temperature, inspection of the results acquired indicate that although values obtained for the different parameters are dependent on the generalization scheme used, some general tendencies can be observed from a given parameter correlation.

As shown in Tables E.11 and E.14 and Figures 40 and E.1, the second correlation exhibits clear temperature and CN dependence for the C_{ij} values obtained, especially at high CN. By comparison, the first correlation produces minor variations in the C_{ij} value with CN and a significant temperature dependence. Accordingly, while the second correlation produces significantly varied values for C_{ij} extending from 0.04 for n-C_4 to 0.13 for n-C_{44}, the first correlation tends to give less variation in C_{ij} with a range of 0.11 to 0.12 for the systems considered. Both correlations give similar behavior for D_{ij} with both CN and temperature, as indicated by Figures 41 and E.2. In general, however, inspection of Table XLIV reveals the relative superiority of the second correlation. This may be attributed to the close representation given by this correlation to the regressed values of C_{ij} and D_{ij}.

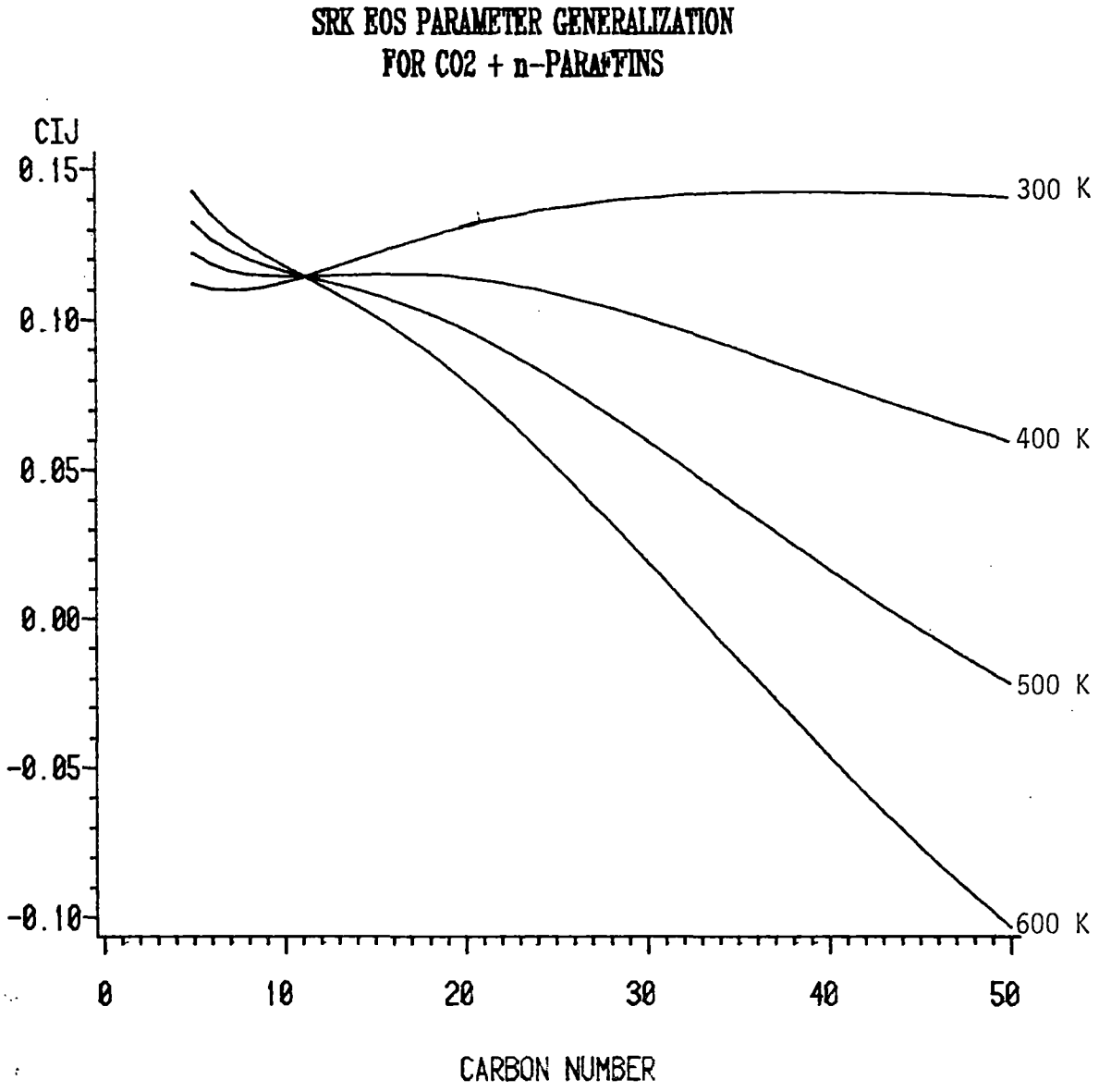

Figure 40. Behavior of SRK Generalized C_{ij} (Case 16)

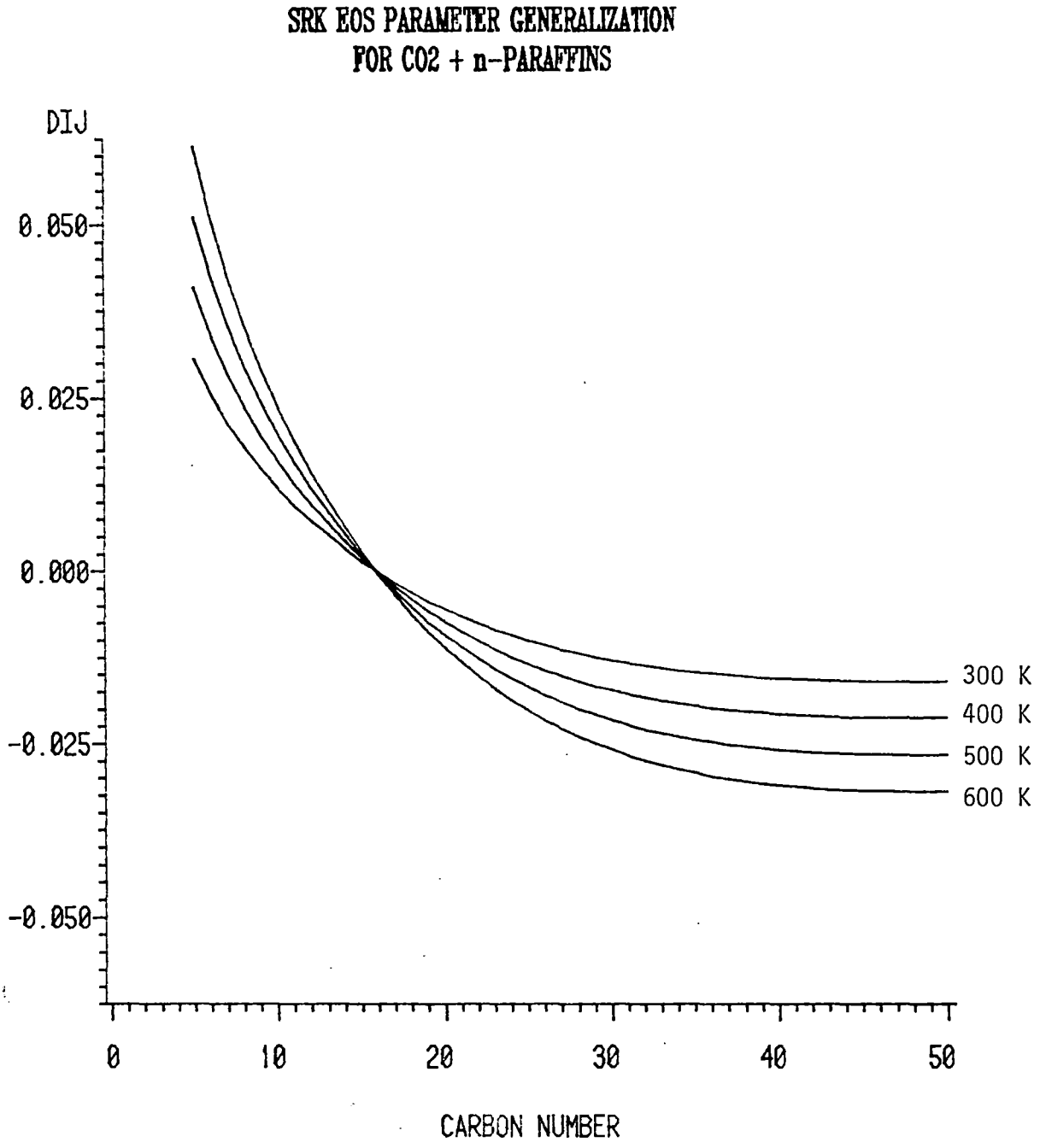

Figure 41. Behavior of SRK Generalized D_{ij} (Case 16)

As indicated by Figures 42 and 43, the values of Ω_{a,CO_2} and Ω_{b,CO_2} given by the second correlation show a definite variation with the CO_2 reduced temperature (exhibiting minima at about 1.2 T_{c,CO_2} then increasing values with temperature). In contrast, Ω_a obtained from the first correlation produces a maximum at 1.2 T_{c,CO_2}, and an increasing dependence of Ω_b with temperature as shown in Figures 44 and E.4.

In retrospect, the variations in the amount of overall deviations from experimental data observed employing the favorable generalization schemes range from 2.0 to 8.0% in terms of %AAD, translating to 0.9 to 3.7 bar in bubble point pressure RMSE (0.0056 to 0.0217 in mole fraction). This constitutes a significant variation if we are to approximate the experimental imprecision of about 0.25 bar RMSE (0.002 mole fraction). And while varying degrees of success are observed for the overall performance of the different schemes, comparisons to the corresponding alternative using individually regressed parameters indicate reasonable approximation is attained for the the experimental precision using selected generalization schemes.

Peng-Robinsons EOS Parameter Generalization

In dealing with PR EOS, as expected, results are very similar to those obtained using the SRK EOS. A detailed account for results of the different approaches is given in Table XLV.

Attempts to retain the structural and temperature dependence obtained for the SRK parameter generalization (by retaining all SRK correlation constants except for A_1 and A_6 of Equations (9.23 and 9.24)) resulted in relatively poor results. By comparison retaining only the SRK parameter temperature dependence (accounted for through C_{ij} and D_{ij}

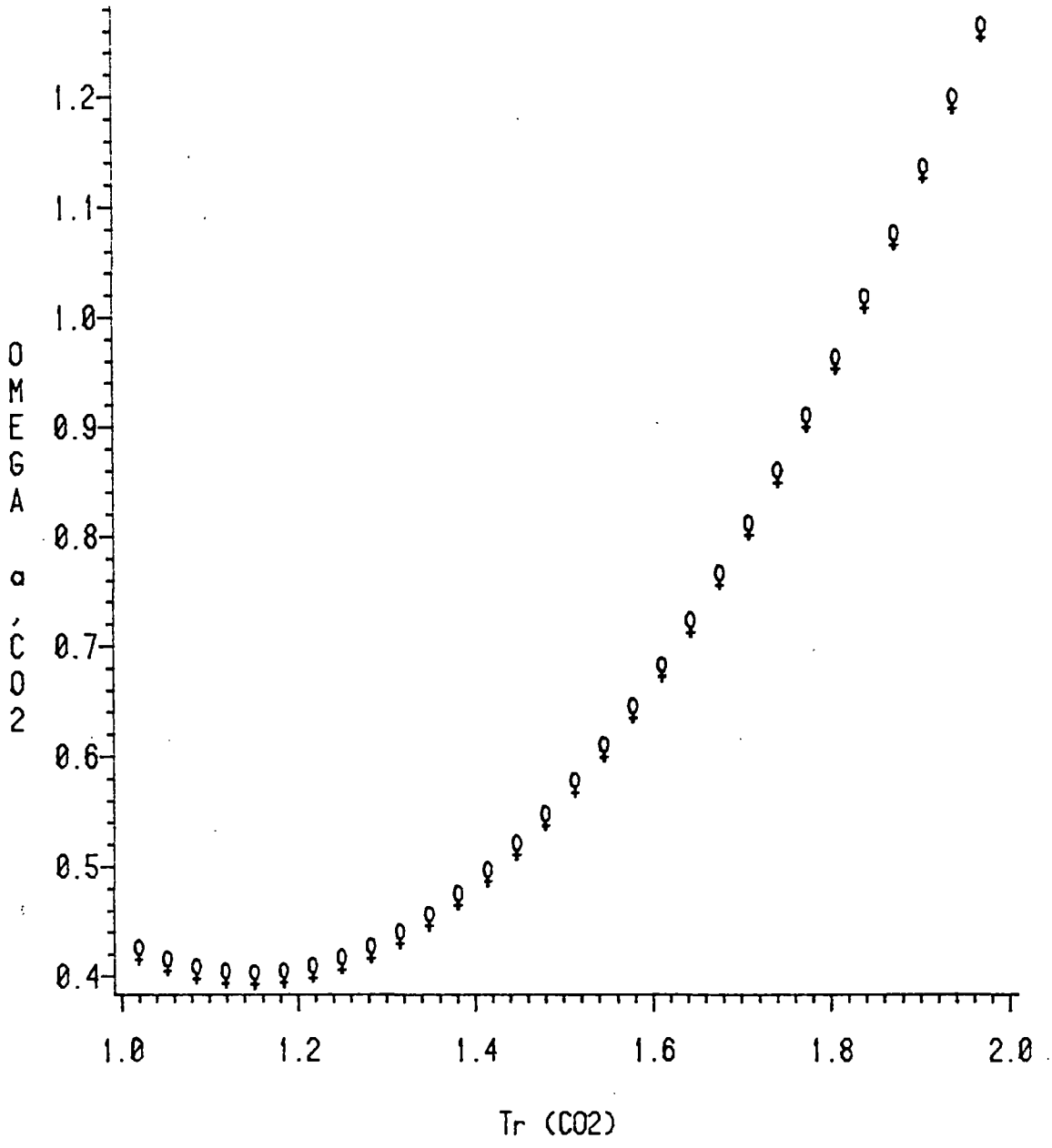

Figure 42. Behavior of SRK Generalized Ω_a (Case 16)

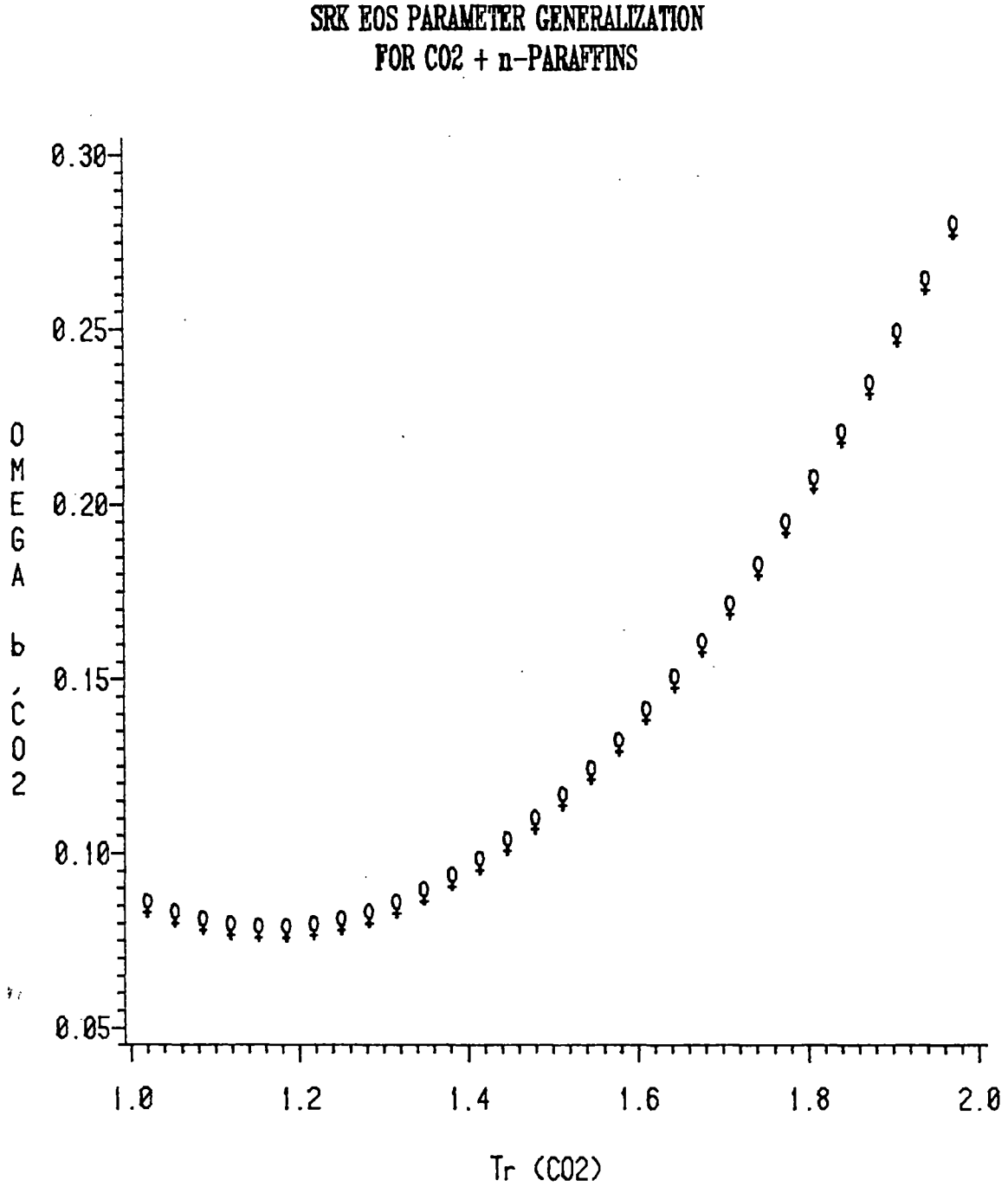

Figure 43. Behavior of SRK Generalized Ω_b (Case 16)

TABLE XLV

SUMMARY OF RESULTS FOR PR PARAMETER GENERALIZATIONS

	BPP , Bar					X_{CO_2}				
Case	RMSE	BIAS	AAD	%AAD	NRMSE*	RMSE	BIAS	AAD	%AAD	NRMSE*
6	6.46	0.164	4.92	13.04	11.13	0.0356	-.0007	0.0286	11.05	6.47
7	3.70	-1.31	2.99	7.99	6.37	0.0229	0.0100	0.0189	8.08	4.16
8	3.00	-.220	2.18	5.94	5.17	0.0182	0.0008	0.0140	5.63	3.10
9	1.96	-.405	1.47	3.73	3.25	0.0111	0.0020	0.0086	3.36	2.01
10	1.90	-.263	1.40	3.75	3.37	0.0112	0.0011	0.0085	3.37	2.04
11	2.58	0.012	1.88	4.72	4.45	0.0160	0.0009	0.012	4.72	2.91
12	1.75	-.354	1.26	3.22	3.01	0.0100	-.0001	0.0076	3.00	1.82
13	1.31	-.105	0.97	2.50	2.25	0.0082	-.0001	0.0062	2.52	1.49
14+	1.22	-.131	0.94	2.60	2.10	0.0078	0.0001	0.0059	2.41	1.42
14++	1.56	-.156	1.17	3.04	2.69	0.0101	0.0021	0.0076	3.01	1.80
15	1.32	-.096	1.02	2.80	2.28	0.0095	-.0006	0.0069	2.81	1.73
16	0.86	-.020	0.66	1.80	1.48	0.0056	0.0000	0.0044	1.78	1.02
16+	0.93	-.048	0.75	2.15	1.50	0.0065	0.0006	0.0051	2.08	1.20
17	2.80	0.426	1.79	5.16	4.83	0.0169	-.0030	0.0118	4.47	3.02
18	10.63	6.402	6.94	18.37	28.67	0.0469	0.0229	0.0339	11.81	8.38

* RMSE / (RMSE of Case 5)
\+ SRK parameter temperature dependence
++ SRK parameter temperature and structure dependence

TABLE XLV (Continued)

CASE GENERALIZED PARAMETER CONSTANTS (A_i) :

	1	2	3	4	5	6	7	8
	9	10	11	12	13	14	15	16
6	0.0850							
7	0.116					-.0240		
8	0.89655D-01	0.10720D000	-.12552D000					
9	0.10446D000	0.00000D000	0.00000D000	0.00000D000	0.00000D000	0.37514D-01	-.48606D000	-.17632D-02
10	0.12679D000	-.69792D-01	0.41908D-01	0.00000D000	0.00000D000	0.34864D-01	-.32706D-01	-.12628D-01
11	0.11400D000	-.22570D000	0.38685D000	-.21290D000	0.75206D00			
12	0.10252D000	0.00000D-00	0.00000D000	0.00000D000	0.00000D000	0.33402D-04	-.18647D-04	-.31344D-04
12	0.17550D004	-.29614D003						
13	0.60320D000	-.59885D-01	0.17933D000	0.20121D001	-.29644D001	0.50509D-01	-.10201D000	0.38422D-01
14	0.65552D-01	-.87412D-01	0.16770D000	0.25144D001	-.31036D001	-.14226D-04	0.10173D-03	-.11188D-03
14	0.32389D004	-.19151D004						
15	0.99817D-01	0.32588D-01	-.17024D-01	0.00000D000	0.00000D000	0.44756D-01	-.70691D-01	0.10174D-01
15	0.00000D000	0.00000D000	0.13180D001	0.35569D001	0.23742D001	0.18426D001	0.38364D001	0.12789D001
16	0.73908D-01	0.19200D-01	0.11919D000	0.83822D000	-.20232D001	0.38979D-04	-.42055D-04	-.25400D-04
16	0.15202D004	-.55452D003	0.95589D000	0.32887D001	0.25592D001	0.12677D001	0.38509D001	0.19917D001

or through Ω_{a,CO_2} and Ω_{b,CO_2} or both) produces comparable results for the PR EOS to those attained using the SRK EOS; thus limiting the variation in the generalization scheme for the two EOS only to structural-dependent parameters. Table XLV presents the results obtained for the selected generalization schemes applied directly to the PR EOS or retaining the results SRK temperature dependence. As signified by such results, in most cases minor gains are realized by refitting the generalized correlation for the PR EOS. Failure to employ the structural dependence of the SRK EOS to the PR EOS may be attributed to the presence of some correlation between constants accounting for molecular size and those accounting for temperature effects in a given generalization scheme.

Comparison of the PR predictions using the different generalization methods suggested in the literature indicates the inadequacies of the previous works in representing the experimental data for heavy paraffins. As indicated by Case 18, RMSE of up to 10.63 bar and %AAD of 18.37 were observed following Lin's recommendation of using a value of 0.125 for C_{ij}. By comparison, Kato's work (4) accounting for C_{ij} temperature effects produced RMSE of only 2.8 bar and %AAD of 5.2, but it failed to approach the reported experimental precision for the data tested (Case 17). Inspection of Table XLV reveals rather obviously that while using Kato's procedures or Lin's recommendations to use a single common interaction parameter may to some degree serve the purpose of giving reasonable predictions for the lighter paraffins up to n-decane, unacceptable deviations are observed for heavier molecules. Furthermore, refitting Kato's correlation to the experimental data considered in this study resulted in deviations comparable to those

obtained using the original correlation constants. This further illustrates the inadequacy of C_{ij} to account for molecular size effects when dealing with heavy solvents.

Table XLIV contains the results obtained by refitting Kato's correlation (4) for the SRK EOS. The summary of the results given by Case 17 indicates a performance equivalent to that obtained from the original correlation given for the PR EOS.

CHAPTER X

CONCLUSIONS AND RECOMMENDATIONS

An experimental apparatus was constructed for the determination of bubble point pressures for binary mixtures of CO_2 + heavy normal paraffins (HNP) at temperatures from 323 K to 423 K and pressures to 96 bar. Bubble point data were obtained for CO_2 binaries involving n-eicosane, n-octacosane, n-hexatriacontane and n-tetratetracontane, all of which are solids at room temperature. Correlative efforts on the data obtained in this study and data found in the literature for CO_2 + n-paraffins (n-C_4 and above) include the following: (1) Interaction parameters were determined for the Soave-Redlich-Kwong (SRK) and Peng-Robinson (PR) equations of state using least squares regressions. A sensitivity analysis was used to investigate the effects of errors in estimated pure hydrocarbon critical properties on the regressed interaction parameters and the predicted phase properties. (2) Several parameter generalization schemes for interaction parameters for the SRK and PR equations in terms of pure hydrocarbon properties been considered. These schemes extend the predictive capabilities of the equations to CO_2 + HNP systems for which no experimental data are available. (3) The data were analyzed using the the Krichevsky-Kasarnovsky solution model. This was done to provide estimates for the Henry's constants and the CO_2 partial molar volumes and to test the internal consistency of the data. Pertinent conclusions and

recommendations regarding the different phases of this study are given below.

Experimental Apparatus

Precise bubble point data have been obtained for CO_2 + HNP using the developed experimental apparatus and procedures. Comparisons of data generated by the apparatus on test systems for which data are available in the literature are very favorable. The bubble point measurements are believed to have an imprecision of no more than 0.25 bar in pressure and 0.002 in liquid mole fraction. Instrumental and internal consistency tests performed on the data indicate a high a degree of experimental consistency. Specific recommendations for the further development of the experimental apparatus are as follows:

1. To eliminate the effects of room temperature variation on the precision of the data obtained, all the pressure elements of the apparatus should be enclosed in constant temperature baths.
2. A modification of the agitation system is needed to prevent mercury spills caused by mercury coil rupture.
3. For more precise measurements, the 5000 psi pressure gauge should be replaced by a high resolution pressure gauge. Similarly, a higher resolution displacement pump should be used.
4. To prevent solvent solidification during apparatus clean-up, the solvent trap should be placed within the constant temperature bath.

Equation of State Representation of Experimental Data

Interaction parameters for the SRK and the PR equations of state using modified mixing rules were obtained for CO_2 + HNP based on recently acquired experimental data. Use of the original SRK mixing rules with a single interaction parameter, C_{ij}, proved inadequate. Thus, two parameters, C_{ij} and D_{ij}, have been used to successfully fit the available data. RMSE of 0.6 bar (0.0055 mole fraction) were obtained, which constitutes a significant improvement over single interaction parameter regressions where RMSE of 1.5 bar (0.02 mole fraction) were obtained for the data considered. The success of EOS representation for the systems considered is attributed to proper accounting for both temperature and molecular size effects.

Molar volume predictions obtained using SRK and PR EOS are significantly improved by volume translation using the Rackett compressibility factor. The SRK and PR EOS give comparable molar volume predictions when using this approach.

Accurate new correlation (asymptotic behavior correlation) based on existing experimental data have been developed for the critical temperature, critical pressure, critical volume, and the acentric factor of pure n-paraffins in terms of the paraffin carbon number. Good extrapolation capabilities, along with a good degree of internal consistency among the different properties, are the main attributes of the proposed correlation. Sensitivity analyses were performed to assess the effects of errors in the estimated hydrocarbon critical properties on the values of the regressed interaction parameters and predicted

phase properties. Results indicate high sensitivity of the EOS predictions to the input variables used.

Previous correlations for SRK and PR EOS parameters are inadequate for CO_2 + HNP systems. Generalized expressions for the binary interaction parameters C_{ij} and D_{ij}, as well as the pure CO_2 parameters, Ω_{a,CO_2} and Ω_{b,CO_2}, have been developed in terms of the paraffin carbon number, the acentric factor and temperature. Both temperature-dependent and temperature-independent generalized expressions are obtained for the interaction parameters. The quality of the predictions obtained using such correlations is dependent on the complexity of the generalization scheme used. For accurate predictions, however, account must be taken of the effects of both temperature and paraffin structure.

While simple correlations for a common C_{ij} and structure dependent D_{ij} may be recommended as adequate for most purposes, use of the complete generalization scheme involving $C_{ij}(\omega,T)$ and $D_{ij}(\omega,T)$ gives the most accurate representation of the data.

The Krichevsky-Kasarnovsky model analysis of the data at mole fraction below 0.45 provided estimates for Henry's constant and CO_2 partial molar volumes. Solubility predictions with average errors of about 0.002 in mole fraction are obtained using the K-K equation. While the Henry's constants obtained are believed accurate within a few percent, the partial volumes may not be as accurate.

Finally, additional experimental data involving CO_2 and other hydrocarbons such as naphthenes and aromatics are needed to develop more general correlations.

REFERENCES

1. Huron, M. J., et. al, Fluid Phase Equilibria 1, 247 (1977).

2. Graboski, M. S. and T. E. Daubert, Ind. Eng. Chem. Proc. Des. Dev. 17, 443-448 (1978).

3. Turek, E. A., et. al, Soc. Petrol Eng. J. 308 (June, 1984).

4. Kato, K., et. al, Fluid Phase Equilibria 7, 219 (1981).

5. Lin, H.-M., Fluid Phase Equilibria 16, 151 (1984) .

6. "The Scientific papers of J. Willard Gibbs," Vol. I, N.Y.: Dover Pub. Inc. (1961).

7. Soave, G., Chem. Eng. Sci. 27, 1197 (1972).

8. Peng, D. Y. and D. B. Robinson, Ind. Eng. Chem. Fund. 15 59 (1976).

9. Prausnitz, J. M., "Molecular Thermodynamics of Fluid-Phase Equilibria" Prentice-Hall, Englewood Cliffs, N.J. (1969).

10. Malanowski, S., Fluid Phase Equilibria 9, 311 (1982).

11. Eubank, P. T. and K. R. Hall, "A review of experimental techniques for Vapor Liquid Equilibria at High Pressure", H. Knapp and S. I. Sandler (Editors), Int. Conf. on Phase Equilibria and Fluid Properties in Chemical Industry, Dechema, Frankfurt, Part II, 675 (1980).

12. Reamer, H. H. and B. H. Sage, J. Chem. Eng. Data 8, 508 (1963).

13. Sage, B. H., et. al, Ind. Eng. Chem. 26, 1219 (1934).

14. Van Ness, H. C., et. al, A.I.Ch.E. J. 19, 238 (1973).

15. Li, Y.-H., et. al, J. Chem. Eng. Data. 26, 53 (1981).

16. Gupta, M. K., et. al, J. Chem. Eng. Data 27, 55 (1982).
    a) Bubble-point pressure measurements;
    b) phase composition measurements.

17. Huie, N., et. al, J. Chem. Eng. Data 18, 311 (1973).

18. McHugh, et. al, Paper presented at the National Meeting of A.I.Ch.E., Houston, TX, March (1983).

19. Fall, D. J. and K. D. Luks, J. Chem. Eng. Data 29 443 (1984).

20. Wichterle, I., et. al, "Vapor Liquid Equilibrium Data Bibliography", Elsevier, (1973).

21. Olds, R. H., et. al, Ind. Eng. Chem. 41, 475 (1949).

22. Kalra, H., et. al, J. Chem. Eng. Data 21, 222 (1976).

23. Vargaftik, N. M., "Tables on The Thermophysical Properties of Liquids and Gases", 2nd Ed., John Wiley & Sons, New York (1970).

24. "International Thermodynamic Tables of Fluid State Carbon Dioxide", International Union of Pure and Applied Chemistry, Vol 3, Oxford, 265 (1976).

25. Legret, D., et. al, Ind. Eng. Chem. Fund. 19, 122 (1980).

26. Lee, K. H. and J. P. Kohn, J. Chem. Eng. Data 4, 292 (1969).

27. Meskel-Lesavre, M., et. al, Ind. Eng. Chem. Fund. 20, 284 (1981).

28 Metcalfe, R. S., Amoco Production Company, Tulsa, OK, Personal Communication, (1981).

29. Krichevsky, I. R. and J. S. Kasarnovsky, J. Am. Chem. Soc. 57, 2168 (1935)

30. Chai, C. P. and M. E. Paulaitis, J. Chem. Eng. Data. 26, (1981).

31. Anderson, T. F., et. al, A.I.Ch.E. J. 24 20 (1978).

32. Fisher, R. A., Phil. Trans. Roy. Soc. London (a), 222, 309 (1922).

33. Sutton, T. L. and J. F. MacGregor, Can. J. Chem. Eng. 55 602 (1977).

34. Kemeny, S. and J. Manczinger, Chem. Eng. Sci. 33, 71 (1978).

35. Kemeny, S., et. al, A.I.Ch.E. J. 28, 20 (1982).

36. Neau, E. and A. Peneloux, Fluid Phase Equilibria 6, 1 (1981).

37. Van Ness, H. C., et. al, A.I.Ch.E. J. 24, 1055 (1978).

38. Luecke, R. H., et al, K. R. Hall, Cryogenics, 284 (1974).

39. Fariss R. H. and V. H. Laws, Comp. Chem. Eng. 3, 95 (1979).

40. Box, M. J., Techonometrics 12, 219 (1970).

41. Barker, J. A., Austr. J Chem. 6, 207 (1953).

42. Hunter, W. G., Ind. Eng. Chem. Fund. 6, 461 (1967).

43. Patino-Leal, H. and P. M. Reilly, A.I.Ch.E. 28, 580 (1982).

44. Kudchadker, A. P., et. al, Chem. Rev. 68, 659 (1968).

45. American Petroleum Institute, Research Project 44.

46. Lee, B. I. and M. G. Kesler, A.I.Ch.E. J. 21, 510 (1975).

47. Nokay, R., Chem. Eng. 66 (4), 147 (1959).

48. Reid, R. C. and T. K. Sherwood, "The Properties of Gases and Liquids", 2nd Ed., McGraw-Hill, New York (1966).

49. Spencer, C. F. and T. E. Daubert, A.I.Ch.E. J. 19, 482 (1973).

50. Richards, F. J., J. Exper. Botany 10 (29), 210 (1959)

51. Stevens, W. L., BIOMETRICS, 247 (Sept., 1951).

52. Kudchadker, A. P., et. al, J. Chem. Eng. Data 2, 253 (1966).

53. Chao, K. C., "Phase Equilibrium in Coal Liquefaction Processes", EPRI AP-3450 Research Project 367-2, Final Report, August (1984).

54. Ely, J. F. and H. J. M. Hanley, NBS Technical Note, 1039 (1981).

55. McGarry, J., Ind. Eng. Chem. Proc. Des. Dev. 22, 313 (1985).

56. Spencer, C. F. and R. P. Danner, J. Chem. Eng. Data. 17, 236 (1972).

57. Hankinson, R. W. and G. H. Thomson, A.I.Ch.E. 25 (4), 653 (1979).

58. Meisner, J., Ind. Eng. Chem. Proc. Des. Dev. 11, 83 (1972).

59. Flory, P. J., et. al, J. Am. Chem. Soc. 86, 3507 (1964).

60. Martin, J. J., Ind. Eng. Chem. 59, 35 (1967).

61. Rowlinson, J. S., Nature 244, 244 (August, 1973).

62. Abbott, M. M., "Cubic Equations of State: An Interpretive Review" in Equations of State in Engineering, Advances In Chemistry Series 182, K. C. Chao and R. L. Robinson, Jr., editors, American Chemical Society, Washington, D.C. (1979).

63. Flory, P. J., et al., J. Am. Chem. Soc. 86, 3507 (1964).

64. Wilson, G. M., Adv. in Cryogenic Eng. 9, 168 (1964).

65. Zudkevitch, D. and J. Joffe, A.I.Ch.E. J. 16, 112 (1970).

66. Chang, S. D. and B. C.-Y. Lu, Can. J. Chem. Eng. 46 21 (1970).

67. Redlich, O. and J. N. S. Kwong, Chem. Rev. 44, 233 (1949).

68. Prausnitz, J. M., "Phase Equilibria and Fluid Properties in the Chemical Industry", A.I.Ch.E. Proceedings 2nd International Cong, Part 2, 231 (1980).

69. Mathias, P. M., Ind. Eng. Chem. Proc. Des. Dev. 22, 385 (1983).

70. Radosz, M., et. al, Ind. Eng. Chem. Proc. Des. Dev. 21, 653 (1982).

71. Huron, M. J. and J. Vidal, Fluid Phase Equilibria 3, 255 (1979).

72. Gray, R. D., Jr., "Industrial Experience in Applying The Redlich-Kwong Equation to Vapor/Liquid Equilibria" in Equations of State in Engineering, Advances In Chemistry Series 182, K. C. Chao and R. L. Robinson, Jr., editors, American Chemical Society, Washington, D.C. (1979).

73. Vidal, J., Fluid Phase Equilibria 14 15 (1983).

74. Jackson, L. W., "A comparison of Selected Gradient Methods for Solving Least Squares Problem", M.S. Thesis, Oklahoma State University, Stillwater, OK (1978).

75. Oellrich, L., et. al, Ind. Chem. Eng. 21, 1 (1981).

76. Robinson, R. L., Jr., Progress Report On "Vapor-Liquid Phase Equilibrium in Coal-Type Fluid Systems", July 1-Dec 31, 1979, U.S. Energy Res. Dev. Admin.

77. Simonet, R. and E. Behar, Chem. Eng. Sci. 31, 37 (1976).

78. Renon, H., Fluid Phase Equilibria 2, 101 (1978).

79. Martin J. J., Ind. Eng. Chem. Fund. 18, 81 (1979).

80. Peneloux, A. and E. Rauzy, Fluid Phase Equilibria 8, 7 (1982).

81. Snedecor, G. W. and W. G. Cohran, "Statistical Methods", 6th Ed., Ames, Iowa: Iowa State University, (1967).

82. Shreider, Yu. A., "The Monte Carlo Method", N.Y., Pergamon Press, (1966).

83. Al-Zakri, A. S. "Estimation of The Performance of Shell and Tube Heat Exchanger Systems When Uncertainties Exist" Ph.D. Thesis, Oklahoma State University , Stillwater, OK (1977).

84. Hamam, S. E., et. al, Ind. Eng. Proc. Des. Dev., 16, 51 (1977).

85. Stein, R. B., Ind. Eng. Proc. Des. Dev., 21, 564 (1982).

86. Pesuit, R. P., Ind. Eng. Chem. Fund. 17, 236 (1976).

87. Ezekwe, J. N., "Effect of Paraffinic, Naphthenic and Aromatic Distribution in the Hydrocarbon Mixture and Water on the Phase Equilibria of Carbon Dioxide-Hydrocarbon Systems Over The Temperature Range from 333 K to 366 K", Ph.D. Thesis, University of Kansas, Kansas (1982).

88. Yarborough, Lyman, "Application of a Generalized Equation of State to Petroleum Reservoir Fluids" in Equations of State in Engineering, Advances In Chemistry Series 182, K. C. Chao and R. L. Robinson, Jr., editors, American Chemical Society, Washington, D.C. 385 (1979).

89. Barrick, M. W., "High Pressure Solubility of Carbon Dioxide in Aromatic Solvents Benzene, Naphthalene, Phenanthrene, and Pyrene", M.S. Thesis, Oklahoma State University, Stillwater, OK (1985).

90. Fall D. J. and K. D. Luks, University of Tulsa, Personal Communication, (1983).

91. Maddox, R. N. and J. H. Erbar, Hydrocarbon Process 63 (1), 119 (1984).

92. "Heat Exchanger Handbook", Hemisphere Publishing Corporation, Vol. 5, N.Y. 5.5.1-5 (1983).

APPENDIX A

CALCULATION PROCEDURE FOR COMPONENT MOLE FRACTION

Component mole fraction by definition is given as:

$$x_i = n_i / \sum_{i}^{N} n_i$$

Thus for a CO_2 binary

$$x_{CO_2} = x_1 = \frac{n_1}{n_1 + n_2}$$

where n_1 and n_2 represent the total number of moles of CO_2 and the hydrocarbon solvent respectively. For multiple CO_2 injections n_1 may be expressed as:

$$n_i = \sum_{j} \rho_{1j} \, v_{1j}$$

where as for the hydrocarbon solvent single injection n_2 is given as:

$$n_2 = \rho_2 \, v_2$$

A slight adjustment is applied to the values of the injected volumes, V_i, to account for the variation of mercury density with temperature, as it is injected at room temperature from the displacement pump into the

equilibrium cell or the fluid reservoirs which are at elevated temperatures. The adjustment factor, which has a value of about 1.004, is calculated using the following relation:

$$V_i, \text{ corrected} = V_i \frac{\rho_{Hg}\ (T_{room})}{\rho_{Hg}\ (T_{oven})}$$

Details of an injection were recorded on an injection sheet (Figure A.1), where a complete record of raw and calculated experiment variables was made along with any observations deemed usefull.

Upon completion of components injections for the desired CO_2 mole fraction, equilibrium data accounting for variations in the system pressure due to alteration in the system total volume were obtained. A PVT data sheet as that given in Figure A.2 was used for to such a purpose.

INJECTION SHEET

Date: _____

SOLVENT INJECTION

Solvent Name: _____

$Time_i$: _____ P_i: _____

Temp Pump Bath : _____ x_i: _____

Temp Cell Bath : _____ x_f: _____

$Time_f$: _____ P_f: _____

ΔV = (_____) (_____) = _____

Solvent ρ = _____ M. Wt. = _____
( )

Δn solvent = _____

n solvent = _____

SOLUTE INJECTION

Solute Name: _____

$Time_i$: _____ P_i: _____

Temp Pump Bath : _____ x_i: _____

Temp Room : _____ x_f: _____

$Time_f$: _____ P_f: _____

ΔV: _____

Solute ρ = _____ M. Wt. = _____
( )

Δn solute: _____ n total: _____

n solute: _____ x solute: _____

OBSERVATIONS: _____

Figure A.1. Fluid Injection Sheet

PVT DATA

System: _____ No. _____

Temp: _____

$x_{(\ \ )}$: _____

DATE	TIME	ROOM TEMP.	V_I			ΔV_{cc}	P ( )	COMMENTS

Chart No.: _____

P_B: _____

Initials: _____

Figure A.2. Equilibrium Data Sheet

APPENDIX B

EXPERIMENTAL DATA ERROR ANALYSIS

Uncertainties in the experimental data presented are analyzed in this Appendix. While repeated instrument calibrations are used to determine the random errors associated with instrument imprecisions, error propagation is employed in estimating uncertainty in the dependent variable, such as the liquid mole fraction. Errors attributed to the procedure used in determining the bubble point pressure are estimated by analyzing repeated runs.

Errors Associated With Temperature Determination

Typical calibrations for the platinum resistance thermometer are given in Table B.1 where a distilled water melting point cell is used for the calibration. Though the cell is used a substitute for a certified triple point cell, a reliable calibration is still obtained by this method. This claim was verified by repeating the calibration procedure against another certified platinum-resistance thermometer with digital read-out (Minco RT 8078).

The combined uncertainty due the thermometer random imprecision and the temperature control fluctuations is estimated at 0.18°F (double the maximum variation observed in Table B.1).

Errors Associated With Volume Determinations

Gravimetric calibrations were preformed to establish the uncertainty in the fluid volumes injected. For such a purpose, known

TABLE B.1

PLATINUM RESISTANCE THERMOMETER
CALIBRATION (FLUKE 2180A)

Date	T, °F	Error, °F	Reference
11/30/81	0.0	0.0	ice point
5/10/82	0.0	-0.08	ice point
8/30/82	75	+0.09	Minco RT8078

TABLE B.2

SCREW PUMP CALIBRATIONS

Date	Pump	AAD	Reference
10/5/81	Ruska (250cc)	0.617%	gravimetric
1/25/81	HIP (60cc)*	0.0425%	gravimetric

*Pump was discontinued on 3/1/82.

volumes of mercury at room temperature were displaced in a tared glass beaker and then weighed using a precision mass balance. Comparison of the mass obtained gravimetrically for the volumes displaced to those calculated using accurate mercury density according to the following relation:

$$\rho_{Hg}, \text{ gm/cc} = [0.07334 + 7.49 \times 10^{-6} \, T \, (^{0}F)]^{-1}$$

results in estimates for the uncertainty in the volume measurements.

Table B.2 gives representative values for the expected errors for volumes injected.

Errors Associated With Pressure Determinations

Pressure measurements are influenced, in varying degrees, by several factors including the accuracy of the calibration system used, head corrections, and the barometeric pressure measurement.

The calibration system used in this study was a Ruska dead weight gauge (model: 2401, serial no. 10381) with a certification traceable to the National Bureau of Standards. The accuracy of this gauge was further established by cross-floating it against another certified dead weight tester (model: 2401, serial no. 14203), imprecisions well within the reported uncertainty of 0.025% psia were observed.

To obtain the true system pressure in the equilibrium cell, head corrections due the added pressure exerted by mercury/oil heads are applied to the pressure gauge set point. This combined with the head correction for the elevation difference between the pressure gauge and

the dead weight plane of reference produce the following gauge correction relation in accordance with Figure B.1.

$$GC = PDW - (PG + hc1 + hc2) \quad (=) \text{ psia}$$

Where

PG = gauge pressure

PDW = dead weight gauge pressure

hc_1 = head correction due to cell mercury/oil head

hc_2 = head correction due to dead weight oil head

Thus the true absolute system pressure is:

$$P = P_G + GC + P_b$$

where P_b is the barometric pressure.

Tables B.3-B.5 presents calibration results in terms of gauge correction for the gauges used, where variations in the value of the correction applied with time signify the imprecision in the pressure determination.

Table B.6 gives a summary for the uncertainties in the pressure measurements of the three gauges used in terms of percent errors and standard deviations.

Finally, barometeric pressure measurements made are believed to be within the reported uncertainty of the equipment used as was discussed in Chapter VI.

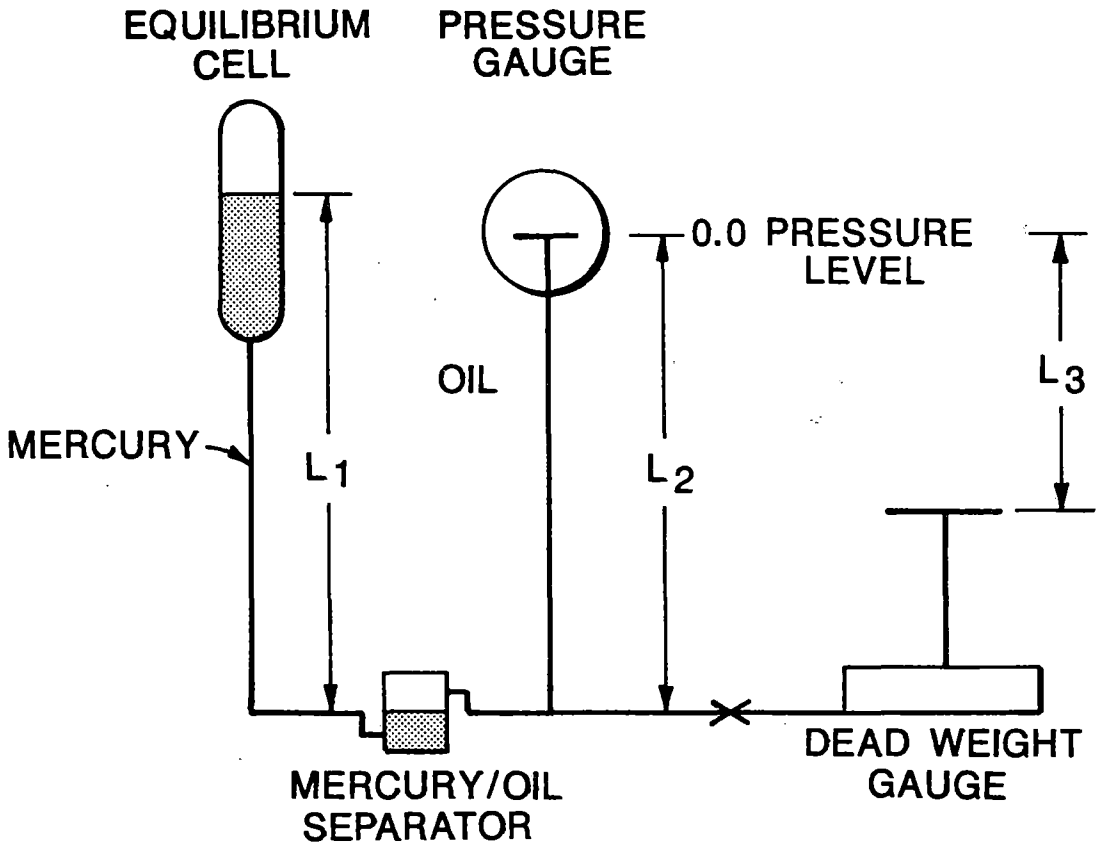

$$hc_1 = 0.491\, L_1 - 0.031\, L_2$$

$$hc_2 = 0.031\, L_3$$

Figure B.1. Apparatus Pressure System

TABLE B.3

PRESSURE GAUGE CALIBRATION (300 PSIG GAUGE, AE05132)

Pressure, Psia	Date				
	10/26/81	12/29/81	6/11/82	9/17/82	
	Gauge Correction, psia				% Error
80	9.30	10.02*	10.0	10.2	0.112**
130	9.41	9.79	10.04	10.19	0.127
180	9.44	10.20	9.98	10.12	0.046
230	9.74	9.92	10.31	10.25	0.019
280	9.79	10.18	10.35	10.38	0.031

ε_p = 0.106 psia, average % Error = 0.067

*Set Point Change
**Not including calibration before set-point shift.

TABLE B.4

PRESSURE GAUGE CALIBRATION (1000 PSIG GAUGE, AD15868)

Pressure, Psia	Date					% Error
	10/26/81	11/15/81	12/1/85	12/29/81	4/3/82	
	Gauge Correction, psia					
121	8.8			9.28	9.31	0.111
221	9.45	9.69	9.69	9.82	10.42	0.066
319	11.0			11.25	11.75	0.056
418	11.34	11.41		11.78	12.39	0.050
519	10.69		11.26	11.12	11.92	0.043
619	10.0	9.96		10.46	10.96	0.033
719	10.40		10.98	10.99	11.29	0.022
818	11.25	11.36	11.86	11.43	11.72	0.013
916	12.60			12.97	13.57	0.025
966	13.04					

Pressure Standard Deviation, $\varepsilon_p = \sqrt{\sum^{n} (Y - \overline{Y})^2/n-1}$ = 0.316 psia, average % Error = 0.0466

TABLE B.5

PRESSURE GAUGE CALIBRATION (5000 PSIG GAUGE, CM5000)

Pressure psia	Date			% Error
	3/1/82	4/14/82	6/11/82	
	Gauge Correction, psia			
800	10.32	10.29	10.97	0.039
900	11.95	9.95	10.85	0.091
1000	12.26	10.76	9.70	0.129
1100	13.60	12.00	13.58	0.105
1200	17.43	13.93	15.45	0.068
1300	18.76	--.--	18.34	-.---
1400	20.60	15.60	19.21	0.151

ε_p = 1.58 psia, average % Error = 0.096

TABLE B.6

PRESSURE GAUGE UNCERTAINTIES

Gauge I.D.	Pressure Range, psia	% Error		ϵ_p (psia)
		Reported	Experimental	
(PENNWALT) AE05132	300	±0.0366*	±0.067	0.20
(PENNWALT) AD15868	1000	±0.066	±0.047	0.32
(HEISE) CMM5000	5000	±0.1	±0.096	1.58

*Certified calibration for this particular gauge.

TABLE B.7

REPRODUCIBILITY OF THE BUBBLE POINT DETERMINATION

Pressure Range (psia)	Reproducibility (psia)
0- 100	0.30
101- 200	0.45
201- 300	0.75
301- 400	1.00
401- 500	1.25
501- 600	1.10
601- 700	1.60
701- 800	2.00
801- 900	2.00
901-1000	2.25

ϵ_{BPP} = 0.0024, P (=) psia

Errors Associated with Mole Fraction Determinations

Component liquid mole fraction is calculated, as shown in Appendix A, based on the component total injected volumes V_i and the pure component densities. Such errors attributed to those variables contribute to the estimated mole fraction uncertainty.

For a binary system the mole fraction is given by:

$$x_1 = n_1/(n_1 + n_2)$$

where n_1 and n_2 signify the total number of moles of CO_2 and the hydrocarbon, respectively. Assuming independent and uncorrelated errors associated with the independent variables n_1 and n_2, the propagated error in the mole fraction can be expressed in terms of variances as:

$$\sigma^2_{x_1} = \sigma^2_{x_2} = (\partial x_1/\partial n_1)^2 \, \sigma^2_{n_1} + (\partial x_1/\partial n_2)^2 \, \sigma^2_{n_2}$$

Since

$$\partial x_1/\partial n_1 = [1/(n_1 + n_2) - n_2/(n_1 + n_2)^2]$$

and

$$\partial x_1/\partial n_2 = -n_1/(n_1 + n_2)^2$$

Therefore,

$$\sigma^2_{x_1} = \sigma^2_{x_2} = [n_2/(n_1 + n_2)^2]\ \sigma^2_{n_1} + [n_1/(n_1 + n_2)^2]\ \sigma^2_{n_2}$$

or

$$(\sigma_{x_1}/x_1x_2)^2 = [n_2^2\sigma^2_{n_1} + n_1^2\sigma^2_{n_2}/(n_1 + n_2)^4][(n_1 + n_2)^4/(n_1n_2)^2]$$

$$= (\sigma_{n_1}/n_1)^2 + (\sigma_{n_2}/n_2)^2$$

$$= \sum_i^2 (\sigma_i/n_i)^2 \qquad (B.1)$$

Errors in Component Number of Moles

To calculate the error contribution due to errors in the number of moles, a similar derivation is followed. By definition:

$$n_i = \sum_j V_j/v_i \text{ and } \sum_j V_j = V_i$$

where v_i is the component specific specific volume $(1/\rho_i)$, and the index j is a counter for the number of injections made. The propagated error is then:

$$\sigma^2_{n_i} = (\partial n_i/\partial V_j)^2\sigma^2_{V_j} + (\partial n_i/\partial v_i)^2\sigma^2_{v_i}$$

Since

$$(\partial n_i/\partial V_j) = 1/v_i, \quad (\partial n_i/\partial v_i) = -(V_j/v_i^2) = -V_j/v_i^2$$

Therefore

$$\sigma^2_{n_i} = (\sigma_V/v_i^2) + (V_j)^2 (\sigma_V/v_i^2)^2$$

or

$$(\sigma_{n_i}/n_i)^2 = v_i^2/V_i^2 (\sigma_{V_i}/v_i)^2 + V_i^2 (\sigma_V^2/v_i^2) v_i^2/V_i^2$$

$$= (\sigma_{V_i}/V_i)^2 + (\sigma_V/v_i)^2 \qquad \text{(B.2)}$$

Errors in Component Injected Volumes

Now, if I_i is to signify the number of injection for a given mole fraction then:

$$V_i = I_i V_j$$

and since

$$\sigma^2_{V_i} = (\partial V_i/\partial V_j)^2 V^2_{V_j} = I_i^2 \sigma^2_{V_j}$$

Therefore

$$(\sigma_{V_i}/V_i)^2 = (I/V)_i^2 \sigma^2_{V_j} \qquad \text{(B.3)}$$

Errors in Component Mole Fraction

Combining Equations B.1, and B.2, and B.3 the following expression is obtained for the mole fraction error estimate:

$$(\sigma_{x_i}/x_1x_2)^2 = \sum_i^2 (\sigma/n)_i^2 = \sum_i^2 [(\sigma_V/V)_i^2 + (\sigma_v/v)_i^2]$$

$$= \sum_i^2 (I/V)_i^2 \sigma_{V_j}^2 + (\sigma_v/v)_i^2 \qquad (B.4)$$

This indicates the error in the liquid mole fraction is dependent on the number of injections made, and the size of the injected volumes along with the errors in the injected volumes and the component densities.

Sample Calculation

Having the following error estimates expressed as standard deviations:

$\sigma_{V_1} = 0.10\%$, $\sigma v_2 = 0.3\%$

$\sigma_V = 0.62\%$ (conservative estimates)

Along with injection data for a typical run where:

$v_1 = 5cc$, $V_2 = 10$ cc

$I_1 = 3$, $I_2 = 1$

Using the above data the effect of the largest error contribution attributed to three consecutive injections is considered.

Then according to Equation B.4:

$$(\sigma_{x_i}/x_1x_2)^2 = \sum_i^2 (I/V)_i^2 \sigma_{V_j}^2 + (\sigma_v/v)_i^2$$

$$= (3/15)^2 (0.62 \times 5/100)^2 + (0.1/100)^2 + (1/10)^2 (0.62 \times 10/100)^2 + (0.3/100)^2$$

$$= 0.00008688$$

or

$$\sigma_{x_1} = \sigma_{x_2} = 0.009 \, x_1 \, (1-x_1)$$

Table B.8 presents the mole fraction error estimates for mole fractions extending from 0.1 to 0.5.

TABLE B.8

LIQUID MOLE FRACTION ERROR ESTIMATES

x_i	σ_{x_i}
0.1	0.0008
0.2	0.0015
0.3	0.0020
0.4	0.0022
0.5	0.0023

APPENDIX C

Derivation of the EOS fugacity coefficient needed for the calculation of equilibrium properties, as discussed in Chapters II and IX, are given in this Appendix.

Also included in this Appendix are:

1. Sample output for EOS data reduction procedure used in the present work.
2. Weighted least squares regression parameter estimates of $C_{ij}(T)$ and $D_{ij}(T)$ for the SRK EOS for the CO_2 systems acquired in this study. These estimates are comparable to those given in Table XXXII using the least squares objective function.
3. Details of PR EOS parameter regressions for the different cases described in Table XXXII.

FORMULATION OF SRK AND PR EOS

(1) SRK EOS

$$p = \frac{RT}{V-b} - \frac{a(T)}{V(V+b)} \qquad (C.1)$$

Where:

$$b = 0.08664 \frac{RT_c}{P_c}$$

$$a(T) = a(T_c)\ \alpha\ (T_r, \omega)$$

$$a(T_c) = 0.42747 \frac{R^2 T_c^{\ 2}}{P_c}$$

$$\alpha^{0.5}\ (T_r, \omega) = 1 + m(1-T_r^{\ 0.5})$$

and

$$m = 0.480 + 1.574\omega - 0.176\omega^2$$

If the mixing rules and the parameters of Equations (9.3-9.14) are recast in reduced form, the following is obtained for the attraction law constant:

$$A = \sum \sum x_j x_j \bar{a}_{ij}$$

where

$$\bar{a}_i = 1/A \sum x_j \bar{a}_{ij}$$

and

$$\bar{a}_{ij} = (1 - C_{ij}) \sqrt{\left(\frac{a_i P}{R^2 T^2}\right)\left(\frac{a_j P}{R^2 T^2}\right)}$$

Similarly for the covolume the following relations are obtained:

$$B = \sum \sum x_i x_j \bar{b}_{ij}$$

where

$$\bar{b}_i = 1/B \sum x_j \bar{b}_{ij}$$

and

$$\bar{b}_{ij} = \left(\frac{1 + D_{ij}}{2}\right) \left[\left(\frac{b_i P}{RT}\right) + \left(\frac{b_j P}{RT}\right)\right]$$

Expressing equation (C.1) in terms of the compressibility factors z(=PV/RT) the fugacity coefficient for the i component as:

$$\ln \hat{\phi}_i = (2\bar{b}_i - 1)(z - 1) - \ln (z - B) - (A/B)(2\bar{a}_i - 2\bar{b}_i - 1) \ln \left(1 + \frac{B}{z}\right)$$

Where:

$$\hat{\phi}_i = \frac{f_i}{x_i P}$$

and

$$z^3 - z^2 (A - B - B^2)z - AB = 0 \qquad (C.3)$$

(2) PR EOS

Similar to the developments for the SRK equation the following equations are obtained for the PR equation of state:

$$p = \frac{RT}{V-b} - \frac{a(T)}{V(V+b)+b(V-b)} \qquad (C.4)$$

Where:

$$b = 0.07780 \frac{RT_c}{P_c}$$

$$a(T) = a(T_c)\ \alpha\ (T_r \omega)$$

$$a(T_c) = 0.45724 \frac{R^2 T^2_c}{P_c}$$

$$\alpha^{0.5}\ (T_r, \omega) = 1 + m(1 - T_r^{0.5})$$

and

$$m = 0.37464 + 1.54226\omega - 0.26992\omega^2$$

The fugacity coefficient is given by:

$$\ln \hat{\phi}_i = (2\overline{b}_i - 1)(z-1) - \ln (z-B)$$

$$- \frac{A}{2.2^{1/2}B} (2\overline{a}_i - 2\overline{b}_i - 1) \ln \left[\frac{z + (1 + 2^{1/2})B}{z + (1 - 2^{1/2})B}\right] \qquad (C.5)$$

where

$$z^3 - (1 - B)z^2 + (A - 3B^2 - 2B)z - (AB - B^2 - B^3) = 0 \qquad (C.6)$$

TABLE C.1

SAMPLE OUTPUT FOR EOS DATA REDUCTION PROCEDURE

BUBBLE-POINT CALCULATIONS
USING SOAVE-RK EQUATION OF STATE

	COMPONENT	TC, K	PC,BAR	TB , K	W	ZRA
1	CO2	0.30421D+03	0.73829D+02	0.36354D+03	0.22510D+00	0.27270D+00
2	N-C20	0.77050D+03	0.11168D+02	0.61778D+03	0.87376D+00	0.20000D-03

PURE COMPONENT VALUES OF OMEGA A AND OMEGA B

ISOTHERM	T,K	1	2
1	0.32315D+03	0.42748D+00	0.42748D+00
1	0.32315D+03	0.86640D-01	0.86640D-01

C(I,J)/K(I,J) MATRIX

	1	2
1	0.00000D+00	0.12661D+00
2	0.12661D+00	0.00000D+00

D(I,J)/L(I,J) MATRIX

	1	2
1	0.00000D+00	-0.44620D-02
2	-0.44620D-02	0.00000D+00

TABLE C.1 (Continued)

BUBBLE-POINT CALCULATIONS
USING SOAVE-RK EQUATION OF STATE

DATA	CN	T(K) EXPTL	X(CO2) EXPTL	P(BAR) EXPTL	P(BAR) CALC	DEV	%DEV
1	20	323.15	0.0734	6.21	6.21	0.00	0.04
2	20	323.15	0.1162	10.10	10.09	-0.01	-0.14
3	20	323.15	0.1796	16.24	16.22	-0.01	-0.08
4	20	323.15	0.2124	19.73	19.60	-0.13	-0.68
5	20	323.15	0.2351	22.01	22.02	0.01	0.06
6	20	323.15	0.2416	22.73	22.73	-0.00	-0.01
7	20	323.15	0.2507	23.84	23.73	-0.10	-0.44
8	20	323.15	0.3004	29.48	29.43	-0.05	-0.16
9	20	323.15	0.3220	31.83	32.03	0.21	0.65
10	20	323.15	0.3349	33.36	33.63	0.27	0.80
11	20	323.15	0.3986	41.88	42.00	0.13	0.30
12	20	323.15	0.4250	46.07	45.74	-0.33	-0.72
13	20	323.15	0.5014	57.69	57.65	-0.04	-0.07

C(1,2) = 0.12661 D(1,2) =-0.00446
CSTDE = 0.00084 DSTDE = 0.00024

RMSE = 0.1449 BAR NO PT = 13
AAD = 0.1005 BAR %AAD = 0.320
MIN DEV= -0.3301 BAR MIN %DEV = -0.716
MAX DEV= 0.2675 BAR MAX %DEV = 0.802
BIAS = -0.0054 BAR C-VAR = 0.290
RESTRICTIONS : NONE R-SQR =0.999460
AUX. MODELS : 000 000 000 EXP REF = 1

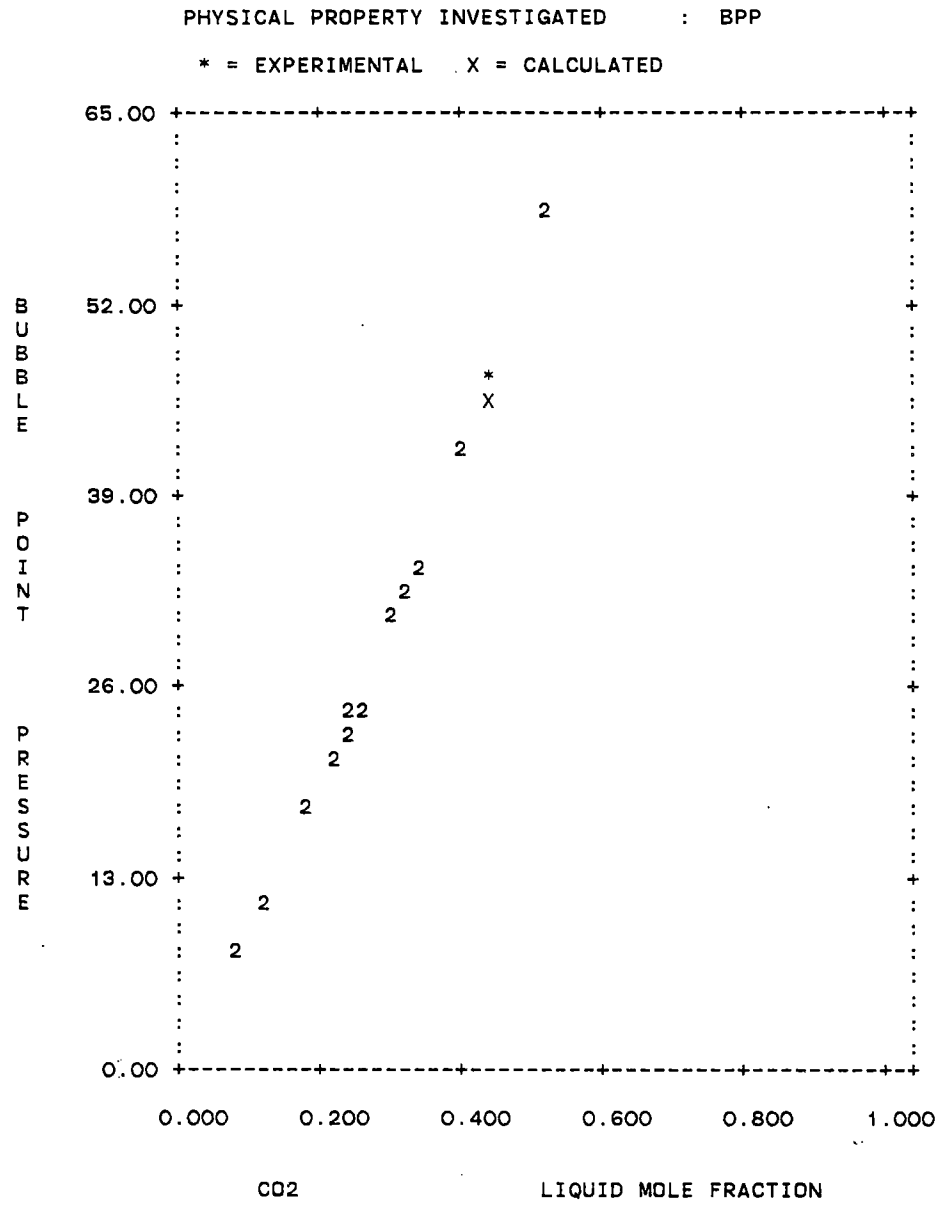

FIGURE C.1. BUBBLE-POINT CALCULATIONS USING SOAVE-RK EQUATION OF STATE

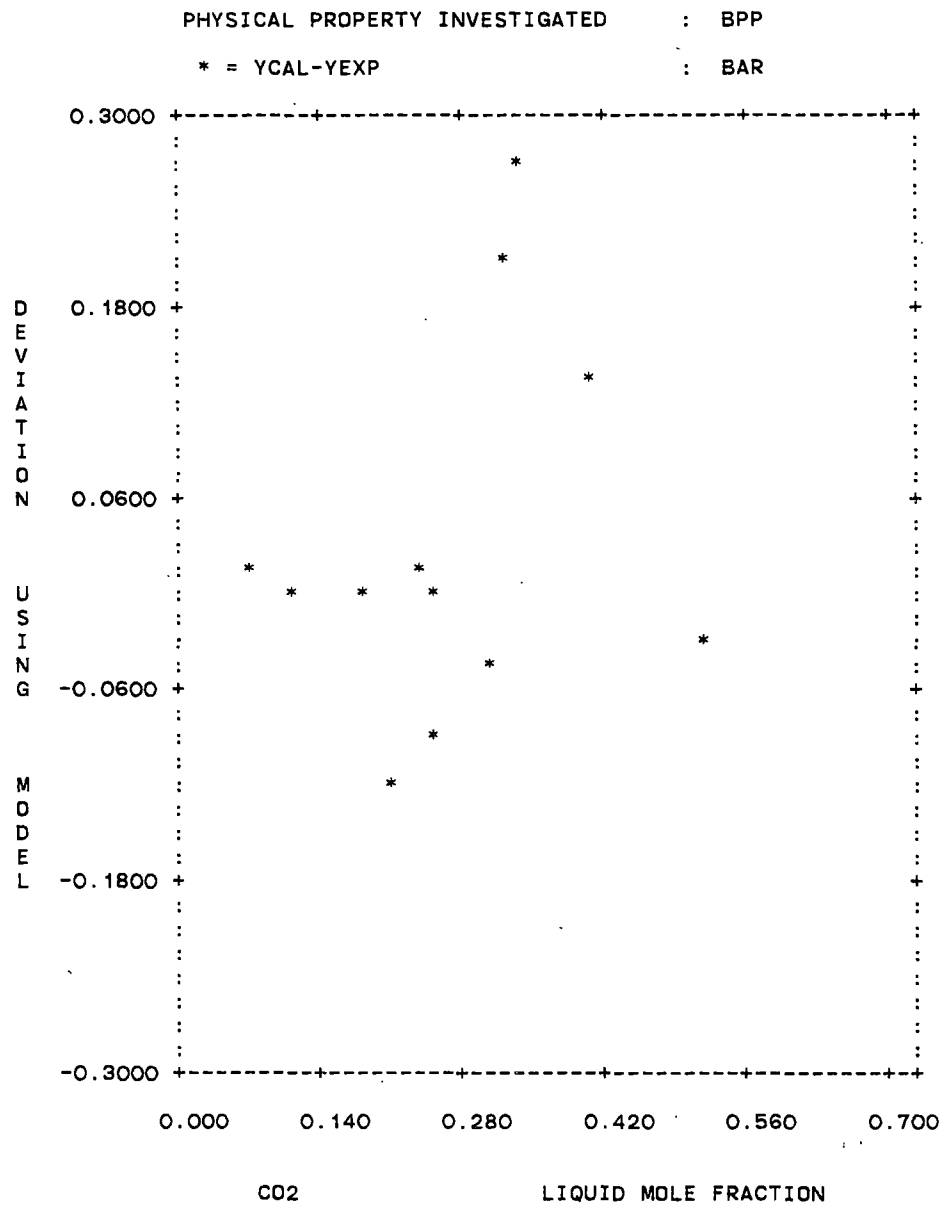

FIGURE C.2. BUBBLE-POINT CALCULATIONS USING SOAVE-RK EQUATION OF STATE

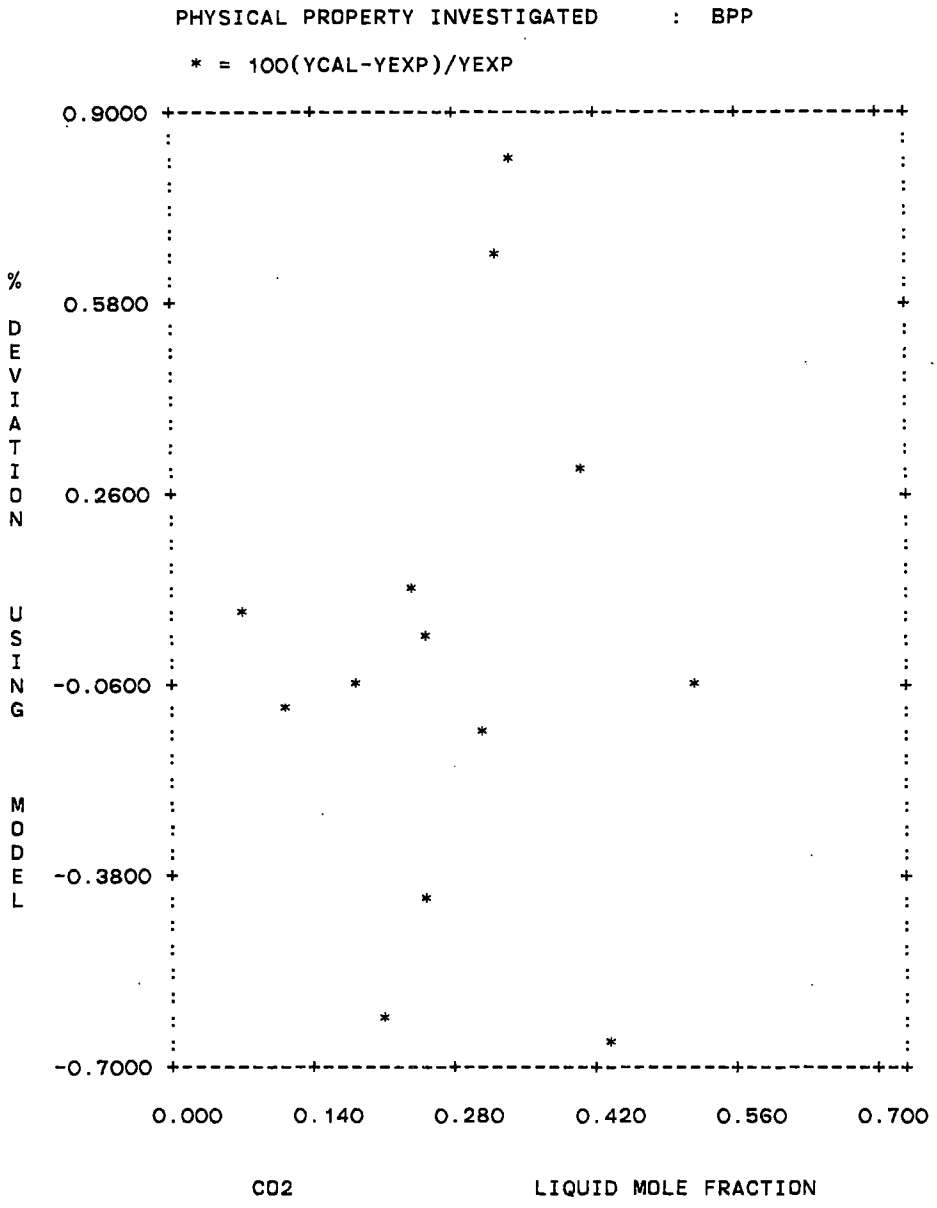

FIGURE C.3. BUBBLE-POINT CALCULATIONS
USING SOAVE-RK EQUATION OF STATE

TABLE C.2

SRK EOS WEIGHTED LEAST SQUARES REGRESSION $C_{ij}(T)$ AND $D_{ij}(T)$

ISO	CN	T(K)	C(I,J)	D(I,J)	RMSE BAR	BIAS BAR	AAD BAR	%AAD	NO PT
1	20	323.1	0.1271	-0.0047	0.14	-0.01	0.10	0.3	13
2	20	373.1	0.1219	-0.0100	0.15	-0.12	0.12	0.4	9
3	28	348.1	0.1224	-0.0119	0.11	0.01	0.09	0.3	8
4	28	373.1	0.1200	-0.0147	0.14	-0.03	0.13	0.6	9
5	28	423.1	0.1180	-0.0215	0.73	-0.06	0.56	2.5	7
6	36	373.1	0.0948	-0.0152	0.29	-0.05	0.25	1.3	10
7	36	423.1	0.0992	-0.0242	0.47	-0.09	0.39	1.5	8
8	44	373.1	0.0776	-0.0170	0.29	-0.05	0.26	1.5	7
9	44	423.1	0.0546	-0.0230	0.30	-0.06	0.28	1.4	7

MODEL OVERALL STATISTICS

RMSE	= 0.3265 BAR	NO PT	= 78
AAD	= 0.2256 BAR	%AAD	= 1.010
MIN DEV	= -0.6059 BAR	MIN %DEV	= -4.697
MAX DEV	= 1.6430 BAR	MAX %DEV	= 5.601
BIAS	= -0.0476 BAR	C-VAR	= 0.010
RESTRICTIONS	: NONE	R-SQR	=0.995127
AUX. MODELS	: 000 000 000/ 000 000		

TABLE C.3

C_{ij} = 0 BPP

CALCULATIONS USING PR EOS

ISO	CN	T(K)	C(I,J)	D(I,J)	RMSE BAR	BIAS BAR	AAD BAR	%AAD	NO PT
1	4	310.9	0.0000	0.0000	6.87	-6.14	6.14	24.4	18
2	4	344.3	0.0000	0.0000	7.56	-6.47	6.47	17.6	17
3	4	377.6	0.0000	0.0000	5.11	-4.53	4.53	10.7	12
4	4	410.9	0.0000	0.0000	1.45	-1.30	1.30	3.1	7
5	6	313.1	0.0000	0.0000	10.44	-9.72	9.72	22.8	8
6	6	353.1	0.0000	0.0000	13.14	-12.20	12.20	27.5	15
7	6	393.1	0.0000	0.0000	15.23	-14.50	14.50	21.7	14
8	7	310.6	0.0000	0.0000	8.01	-6.67	6.67	22.2	23
9	7	352.6	0.0000	0.0000	13.48	-12.51	12.51	23.0	17
10	7	394.3	0.0000	0.0000	12.83	-11.92	11.92	16.4	16
11	7	477.2	0.0000	0.0000	7.15	-6.29	6.29	9.1	7
12	10	277.6	0.0000	0.0000	8.64	-7.90	7.90	44.0	11
13	10	310.9	0.0000	0.0000	14.76	-13.73	13.73	37.4	11
14	10	344.3	0.0000	0.0000	19.37	-17.93	17.93	31.1	8
15	10	377.6	0.0000	0.0000	23.21	-21.01	21.01	27.3	10
16	10	410.9	0.0000	0.0000	22.88	-20.39	20.39	23.4	11
17	10	444.3	0.0000	0.0000	20.54	-18.11	18.11	20.4	11
18	10	477.6	0.0000	0.0000	18.73	-16.47	16.47	18.4	11
19	10	510.9	0.0000	0.0000	15.59	-13.52	13.52	18.0	9
20	16	463.0	0.0000	0.0000	4.30	-4.08	4.08	11.5	4
21	20	323.1	0.0000	0.0000	10.97	-9.56	9.56	33.4	13
22	20	373.1	0.0000	0.0000	10.63	-9.35	9.35	21.6	9
23	22	323.1	0.0000	0.0000	17.18	-15.27	15.27	33.5	14
24	22	348.1	0.0000	0.0000	11.89	-10.18	10.18	23.7	19
25	22	373.1	0.0000	0.0000	8.05	-6.67	6.67	17.6	11
26	28	348.1	0.0000	0.0000	15.65	-11.61	11.61	21.0	8
27	28	373.1	0.0000	0.0000	9.86	-6.68	6.68	12.4	9
28	28	423.1	0.0000	0.0000	4.98	-2.17	3.21	6.4	7
29	32	348.1	0.0000	0.0000	9.42	-7.53	7.53	15.3	11
30	32	373.1	0.0000	0.0000	6.46	-5.41	5.44	9.6	11
31	32	398.1	0.0000	0.0000	2.20	-0.20	1.76	5.3	15
32	36	373.1	0.0000	0.0000	2.22	-0.68	1.50	5.6	10
33	36	423.1	0.0000	0.0000	3.29	2.18	3.19	11.4	8
34	44	373.1	0.0000	0.0000	2.48	1.84	2.42	14.6	7
35	44	423.1	0.0000	0.0000	7.23	6.94	6.94	27.2	7

MODEL OVERALL STATISTICS

RMSE	= 12.2339 BAR	NO PT	= 399
AAD	= 9.5801 BAR	%AAD	= 20.513
MIN DEV	=-33.1148 BAR	MIN %DEV	= -57.980
MAX DEV	= 9.1546 BAR	MAX %DEV	= 40.010
BIAS	= -9.0557 BAR	C-VAR	= 24.468
RESTRICTIONS	: NONE	R-SQR	=0.675413
AUX. MODELS	: 000 000 000		

TABLE C.4

C_{ij} BPP

CALCULATIONS USING PR EOS

ISO	CN	T(K)	C(I,J)	D(I,J)	RMSE BAR	BIAS BAR	AAD BAR	%AAD	NO PT
1	4	310.9	0.1343	0.0000	0.66	0.24	0.46	1.3	18
2	4	344.3	0.1343	0.0000	0.26	-0.09	0.19	0.6	17
3	4	377.6	0.1343	0.0000	0.96	-0.77	0.77	1.6	12
4	4	410.9	0.1343	0.0000	1.22	-1.08	1.09	2.5	7
5	6	313.1	0.1227	0.0000	1.06	0.18	0.90	1.8	8
6	6	353.1	0.1227	0.0000	1.16	0.09	0.97	2.5	14
7	6	393.1	0.1227	0.0000	0.98	-0.86	0.86	2.0	15
8	7	310.6	0.1000	0.0000	0.99	-0.54	0.81	2.5	23
9	7	352.6	0.1000	0.0000	0.87	-0.26	0.54	0.9	17
10	7	394.3	0.1000	0.0000	1.60	1.24	1.56	3.4	16
11	7	477.2	0.1000	0.0000	0.75	-0.35	0.60	1.0	7
12	10	277.6	0.1073	0.0000	1.69	-1.34	1.55	10.5	11
13	10	310.9	0.1073	0.0000	1.74	-1.09	1.52	5.9	11
14	10	344.3	0.1073	0.0000	3.29	0.53	2.55	4.0	8
15	10	377.6	0.1073	0.0000	2.47	0.63	1.73	1.8	10
16	10	410.9	0.1073	0.0000	1.63	0.14	1.27	1.4	11
17	10	444.3	0.1073	0.0000	1.32	-0.79	1.03	1.1	11
18	10	477.6	0.1073	0.0000	2.80	-2.34	2.34	2.6	11
19	10	510.9	0.1073	0.0000	5.16	-4.43	4.43	6.0	9
20	16	463.0	0.0601	0.0000	0.21	-0.01	0.19	0.6	4
21	20	323.1	0.0911	0.0000	1.50	-1.08	1.08	3.1	13
22	20	373.1	0.0911	0.0000	1.84	1.79	1.79	5.3	9
23	22	323.1	0.0865	0.0000	2.67	-2.02	2.07	3.9	14
24	22	348.1	0.0865	0.0000	1.55	1.41	1.45	5.2	19
25	22	373.1	0.0865	0.0000	2.75	2.57	2.57	8.5	11
26	28	348.1	0.0688	0.0000	4.02	-1.41	2.78	6.8	8
27	28	373.1	0.0688	0.0000	2.39	1.65	2.28	9.5	9
28	28	423.1	0.0688	0.0000	5.45	5.08	5.08	17.5	7
29	32	348.1	0.0352	0.0000	4.21	-2.74	3.03	5.6	11
30	32	373.1	0.0352	0.0000	1.64	-0.10	1.39	3.7	11
31	32	398.1	0.0352	0.0000	4.30	4.09	4.09	12.7	15
32	36	373.1	0.0023	0.0000	2.07	-0.49	1.44	5.8	10
33	36	423.1	0.0023	0.0000	3.39	2.43	3.31	11.8	8
34	44	373.1	-0.0379	0.0000	3.64	-1.30	2.34	8.6	7
35	44	423.1	-0.0379	0.0000	3.82	3.42	3.46	16.4	7

MODEL OVERALL STATISTICS

RMSE	= 2.3727 BAR	NO PT	= 399
AAD	= 1.6710 BAR	%AAD	= 4.615
MIN DEV	= -9.5380 BAR	MIN %DEV	= -17.525
MAX DEV	= 7.6830 BAR	MAX %DEV	= 28.988
BIAS	= 0.0376 BAR	C-VAR	= 4.745
RESTRICTIONS	: NONE	R-SQR	=0.994814
AUX. MODELS	: 000 000 000		

TABLE C.5

C_{ij} AND D_{ij} BPP
CALCULATIONS USING PR EOS

ISO	CN	T(K)	C(I,J)	D(I,J)	RMSE BAR	BIAS BAR	AAD BAR	%AAD	NO PT
1	4	310.9	0.1364	-0.0017	0.72	0.30	0.49	1.4	18
2	4	344.3	0.1364	-0.0017	0.25	-0.02	0.20	0.6	17
3	4	377.6	0.1364	-0.0017	0.89	-0.72	0.73	1.5	12
4	4	410.9	0.1364	-0.0017	1.21	-1.07	1.08	2.5	7
5	6	313.1	0.1203	0.0078	1.10	0.34	0.97	1.8	8
6	6	353.1	0.1203	0.0078	0.96	0.21	0.78	1.7	14
7	6	393.1	0.1203	0.0078	0.92	-0.75	0.76	1.4	15
8	7	310.6	0.0923	0.0078	1.04	-0.80	0.83	2.5	23
9	7	352.6	0.0923	0.0078	1.45	-0.91	0.99	1.4	17
10	7	394.3	0.0923	0.0078	1.85	0.54	1.60	3.5	16
11	7	477.2	0.0923	0.0078	1.27	-0.69	0.98	1.5	7
12	10	277.6	0.1021	0.0144	0.74	-0.42	0.65	3.6	11
13	10	310.9	0.1021	0.0144	0.63	-0.05	0.52	1.2	11
14	10	344.3	0.1021	0.0144	2.06	1.38	1.38	2.1	8
15	10	377.6	0.1021	0.0144	1.62	1.45	1.45	2.8	10
16	10	410.9	0.1021	0.0144	1.23	0.93	1.02	2.5	11
17	10	444.3	0.1021	0.0144	1.23	-0.04	1.15	2.1	11
18	10	477.6	0.1021	0.0144	2.74	-1.87	2.15	2.1	11
19	10	510.9	0.1021	0.0144	4.80	-3.84	3.84	4.6	9
20	16	463.0	0.0630	-0.0011	0.20	-0.02	0.19	0.6	4
21	20	323.1	0.1091	-0.0081	1.41	-1.33	1.33	5.3	13
22	20	373.1	0.1091	-0.0081	1.64	1.50	1.50	3.6	9
23	22	323.1	0.1139	-0.0145	1.85	-1.76	1.76	5.6	14
24	22	348.1	0.1139	-0.0145	0.91	0.38	0.72	1.9	19
25	22	373.1	0.1139	-0.0145	1.53	0.93	1.10	2.8	11
26	28	348.1	0.1133	-0.0211	2.08	-1.98	1.98	6.9	8
27	28	373.1	0.1133	-0.0211	0.82	-0.52	0.75	3.6	9
28	28	423.1	0.1133	-0.0211	3.00	2.31	2.31	5.2	7
29	32	348.1	0.0975	-0.0227	2.70	-2.65	2.65	9.4	11
30	32	373.1	0.0975	-0.0227	1.24	-0.95	1.11	3.3	11
31	32	398.1	0.0975	-0.0227	2.77	2.00	2.27	5.1	15
32	36	373.1	0.0686	-0.0186	1.76	-1.59	1.59	6.7	10
33	36	423.1	0.0686	-0.0186	1.92	1.72	1.72	4.8	8
34	44	373.1	0.0589	-0.0243	2.56	-2.36	2.36	11.2	7
35	44	423.1	0.0589	-0.0243	2.29	1.84	1.84	4.8	7

MODEL OVERALL STATISTICS

RMSE	= 1.7238 BAR	NO PT	= 399
AAD	= 1.2601 BAR	%AAD	= 3.253
MIN DEV	= -8.4170 BAR	MIN %DEV	= -23.155
MAX DEV	= 5.7226 BAR	MAX %DEV	= 18.216
BIAS	= -0.2571 BAR	C-VAR	= 3.448
RESTRICTIONS	: NONE	R-SQR	=0.990450
AUX. MODELS	: 000 000 000		

TABLE C.6

$C_{ij}(T)$ BPP
CALCULATIONS USING PR EOS

ISO	CN	T(K)	C(I,J)	D(I,J)	RMSE BAR	BIAS BAR	AAD BAR	%AAD	NO PT
1	4	310.9	0.1273	0.0000	0.47	-0.16	0.39	1.7	18
2	4	344.3	0.1346	0.0000	0.45	-0.15	0.26	0.7	17
3	4	377.6	0.1515	0.0000	0.16	0.05	0.14	0.4	12
4	4	410.9	0.1993	0.0000	0.29	-0.08	0.26	0.6	7
5	6	313.1	0.1183	0.0000	0.94	-0.26	0.86	1.9	8
6	6	353.1	0.1199	0.0000	1.09	-0.28	0.90	2.7	14
7	6	393.1	0.1283	0.0000	0.57	-0.14	0.43	1.2	15
8	7	310.6	0.1032	0.0000	0.94	-0.30	0.77	2.2	23
9	7	352.6	0.1008	0.0000	0.86	-0.13	0.55	0.8	17
10	7	394.3	0.0943	0.0000	1.19	0.34	1.00	2.4	16
11	7	477.2	0.1082	0.0000	0.48	0.21	0.45	1.1	7
12	10	277.6	0.1188	0.0000	1.26	-0.35	1.05	6.9	11
13	10	310.9	0.1105	0.0000	1.63	-0.56	1.46	5.3	11
14	10	344.3	0.1011	0.0000	2.64	-1.16	2.44	4.9	8
15	10	377.6	0.1027	0.0000	1.93	-0.67	1.65	2.3	10
16	10	410.9	0.1056	0.0000	1.52	-0.30	1.24	1.4	11
17	10	444.3	0.1104	0.0000	1.08	-0.17	0.83	0.9	11
18	10	477.6	0.1199	0.0000	1.28	-0.30	0.90	0.9	11
19	10	510.9	0.1493	0.0000	0.96	-0.13	0.68	0.9	9
20	16	463.0	0.0601	0.0000	0.21	-0.01	0.19	0.6	4
21	20	323.1	0.1014	0.0000	0.43	0.17	0.39	1.7	13
22	20	373.1	0.0806	0.0000	0.73	0.27	0.67	2.3	9
23	22	323.1	0.0972	0.0000	0.68	0.27	0.56	1.9	14
24	22	348.1	0.0805	0.0000	1.09	0.43	0.97	3.5	19
25	22	373.1	0.0611	0.0000	1.26	-0.50	0.91	2.4	11
26	28	348.1	0.0826	0.0000	2.28	1.27	2.11	8.4	8
27	28	373.1	0.0641	0.0000	2.32	0.99	2.03	8.3	9
28	28	423.1	0.0346	0.0000	2.66	1.26	2.27	9.1	7
29	32	348.1	0.0567	0.0000	1.64	0.67	1.47	5.3	11
30	32	373.1	0.0387	0.0000	1.52	0.48	1.34	3.9	11
31	32	398.1	0.0076	0.0000	1.97	0.68	1.71	5.9	15
32	36	373.1	0.0156	0.0000	1.59	0.65	1.31	7.2	10
33	36	423.1	-0.0083	0.0000	3.13	1.30	2.77	9.7	8
34	44	373.1	-0.0089	0.0000	2.30	1.07	2.14	12.4	7
35	44	423.1	-0.0639	0.0000	2.85	1.23	2.58	11.5	7

MODEL OVERALL STATISTICS

RMSE	= 1.4178 BAR	NO PT	= 399
AAD	= 1.0374 BAR	%AAD	= 3.382
MIN DEV=	-5.8811 BAR	MIN %DEV	= -12.095
MAX DEV=	4.7510 BAR	MAX %DEV	= 24.209
BIAS	= 0.1096 BAR	C-VAR	= 2.836
RESTRICTIONS	: NONE	R-SQR	=0.998302
AUX. MODELS	: 000 000 000		

TABLE C.7

$C_{ij}(T)$ AND $D_{ij}(T)$ BPP
CALCULATIONS USING PR EOS

ISO	CN	T(K)	C(I,J)	D(I,J)	RMSE BAR	BIAS BAR	AAD BAR	%AAD	NO PT
1	4	310.9	0.1187	0.0138	0.42	-0.14	0.29	0.9	18
2	4	344.3	0.1367	-0.0038	0.24	-0.08	0.20	0.7	17
3	4	377.6	0.1533	-0.0036	0.15	0.04	0.12	0.3	12
4	4	410.9	0.1530	0.0654	0.20	-0.12	0.17	0.4	7
5	6	313.1	0.1109	0.0138	0.82	-0.32	0.60	1.1	8
6	6	353.1	0.1152	0.0129	0.79	-0.19	0.63	1.4	14
7	6	393.1	0.1264	0.0057	0.48	-0.07	0.40	1.0	15
8	7	310.6	0.0954	0.0141	0.79	-0.30	0.55	1.9	23
9	7	352.6	0.1014	-0.0017	0.85	-0.15	0.57	1.0	17
10	7	394.3	0.0987	-0.0144	0.45	0.04	0.31	0.9	16
11	7	477.2	0.1081	-0.0088	0.36	0.09	0.29	0.6	7
12	10	277.6	0.0938	0.0257	0.43	-0.01	0.33	2.3	11
13	10	310.9	0.0986	0.0187	0.50	-0.05	0.36	1.0	11
14	10	344.3	0.0942	0.0198	0.59	0.13	0.53	1.6	8
15	10	377.6	0.0981	0.0135	0.68	0.16	0.61	1.6	10
16	10	410.9	0.1017	0.0100	0.93	0.18	0.82	1.8	11
17	10	444.3	0.1075	0.0073	0.81	0.16	0.75	1.4	11
18	10	477.6	0.1183	0.0079	0.90	0.19	0.77	1.2	11
19	10	510.9	0.1443	0.0092	0.84	0.11	0.70	1.1	9
20	16	463.0	0.0630	-0.0011	0.20	-0.02	0.19	0.6	4
21	20	323.1	0.1109	-0.0044	0.14	-0.00	0.10	0.3	13
22	20	373.1	0.1032	-0.0099	0.11	-0.02	0.09	0.3	9
23	22	323.1	0.1044	-0.0047	0.28	-0.00	0.23	0.7	14
24	22	348.1	0.1010	-0.0100	0.39	-0.01	0.33	1.1	19
25	22	373.1	0.0894	-0.0086	0.48	-0.01	0.38	1.4	11
26	28	348.1	0.1041	-0.0123	0.11	0.01	0.09	0.3	8
27	28	373.1	0.1010	-0.0155	0.14	-0.03	0.13	0.6	9
28	28	423.1	0.0978	-0.0232	0.73	-0.06	0.56	2.5	7
29	32	348.1	0.0826	-0.0111	0.41	-0.05	0.33	1.5	11
30	32	373.1	0.0756	-0.0134	0.41	-0.00	0.34	0.8	11
31	32	398.1	0.0638	-0.0179	0.77	-0.06	0.57	1.9	15
32	36	373.1	0.0768	-0.0162	0.29	-0.05	0.25	1.3	10
33	36	423.1	0.0806	-0.0261	0.48	-0.09	0.40	1.5	8
34	44	373.1	0.0610	-0.0183	0.28	-0.06	0.25	1.5	7
35	44	423.1	0.0387	-0.0251	0.31	-0.06	0.29	1.4	7

MODEL OVERALL STATISTICS

RMSE	= 0.5596 BAR	NO PT	= 399
AAD	= 0.3958 BAR	%AAD	= 1.149
MIN DEV	= -2.7592 BAR	MIN %DEV	= -11.740
MAX DEV	= 2.0505 BAR	MAX %DEV	= 10.477
BIAS	= -0.0370 BAR	C-VAR	= 1.119
RESTRICTIONS	: NONE	R-SQR	=0.998506
AUX. MODELS	: 000 000 000		

APPENDIX D

EOS SENSITIVITY ANALYSIS

This Appendix presents sample simulation runs performed on CO_2 + n-C_{36} system to investigate the sensitivity of SRK EOS predictions to variations in input data.

TABLE D.1

SENSITIVITY OF SRK EOS NORMAL BOILING POINT PREDICTION TO VARIATIONS IN HYDROCARBON PURE PROPERTIES ($n\text{-}C_{36}$)

RUN	T(K)	TC DEV	PC DEV	W DEV	CIJ DEV	DIJ DEV	P RMSE	RMSE DEV
1	770.74	0.00	0.00	0.0000	0.0000	0.0000	0.0124	0.0000
2	770.74	0.00	0.00	0.0257	0.0000	0.0000	0.0049	-0.0075
3	770.74	0.00	0.00	-0.0257	0.0000	0.0000	0.0302	0.0178
4	770.74	0.00	0.07	0.0000	0.0000	0.0000	0.0227	0.0103
5	770.74	0.00	0.07	0.0257	0.0000	0.0000	0.0052	-0.0073
6	770.74	0.00	0.07	-0.0257	0.0000	0.0000	0.0406	0.0282
7	770.74	0.00	-0.07	0.0000	0.0000	0.0000	0.0022	-0.0103
8	770.74	0.00	-0.07	0.0257	0.0000	0.0000	0.0150	0.0026
9	770.74	0.00	-0.07	-0.0257	0.0000	0.0000	0.0198	0.0073
10	770.74	4.51	0.00	0.0000	0.0000	0.0000	0.0555	0.0431
11	770.74	4.51	0.00	0.0257	0.0000	0.0000	0.0724	0.0600
12	770.74	4.51	0.00	-0.0257	0.0000	0.0000	0.0383	0.0259
13	770.74	4.51	0.07	0.0000	0.0000	0.0000	0.0460	0.0335
14	770.74	4.51	0.07	0.0257	0.0000	0.0000	0.0630	0.0505
15	770.74	4.51	0.07	-0.0257	0.0000	0.0000	0.0285	0.0161
16	770.74	4.51	-0.07	0.0000	0.0000	0.0000	0.0651	0.0527
17	770.74	4.51	-0.07	0.0257	0.0000	0.0000	0.0818	0.0694
18	770.74	4.51	-0.07	-0.0257	0.0000	0.0000	0.0480	0.0356
19	770.74	-4.51	0.00	0.0000	0.0000	0.0000	0.0850	0.0726
20	770.74	-4.51	0.00	0.0257	0.0000	0.0000	0.0671	0.0547
21	770.74	-4.51	0.00	-0.0257	0.0000	0.0000	0.1032	0.0908
22	770.74	-4.51	0.07	0.0000	0.0000	0.0000	0.0960	0.0835
23	770.74	-4.51	0.07	0.0257	0.0000	0.0000	0.0779	0.0655
24	770.74	-4.51	0.07	-0.0257	0.0000	0.0000	0.1144	0.1020
25	770.74	-4.51	-0.07	0.0000	0.0000	0.0000	0.0740	0.0616
26	770.74	-4.51	-0.07	0.0257	0.0000	0.0000	0.0563	0.0439
27	770.74	-4.51	-0.07	-0.0257	0.0000	0.0000	0.0921	0.0797

TC...PC...W	NOMINAL VALUES:	901.07	K	6.82	BAR	1.2847		
TC...PC...W	ERROR LEVELS:	0.50	%	1.00	%	2.00	%	
CIJ.....DIJ	NOMINAL VALUES:	0.0948		-0.0152				
CIJ.... DIJ	ERROR LEVELS:	0.00	%	0.00	%			

TABLE D.1 (Continued)

RUN	CIJ.....STDE		DIJ.....STDE		P RMSE	FN(CIJ)	FN(DIJ)	FN(PRM)
1	0.0948	0.0000	-0.0152	0.0000	0.0124	0.3989	0.3989	0.3989
2	0.0948	0.0000	-0.0152	0.0000	0.0049	0.3989	0.3989	0.3947
3	0.0948	0.0000	-0.0152	0.0000	0.0302	0.3989	0.3989	0.3756
4	0.0948	0.0000	-0.0152	0.0000	0.0227	0.3989	0.3989	0.3910
5	0.0948	0.0000	-0.0152	0.0000	0.0052	0.3989	0.3989	0.3949
6	0.0948	0.0000	-0.0152	0.0000	0.0406	0.3989	0.3989	0.3427
7	0.0948	0.0000	-0.0152	0.0000	0.0022	0.3989	0.3989	0.3910
8	0.0948	0.0000	-0.0152	0.0000	0.0150	0.3989	0.3989	0.3984
9	0.0948	0.0000	-0.0152	0.0000	0.0198	0.3989	0.3989	0.3949
10	0.0948	0.0000	-0.0152	0.0000	0.0555	0.3989	0.3989	0.2797
11	0.0948	0.0000	-0.0152	0.0000	0.0724	0.3989	0.3989	0.2007
12	0.0948	0.0000	-0.0152	0.0000	0.0383	0.3989	0.3989	0.3511
13	0.0948	0.0000	-0.0152	0.0000	0.0460	0.3989	0.3989	0.3218
14	0.0948	0.0000	-0.0152	0.0000	0.0630	0.3989	0.3989	0.2448
15	0.0948	0.0000	-0.0152	0.0000	0.0285	0.3989	0.3989	0.3797
16	0.0948	0.0000	-0.0152	0.0000	0.0651	0.3989	0.3989	0.2347
17	0.0948	0.0000	-0.0152	0.0000	0.0818	0.3989	0.3989	0.1591
18	0.0948	0.0000	-0.0152	0.0000	0.0480	0.3989	0.3989	0.3131
19	0.0948	0.0000	-0.0152	0.0000	0.0850	0.3989	0.3989	0.1459
20	0.0948	0.0000	-0.0152	0.0000	0.0671	0.3989	0.3989	0.2252
21	0.0948	0.0000	-0.0152	0.0000	0.1032	0.3989	0.3989	0.0825
22	0.0948	0.0000	-0.0152	0.0000	0.0960	0.3989	0.3989	0.1051
23	0.0948	0.0000	-0.0152	0.0000	0.0779	0.3989	0.3989	0.1757
24	0.0948	0.0000	-0.0152	0.0000	0.1144	0.3989	0.3989	0.0547
25	0.0948	0.0000	-0.0152	0.0000	0.0740	0.3989	0.3989	0.1933
26	0.0948	0.0000	-0.0152	0.0000	0.0563	0.3989	0.3989	0.2760
27	0.0948	0.0000	-0.0152	0.0000	0.0921	0.3989	0.3989	0.1187
CIJ STATISTICS : MEAN..MIN..MAX..STDV=					0.0948	0.0948	0.0948	0.0000
DIJ STATISTICS : MEAN..MIN..MAX..STDV=					-0.0152	-0.0152	-0.0152	0.0000
P RMSE (BAR) : MEAN..MIN..MAX..STDV=					0.0525	0.0022	0.1144	0.0512

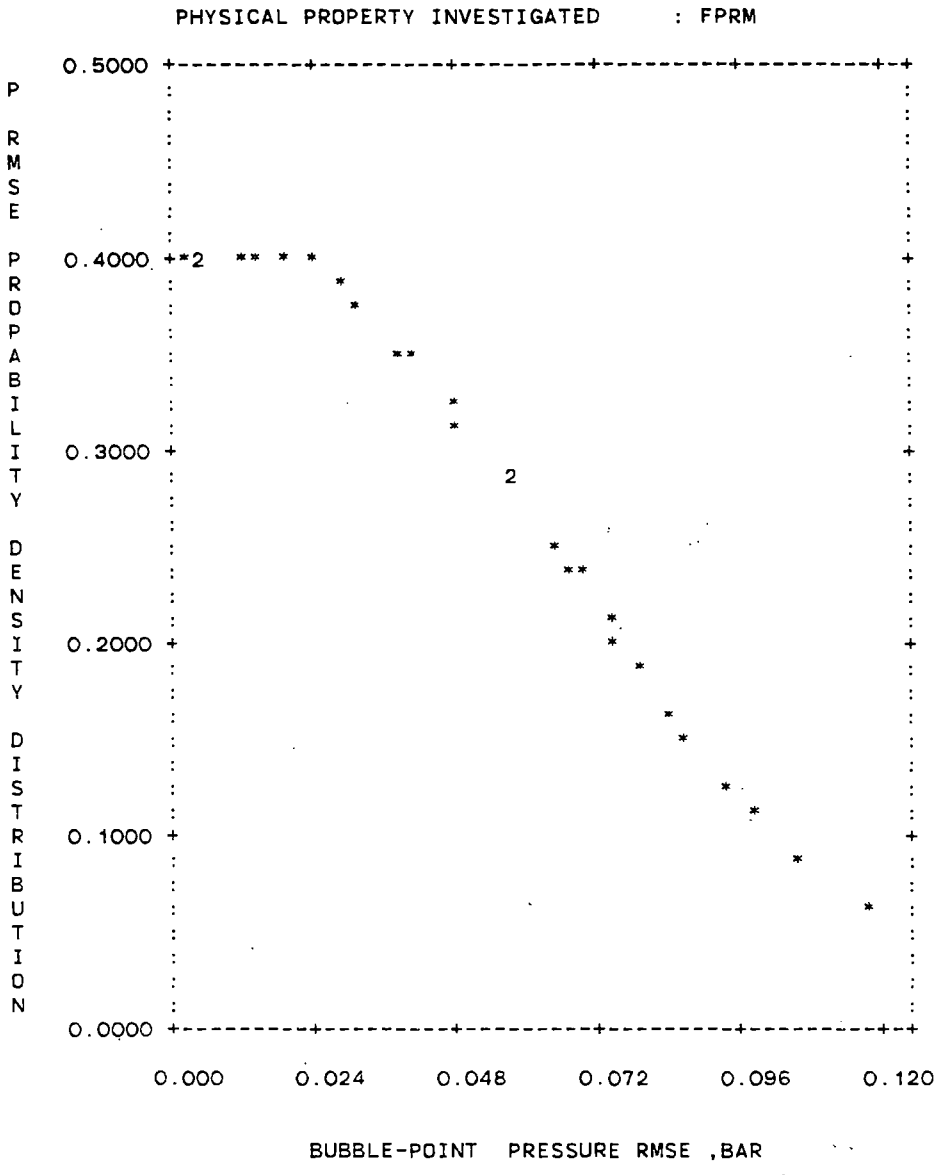

Figure D.1. Probability Density Distribution of BPP RMSE for n-C_{36}. Normal Boiling Point Prediction

TABLE D.2

SENSITIVITY OF SRK EOS BPP PREDICTIONS TO VARIATIONS IN HYDROCARBON PURE PROPERTIES
(CO_2 + n-C_{36} at 373.2K)

RUN	T(K)	TC DEV	PC DEV	W DEV	CIJ DEV	DIJ DEV	P RMSE	RMSE DEV
1	373.15	0.00	0.00	0.0000	0.0000	0.0000	0.2936	0.0000
2	373.15	0.00	0.00	0.0257	0.0000	0.0000	0.3441	0.0505
3	373.15	0.00	0.00	-0.0257	0.0000	0.0000	0.3412	0.0476
4	373.15	0.00	0.07	0.0000	0.0000	0.0000	0.3534	0.0598
5	373.15	0.00	0.07	0.0257	0.0000	0.0000	0.4755	0.1819
6	373.15	0.00	0.07	-0.0257	0.0000	0.0000	0.2950	0.0014
7	373.15	0.00	-0.07	0.0000	0.0000	0.0000	0.3492	0.0556
8	373.15	0.00	-0.07	0.0257	0.0000	0.0000	0.2944	0.0008
9	373.15	0.00	-0.07	-0.0257	0.0000	0.0000	0.4673	0.1737
10	373.15	4.51	0.00	0.0000	0.0000	0.0000	0.2971	0.0035
11	373.15	4.51	0.00	0.0257	0.0000	0.0000	0.3678	0.0742
12	373.15	4.51	0.00	-0.0257	0.0000	0.0000	0.3222	0.0286
13	373.15	4.51	0.07	0.0000	0.0000	0.0000	0.3779	0.0843
14	373.15	4.51	0.07	0.0257	0.0000	0.0000	0.5093	0.2157
15	373.15	4.51	0.07	-0.0257	0.0000	0.0000	0.2995	0.0060
16	373.15	4.51	-0.07	0.0000	0.0000	0.0000	0.3297	0.0361
17	373.15	4.51	-0.07	0.0257	0.0000	0.0000	0.2961	0.0025
18	373.15	4.51	-0.07	-0.0257	0.0000	0.0000	0.4369	0.1434
19	373.15	-4.51	0.00	0.0000	0.0000	0.0000	0.2965	0.0029
20	373.15	-4.51	0.00	0.0257	0.0000	0.0000	0.3241	0.0305
21	373.15	-4.51	0.00	-0.0257	0.0000	0.0000	0.3648	0.0712
22	373.15	-4.51	0.07	0.0000	0.0000	0.0000	0.3324	0.0388
23	373.15	-4.51	0.07	0.0257	0.0000	0.0000	0.4428	0.1492
24	373.15	-4.51	0.07	-0.0257	0.0000	0.0000	0.2969	0.0033
25	373.15	-4.51	-0.07	0.0000	0.0000	0.0000	0.3731	0.0795
26	373.15	-4.51	-0.07	0.0257	0.0000	0.0000	0.2990	0.0054
27	373.15	-4.51	-0.07	-0.0257	0.0000	0.0000	0.5002	0.2066

TC...PC...W	NOMINAL VALUES:	901.07	K	6.82	BAR	1.2847
TC...PC...W	ERROR LEVELS:	0.50	%	1.00	%	2.00 %
CIJ.....DIJ	NOMINAL VALUES:	0.0000		0.0000		
CIJ.... DIJ	ERROR LEVELS:	0.00	%	0.00	%	

TABLE D.2 (Continued)

RUN	CIJ.....STDE		DIJ.....STDE		P RMSE	FN(CIJ)	FN(DIJ)	FN(PRM)
1	0.0948	0.0000	-0.0152	0.0000	0.2936	0.3989	0.3989	0.3989
2	0.0948	0.0000	-0.0152	0.0000	0.3441	0.3989	0.3989	0.3447
3	0.0948	0.0000	-0.0152	0.0000	0.3412	0.3989	0.3989	0.3503
4	0.0948	0.0000	-0.0152	0.0000	0.3534	0.3989	0.3989	0.3250
5	0.0948	0.0000	-0.0152	0.0000	0.4755	0.3989	0.3989	0.0598
6	0.0948	0.0000	-0.0152	0.0000	0.2950	0.3989	0.3989	0.3989
7	0.0948	0.0000	-0.0152	0.0000	0.3492	0.3989	0.3989	0.3342
8	0.0948	0.0000	-0.0152	0.0000	0.2944	0.3989	0.3989	0.3989
9	0.0948	0.0000	-0.0152	0.0000	0.4673	0.3989	0.3989	0.0707
10	0.0948	0.0000	-0.0152	0.0000	0.2971	0.3989	0.3989	0.3987
11	0.0948	0.0000	-0.0152	0.0000	0.3678	0.3989	0.3989	0.2909
12	0.0948	0.0000	-0.0152	0.0000	0.3222	0.3989	0.3989	0.3806
13	0.0948	0.0000	-0.0152	0.0000	0.3779	0.3989	0.3989	0.2654
14	0.0948	0.0000	-0.0152	0.0000	0.5093	0.3989	0.3989	0.0277
15	0.0948	0.0000	-0.0152	0.0000	0.2995	0.3989	0.3989	0.3981
16	0.0948	0.0000	-0.0152	0.0000	0.3297	0.3989	0.3989	0.3703
17	0.0948	0.0000	-0.0152	0.0000	0.2961	0.3989	0.3989	0.3988
18	0.0948	0.0000	-0.0152	0.0000	0.4369	0.3989	0.3989	0.1228
19	0.0948	0.0000	-0.0152	0.0000	0.2965	0.3989	0.3989	0.3987
20	0.0948	0.0000	-0.0152	0.0000	0.3241	0.3989	0.3989	0.3782
21	0.0948	0.0000	-0.0152	0.0000	0.3648	0.3989	0.3989	0.2983
22	0.0948	0.0000	-0.0152	0.0000	0.3324	0.3989	0.3989	0.3659
23	0.0948	0.0000	-0.0152	0.0000	0.4428	0.3989	0.3989	0.1113
24	0.0948	0.0000	-0.0152	0.0000	0.2969	0.3989	0.3989	0.3987
25	0.0948	0.0000	-0.0152	0.0000	0.3731	0.3989	0.3989	0.2777
26	0.0948	0.0000	-0.0152	0.0000	0.2990	0.3989	0.3989	0.3983
27	0.0948	0.0000	-0.0152	0.0000	0.5002	0.3989	0.3989	0.0345

CIJ STATISTICS : MEAN..MIN..MAX..STDV=	0.0948	0.0948	0.0948	0.0000
DIJ STATISTICS : MEAN..MIN..MAX..STDV=	-0.0152	-0.0152	-0.0152	0.0000
P RMSE (BAR) : MEAN..MIN..MAX..STDV=	0.3585	0.2936	0.5093	0.0934

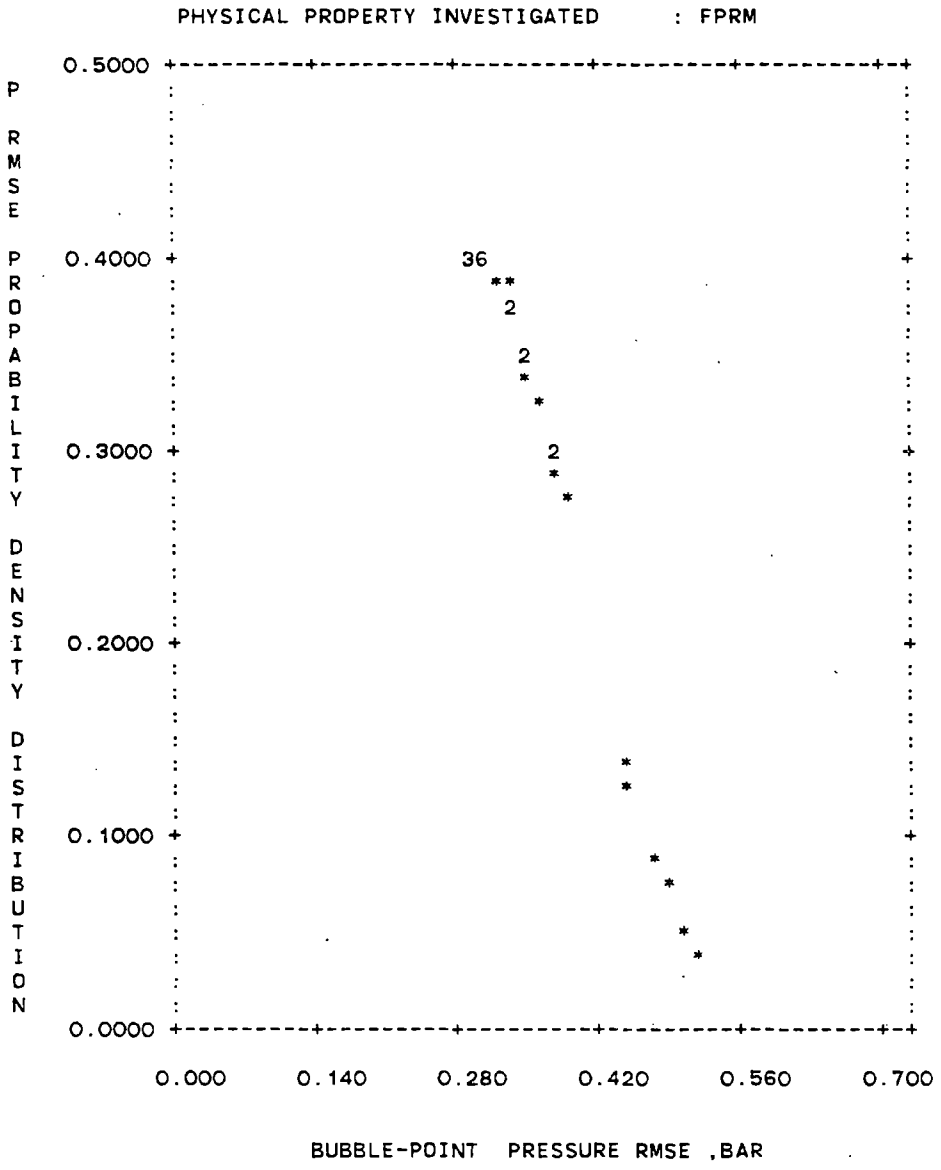

Figure D.2. Probability Density Distribution of BPP RMSE for CO_2 + n-C_{36} Binary at 373.2 K

TABLE D.3

SENSITIVITY OF SRK EOS BPP PREDICTIONS TO VARIATIONS IN C_{ij} AND D_{ij} VALUES (CO_2 + n-C_{36} at 373.2 K)

RUN	T(K)	TC DEV	PC DEV	W DEV	CIJ DEV	DIJ DEV	P RMSE	RMSE DEV
1	373.15	0.00	0.00	0.0000	0.0000	0.0000	0.2936	0.0000
2	373.15	0.00	0.00	0.0000	0.0000	-0.0010	0.5084	0.2148
3	373.15	0.00	0.00	0.0000	0.0000	0.0010	0.5179	0.2243
4	373.15	0.00	0.00	0.0000	0.0043	0.0000	0.5296	0.2361
5	373.15	0.00	0.00	0.0000	0.0043	-0.0010	0.3112	0.0176
6	373.15	0.00	0.00	0.0000	0.0043	0.0010	0.9146	0.6210
7	373.15	0.00	0.00	0.0000	-0.0043	0.0000	0.5198	0.2262
8	373.15	0.00	0.00	0.0000	-0.0043	-0.0010	0.8836	0.5900
9	373.15	0.00	0.00	0.0000	-0.0043	0.0010	0.3112	0.0176

TC...PC...W	NOMINAL VALUES:	901.07	K	6.82	BAR	1.2847	
TC...PC...W	ERROR LEVELS:	0.00	%	0.00	%	0.00	%
CIJ.....DIJ	NOMINAL VALUES:	0.0948		-0.0152			
CIJ.... DIJ	ERROR LEVELS:	4.50	%	6.60	%		

TABLE D.3 (Continued)

RUN	CIJ.....STDE		DIJ.....STDE		P RMSE	FN(CIJ)	FN(DIJ)	FN(PRM)
1	0.0948	0.0000	-0.0152	0.0000	0.2936	0.3989	0.3989	0.3989
2	0.0948	0.0000	-0.0162	0.0000	0.5084	0.3989	0.1884	0.3197
3	0.0948	0.0000	-0.0142	0.0000	0.5179	0.3989	0.1884	0.3133
4	0.0990	0.0000	-0.0152	0.0000	0.5296	0.1884	0.3989	0.3053
5	0.0990	0.0000	-0.0162	0.0000	0.3112	0.1884	0.1884	0.3983
6	0.0990	0.0000	-0.0142	0.0000	0.9146	0.1884	0.1884	0.0627
7	0.0905	0.0000	-0.0152	0.0000	0.5198	0.1884	0.3989	0.3121
8	0.0905	0.0000	-0.0162	0.0000	0.8836	0.1884	0.1884	0.0751
9	0.0905	0.0000	-0.0142	0.0000	0.3112	0.1884	0.1884	0.3983

CIJ STATISTICS : MEAN..MIN..MAX..STDV=	0.0948	0.0905	0.0990	0.0035
DIJ STATISTICS : MEAN..MIN..MAX..STDV=	-0.0152	-0.0162	-0.0142	0.0008
P RMSE (BAR) : MEAN..MIN..MAX..STDV=	0.5322	0.2936	0.9146	0.3228

APPENDIX E

EOS PARAMETER GENERALIZATION

This Appendix contains the details of SRK EOS parameters generalization. Specific cases listed in Table XLIII are presented here in numerical order. Also included in this Appendix are graphical representations for the behavior of SRK generalized parameters of Case 16a.

TABLE E.1

SRK EOS PARAMETER GENERALIZATION

CASE 6

ISO	CN	T(K)	C(I,J)	D(I,J)	RMSE BAR	BIAS BAR	AAD BAR	%AAD	NO PT
1	4	310.9	0.0987	0.0000	2.21	-2.04	2.04	8.5	18
2	4	344.3	0.0987	0.0000	3.16	-2.72	2.72	7.0	17
3	4	377.6	0.0987	0.0000	3.43	-2.86	2.89	6.1	12
4	4	410.9	0.0987	0.0000	2.06	-1.81	1.83	4.1	7
5	6	313.1	0.0987	0.0000	2.96	-2.76	2.76	6.8	8
6	6	353.1	0.0987	0.0000	4.34	-4.11	4.11	9.1	14
7	6	393.1	0.0987	0.0000	5.51	-5.16	5.16	8.7	15
8	10	310.9	0.0987	0.0000	4.07	-3.84	3.84	12.1	11
9	10	344.3	0.0987	0.0000	4.86	-4.51	4.51	8.8	8
10	10	377.6	0.0987	0.0000	5.61	-5.16	5.16	7.2	10
11	10	410.9	0.0987	0.0000	6.00	-5.39	5.39	6.4	11
12	10	444.3	0.0987	0.0000	6.24	-5.58	5.58	6.6	11
13	10	477.6	0.0987	0.0000	6.87	-6.14	6.14	7.5	11
14	10	510.9	0.0987	0.0000	8.25	-7.35	7.35	10.4	9
15	20	323.1	0.0987	0.0000	2.42	-1.89	1.89	5.9	13
16	20	373.1	0.0987	0.0000	0.73	0.25	0.67	2.3	9
17	22	323.1	0.0987	0.0000	3.43	-2.68	2.70	5.1	14
18	22	348.1	0.0987	0.0000	1.14	0.65	0.99	3.8	19
19	22	373.1	0.0987	0.0000	1.76	1.66	1.66	6.4	10
20	28	348.1	0.0987	0.0000	2.37	0.93	2.18	8.3	8
21	28	373.1	0.0987	0.0000	3.61	3.42	3.42	15.4	7
22	28	423.1	0.0987	0.0000	6.43	5.94	5.94	19.4	7
23	32	348.1	0.0987	0.0000	5.34	5.10	5.10	14.5	11
24	32	373.1	0.0987	0.0000	8.26	8.03	8.03	18.0	11
25	32	398.1	0.0987	0.0000	10.44	9.92	9.92	28.8	12
26	36	373.1	0.0987	0.0000	7.83	7.20	7.20	29.4	10
27	36	423.1	0.0987	0.0000	11.79	11.00	11.00	35.2	7
28	44	373.1	0.0987	0.0000	11.70	10.51	10.51	45.7	7
29	44	423.1	0.0987	0.0000	17.49	15.91	15.91	54.2	7

MODEL OVERALL STATISTICS

PAR(1).. PAR(N)= 0.987041D-01* 0.000000D+00 0.000000D+00
0.000000D+00

RMSE = 6.0891 BAR NO PT = 314
AAD = 4.6362 BAR %AAD = 12.223
MIN DEV=-12.7440 BAR MIN %DEV = -18.606
MAX DEV= 27.3078 BAR MAX %DEV = 66.142
BIAS = -0.1013 BAR C-VAR = 0.125
RESTRICTIONS : NONE R-SQR =0.896427
AUX. MODELS : 000 003 000/ 004 000
SQUARE ERROR IN PRESSURE MINIMIZED

*Use of $\overline{C}_{ij}$ value of 0.1 give comparable results

TABLE E.2

SRK EOS PARAMETER GENERALIZATION

CASE 7

ISO	CN	T(K)	C(I,J)	D(I,J)	RMSE BAR	BIAS BAR	AAD BAR	%AAD	NO PT
1	4	310.9	0.1278	-0.0202	1.37	-1.25	1.25	6.1	18
2	4	344.3	0.1278	-0.0202	1.97	-1.75	1.75	5.0	17
3	4	377.6	0.1278	-0.0202	2.56	-2.17	2.19	4.8	12
4	4	410.9	0.1278	-0.0202	1.84	-1.62	1.64	3.8	7
5	6	313.1	0.1278	-0.0202	1.72	-1.04	1.42	3.9	8
6	6	353.1	0.1278	-0.0202	2.57	-1.69	2.29	6.6	14
7	6	393.1	0.1278	-0.0202	3.20	-2.84	2.85	6.0	15
8	10	310.9	0.1278	-0.0202	3.36	-1.87	3.10	11.6	11
9	10	344.3	0.1278	-0.0202	6.16	-0.15	4.98	9.3	8
10	10	377.6	0.1278	-0.0202	5.01	-0.70	4.26	6.6	10
11	10	410.9	0.1278	-0.0202	4.32	-1.52	3.83	5.5	11
12	10	444.3	0.1278	-0.0202	4.04	-2.64	3.66	5.5	11
13	10	477.6	0.1278	-0.0202	5.00	-3.63	4.62	6.6	11
14	10	510.9	0.1278	-0.0202	6.79	-6.22	6.22	9.6	9
15	20	323.1	0.1278	-0.0202	4.55	-4.35	4.35	17.5	13
16	20	373.1	0.1278	-0.0202	2.87	-2.79	2.79	7.8	9
17	22	323.1	0.1278	-0.0202	4.44	-4.37	4.37	12.2	14
18	22	348.1	0.1278	-0.0202	2.44	-2.38	2.38	7.5	19
19	22	373.1	0.1278	-0.0202	1.86	-1.81	1.81	7.2	10
20	28	348.1	0.1278	-0.0202	2.70	-2.59	2.59	8.1	8
21	28	373.1	0.1278	-0.0202	1.24	-1.20	1.20	5.8	7
22	28	423.1	0.1278	-0.0202	1.91	1.39	1.39	2.9	7
23	32	348.1	0.1278	-0.0202	1.66	0.01	1.46	5.3	11
24	32	373.1	0.1278	-0.0202	2.37	1.67	1.88	3.6	11
25	32	398.1	0.1278	-0.0202	4.05	3.51	3.51	8.4	12
26	36	373.1	0.1278	-0.0202	1.50	0.85	1.09	3.6	10
27	36	423.1	0.1278	-0.0202	4.74	4.06	4.06	11.1	7
28	44	373.1	0.1278	-0.0202	4.25	3.00	3.00	8.2	7
29	44	423.1	0.1278	-0.0202	9.12	7.57	7.57	22.0	7

MODEL OVERALL STATISTICS

PAR(1).. PAR(N)= 0.127800D+00 0.000000D+00 0.000000D+00
0.000000D+00 -0.202000D-01 0.000000D+00
0.000000D+00

RMSE = 3.6845 BAR
AAD = 2.9261 BAR
MIN DEV= -9.7710 BAR
MAX DEV= 16.8511 BAR
BIAS = -1.2367 BAR
RESTRICTIONS : NONE
AUX. MODELS : 000 003 003/ 004 003

NO PT = 314
%AAD = 7.556
MIN %DEV = -25.037
MAX %DEV = 24.208
C-VAR = 0.076
R-SQR =0.971579

TABLE E.3

SRK EOS PARAMETER GENERALIZATION

CASE 8

ISO	CN	T(K)	C(I,J)	D(I,J)	RMSE BAR	BIAS BAR	AAD BAR	%AAD	NO PT
1	4	310.9	0.1145	0.0000	1.36	-1.26	1.26	5.5	18
2	4	344.3	0.1167	0.0000	2.04	-1.76	1.76	4.5	17
3	4	377.6	0.1188	0.0000	2.48	-2.05	2.08	4.3	12
4	4	410.9	0.1210	0.0000	1.73	-1.52	1.54	3.5	7
5	6	313.1	0.1190	0.0000	1.24	-0.97	1.04	2.7	8
6	6	353.1	0.1214	0.0000	1.78	-1.53	1.57	4.4	14
7	6	393.1	0.1239	0.0000	2.57	-2.41	2.41	4.5	15
8	10	310.9	0.1224	0.0000	1.66	-0.28	1.50	5.0	11
9	10	344.3	0.1244	0.0000	4.54	1.80	3.00	3.9	8
10	10	377.6	0.1263	0.0000	3.80	1.81	2.30	2.0	10
11	10	410.9	0.1283	0.0000	3.04	1.25	1.91	1.7	11
12	10	444.3	0.1303	0.0000	2.11	0.09	1.39	1.3	11
13	10	477.6	0.1323	0.0000	2.81	-1.37	2.36	2.9	11
14	10	510.9	0.1342	0.0000	4.79	-4.27	4.27	6.4	9
15	20	323.1	0.1026	0.0000	1.94	-1.46	1.46	4.3	13
16	20	373.1	0.1051	0.0000	1.20	1.13	1.13	3.7	9
17	22	323.1	0.0954	0.0000	4.13	-3.32	3.32	6.3	14
18	22	348.1	0.0965	0.0000	1.12	0.30	1.00	3.5	19
19	22	373.1	0.0976	0.0000	1.65	1.54	1.54	6.1	10
20	28	348.1	0.0717	0.0000	6.73	-3.88	4.34	7.3	8
21	28	373.1	0.0726	0.0000	1.20	1.06	1.10	6.8	7
22	28	423.1	0.0743	0.0000	3.55	3.19	3.19	12.7	7
23	32	348.1	0.0543	0.0000	3.90	-2.42	2.80	5.4	11
24	32	373.1	0.0550	0.0000	1.55	0.20	1.34	3.8	11
25	32	398.1	0.0556	0.0000	4.55	4.39	4.39	14.4	12
26	36	373.1	0.0376	0.0000	1.66	1.07	1.56	8.5	10
27	36	423.1	0.0385	0.0000	4.94	4.81	4.81	17.3	7
28	44	373.1	0.0054	0.0000	2.33	0.90	2.09	12.0	7
29	44	423.1	0.0055	0.0000	6.03	5.81	5.81	23.7	7

MODEL OVERALL STATISTICS

PAR(1).. PAR(N)=	0.766547D-01	0.111954D+00	-0.114887D+00
	0.000000D+00	0.247125D+00	0.215867D+00
	0.000000D+00	0.000000D+00	0.000000D+00
	0.000000D+00	0.000000D+00	0.000000D+00
	0.000000D+00	0.000000D+00	0.427480D+00
	0.000000D+00	0.000000D+00	0.000000D+00
	0.866400D-01	0.000000D+00	0.000000D+00
	0.000000D+00		

RMSE = 3.0306 BAR		NO PT =	314
AAD = 2.2185 BAR		%AAD =	5.929
MIN DEV=-15.3772 BAR		MIN %DEV =	-16.011
MAX DEV= 10.7040 BAR		MAX %DEV =	36.302
BIAS = -0.2490 BAR		C-VAR =	0.062
RESTRICTIONS : NONE		R-SQR =	0.996297

AUX. MODELS : 000 202 202/ 407 407
SQUARE ERROR IN PRESSURE MINIMIZED

TABLE E.4

SRK EOS PARAMETER GENERALIZATION

CASE 9

ISO	CN	T(K)	C(I,J)	D(I,J)	RMSE BAR	BIAS BAR	AAD BAR	%AAD	NO PT
1	4	310.9	0.1183	0.0317	0.52	-0.03	0.37	1.2	18
2	4	344.3	0.1183	0.0317	1.23	-0.73	0.76	1.4	17
3	4	377.6	0.1183	0.0317	1.82	-1.32	1.37	2.6	12
4	4	410.9	0.1183	0.0317	1.45	-1.26	1.30	3.0	7
5	6	313.1	0.1183	0.0264	1.04	0.15	0.91	1.9	8
6	6	353.1	0.1183	0.0264	1.12	-0.66	0.71	1.0	14
7	6	393.1	0.1183	0.0264	2.33	-1.89	1.89	2.5	15
8	10	310.9	0.1183	0.0160	1.45	1.13	1.13	2.8	11
9	10	344.3	0.1183	0.0160	3.14	2.49	2.49	4.0	8
10	10	377.6	0.1183	0.0160	2.28	2.01	2.01	3.5	10
11	10	410.9	0.1183	0.0160	1.41	1.01	1.24	2.6	11
12	10	444.3	0.1183	0.0160	1.25	-0.33	1.09	1.7	11
13	10	477.6	0.1183	0.0160	2.83	-2.13	2.17	2.1	11
14	10	510.9	0.1183	0.0160	5.34	-4.59	4.59	6.2	9
15	20	323.1	0.1183	-0.0043	1.12	-0.95	0.95	3.3	13
16	20	373.1	0.1183	-0.0043	1.48	1.42	1.42	3.9	9
17	22	323.1	0.1183	-0.0076	1.75	-1.64	1.64	4.1	14
18	22	348.1	0.1183	-0.0076	0.94	0.81	0.81	2.3	19
19	22	373.1	0.1183	-0.0076	1.37	1.19	1.19	3.8	10
20	28	348.1	0.1183	-0.0162	2.95	-2.63	2.63	6.8	8
21	28	373.1	0.1183	-0.0162	0.70	-0.67	0.67	3.1	7
22	28	423.1	0.1183	-0.0162	2.22	1.84	1.84	5.0	7
23	32	348.1	0.1183	-0.0209	1.98	-1.86	1.86	7.5	11
24	32	373.1	0.1183	-0.0209	1.01	-0.29	0.84	2.5	11
25	32	398.1	0.1183	-0.0209	2.49	2.09	2.12	4.9	12
26	36	373.1	0.1183	-0.0250	1.82	-1.78	1.78	9.3	10
27	36	423.1	0.1183	-0.0250	1.72	1.21	1.27	2.9	7
28	44	373.1	0.1183	-0.0316	2.44	-2.34	2.34	14.3	7
29	44	423.1	0.1183	-0.0316	2.84	1.56	1.95	5.0	7

MODEL OVERALL STATISTICS

PAR(1).. PAR(N)=	0.118251D+00	0.000000D+00	0.000000D+00
	0.000000D+00	0.000000D+00	0.000000D+00
	0.000000D+00	0.429385D-01	-0.564916D-01
	0.279034D-02	0.000000D+00	0.000000D+00
	0.000000D+00	0.000000D+00	0.427480D+00
	0.000000D+00	0.000000D+00	0.000000D+00
	0.866400D-01	0.000000D+00	0.000000D+00
	0.000000D+00		

RMSE	= 1.9816 BAR	NO PT	= 314
AAD	= 1.4645 BAR	%AAD	= 3.605
MIN DEV=	-8.8881 BAR	MIN %DEV	= -25.138
MAX DEV=	6.3021 BAR	MAX %DEV	= 11.979
BIAS	= -0.3189 BAR	C-VAR	= 0.041
RESTRICTIONS	: NONE	R-SQR	=0.988946
AUX. MODELS	: 000 202 202/ 407 407		
	SQUARE ERROR IN PRESSURE MINIMIZED		

TABLE E.5

SRK EOS PARAMETER GENERALIZATION

CASE 10

ISO	CN	T(K)	C(I,J)	D(I,J)	RMSE BAR	BIAS BAR	AAD BAR	%AAD	NO PT
1	4	310.9	0.1275	0.0278	0.70	0.33	0.62	2.4	18
2	4	344.3	0.1275	0.0278	0.85	-0.33	0.50	1.1	17
3	4	377.6	0.1275	0.0278	1.47	-1.03	1.09	2.1	12
4	4	410.9	0.1275	0.0278	1.36	-1.17	1.21	2.8	7
5	6	313.1	0.1230	0.0240	1.27	0.51	1.19	2.5	8
6	6	353.1	0.1230	0.0240	0.83	-0.18	0.63	1.0	14
7	6	393.1	0.1230	0.0240	1.82	-1.44	1.45	1.9	15
8	10	310.9	0.1169	0.0159	1.20	0.88	0.88	2.2	11
9	10	344.3	0.1169	0.0159	2.77	2.12	2.12	3.4	8
10	10	377.6	0.1169	0.0159	1.86	1.62	1.62	3.0	10
11	10	410.9	0.1169	0.0159	1.21	0.67	1.12	2.4	11
12	10	444.3	0.1169	0.0159	1.42	-0.60	1.17	1.7	11
13	10	477.6	0.1169	0.0159	3.03	-2.34	2.34	2.4	11
14	10	510.9	0.1169	0.0159	5.48	-4.72	4.72	6.3	9
15	20	323.1	0.1153	-0.0034	1.23	-1.01	1.01	3.3	13
16	20	373.1	0.1153	-0.0034	1.39	1.35	1.35	3.8	9
17	22	323.1	0.1164	-0.0069	1.91	-1.76	1.76	4.2	14
18	22	348.1	0.1164	-0.0069	0.90	0.78	0.78	2.3	19
19	22	373.1	0.1164	-0.0069	1.39	1.22	1.22	4.0	10
20	28	348.1	0.1213	-0.0168	2.56	-2.35	2.35	6.4	8
21	28	373.1	0.1213	-0.0168	0.65	-0.63	0.63	3.1	7
22	28	423.1	0.1213	-0.0168	2.35	1.92	1.92	5.0	7
23	32	348.1	0.1252	-0.0227	1.90	-1.55	1.64	7.3	11
24	32	373.1	0.1252	-0.0227	1.25	-0.06	1.06	3.0	11
25	32	398.1	0.1252	-0.0227	2.59	2.10	2.16	4.9	12
26	36	373.1	0.1293	-0.0280	2.02	-1.96	1.96	10.6	10
27	36	423.1	0.1293	-0.0280	1.65	0.95	1.23	3.2	7
28	44	373.1	0.1374	-0.0369	2.99	-2.79	2.79	17.5	7
29	44	423.1	0.1374	-0.0369	2.82	0.93	2.01	6.5	7

MODEL OVERALL STATISTICS

PAR(1).. PAR(N)= 0.139494D+00 -0.697235D-01 0.481242D-01
0.000000D+00 0.000000D+00 0.000000D+00
0.000000D+00 0.348643D-01 -0.327060D-01
-0.126284D-01 0.000000D+00 0.000000D+00
0.000000D+00 0.000000D+00 0.427480D+00
0.000000D+00 0.000000D+00 0.000000D+00
0.866400D-01 0.000000D+00 0.000000D+00
0.000000D+00

RMSE = 1.9428 BAR NO PT = 314
AAD. = 1.4283 BAR %AAD = 3.744
MIN DEV= -9.0999 BAR MIN %DEV = -31.207
MAX DEV= 6.5029 BAR MAX %DEV = 11.970
BIAS = -0.2909 BAR C-VAR = 0.040
RESTRICTIONS : NONE R-SQR =0.988540
AUX. MODELS : 000 202 202/ 407 407
SQUARE ERROR IN PRESSURE MINIMIZED

TABLE E.6

SRK EOS PARAMETER GENERALIZATION

CASE 11

ISO	CN	T(K)	C(I,J)	D(I,J)	RMSE BAR	BIAS BAR	AAD BAR	%AAD	NO PT
1	4	310.9	0.1453	0.0000	0.75	0.35	0.52	1.4	18
2	4	344.3	0.1509	0.0000	0.36	0.16	0.26	0.6	17
3	4	377.6	0.1564	0.0000	0.65	-0.44	0.50	1.1	12
4	4	410.9	0.1619	0.0000	1.12	-0.96	1.01	2.3	7
5	6	313.1	0.1268	0.0000	0.93	-0.24	0.87	1.9	8
6	6	353.1	0.1319	0.0000	1.11	-0.23	0.91	2.7	14
7	6	393.1	0.1371	0.0000	1.12	-0.85	0.97	2.2	15
8	10	310.9	0.1136	0.0000	2.08	-1.68	1.80	6.8	11
9	10	344.3	0.1170	0.0000	2.92	-0.25	2.46	4.4	8
10	10	377.6	0.1203	0.0000	2.49	0.16	1.90	2.2	10
11	10	410.9	0.1237	0.0000	2.30	0.13	1.73	1.7	11
12	10	444.3	0.1270	0.0000	1.98	-0.54	1.58	1.7	11
13	10	477.6	0.1303	0.0000	2.93	-1.65	2.55	3.2	11
14	10	510.9	0.1337	0.0000	4.84	-4.32	4.32	6.4	9
15	20	323.1	0.1069	0.0000	1.40	-0.97	0.97	2.7	13
16	20	373.1	0.1109	0.0000	2.01	1.96	1.96	5.7	9
17	22	323.1	0.1021	0.0000	2.70	-2.02	2.08	3.9	14
18	22	348.1	0.1039	0.0000	1.63	1.49	1.51	5.4	19
19	22	373.1	0.1058	0.0000	2.58	2.43	2.43	8.8	10
20	28	348.1	0.0792	0.0000	5.34	-2.63	3.54	7.1	8
21	28	373.1	0.0806	0.0000	1.81	1.76	1.76	9.3	7
22	28	423.1	0.0833	0.0000	4.49	4.18	4.18	15.1	7
23	32	348.1	0.0559	0.0000	3.66	-2.19	2.64	5.2	11
24	32	373.1	0.0568	0.0000	1.52	0.50	1.35	4.0	11
25	32	398.1	0.0577	0.0000	4.65	4.29	4.29	14.5	12
26	36	373.1	0.0292	0.0000	1.63	0.34	1.30	6.7	10
27	36	423.1	0.0301	0.0000	4.14	4.04	4.04	15.1	7
28	44	373.1	-0.0312	0.0000	4.31	-1.98	2.65	8.2	7
29	44	423.1	-0.0321	0.0000	3.19	2.51	3.07	14.3	7

MODEL OVERALL STATISTICS

PAR(1).. PAR(N)=	0.125170D+00	-0.225704D+00	0.386846D+00
	-0.212900D+00	0.752060D+00	0.000000D+00
	0.000000D+00	0.000000D+00	0.000000D+00
	0.000000D+00	0.000000D+00	0.000000D+00
	0.000000D+00	0.000000D+00	0.427480D+00
	0.000000D+00	0.000000D+00	0.000000D+00
	0.866400D-01	0.000000D+00	0.000000D+00
	0.000000D+00		

RMSE	= 2.5900 BAR	NO PT	= 314
AAD	= 1.8533 BAR	%AAD	= 5.019
MIN DEV=	-12.4908 BAR	MIN %DEV	= -17.157
MAX DEV=	6.9171 BAR	MAX %DEV	= 25.903
BIAS	= 0.0541 BAR	C-VAR	= 0.053
RESTRICTIONS	: NONE	R-SQR	=0.983691
AUX. MODELS	: 000 202 202/ 407 407		

TABLE E.7

SRK EOS PARAMETER GENERALIZATION

CASE 12

ISO	CN	T(K)	C(I,J)	D(I,J)	RMSE BAR	BIAS BAR	AAD BAR	%AAD	NO PT
1	4	310.9	0.1185	0.0368	0.63	0.09	0.51	2.0	18
2	4	344.3	0.1185	0.0407	1.20	-0.50	0.74	1.6	17
3	4	377.6	0.1185	0.0446	1.62	-1.03	1.14	2.1	12
4	4	410.9	0.1185	0.0486	1.30	-1.11	1.16	2.6	7
5	6	313.1	0.1185	0.0264	1.07	0.01	0.92	1.8	8
6	6	353.1	0.1185	0.0298	1.24	-0.59	0.80	1.1	14
7	6	393.1	0.1185	0.0332	2.30	-1.64	1.77	2.2	15
8	10	310.9	0.1185	0.0136	1.08	0.64	0.67	1.3	11
9	10	344.3	0.1185	0.0150	2.88	2.16	2.16	3.4	8
10	10	377.6	0.1185	0.0165	2.13	1.91	1.91	3.5	10
11	10	410.9	0.1185	0.0179	1.47	1.15	1.27	2.8	11
12	10	444.3	0.1185	0.0194	1.19	-0.03	1.11	2.0	11
13	10	477.6	0.1185	0.0208	2.54	-1.78	1.89	1.9	11
14	10	510.9	0.1185	0.0223	4.98	-4.18	4.18	5.4	9
15	20	323.1	0.1185	-0.0044	1.21	-1.03	1.03	3.6	13
16	20	373.1	0.1185	-0.0051	1.12	1.07	1.07	3.0	9
17	22	323.1	0.1185	-0.0071	1.66	-1.54	1.54	3.8	14
18	22	348.1	0.1185	-0.0076	0.86	0.73	0.74	2.1	19
19	22	373.1	0.1185	-0.0082	1.13	0.96	0.96	3.0	10
20	28	348.1	0.1185	-0.0150	2.50	-2.19	2.19	5.4	8
21	28	373.1	0.1185	-0.0160	0.68	-0.65	0.65	3.0	7
22	28	423.1	0.1185	-0.0182	1.45	1.08	1.08	2.7	7
23	32	348.1	0.1185	-0.0190	1.34	-1.05	1.13	5.3	11
24	32	373.1	0.1185	-0.0203	0.99	-0.05	0.81	2.3	11
25	32	398.1	0.1185	-0.0217	2.11	1.72	1.78	4.1	12
26	36	373.1	0.1185	-0.0240	1.49	-1.46	1.46	8.0	10
27	36	423.1	0.1185	-0.0272	0.95	0.30	0.77	2.6	7
28	44	373.1	0.1185	-0.0300	1.95	-1.80	1.80	11.9	7
29	44	423.1	0.1185	-0.0340	2.05	0.55	1.54	5.4	7

MODEL OVERALL STATISTICS

PAR(1).. PAR(N)=	0.118500D+00	0.000000D+00	0.000000D+00
	0.000000D+00	0.000000D+00	0.000000D+00
	0.000000D+00	0.350840D-04	-0.176780D-04
	-0.359260D-04	0.175670D-07	0.180410D+04
	-0.720300D+03	0.216110D+03	0.427480D+00
	0.000000D+00	0.000000D+00	0.000000D+00
	0.864400D-01	0.000000D+00	0.000000D+00
	0.000000D+00		

RMSE	= 1.7625 BAR	NO PT	= 314
AAD	= 1.2770 BAR	%AAD	= 3.185
MIN DEV	= -8.5264 BAR	MIN %DEV	= -22.141
MAX DEV	= 5.9705 BAR	MAX %DEV	= 10.293
BIAS	= -0.2873 BAR	C-VAR	= 0.036
RESTRICTIONS	: NONE	R-SQR	=0.987363
AUX. MODELS	: 000 202 202/ 407 407		

TABLE E.8

SRK EOS PARAMETER GENERALIZATION

CASE 13

ISO	CN	T(K)	C(I,J)	D(I,J)	RMSE BAR	BIAS BAR	AAD BAR	%AAD	NO PT
1	4	310.9	0.1283	0.0388	1.15	0.76	1.03	4.6	18
2	4	344.3	0.1359	0.0388	1.06	0.49	0.92	2.9	17
3	4	377.6	0.1435	0.0388	0.71	-0.07	0.60	1.5	12
4	4	410.9	0.1511	0.0388	0.88	-0.75	0.80	1.9	7
5	6	313.1	0.1129	0.0296	0.94	-0.21	0.72	1.3	8
6	6	353.1	0.1195	0.0296	1.11	-0.34	0.77	1.2	14
7	6	393.1	0.1262	0.0296	1.45	-0.82	1.13	1.6	15
8	10	310.9	0.1084	0.0140	0.91	-0.77	0.78	2.3	11
9	10	344.3	0.1117	0.0140	1.29	0.43	0.95	1.5	8
10	10	377.6	0.1151	0.0140	1.22	0.83	0.95	2.0	10
11	10	410.9	0.1184	0.0140	1.33	0.77	1.19	2.3	11
12	10	444.3	0.1218	0.0140	1.13	0.10	0.97	1.6	11
13	10	477.6	0.1251	0.0140	2.12	-1.28	1.71	1.6	11
14	10	510.9	0.1285	0.0140	4.41	-3.81	3.81	5.2	9
15	20	323.1	0.1259	-0.0078	1.19	-1.12	1.12	4.5	13
16	20	373.1	0.1222	-0.0078	0.75	0.70	0.70	1.8	9
17	22	323.1	0.1276	-0.0102	0.85	-0.68	0.78	2.7	14
18	22	348.1	0.1246	-0.0102	1.06	0.84	0.88	2.1	19
19	22	373.1	0.1216	-0.0102	0.91	0.70	0.79	2.5	10
20	28	348.1	0.1205	-0.0147	1.74	-1.56	1.56	4.1	8
21	28	373.1	0.1135	-0.0147	0.59	-0.54	0.54	2.3	7
22	28	423.1	0.0994	-0.0147	1.06	0.46	0.65	2.3	7
23	32	348.1	0.1138	-0.0161	0.88	-0.38	0.75	3.5	11
24	32	373.1	0.1039	-0.0161	0.56	-0.14	0.42	1.2	11
25	32	398.1	0.0939	-0.0161	1.69	1.52	1.52	4.1	12
26	36	373.1	0.0921	-0.0167	0.91	-0.83	0.83	3.9	10
27	36	423.1	0.0664	-0.0167	0.38	0.25	0.35	1.2	7
28	44	373.1	0.0661	-0.0164	0.97	-0.75	0.75	3.1	7
29	44	423.1	0.0293	-0.0164	0.91	0.62	0.85	3.3	7

MODEL OVERALL STATISTICS

PAR(1).. PAR(N)=	0.610253D-01	-0.534423D-01	0.176704D+00
	0.000000D+00	0.230162D+01	-0.306177D+01
	0.000000D+00	0.604094D-01	-0.116491D+00
	0.439747D-01	0.000000D+00	0.000000D+00
	0.000000D+00	0.000000D+00	0.427480D+00
	0.000000D+00	0.000000D+00	0.000000D+00
	0.866400D-01	0.000000D+00	0.000000D+00
	0.000000D+00		

RMSE = 1.3492 BAR		NO PT =	314
AAD = 0.9989 BAR		%AAD =	2.590
MIN DEV= -7.4326 BAR		MIN %DEV =	-13.723
MAX DEV= 2.7645 BAR		MAX %DEV =	9.095
BIAS = -0.1304 BAR		C-VAR =	0.028
RESTRICTIONS : NONE		R-SQR =	0.986007
AUX. MODELS : 000 202 202/ 407 407			
SQUARE ERROR IN PRESSURE MINIMIZED			

TABLE E.9

SRK EOS PARAMETER GENERALIZATION

CASE 14

ISO	CN	T(K)	C(I,J)	D(I,J)	RMSE BAR	BIAS BAR	AAD BAR	%AAD	NO PT
1	4	310.9	0.1386	0.0146	0.83	0.48	0.68	2.4	18
2	4	344.3	0.1472	0.0161	0.70	0.47	0.61	1.8	17
3	4	377.6	0.1558	0.0177	0.41	-0.03	0.36	1.0	12
4	4	410.9	0.1644	0.0193	0.88	-0.74	0.80	1.9	7
5	6	313.1	0.1173	0.0166	0.79	-0.39	0.56	1.0	8
6	6	353.1	0.1247	0.0188	0.70	-0.23	0.55	1.0	14
7	6	393.1	0.1321	0.0209	0.85	-0.49	0.70	1.1	15
8	10	310.9	0.1065	0.0129	1.32	-1.20	1.20	3.6	11
9	10	344.3	0.1103	0.0143	1.06	0.10	0.88	1.5	8
10	10	377.6	0.1141	0.0156	1.11	0.82	0.91	2.1	10
11	10	410.9	0.1179	0.0170	1.43	1.07	1.25	2.7	11
12	10	444.3	0.1217	0.0184	1.17	0.62	1.04	2.1	11
13	10	477.6	0.1256	0.0198	1.66	-0.71	1.39	1.6	11
14	10	510.9	0.1294	0.0212	3.85	-3.20	3.20	4.1	9
15	20	323.1	0.1218	-0.0050	0.86	-0.76	0.76	2.7	13
16	20	373.1	0.1201	-0.0058	1.18	1.13	1.13	3.0	9
17	22	323.1	0.1241	-0.0079	0.64	-0.54	0.57	1.8	14
18	22	348.1	0.1223	-0.0086	1.26	1.09	1.09	2.8	19
19	22	373.1	0.1204	-0.0092	0.96	0.73	0.76	2.4	10
20	28	348.1	0.1212	-0.0150	1.75	-1.59	1.59	4.3	8
21	28	373.1	0.1159	-0.0161	0.88	-0.82	0.82	3.6	7
22	28	423.1	0.1052	-0.0182	0.92	-0.19	0.72	2.2	7
23	32	348.1	0.1167	-0.0170	1.01	-0.33	0.90	3.9	11
24	32	373.1	0.1089	-0.0182	0.77	-0.42	0.65	1.9	11
25	32	398.1	0.1010	-0.0195	1.08	0.86	0.93	2.4	12
26	36	373.1	0.0998	-0.0188	1.05	-1.01	1.01	5.1	10
27	36	423.1	0.0789	-0.0213	0.59	-0.54	0.54	2.0	7
28	44	373.1	0.0785	-0.0169	0.31	0.04	0.24	1.3	7
29	44	423.1	0.0478	-0.0192	1.08	0.94	0.94	3.1	7

MODEL OVERALL STATISTICS

PAR(1).. PAR(N)=	0.661930D-01	-0.750620D-01	0.173050D+00
	0.000000D+00	0.251560D+01	-0.310360D+01
	0.000000D+00	-0.505080D-05	0.787500D-04
	-0.935190D-04	0.000000D+00	0.323890D+04
	-0.191510D+04	0.000000D+00	

RMSE	= 1.1968 BAR	NO PT	= 314
AAD	= 0.9040 BAR	%AAD	= 2.377
MIN DEV=	-6.8016 BAR	MIN %DEV	= -14.668
MAX DEV=	2.1641 BAR	MAX %DEV	= 9.175
BIAS	= -0.0925 BAR	C-VAR	= 0.025
RESTRICTIONS	: NONE	R-SQR	=0.994256
AUX. MODELS	: 000 002 002/ 007 007		

TABLE E.10

SRK EOS PARAMETER GENERALIZATION

CASE 14a

ISO	CN	T(K)	C(I,J)	D(I,J)	RMSE BAR	BIAS BAR	AAD BAR	%AAD	NO PT
1	4	310.9	0.1195	0.0135	0.66	-0.57	0.57	2.2	18
2	4	344.3	0.1211	0.0260	1.15	-0.74	0.76	1.4	17
3	4	377.6	0.1227	0.0384	1.51	-0.98	1.07	2.0	12
4	4	410.9	0.1242	0.0509	1.18	-1.01	1.06	2.4	7
5	6	313.1	0.1182	0.0102	0.87	-0.59	0.70	1.6	8
6	6	353.1	0.1201	0.0209	1.00	-0.71	0.74	1.4	14
7	6	393.1	0.1219	0.0315	1.86	-1.23	1.43	1.9	15
8	10	310.9	0.1156	0.0047	1.33	-0.79	1.16	4.3	11
9	10	344.3	0.1171	0.0091	2.49	1.10	1.63	2.0	8
10	10	377.6	0.1186	0.0134	2.15	1.72	1.72	2.8	10
11	10	410.9	0.1201	0.0178	1.95	1.71	1.71	3.3	11
12	10	444.3	0.1216	0.0221	1.41	1.05	1.19	2.6	11
13	10	477.6	0.1232	0.0265	1.55	-0.50	1.35	1.9	11
14	10	510.9	0.1247	0.0309	3.75	-2.93	2.93	3.4	9
15	20	323.1	0.1118	-0.0026	1.47	-1.18	1.18	3.8	13
16	20	373.1	0.1140	-0.0052	0.54	0.49	0.49	1.6	9
17	22	323.1	0.1113	-0.0038	1.94	-1.61	1.61	3.3	14
18	22	348.1	0.1124	-0.0057	0.74	0.59	0.64	2.2	19
19	22	373.1	0.1135	-0.0077	0.79	0.65	0.69	2.4	10
20	28	348.1	0.1115	-0.0104	2.05	-1.40	1.40	2.2	8
21	28	373.1	0.1126	-0.0140	0.45	-0.40	0.40	1.7	7
22	28	423.1	0.1147	-0.0211	0.78	-0.23	0.68	2.7	7
23	32	348.1	0.1115	-0.0130	1.16	0.66	0.97	2.7	11
24	32	373.1	0.1126	-0.0175	1.07	0.56	0.82	1.8	11
25	32	398.1	0.1136	-0.0219	1.35	0.97	1.08	2.7	12
26	36	373.1	0.1130	-0.0206	0.67	-0.56	0.59	4.1	10
27	36	423.1	0.1152	-0.0310	1.36	-1.31	1.31	5.7	7
28	44	373.1	0.1153	-0.0258	1.19	-0.44	1.09	6.9	7
29	44	423.1	0.1175	-0.0389	1.84	-1.34	1.74	9.0	7

MODEL OVERALL STATISTICS

PAR(1).. PAR(N)= 0.125755D+00 -0.880568D-03 0.146232D-04
0.213588D-03 0.729327D-01 -0.260875D-01
0.563841D-02

RMSE = 1.5040 BAR
AAD = 1.0969 BAR
MIN DEV= -6.8834 BAR
MAX DEV= 5.6399 BAR
BIAS = -0.2936 BAR
RESTRICTIONS : NONE
AUX. MODELS : 000 003 003/ 004 003
SQUARE ERROR IN PRESSURE MINIMIZED

NO PT = 314
%AAD = 2.769
MIN %DEV = -19.561
MAX %DEV = 10.208
C-VAR = 0.031
R-SQR =0.998416

TABLE E.11

SRK EOS PARAMETER GENERALIZATION

CASE 15

ISO	CN	T(K)	C(I,J)	D(I,J)	RMSE BAR	BIAS BAR	AAD BAR	%AAD	NO PT
1	4	310.9	0.1227	0.0274	0.47	0.22	0.40	1.5	18
2	4	344.3	0.1227	0.0274	0.35	-0.21	0.23	0.5	17
3	4	377.6	0.1227	0.0274	1.24	-0.94	0.99	2.0	12
4	4	410.9	0.1227	0.0274	1.33	-1.15	1.19	2.7	7
5	6	313.1	0.1206	0.0234	1.06	0.59	1.00	2.1	8
6	6	353.1	0.1206	0.0234	0.55	0.02	0.40	0.9	14
7	6	393.1	0.1206	0.0234	1.55	-1.33	1.33	2.3	15
8	10	310.9	0.1181	0.0150	1.45	1.09	1.09	2.5	11
9	10	344.3	0.1181	0.0150	1.98	1.50	1.50	2.6	8
10	10	377.6	0.1181	0.0150	0.90	-0.16	0.78	1.8	10
11	10	410.9	0.1181	0.0150	1.63	-0.78	1.32	2.1	11
12	10	444.3	0.1181	0.0150	1.35	-0.20	1.09	1.5	11
13	10	477.6	0.1181	0.0150	1.98	0.62	1.13	1.3	11
14	10	510.9	0.1181	0.0150	1.08	-0.46	0.80	1.0	9
15	20	323.1	0.1193	-0.0039	0.79	-0.62	0.62	2.0	13
16	20	373.1	0.1193	-0.0039	1.00	0.96	0.96	3.0	9
17	22	323.1	0.1203	-0.0073	1.14	-1.05	1.05	2.7	14
18	22	348.1	0.1203	-0.0073	1.05	0.94	0.94	2.8	19
19	22	373.1	0.1203	-0.0073	1.14	1.01	1.01	3.4	10
20	28	348.1	0.1241	-0.0166	2.47	-2.20	2.20	5.7	8
21	28	373.1	0.1241	-0.0166	0.68	-0.64	0.64	2.9	7
22	28	423.1	0.1241	-0.0166	1.97	1.65	1.65	4.7	7
23	32	348.1	0.1270	-0.0221	1.64	-1.28	1.38	6.4	11
24	32	373.1	0.1270	-0.0221	1.00	-0.26	0.83	2.5	11
25	32	398.1	0.1270	-0.0221	2.04	1.60	1.63	3.9	12
26	36	373.1	0.1298	-0.0270	1.88	-1.84	1.84	9.8	10
27	36	423.1	0.1298	-0.0270	1.53	0.97	1.13	2.7	7
28	44	373.1	0.1353	-0.0351	2.75	-2.61	2.61	16.1	7
29	44	423.1	0.1353	-0.0351	2.58	1.04	1.80	5.5	7

MODEL OVERALL STATISTICS

PAR(1).. PAR(N)=	0.128653D+00	-0.353648D-01	0.282510D-01
	0.000000D+00	0.000000D+00	0.000000D+00
	0.000000D+00	0.350665D-01	-0.366378D-01
	-0.907716D-02	0.000000D+00	0.000000D+00
	0.000000D+00	0.000000D+00	0.427480D+00
	0.404032D+00	0.422705D+00	-0.302209D+00
	0.866400D-01	0.443973D+00	-0.747006D+00
	-0.271510D+01		

RMSE = 1.4298 BAR		NO PT =	314
AAD = 1.0734 BAR		%AAD =	3.072
MIN DEV= -4.1587 BAR		MIN %DEV =	-28.603
MAX DEV= 6.1211 BAR		MAX %DEV =	11.791
BIAS = -0.1180 BAR		C-VAR =	0.029
RESTRICTIONS : NONE		R-SQR =	0.996331
AUX. MODELS : 000 202 202/ 407 407			
SQUARE ERROR IN PRESSURE MINIMIZED			

TABLE E.12

SRK EOS PARAMETER GENERALIZATION

CASE 15a

ISO	CN	T(K)	C(I,J)	D(I,J)	RMSE BAR	BIAS BAR	AAD BAR	%AAD	NO PT
1	4	310.9	0.1146	0.0538	0.82	0.73	0.73	3.2	18
2	4	344.3	0.1146	0.0538	0.25	0.06	0.22	0.8	17
3	4	377.6	0.1146	0.0538	1.02	-0.71	0.78	1.6	12
4	4	410.9	0.1146	0.0538	1.19	-1.03	1.07	2.5	7
5	6	313.1	0.1218	0.0395	1.15	0.56	1.08	2.5	8
6	6	353.1	0.1218	0.0395	0.56	-0.14	0.38	0.8	14
7	6	393.1	0.1218	0.0395	1.35	-1.01	1.05	1.6	15
8	10	310.9	0.1331	0.0176	1.52	1.12	1.42	4.1	11
9	10	344.3	0.1331	0.0176	1.08	0.62	1.03	2.6	8
10	10	377.6	0.1331	0.0176	0.99	0.17	0.89	2.4	10
11	10	410.9	0.1331	0.0176	1.28	0.05	1.13	2.3	11
12	10	444.3	0.1331	0.0176	1.54	0.03	1.21	1.7	11
13	10	477.6	0.1331	0.0176	2.90	0.04	1.77	1.5	11
14	10	510.9	0.1331	0.0176	2.57	-1.96	2.24	3.4	9
15	20	323.1	0.1445	-0.0093	0.84	-0.79	0.79	3.2	13
16	20	373.1	0.1445	-0.0093	0.73	0.69	0.69	1.8	9
17	22	323.1	0.1449	-0.0123	0.94	-0.90	0.90	2.8	14
18	22	348.1	0.1449	-0.0123	0.88	0.68	0.73	1.9	19
19	22	373.1	0.1449	-0.0123	0.85	0.64	0.74	2.4	10
20	28	348.1	0.1439	-0.0194	2.54	-2.31	2.31	6.4	8
21	28	373.1	0.1439	-0.0194	0.85	-0.82	0.82	4.0	7
22	28	423.1	0.1439	-0.0194	1.71	1.35	1.35	3.5	7
23	32	348.1	0.1421	-0.0231	1.60	-1.32	1.36	6.4	11
24	32	373.1	0.1421	-0.0231	0.99	-0.18	0.82	2.5	11
25	32	398.1	0.1421	-0.0231	2.30	1.92	1.96	4.6	12
26	36	373.1	0.1397	-0.0263	1.67	-1.63	1.63	8.8	10
27	36	423.1	0.1397	-0.0263	1.56	1.08	1.15	2.7	7
28	44	373.1	0.1344	-0.0322	2.44	-2.36	2.36	14.1	7
29	44	423.1	0.1344	-0.0322	2.38	1.26	1.68	4.6	7

MODEL OVERALL STATISTICS

PAR(1).. PAR(N)=

0.966803D-01	0.997532D-01	-0.515696D-01
0.000000D+00	0.000000D+00	0.000000D+00
0.000000D+00	0.907359D-01	-0.212932D+00
0.150579D+00	-0.434119D-01	0.000000D+00
0.000000D+00	0.000000D+00	0.346916D+00
0.150606D+00	-0.123241D+00	0.569600D-01
0.294283D-01	-0.168484D-01	

RMSE = 1.4638 BAR
AAD = 1.1013 BAR
MIN DEV= -4.1760 BAR
MAX DEV= 8.5434 BAR
BIAS = -0.1068 BAR
RESTRICTIONS : NONE
AUX. MODELS : 100 102 102/ 307 307
SQUARE ERROR IN PRESSURE MINIMIZED

NO PT = 314
%AAD = 3.157
MIN %DEV = -24.699
MAX %DEV = 10.491
C-VAR = 0.030
R-SQR =0.998465

TABLE E.13

SRK EOS PARAMETER GENERALIZATION

CASE 16

ISO	CN	T(K)	C(I,J)	D(I,J)	RMSE BAR	BIAS BAR	AAD BAR	%AAD	NO PT
1	4	310.9	0.1166	0.0385	0.47	0.28	0.44	1.9	18
2	4	344.3	0.1208	0.0427	0.51	0.46	0.46	1.6	17
3	4	377.6	0.1251	0.0468	0.57	-0.20	0.45	1.1	12
4	4	410.9	0.1294	0.0509	1.01	-0.86	0.91	2.1	7
5	6	313.1	0.1109	0.0269	0.54	-0.24	0.37	0.7	8
6	6	353.1	0.1143	0.0303	0.66	0.19	0.46	0.8	14
7	6	393.1	0.1176	0.0337	1.13	-0.80	0.93	1.4	15
8	10	310.9	0.1126	0.0123	0.75	-0.47	0.67	2.1	11
9	10	344.3	0.1132	0.0137	0.82	-0.15	0.72	1.4	8
10	10	377.6	0.1137	0.0150	0.98	-0.30	0.86	1.8	10
11	10	410.9	0.1143	0.0163	1.18	0.09	1.04	2.2	11
12	10	444.3	0.1149	0.0176	1.16	0.65	1.02	2.1	11
13	10	477.6	0.1154	0.0189	1.16	0.69	0.87	1.7	11
14	10	510.9	0.1160	0.0203	1.15	-0.39	0.83	1.1	9
15	20	323.1	0.1268	-0.0060	0.63	-0.55	0.55	2.0	13
16	20	373.1	0.1182	-0.0069	0.34	0.10	0.31	0.9	9
17	22	323.1	0.1286	-0.0082	0.38	-0.06	0.30	1.0	14
18	22	348.1	0.1232	-0.0088	0.90	0.78	0.78	2.3	19
19	22	373.1	0.1178	-0.0094	0.51	0.33	0.43	1.8	10
20	28	348.1	0.1222	-0.0139	1.89	-1.46	1.46	3.0	8
21	28	373.1	0.1133	-0.0149	0.80	-0.70	0.70	2.8	7
22	28	423.1	0.0954	-0.0169	1.34	-0.53	1.03	2.5	7
23	32	348.1	0.1196	-0.0160	1.05	0.34	0.91	3.0	11
24	32	373.1	0.1083	-0.0171	0.55	-0.23	0.45	1.3	11
25	32	398.1	0.0970	-0.0183	1.03	0.86	0.89	2.4	12
26	36	373.1	0.1024	-0.0185	0.73	-0.68	0.68	3.7	10
27	36	423.1	0.0753	-0.0210	0.58	-0.52	0.52	1.9	7
28	44	373.1	0.0899	-0.0198	0.40	-0.14	0.36	2.6	7
29	44	423.1	0.0545	-0.0224	0.56	0.36	0.42	1.3	7

MODEL OVERALL STATISTICS

PAR(1).. PAR(N)=	0.679934D-01	0.169949D-01	0.130167D+00
	0.000000D+00	0.114065D+01	-0.213571D+01
	0.000000D+00	0.363949D-04	-0.213527D-04
	-0.393921D-04	0.000000D+00	0.189541D+04
	-0.855258D+03	0.000000D+00	0.427480D+00
	0.955886D+00	0.328868D+01	0.255916D+01
	0.864400D-01	0.126765D+01	0.385093D+01
	0.199174D+01		

RMSE =	0.8669 BAR	NO PT =	314
AAD =	0.6713 BAR	%AAD =	1.842
MIN DEV=	-3.9369 BAR	MIN %DEV =	-11.283
MAX DEV=	2.7166 BAR	MAX %DEV =	7.622
BIAS =	-0.0336 BAR	C-VAR =	0.018
RESTRICTIONS :	NONE	R-SQR =	0.995472
AUX. MODELS :	000 202 202/ 407 407		
	SQUARE ERROR IN PRESSURE MINIMIZED		

TABLE E.14

SRK EOS PARAMETER GENERALIZATION

CASE 16a

ISO	CN	T(K)	C(I,J)	D(I,J)	RMSE BAR	BIAS BAR	AAD BAR	%AAD	NO PT
1	4	310.9	0.1333	0.0198	0.64	0.43	0.44	1.2	18
2	4	344.3	0.1200	0.0303	0.26	-0.18	0.20	0.5	17
3	4	377.6	0.1066	0.0408	1.28	-0.91	0.97	1.9	12
4	4	410.9	0.0933	0.0513	1.25	-1.07	1.12	2.5	7
5	6	313.1	0.1321	0.0147	0.91	0.39	0.80	1.5	8
6	6	353.1	0.1161	0.0237	0.76	-0.17	0.64	1.5	14
7	6	393.1	0.1001	0.0327	1.44	-1.16	1.17	1.6	15
8	10	310.9	0.1325	0.0071	1.00	0.16	0.81	2.1	11
9	10	344.3	0.1192	0.0108	0.98	-0.00	0.82	1.4	8
10	10	377.6	0.1060	0.0146	0.95	-0.01	0.86	1.8	10
11	10	410.9	0.0927	0.0183	1.26	0.50	1.14	2.5	11
12	10	444.3	0.0794	0.0221	1.42	0.98	1.21	2.5	11
13	10	477.6	0.0662	0.0258	1.38	0.73	1.05	2.0	11
14	10	510.9	0.0529	0.0296	1.70	-0.96	1.22	1.4	9
15	20	323.1	0.1273	-0.0030	0.61	-0.31	0.34	0.9	13
16	20	373.1	0.1074	-0.0050	0.45	0.12	0.41	1.3	9
17	22	323.1	0.1273	-0.0046	0.71	-0.32	0.50	1.1	14
18	22	348.1	0.1174	-0.0061	0.85	0.68	0.74	2.6	19
19	22	373.1	0.1075	-0.0077	0.61	0.45	0.50	2.0	10
20	28	348.1	0.1179	-0.0115	2.18	-1.42	1.42	2.1	8
21	28	373.1	0.1079	-0.0143	0.59	-0.51	0.51	2.0	7
22	28	423.1	0.0880	-0.0201	0.81	-0.04	0.58	2.1	7
23	32	348.1	0.1184	-0.0144	1.14	0.64	0.98	2.8	11
24	32	373.1	0.1084	-0.0180	0.74	0.19	0.55	1.4	11
25	32	398.1	0.0983	-0.0216	1.39	1.11	1.19	3.0	12
26	36	373.1	0.1090	-0.0213	0.81	-0.76	0.76	4.7	10
27	36	423.1	0.0888	-0.0298	0.98	-0.89	0.89	4.3	7
28	44	373.1	0.1107	-0.0268	1.18	-0.82	1.08	7.6	7
29	44	423.1	0.0903	-0.0375	1.57	-0.95	1.44	7.6	7

MODEL OVERALL STATISTICS

PAR(1).. PAR(N)= 0.109039D+00 -0.179888D-03 0.495417D-05
-0.205265D-02 0.776553D-01 -0.276047D-01
0.443644D-02 0.147758D+00 0.403072D+00
-0.161668D+00 0.678514D-01 -0.890407D-02
0.150625D-01

RMSE = 1.0694 BAR NO PT = 314
AAD = 0.8024 BAR %AAD = 2.189
MIN DEV= -4.9534 BAR MIN %DEV = -17.315
MAX DEV= 3.3224 BAR MAX %DEV = 8.640
BIAS = -0.0706 BAR C-VAR = 0.022
RESTRICTIONS : NONE R-SQR =0.999861
AUX. MODELS : 000 103 103/ 304 303
SQUARE ERROR IN PRESSURE MINIMIZED

TABLE E.15

SRK EOS PARAMETER GENERALIZATION

CASE 17

ISO	CN	T(K)	C(I,J)	D(I,J)	RMSE BAR	BIAS BAR	AAD BAR	%AAD	NO PT
1	4	310.9	0.1326	0.0000	0.51	-0.33	0.44	2.0	18
2	4	344.3	0.1481	0.0000	0.20	0.02	0.15	0.4	17
3	4	377.6	0.1762	0.0000	0.51	0.46	0.46	1.2	12
4	4	410.9	0.2171	0.0000	0.38	-0.18	0.35	0.8	7
5	6	313.1	0.1244	0.0000	0.97	-0.46	0.88	2.1	8
6	6	353.1	0.1302	0.0000	1.14	-0.45	0.90	2.8	14
7	6	393.1	0.1497	0.0000	1.32	0.72	1.05	1.6	15
8	10	310.9	0.1246	0.0000	1.79	0.09	1.54	4.8	11
9	10	344.3	0.1168	0.0000	2.85	-0.32	2.44	4.4	8
10	10	377.6	0.1146	0.0000	2.32	-1.34	2.04	3.0	10
11	10	410.9	0.1180	0.0000	2.25	-1.18	1.86	2.2	11
12	10	444.3	0.1271	0.0000	1.99	-0.51	1.57	1.7	11
13	10	477.6	0.1419	0.0000	2.92	0.10	1.86	1.9	11
14	10	510.9	0.1623	0.0000	2.25	-1.65	2.07	3.3	9
15	20	323.1	0.1109	0.0000	0.91	-0.50	0.55	1.5	13
16	20	373.1	0.1043	0.0000	1.11	1.02	1.02	3.5	9
17	22	323.1	0.1029	0.0000	2.52	-1.85	1.93	3.6	14
18	22	348.1	0.1011	0.0000	1.29	1.02	1.14	4.4	19
19	22	373.1	0.0995	0.0000	1.85	1.74	1.74	6.7	10
20	28	348.1	0.0725	0.0000	6.58	-3.74	4.24	7.3	8
21	28	373.1	0.0763	0.0000	1.46	1.38	1.38	7.9	7
22	28	423.1	0.0824	0.0000	4.39	4.08	4.08	14.9	7
23	32	348.1	0.0475	0.0000	4.94	-3.41	3.59	6.6	11
24	32	373.1	0.0552	0.0000	1.54	0.23	1.34	3.8	11
25	32	398.1	0.0620	0.0000	5.32	5.15	5.15	16.4	12
26	36	373.1	0.0312	0.0000	1.60	0.52	1.29	7.0	10
27	36	423.1	0.0508	0.0000	6.21	5.99	5.99	20.7	7
28	44	373.1	-0.0196	0.0000	3.48	-1.11	2.27	8.8	7
29	44	423.1	0.0126	0.0000	6.74	6.48	6.48	25.7	7

MODEL OVERALL STATISTICS

PAR(1).. PAR(N)= -0.820890D-05 -0.132000D-07 0.301580D+03
0.226570D+03 -0.434150D-01 0.944420D+00
0.131960D+00

RMSE = 2.7982 BAR
AAD = 1.8290 BAR
MIN DEV=-15.0735 BAR
MAX DEV= 8.6082 BAR
BIAS = 0.2725 BAR
RESTRICTIONS : NONE
AUX. MODELS : 000 007 000/ 007 000

NO PT = 314
%AAD = 5.065
MIN %DEV = -15.694
MAX %DEV = 38.373
C-VAR = 0.058
R-SQR =0.991091

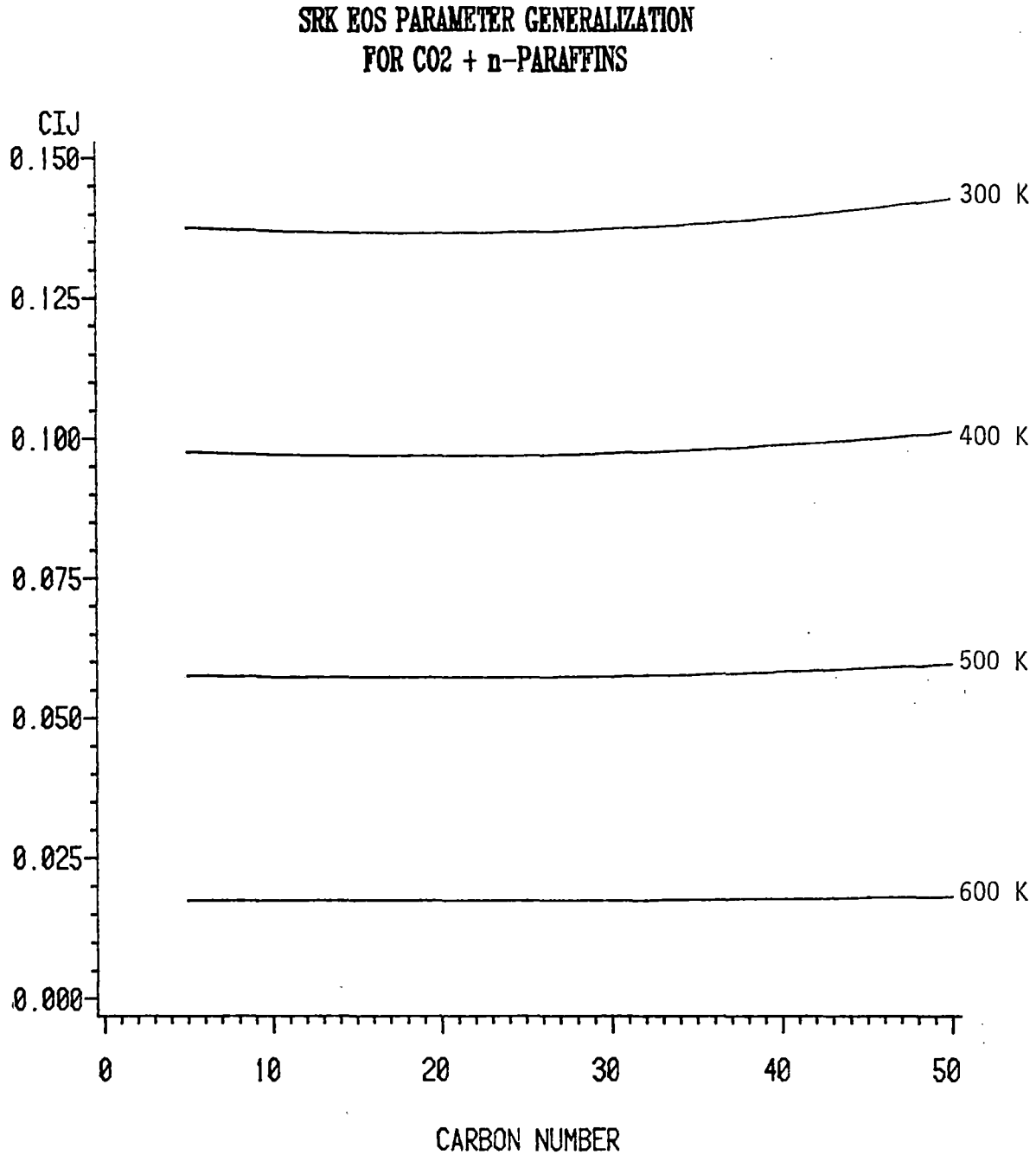

Figure E.1. Behavior of SRK Generalized C_{ij} (Case 16a)

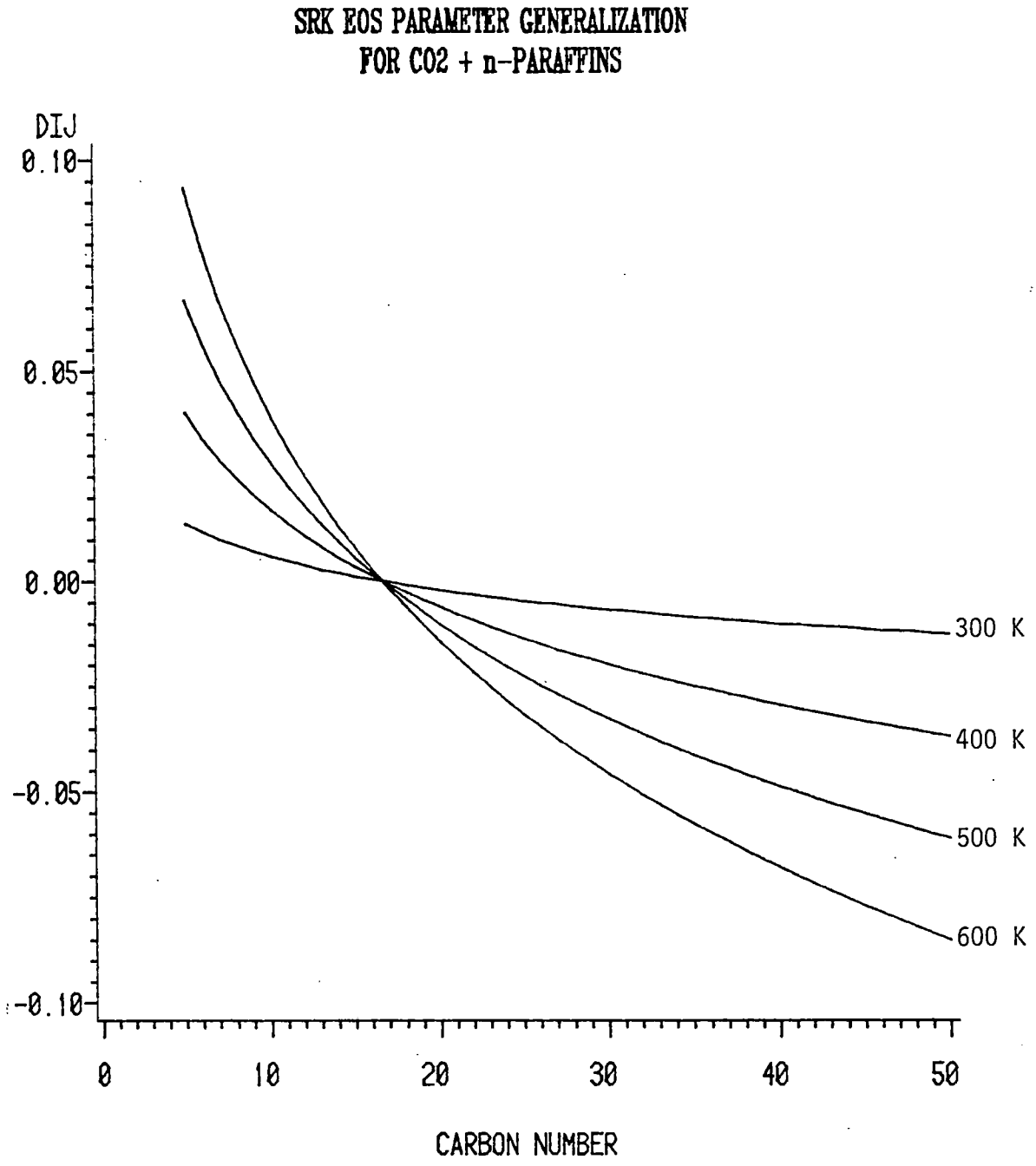

Figure E.2. Behavior of SRK Generalized D_{ij} (Case 16a)

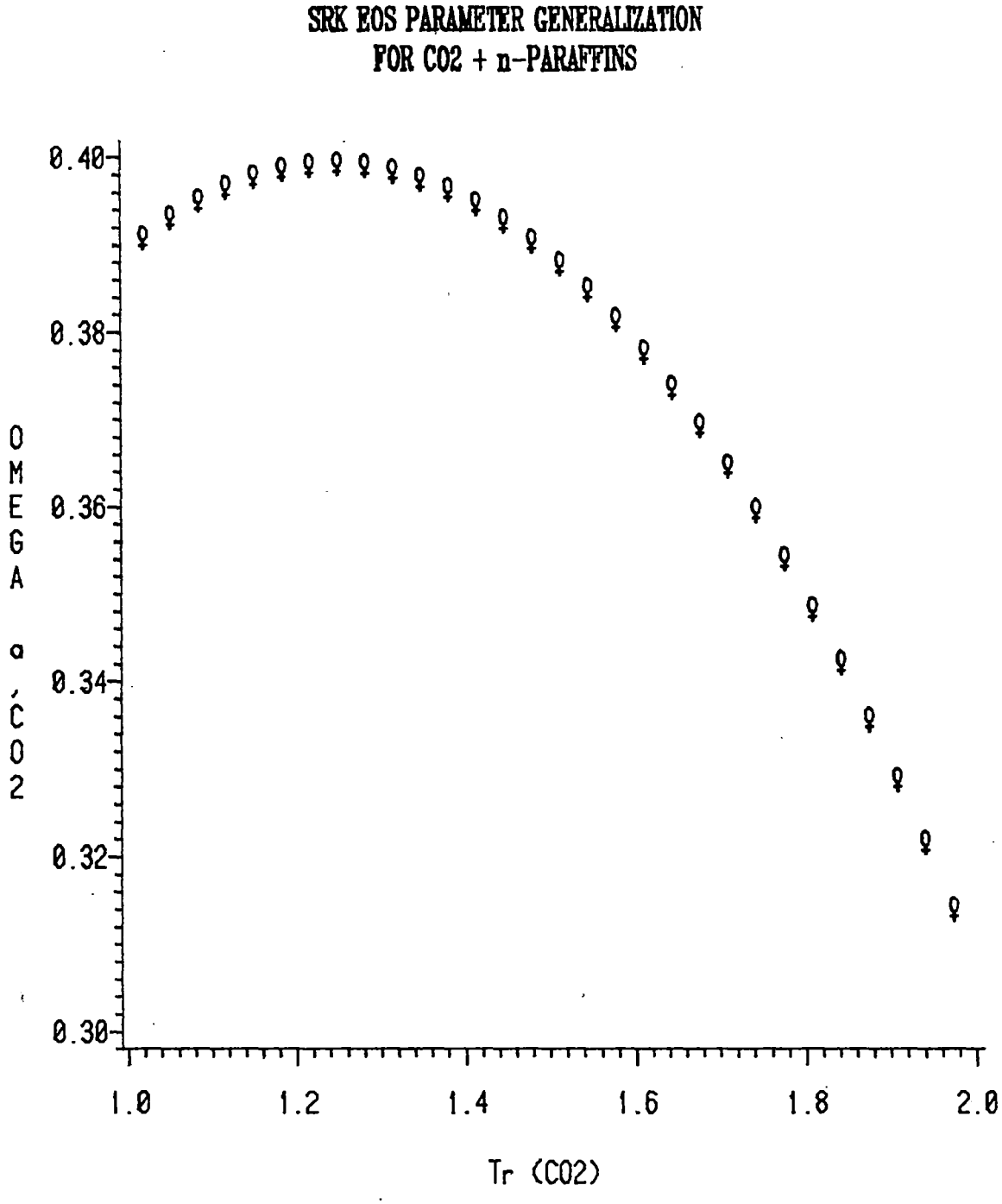

Figure E.3. Behavior of SRK Generalized Ω_{a,CO_2} (Case 16a)

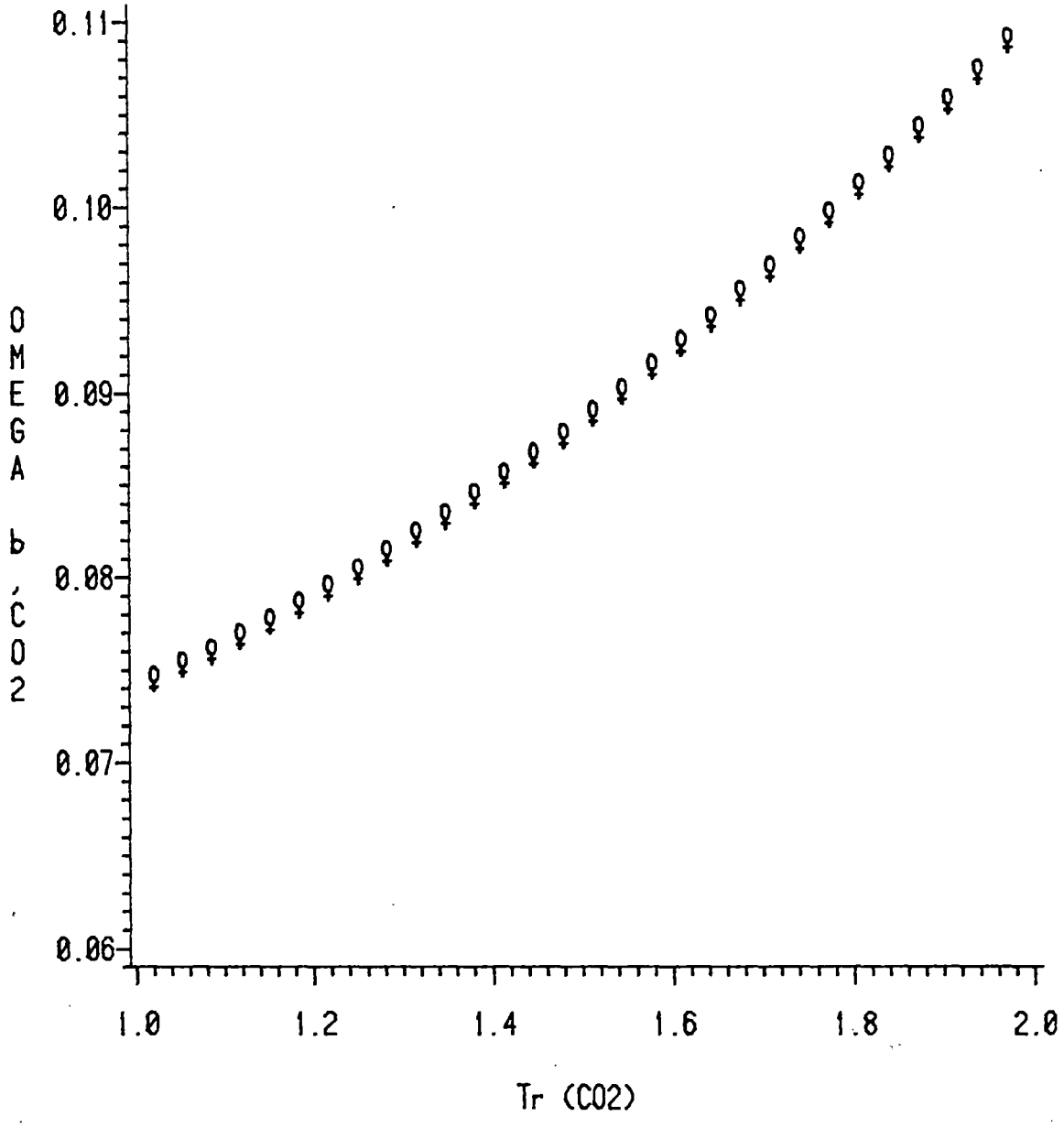

Figure E.4. Behavior of SRK Generalized Ω_{b,CO_2} (Case 16a)

VITA

Khaled A. Massoud-Gasem

Candidate for the Degree of

Doctor of Philosophy

Thesis: BINARY VAPOR-LIQUID PHASE EQUILIBRIUM FOR CARBON DIOXIDE + HEAVY NORMAL PARAFFINS

Major Field: Chemical Engineering

Biographical:

Personal Data: Born in Kabaow, Libya, February 5, 1954, the son of Aboulgasem M. Gasem and Saida Y. Elbarouni.

Education: Attended elementary school in Tripoli and Kabaow, Libya; graduated in 1971 from Tripoli High School. Received the Bachelor of Science degree in Chemical Engineering from the University of California at Berkeley in June, 1976. Received Master of Science in Chemical and Petroleum Refining Engineering from the Colorado School of Mines in December, 1979. Completed the requirements for Doctor of Philosophy degree in May, 1986.

Professional Experience: Graduate teaching assistant, Chemical Engineering Department, University of AL-fatah, Libya, 1976-1977. Instructor, Chemical Engineering Department, University of AL-fatah, Libya, 1980. Graduate research and teaching assistant, School of Chemical Engineering, Oklahoma State University, 1981-1983.